IASJ
المجلات الاكاديمية العراقية

KJPS
AL-Kitab Journal For Pure Sciences

AL-Kitab Journal For Pure Sciences

Volume : 8 (2024)

Issue: 1

ISSN: 2617-1260 (print)

ISSN: 2617-8141 (online)

DOI: http://10.32441/kjps

Deposit number at the Notional House of Books and Archives, Iraq, 2271 in 2017

Al-Kitab Journal for Pure Science

KJPS

ISSN: 2617-1260 (print), 2617-8141(online)
DOI: http://10.32441/kjps
https://isnra.net/index.php/kjps

An Academic Semi-Annual Journal

Volume: 8 Issue: 1 June 2024

University Website: **www.uoalkitab.edu.iq**
Journal Website: **https://isnra.net/index.php/kjps**
E-mail: **kjps@uoalkitab.edu.iq**

Editorial Board

Aims and Scope

The aim of Al-Kitab Journal for Pure Sciences is to provide an international forum for the publication and dissemination of original work that contributes to the understanding of the principal and related disciplines of science. Al-Kitab Journal for Pure Sciences publishes two peer-reviewed issues per year, an online and print journal, which publishes innovative research papers, literature reviews, and technical notes on the fields of Biology, Computer Sciences, Chemistry, Physics, and Mathematics.

Authors Guidelines

Rules and Instructions for Publication in Al-Kitab Journal for Pure Sciences

First: General requirements

1. The paper is submitted to the Editorial Secretariat directly in four copies with CD-ROM or E-mail of the magazine in MS Word and PDF files.
2. Research before being sent to scientific evaluators is subject to the quotation Turnitin program.
3. Research shall be accepted for publication after being judged by scientific evaluators and according to the rules.
4. The publication fee is (50$) for researchers from Iraqi Universities and (free of charge) for foreign researchers.

Second: To prepare research for publication, authors must follow the following procedures.

1. **The article:**

   The article needs to be typed on one side of A4 paper (Right margin =2.5 cm, left margin =2.5 cm, and 2cm for the top and bottom) with 1.5 space, and the pages must be numbered.

2. **The content organization:**

   MS Word is to be used as follows: "Simplified Arabic" font for the Arabic articles, and "Times New Roman" for the English articles. The Size of the title is 18 bold. The names of the authors will be typed in 11 bold in Arabic and 11 bold in English. Abbreviations, keywords, the main headings, the reference, and the acknowledgment will be typed in 14. Subheadings will be in 12 bold. The abstract will be size 12. The body of the article/paper is in size 12. The order of the paper's content will be as follows:

The article heading, the names of authors and their addresses, and the abstract (Both in Arabic and English).

3. **Research paper title:**

The title must be as short as possible and indicates the contents of the subject together with the name (names) of the authors. The names of the authors to whom correspondence is to be made should be indicated with (*) and show his / her email.

4. **The size:**

The paper should contain no more than 15 pages of journal pages including charts and diagrams. Extra pages will be charged at (3$) each.

5. **Abstract:**

The abstract should include the purpose and the means of the founding results and the conclusions. It should also contain the knowledge values of the subject of research. It is meant to be no more than 250 words. It should also emphasize the content of the subject and include the keywords used throughout the paper.

6. **Diagrams:**

Figures and diagrams must be given following the explanation referring to the diagram. Each diagram must contain its title below the diagram at the first size of 12. The diagram should be editable in terms of enlargement or reduction within the margins of the paper size. The parts of each diagram must be grouped into drawing parts.

7. **Tables:**

The tables should follow the parts of the main body and should be located below the indicated part of the text. Tables must have titles with a text size of 12. The text used inside the tables should be of size 12 and kept within the cells of the table.

8. **References:**

The references used in the paper must be given in order and their numbers given inside the square bracket **[ ]**. The following instructions are to be followed:

If the reference is a book, the First name of the reference must be given first followed by the other names. Then the title (bold and Italic) of the book, edition, year of publication, the publisher, and place of publication (year of publication).

Example: **[1]** P. Ring and P. Schuck, "**The Nuclear Many-Body Problem**", First Edition, Springer-Verlag, New York (1980).

(b) If the reference is a research paper or an article in a journal: The name of the author must be given first, the title of the article, the name of the journal, the volume (issue), page (Year). **Example:** **[1]** Ali H. Taqi, R. A. Radhi, and Adil M. Hussein,

"Electroexcitation of Low-lying Particle-Hole RPA States of ^{16}O with WBP Interaction", Communication

Theoretical Physics, 62(6), 839 (2014).

c) If the reference is an M.Sc. or Ph.D. thesis, the name of the anther must be written with the first name first followed by the surname, title of the thesis, the name of the university, and Country (Year).

Example: [1] R. A. Radhi, **"Calculations of Elastic and Inelastic Electron Scattering in Light Nuclei with Shell-Model Wave Functions**", Ph.D. Thesis, Michigan State University, USA (1983).

(d) If the reference is from the conference. Authors Name, "**Paper Title**", Conference, Country, Publisher, volume, page (Year).

Example: [1] Ali H. Taqi and Sarah S. Darwesh, **"Charge-Changing Particle-Hole Excitation of ^{16}N and ^{16}F Nuclei"**, 3rdInternational Advances in Applied Physics and Materials Science Congress, Turkey, AIP Conf. Proc., 1569, 27 (2013)

Third: Privacy Statement

1. The names and e-mail addresses entered into the journal's website will be used exclusively for the purposes stated in this journal and will not be provided for any other purpose or to any other party.
2. The editor of the journal has the right to change any statement or phrase of the research content he may find necessary in order to express the work suitable to the general style of the journal.
3. After publishing the paper and its presentation on the journal page, the editors' team will destroy all the scrap papers. The author has no right to ask for them in any case.

Fourth: Modernity of sources:

The percentage of modern references used in the research should not be less than 50% of the total references used in the research. Modernity is measured within the last ten years of the year of submission of the research. For example, when submitting the research in 2018, the references should be from 2008 upwards and not less than 50%. The journal prefers to have at least one of the reference types of research published in the previous journal issues.

Note: For more information, visit:

Al-Kitab University Website: www.uoalkitab.edu.iq

Or Journal Website: https://isnra.net/index.php/kjps

The Journal can also be e-mailed to kjps@uoalkitab.edu.iq

Table of Contents

Volume: 8 Issue: 1 June 2024

Al-Kitab Journal for Pure Sciences (2024); 8(1):1-9.
https://doi.org/10.32441/kjps.08.01.p1

Al-Kitab Journal for Pure Sciences
ISSN: 2617-1260 (print), 2617-8141(online)

https://isnra.net/index.php/kjps

Detection of Hematological Correlations of People Lived at Al-Ahdab Oil Field in Al-Kut City, Iraq

Eman A. Muhsin[*1], Afrah F. Abdulkareem[2] , Shahrazad A. Khalaf [3]

[1] Ministry of science and technology, Baghdad, Iraq
[2] Microbiology Department, College of Science, Mustansiriyah University, Baghdad, Iraq
[3] Biotechnology Department, College of Science, Diyala University, Diyala, Iraq

*Corresponding Author: eman2014bio@gmail.com

Citation: Muhsin EA, Abdulkareem AF, Khalaf SA. Detection of Hematological Correlations of People Lived at Al-Ahdab Oil Field in Al-Kut City, Iraq. Al-Kitab J. Pure Sci. [Internet]. 2024 Jan 13 [cited 2024 Jan 13];8(1):1-9. Available from: https://doi.org/10.32441/kjps.08.01.p1.

Keywords: Renal function, Hb, CRP, Wassit.

Article History
Received 04 Oct. 2023
Accepted 25 Dec. 2023
Available online 13 Jan. 2024

Abstract:

This study was done in Wassit province, Al-Kut city in December 2023. Two groups were selected in this study: the first one consists of 25 people who have lived near the Al-Ahdab oil field, while the second one consists of controls with no significant difference in age between them and of both genders. This study aims to detect the influence of environmental pollution on the measured parameters of the blood (Urea, Creatinine, Hb, PCV, and CRP) with the presence of a significant relation among them. The results indicate that there is a highly significant relationship between Urea and creatinine and between Hb and PCV in both study groups. There is also a significant correlation between Urea and both Hb and PCV in the exposed group. While it was a significant correlation between Urea and CRP was detected in the control group only.

Keywords: Renal function, Hb, CRP, Wassit.

الكشف عن علاقات المؤشرات الدموية للأشخاص الذين يعيشون في حقل الأحدب النفطي في مدينة الكوت، العراق

إيمان عباس محسن[1]*, أفراح فهد عبدالكريم[2]، شهرزاد أحمد خلف[3]

eman2014bio@gmail.com, aalfahad17@uomustansiriyah.edu.iq, ShahrazadAh.Kh@uodiyala.edu.iq

[1]وزارة العلوم والتكنولوجيا العراقية، دائرة البيئة والمياه والطاقات المتجددة، بغداد، العراق
[2] قسم الأحياء المجهرية، كلية العلوم، الجامعة المستنصرية، بغداد، العراق
[3] قسم التقانة الإحيائية، كلية العلوم، جامعة ديالى، ديالى، العراق

إيميل الباحث الرئيس eman2014bio@gmail.com

الخلاصة:

أجريت هذه الدراسة في محافظة واسط، مدينة الكوت في كانون الأول ٢٠٢٣. تم اختيار مجموعتين في هذه الدراسة: الأولى تتكون من ٢٥ شخصا يسكنون بالقرب من حقل الأحدب النفطي، بينما تتكون المجموعة الثانية من افراد مجموعة السيطرة ولا يوجد فرق كبير في العمر بينهم وبين كلا الجنسين. تهدف هذه الدراسة إلى الكشف عن تأثير التلوث البيئي على مؤشرات الدم المقاسة (اليوريا، الكرياتينين، *Hb*، *PCV*، و*CRP*) مع وجود علاقة معنوية فيما بينها. تشير النتائج إلى وجود علاقة ذات دلالة إحصائية كبيرة بين اليوريا والكرياتينين وبين *Hb* و*PCV* في كلا المجموعتين. كما أنه يوجد ارتباط كبير بين اليوريا وكل من *Hb* و*PCV* في المجموعة قيد الدراسة. في حين أنه تم الكشف عن وجود ارتباط كبير بين اليوريا و*CRP* في المجموعة الضابطة فقط.

الكلمات المفتاحية: وظيفة الكلى، Hb، CRP، واسط.

1. Introduction:

Iraq has suffered in recent periods of wars and the introduction of various pollutants in large quantities to the ecosystem and thus arrived at the man either directly or cumulatively or through food and water, air and soil and then suffering from disease never encountered, in the forefront of their cancer and respiratory diseases, in the modern era **[1]**. Some scientific studies have reported that the city of Kut was one of the cities exposed to radiation in 2003, as mentioned by UN reports about the environment in the United Nations Environmental Programs (UNEP) and WHO **[2]**. Air pollution has long been thought to exacerbate minor acute illnesses, recent studies have suggested that air pollution, particularly hydrocarbon-related pollution, is associated with high levels of mortality and the development of certain disorders in areas where particle concentrations have fallen **[3]**. Although many of these associations seem likely to be causal, others require and warrant additional investigation because although the role of air pollution in

exacerbating existing illness has been well established, recent evidence has implicated pollution exposure with the development of chronic disease or impairments [4]. For several decades, studies tended to determine the relationship of biological indicators and hydrocarbon environmental contaminants, previous studies have highlighted natural emission exposure (environmental) or in other areas such as industry and medicine [5]. In general, the effect was strongly associated with immune system disorders and more mixed results have been reported mainly in the levels of some blood components. It was discovered that exposure to environmental pollutants has a toxic effect on the immune system and its effect on the vitality and functions of immune cells, rendering the intact human cells into cancerous ones [6]. Several proteins and biomarkers were measured for the efficient work of the kidneys where the structural change of the nephron (functional and structural unit of the kidney) by taking an autopsy. The same procedure was done by taking samples of renal biopsy from some people within the scope of exposure showed that several histological changes of renal cells even in the absence of a direct cause of the emergence of kidney damage; but when exposed to constant increase, the chance the continued evolution of this damage [7]. This study aimed to measure some blood factors in both groups (study and control group) and find the interactions between factors measured in terms of the correlated effects among all factors.

2. Materials and methods:

The systematic execution of the research included the following steps:

1) The creation of scientific and material supplies: the creation of laboratory supplies for the withdrawal of blood and look at the scientific sources, considering that the city of Kut from cities exposed to radiation in 2003, and recorded a high rate of environmental pollution by sources [2,8]

2) Collection of blood samples from people in the surrounding areas Ahdab oil field (residents and staff) and filling in the questionnaires, and people living in areas far from Kut as a control group.

The samples were collected from the people near the Al-Ahdab area and people far from the city of Kut and considered as a control group. Sera were separated from blood samples and then frozen until use [9]. The levels of urea, creatinine, and C-reactive protein were measured. Blood hemoglobin ratio and packed cell volume were also applied (all were done according to the manufacturing companies' instructions). These tests reveal the performance of the kidneys and the nature of the blood and immune components in each of the exposed people and the control group for comparison.

3. Statistical analysis:

The results were analyzed statistically by SPSS ver. 17 using Chi-square for the parameter within the same category, and T-Test in parameters comparison between two categories.

4. Results and discussion:

As seen in **Tables 1** and **2**, the results show that a significant relation was recorded between urea and creatinine in both the exposed and control groups. Also, a significant correlation was detected between each of the hemoglobin and packed cell volume in both groups. There was no significant difference between age and smoking in both groups.

Table 1: Correlations of parameters in the exposed group

		Urea	Creatinine	Hb	PCV	CRP	Age
Urea	Pearson Correlation	1	.608**	.406*	.408*	-.104-	.131
	Sig. (2-tailed)		.001	.044	.043	.622	.532
	N	25	25	25	25	25	25
Creatinine	Pearson Correlation	.608**	1	.344	.344	-.014-	-.060-
	Sig. (2-tailed)	.001		.092	.093	.948	.777
	N	25	25	25	25	25	25
Hb	Pearson Correlation	.406*	.344	1	1.000**	.341	.356
	Sig. (2-tailed)	.044	.092		.000	.096	.081
	N	25	25	25	25	25	25
PCV	Pearson Correlation	.408*	.344	1.000**	1	.336	.358
	Sig. (2-tailed)	.043	.093	.000		.101	.079
	N	25	25	25	25	25	25
CRP	Pearson Correlation	-.104-	-.014-	.341	.336	1	.099
	Sig. (2-tailed)	.622	.948	.096	.101		.636
	N	25	25	25	25	25	25
Age	Pearson Correlation	.131	-.060-	.356	.358	.099	1
	Sig. (2-tailed)	.532	.777	.081	.079	.636	
	N	25	25	25	25	25	25

**. Correlation is significant at the 0.01 level (2-tailed).

*. Correlation is significant at the 0.05 level (2-tailed).

The relation between urea and creatinine indicates the linear relationship between these two indicators of renal function. In the exposed group, there was a rise in urea accompanied by a rise in creatinine where they are affected together in the same pattern. There were natural values of urea and creatinine in the healthy range, and this demonstrates the safety of renal function **[10,11]**. These results coincided with the results of each of **[12.13]**on renal function assessment

and the role of each of urea and creatinine in the credibility of the measure, as reflected in turn damage caused in the nephron, the structural and functional unit of the kidney, by its two parts: glomeruli and tubule [7]. These recordings agreed with [14] and [15].

Table (2): Correlations of parameters in the control group

		Urea	Creatinine	Hb	PCV	CRP	Age
Urea	Pearson Correlation	1	-.476-*	.022	.024	-.490-*	-.025-
	Sig. (2-tailed)		.016	.917	.911	.013	.906
	N	25	25	25	25	25	25
Creatinine	Pearson Correlation	-.476-*	1	.318	.315	.189	-.022-
	Sig. (2-tailed)	.016		.121	.125	.365	.917
	N	25	25	25	25	25	25
Hb	Pearson Correlation	.022	.318	1	1.000**	-.183-	.097
	Sig. (2-tailed)	.917	.121		.000	.381	.645
	N	25	25	25	25	25	25
PCV	Pearson Correlation	.024	.315	1.000**	1	-.186-	.099
	Sig. (2-tailed)	.911	.125	.000		.372	.636
	N	25	25	25	25	25	25
CRP	Pearson Correlation	-.490-*	.189	-.183-	-.186-	1	.029
	Sig. (2-tailed)	.013	.365	.381	.372		.889
	N	25	25	25	25	25	25
Age	Pearson Correlation	-.025-	-.022-	.097	.099	.029	1
	Sig. (2-tailed)	.906	.917	.645	.636	.889	
	N	25	25	25	25	25	25

*. Correlation is significant at the 0.05 level (2-tailed).

**. Correlation is significant at the 0.01 level (2-tailed).

Urea is one of the important tests to assess renal function as it has a standard rise in many cases, including factors related to the kidney and its performance, or other factors that are not directly related to it such as the nature of food and metabolism of proteins, drought and lack of fluid intake. The rise in urea level reflects the state of the kidneys and the possibility of being affected negatively by certain stimuli in the urinary system hindering his performance properly [16]. Creatinine is deemed to be the most honest cursor in the expression of the efficiency of renal function because it is not affected by the nature of the food, or metabolism and because it raises through the kidney only and not through other outlets such as skin and intestine like urea,

so the height is a clear indication of a defect in renal function and effect and evolve it to real renal disease **[17]**.

Numerous studies have found that these percentages have increased with time or dose exposure to environmental pollutants, as gene expression of the components of the blood increases excessively so the body will consider it as an inflammatory state **[18]**. Hemoglobin levels are associated with the packed cell volume of red blood cells in both groups. Because hemoglobin is a certain size of the red blood cells, it means that the change in the total size of the cells will be affected by a parallel pattern and there will be a regular effect on hemoglobin, and the relationship between these two variables would be according to the following equation (equation.1) as mentioned by Connor *et al.* (1994) as it is simple and scientifically supported method **[19]**: **Hb (g/dl)+PCV(L/L)/3**.

The hemoglobin rose steadily as in the study of Hemoglobin and hematocrit values are age-dependent **[3]**. The strong relationship recorded only in the exposed group is the urea relationship with both hemoglobin and packed cell volume. According to the equation above, the effect of urea with both variables is linked by the fixed pattern with both hemoglobin and packed cell volume. When urea rises will cause an increase "in blood pressure and this refers to the injury shocked size (increase in size is controlled by the body) as in cases of deterioration of renal function itself. **[20,21]**. The style of life and inhalation of toxic materials and gases, affected by the ecosystem and the kind of food, will lead to genetic mutations and overproduction of blood cells after free radicals' formation **[22]**.

Finally, a significant relationship was recorded between urea and C-reactive protein in the control group. That can be explained by the relationship between these two variables is that the urea is produced by the liver which also produces a protein called C-reactive protein **[18]**. This last one has a natural level in the blood and so as long as the function of the liver is intact, the production of these two hematological will be less than the allowable limit, without any effect or infection **[22]**. While this relation was not detected in the exposed group due to non-intact healthy function, agreed with **[13]**.

Increased human exposure to pollutants leads to an imbalance in the proportions of blood components in humans according to potions and exposure time **[1,23]**. A mechanism was suggested to give a certain explanation, about blood components that are not within normal limits, which is an irregular and frequent production of proteins and cellular secretions by recurrent exposure to toxic materials or pollutants. So, recurrent exposure to emitted airborne particulate matter (PM) and gaseous pollutants leads the body to suffer an inflammatory or infectious case which results in a wide range of health hazardous problems, including

respiratory and cardiovascular diseases [5]. Other factors, like poor diet, low exercise, underlying diseases, and individual diversity of human genes, may worsen the effects of air pollution and bring on adverse chronic organ pathology [24].

5. Conclusions:

1) The presence of a high-significant correlation between renal function parameters (urea, creatinine) as well as blood indicators (hemoglobin and PCV) in the exposed group and the control group.

2) There was a significant relationship between urea and the level of each of the hemoglobin and the PCV in the exposed group.

3) There was a significant relationship between urea and C-reactive protein in the control group.

6. Recommendations:

Periodic hematological and genetic tests should be performed particularly for people who live near oil fields or workers in industry and energy generation fields.

7. REFERENCES

[1]Bortman M. Environmental encyclopedia. 1, A - M. Detroit: Gale; 2003.

[2]Kapita's Research team. Climate Change Overview: Impacts, Mitigation, and Adaptation in Iraq. A booklet. © KAPITA. 2022. pp 38-41.

[3]Ramsy G, Rusi M. Biological Individuality: A book. Chapter 1. In: McConwell AK, editor. 1st edition. USA: Alison K. McConwell; 2023. p. 26-29. DOI: 10.1017/9781108942775

[4]Hegerl G. Climate change is physics. Communications Earth & Environment. 2022;3:14. https://doi.org/10.1038/s43247-022-00342-8, www.nature.com/commsen

[5]Gurjar B, Molina L, Ojha C. Air pollution. A book. Chapter 7. In: CRC Press, editor. 1st edition. India: CRC Press; 2010. p. 203.

[6]Yu P, Xu R, et al. Cancer and Ongoing Climate Change: Who Are the Most Affected. ACS Environ. 2023;3:5−11.

[7]Ho Yu M. Environmental toxicology. A book. Chapter 2. In: CRC Press, editor. 2nd edition. India: CRC Press; 2005. p. 15-16.

[8]Ahmed W, Abed T, et al. Environmental impact of using generators in the University of Technology in Baghdad, Iraq. J Thermal Eng. 2020;6:6. pp. 272-281.

[9]Polnay L, Hampshire M, Lakhanpaul M. Manual of pediatrics, an integrated approach. 1st ed. China: Churchill Livingstone Elsevier; 2006. p. 14-16.

[10] Landrigan P, Fuller R, Acosta J, et al. The Lancet Commission on pollution and health. The Lancet. 2018;391:10119. pp:462-512.

[11] Hartley A, Tandon A. The impacts of climate changes. Frontiersin.org. 2022;716479:10:1-6.

[12] Babayemi JO, Ogundiran MB, Osibanjo O. Overview of environmental hazards and health effects of pollution in developing countries: a case study of Nigeria. Environ Qual Manage. 2016;26:1. Pp: 51-71.

[13] Tosun J. Addressing climate change through climate action. Climate Action. 2022;1:1. pp1-8. https://doi.org/10.1007/s44168-022-00003-8

[14] Ubong I, Osaghae O. Investigation and evaluation of health hazards associated with smoke emissions from the proliferation of generators in Port Harcourt Metropolis. Int J Dev Sustain. 2018;7:5. Pp: 1654-1675.

[15] Jiang SY, Ma A, Ramachandran S. Negative air ions and their effects on human health and air quality improvement. Int J Mol Sci. 2018;19:10. Pp: 2966.

[16] Santos O, Melly P, et al. Climate Change, Environmental Health, and Challenges for Nursing Discipline. Int J Environ Res Public Health. 2023;20:5682. https://doi.org/10.3390/ijerph20095682

[17] Jan C, Semenza R, et al. Climate Change and Cascading Risks from Infectious Disease. Infect Dis Ther. 2022;11:1371–1390. https://doi.org/10.1007/s40121-022-00647-3

[18] Luschkova D, Traidl-Hoffmann C, Ludwig A. Climate change and allergies. A review. Allergo J Int. Springer. https://doi.org/10.1007/s40629-022-00212-x

[19] Connor G, Molloy A, Daly L, Scott J. Deriving useful packed cell volume estimation from hemoglobin analysis. J Clin Pathol. 1994;47(1):78-79.

[20] Macedo J. Climate change: a bioethical emergency and health priority. The Author(s). Published by Elsevier Masson SAS. 2023. https://doi.org/10.1016/j.jemep.2023.100872

[21] Rahman M, Arafa A, Ali Md, Ali S. Immunogenetics: A Molecular and Clinical Overview. A book. Chapter 1. In: Academic press and Elsevier, editor. 1st edition. UK: Academic press and Elsevier; 2022. p: 30. ISBN: 978-0-323-90053-9.

[22] Remadevi O, Kumar V, Singh R. Biodiversity, ecosystem services and climate change biodiversity, ecosystem services and climate change. A book. Chapter 1. In: Environmental Management and Policy Research Institute, editor. Bangalore. India: Environmental Management and Policy Research Institute; 2022. p: 119.

[23] Hammadi A, Idress M, Hussain B. Evaluation and Assessment of Generated Greenhouse Gases Produced from Collection and Disposal of Municipal Solid Wastes in Baghdad. MEIJSS. 2021;3:3. pp:175-183. e-ISSN: 2682-8766.

[24] Fakinle BS, Okedere OB, Adebanjo SA, Adesanmi AJ, Sonibare JA. Air quality impact of carbon monoxide emission from diesel engine electric power generators. Environ Qual Manage. 2019;28:3. pp: 97-102.

Al-Kitab Journal for Pure Sciences (2024); 8(1):10-18.
https://doi.org/10.32441/kjps.08.01.p2

Al-Kitab Journal for Pure Sciences
ISSN: 2617-1260 (print), 2617-8141(online)
https://isnra.net/index.php/kjps

Sensitivity of some types of Gr+ and Gr- bacteria to some types of commercial soaps

Mahmood A. Al-Toobjee, Fulla Q. Yahya, Ashwaq H. Najem*

Department of Biology, College of Science, University of Mosul.

*Corresponding Author: ashsbio102@uomosul.edu.iq

Citation: Al-Toobjee MA, Yahya FQ, Najem AH. Sensitivity of some types of Gr+ and Gr- bacteria to some types of commercial soaps. Al-Kitab J. Pure Sci. [Internet]. 2024 Jan 13 [cited 2024 Jan 13];8(1):10-18. Available from: https://doi.org/10.32441/kjps.08.01.p2.

Keywords: sensitivity test, detergent, gram-positive bacteria, gram-negative bacteria, antibacterial agents.

Article History

Received	12	Oct.	2023
Accepted	19	Dec.	2023
Available online	13	Jan.	2024

Abstract:

The use of soap is one of the most important means of ionic cleansing and getting rid of some types of bacteria that may be harmful and present on the skin, especially after using the toilet, as part of them may remain on the surface of the skin, causing some pathological injuries, and the ability of soap to remove or eliminate these germs varies according to the soap type and the period of its use in washing, the study aimed to determine the ability of some types of liquid soap to eliminate different types of Gram-positive and gram-negative bacteria.

The plate method was used to find out the sensitivity of each of the types of bacteria(Klebsiella, E.coli Staph aureus, Pseudomonas, Streptococcus,) towards types of liquid soaps produced by international companies, including Bivy, Dettol, ActiveX, Lifebuoy, Oud, using the tablet method, and it was determined The minimum inhibitory concentration for each type of liquid soap (depending on the bacterial species used). Klebsiella E.coli showed high sensitivity to Dettol soap, while Pseudomonas and Staph aureus bacteria showed high sensitivity to Bivy soap. Streptococcus bacteria appeared to be highly sensitive to Lifebuoy soap, and the sensitivity of bacterial species to the rest of the soaps varied between medium and weak.

Keywords: sensitivity test, detergent, gram-positive bacteria, gram-negative bacteria, antibacterial agents.

حساسية بعض أنواع البكتريا الموجبة والسالبة لصبغة كرام تجاه أنواع من الصوابين التجارية

محمود عبد الجبار الطوبجي، فلة قيدار محمد يحيى، أشواق حازم نجم*

قسم الأحياء، كلية العلوم، جامعة الموصل، العراق

mahtsbio30@uomosul.edu.iq, Fulla.Kaydar@uomosul.edu.iq, ashsbio102@uomosul.edu.iq

الخلاصة:

يعد استخدام الصابون من اهم الوسائل للتطهير الأيوني والتخلص من بعض أنواع البكتريا التي قد تكون ضارة والمتواجدة على الجلد وخاصة بعد استخدام التواليت إذ قد يتبقى جزء منها على سطح الجلد مما يسبب بعض الإصابات المرضية، وتختلف قدرة الصابون على إزالة تلك الجراثيم أو القضاء عليها حسب نوع الصابون وفترة استخدامه بالغسل، هدفت الدراسة الى تحديد قدرة بعض أنواع الصابون السائل على القضاء على أنواع مختلفة من البكتريا الموجبة والسالبة لصبغة كرام.

تم استخدام طريقة الأطباق لغرض إيجاد حساسية كل من أنواع البكتريا *Staph aureus, E.coli , Klebsiella Pseudomonas, Streptococcus*, تجاه أنواع من الصوابين المنتجة السائلة من شركات عالمية ضمت *Bivy, Dettol, Activex, Lifebuoy, Oud*. وذلك باستخدام طريقة الأقراص، وتم تحديد التركيز المثبط الأدنى لكل نوع من الصوابين السائلة (على الأنواع البكتيرية المستخدمة). وظهرت كل من بكتريا *E.coli Klebsiella*, بحساسية عالية تجاه صابون *Dettol* في حين ظهرت بكتريا *Pseudomonas, Staph aureus* بحساسية عالية تجاه صابون *Bivy* ظهرت بكتريا *Streptococcus* بحساسية عالية تجاه صابون *Lifebuoy* ، وكانت حساسية الأنواع البكتيرية لباقي أنواع الصوابين متفاوتة بين متوسطة وضعيفة.

الكلمات المفتاحية: اختبار الحساسية، مطهر، البكتريا الموجبة لصبغة كرام، البكتريا السالبة لصبغة كرام، العوامل المضادة للبكتيريا.

1. Introduction:

As the body's initial line of defense, skin contains most of the bacteria that cause skin infections, including Pseudomonas aeruginosa and Staphylococcus aureus. According to health care professionals, hand washing with antibacterial soap is particularly crucial since it may be the primary source of bacterial contamination from infections or opportunistic germs. **[1-2]**. Staphylococcus aureus and other gram-negative bacterial species cause pyogenic skin infections, and soaps include active chemicals that are both antibacterial and have reducing action. **[3]**. According to studies, antibacterial soap removes bacteria more effectively than regular soap **[4]**. There is a wide variety of chemicals that may kill germs and prevent their development. There may be as many as 10,000 different compounds, with just around 1,000 of them seeing regular usage in healthcare facilities and private residences. All three of those states

are possible for these chemical substances. There are several classes of compounds used to kill or inhibit microorganisms.

When it comes to stopping the spread of disease, few things have been as useful as detergents, which are chemicals with both lipophilic and hydrophilic components that can kill or inhibit the growth of microorganisms on inanimate objects. Soap is a chemical molecule formed when fatty acids, oils, and salt mix **[5, 6]**. Soap, liquid hand-wash, detergent, etc. are only a few examples of the many cleaning chemicals that have been in use for centuries all around us. For decades, antibacterial soaps have been helping people keep their hygiene in check. Some antibacterial soaps can eradicate as much as 85% of germs from the skin with a single use. **[7]**. It was recommended in a 1961 report by the U.S. Public Health Service that Before and after having contact with customers, staff members spend one to two minutes using soap and water. When it comes to healthcare providers, hand hygiene is of the utmost importance because of the prevalence of harmful and opportunistic microorganisms in the workplace **[8]**.

Products with antimicrobial components are referred to as "antiseptics" because of their ability to prevent the spread of bacteria and other pathogens. Antimicrobials are available without a prescription and fall under this category. Their usefulness and safety are legal in the United States according to the Food and Drug Administration. Antibacterial soaps, hand washes, body washes, sanitizers, surface sprays, and mouthwashes are only some of the consumer antiseptic medication items available in stores today **[9]**. Chloroxylenol, triclosan, and triclocarban are some of the active components in these products, and the US Food and Drug Administration **[10]** names them as active ingredients in over-the-counter antiseptics, but further study is required to confirm their safety and effectiveness. Antiseptic body washes and other consumer antiseptic products get heavy daily use **[11]**. That's why it's so important to track how well this product works so we can keep an eye out for any signs of a resistance pattern developing over time. **[11]**. Soaps containing antimicrobial compounds are another option, although those without are the most common. Medicated soaps feature antimicrobial chemicals in addition to the soap base **[12]**. Microorganisms may be found almost anywhere in the air, water, soil, and rock, as well as in plants, animals, and people **[13]**, and they play an essential role in maintaining human health **[14]**. Bacteria from the environment, both Gram-positive and --negative, may cause skin infections when they settle on the skin's surface **[17]**.

2. Material and methods :

The work was done in the Department of Biology College of Science University of Mosul and used the disc method to process different soaps to types of bacteria **[15]**.

1 -Sample Collection: Five types of liquid soap have been prepared from different international origins available in the local markets, namely Dettol soap, Activex, Lifebuoy, Bivy, and Oud. Use the double dilution method by taking 1 ml of liquid soap and adding 9 ml of distilled water. Several concentrations: 1/2, 1/4, 1/8, 1/16, 1/32. it was sterilized in a water bath at 80°C for 1/2 hour.

2 -Bacterial use: The bacterial used were obtained from postgraduate students in the department and were previously diagnosed and included E.coli, Klebsiella sp, Pseudomonas sp, Staph aureus, Streptococcus sp was isolated on Nutrient agar (N.a).

3 -Paper discs: Prepared from What Man No. 1 filter paper, 100 tablets were dispensed into a vial and sterilized in an autoclave at 121 and 15 degrees for 15 minutes, then 10 ml of the prepared dilution of liquid soap was added so that each tablet was saturated with 100 µl. They were sterilized by pasteurization in a water bath at 80°C for half an hour.

4 -Bacterial activity: Bacteria were cultured on a Nutrient agar medium. Distribute the bacteria evenly on the plate by swab. The tablets saturated with soap were placed in the dish at equal and appropriate distances and incubated at 37 °C for 24 hours and then read by measuring the inhibition zone. Each experiment was repeated three times.

3.Results and discussion:

The effect of liquid soaps of international origin was tested on five species of bacteria, including Gr+ and Gr-, and the preliminary results were shown in the following table.

Table 1: Inhibitory effect of liquid soaps on gram-positive and negative bacteria

Bacteria type	Oud/mm	Bivy/mm	Lifebuoy/mm	Activex/mm	Dettol/mm
E.coli	15	17	25	21	23
Klebsiella sp.	14	13	17	14	19
Pseudomonas sp	23	40	30	18	32
Staph aureus	20	27	25	14	24
Streptococcus sp.	15	11	29	22	22

The results showed an inhibitory effect of (Dettol) liquid soap at a concentration of 1/2 on each of (E.coli, Klebsiella sp, Pseudomonas sp, Staph aureus, Streptococcus sp) Inhibitory diameters amounted to 23 mm, 19 mm, 32 mm, 24 mm, and 22 mm, respectively; the highest effect was on the bacteria Pseudomonas. The effect of (Activex) soap appeared at a concentration of 1/2 to highly inhibit specially Streptococcus in diameter 22 mm Also, the results showed an inhibitory effect of (Lifebuoy) liquid soap at a concentration of 1/2 on bacteria,(E.coli, Klebsiella sp, Pseudomonas sp, Staph aureus, Streptococcus sp) Inhibitory

diameters amounted to 25mm,17mm, 30mm, 25mm, 29mm respectively, the highest effect was on bacteria Pseudomonas.

Also, Pseudomonas bacteria were highly sensitive to each of Bivy and Oud soap, with inhibition diameters of 40 mm and 23 mm, respectively, while type of the bacteria showed lower inhibition diameters from both types of soap.

Table 2: the minimum inhibitory concentration of E.coli bacteria for the types of soaps used Dilutions.

Soap type	Dilutions/mm				
	1\2	1\4	1\8	1\16	1\23
Dettol	23	21	18	16	-
Activex	21	18	13	11	-
Lifebuoy	25	19	9	7	-
Bivy	17	12	8	-	-
Oud	15	10	8	-	-

When tested on E. coli bacteria, the MIC for Dettol soap was at a dilution of 1/32, whereas the MICs for Activex and Lifebuoy soap were at a dilution of 1/16. Bivy and Oud soaps showed a MIC against E. coli at a dilution of 1/8. These results show that the effect of Dettol soap was higher than other types of soaps on E.coli bacteria, followed by Activex and Lifebuoy soaps, while the effect of Bivy and Oud was less on the same bacteria.

Table 3: the minimum inhibitory concentration of Klebsiella sp bacteria for the types of soaps used.

Soap type	Dilutions /mm				
	1\2	1\4	1\8	1\16	1\23
Dettol	19	6	-	-	-
Activex	14	9	7	-	-
Lifebuoy	17	16	11	-	-
Bivy	13	9	-	-	-
Oud	14	13	7	-	-

The Klebsiella bacteria appeared with a high resistance to the most used types of soap, as the Mic appeared to Dettol soap at a dilution of 1/4, while the MIC of actives soap appeared at a dilution of 1/8, and the MIC of Lifebuoy soap appeared at a dilution of 1/8. Likewise, the MIC of Bivysoap appeared on Klebsiella sp at a dilution of 1/4, while the MIC of Oud soap appeared at a dilution of 1/8.

Table 4: the minimum inhibitory concentration (MIC) of Pseudomonas sp for the types of soaps used.

Soap type	Dilutions/mm				
	1\2	1\4	1\8	1\16	1\23
Dettol	23	16	14	12	-
Activex	18	20	18	15	12
Lifebuoy	30	18	15	12	18
Bivy	40	10	8	7	-
Oud	23	15	10	8	-

Pseudomonas bacteria appeared with average sensitivity to the types of soaps used, as the mic appeared Dettol soap at a dilution of 1/16, while the MIC of Activex soap at a dilution of 1/32, and the MIC of Lifebuoy soap appeared at a dilution of 1/32. Likewise, the MIC of Bivy soap appeared on Pseudomonas sp at a 1/16 dilution, while the MIC of Oud soap appeared at a 1/16 dilution.

Table 5: the minimum inhibitory concentration (MIC) of Staph aureus bacteria for the types of soaps used.

Soap type	Dilutions /mm				
	1\2	1\4	1\8	1\16	1\23
Dettol	24	11	9	-	-
Activex	14	9	-	-	-
Lifebuoy	25	14	9	-	-
Bivy	27	10	-	-	-
Oud	20	14	11	-	-

The Staph aureus bacteria had more resistance to soap types than the while type of the bacteria, as the mic appeared Dettol soap on Staph aureus at a dilution of 1/8, while the MIC of Activex soap appeared at a dilution of 1/4, and the MIC of Lifebuoy soap at a dilution of 1/8. Likewise, the MIC of Bivy soap appeared on Staph aureus at a dilution of 1/4, while the MIC of Oud soap appeared at a dilution of 1/8.

Table (6) the minimum inhibitory concentration of Streptococcus sp. for the types of soaps used.

Soap type	Dilutions /mm				
	1\2	1\4	1\8	1\16	1\23
Dettol	22	16	12	8	-
Activex	22	-	-	-	-
Lifebuoy	29	20	15	15	11
Bivy	11	8	-	-	-
Oud	15	12	9	9	-

Our results in **Table (1)** agreed with the results of the scientist Ecor in 2018 **[16]** and the scientist Bashir in 2018 **[17]** on the effect of Dettol soap on different types of bacteria.

The results of **Table (2)** agreed with the results of the scientist Ishur T. In Nigeria in 2018 **[16]** and the scientist Bashir in Algeria in 2018 **[17]** and the scientist Abbas in Pakistan in 2016 **[18]** about the effect of Dettol soap on different types of bacteria, where the study concluded that according to our results, the width of the inhibitory zones increased with increasing amount or concentration of liquid soap applied. The above-mentioned inhibition diameters appeared with increasing concentration.

The results of **Table (3)** also agreed with the results of the scientist EcoR in 2018 **[16]** on the effect of Dettol soap on different types of bacteria, as the study concluded that the diameters of inhibition increase with the increase in the volume or concentration of the liquid soap added, and this is consistent with our results, as the diameters of inhibition appeared the above inhibition increases with increasing concentration .

The results of **Table (4)** are consistent with the results of the scientist Ecore T. In Nigeria in 2018 **[16]** and the scientist Bashir in Algeria in 2018 **[17]** about the effect of Dettol soap on different types of bacteria. Above with increasing concentration .

The results of **Table (5)** agreed with the results of the scientist Ecore T. In Nigeria in 2018 **[16]**, the scientist Bashir in Algeria in 2018 **[17]**, and the scientist Abbas in Pakistan in 2016 **[18]** about the effect of Dettol soap on different types of bacteria, where the study concluded that the diameters of inhibition increase with the increase in the volume or concentration of the added liquid soap. This is consistent with our results, as the inhibition diameters appeared higher with increasing concentration .

The results of **Table (6)** agreed with a study conducted by the scientist Ishur T. In Nigeria in 2018 **[16]**, scientist Bashir in Algeria in 2018 **[17]**, and scientist Abbas in Pakistan in 2016 **[18]** about the effect of Dettol soap and Lifebuoy soap on different types of bacteria. The diameters of inhibition are higher depending on the concentration, or proportionally to the amount of soap used the species Streptococcus showed high sensitivity to each of Oud, Life, and Dettol soaps, as the MIC appeared for each of them at a dilution of 1/32, while it appeared for the whole type of the soaps with an amount of 0 respectively .

4. CONCLUSION:

The ability of soap to remove or eliminate harmful bacteria varies depending on the type of soap and how long it is used for washing. Using soap is one of the most important ways to achieve ionic cleansing and get rid of some types of bacteria that may be present on the skin, especially after using the restroom. Some of these germs may remain on the skin's surface and

cause pathological injuries. the bacterial species used). Klebsiella E.coli showed high sensitivity to Dettol soap, while Pseudomonas and Staph aureus bacteria showed high sensitivity to Bivy soap. Streptococcus bacteria appeared to be highly sensitive to Lifebuoy soap, and the sensitivity of bacterial species to the rest of the soaps varied between medium and weak .

5. REFERENCES

[1] Stewart S, Robertson C, Pan J, Kennedy S, Dancer S, Haahr L, Manoukian S, Mason H, Kavanagh K, Cook B, Reilly J. Epidemiology of healthcare-associated infection reported from a hospital-wide incidence study: considerations for infection prevention and control planning. J Hosp Infect. 2021;114:10–22. https://doi.org/10.1016/j.jhin.2021.03.031.

[2] Higaki S, Kitagawa T, Kagoura M, Morohashi M, Yamagish T. Predominant Staphylococcus aureus isolated from various skin diseases. J Int Med. 2000;28:87-190.

[3] Baig FK, Mehboob R. Nosocomial infections: Epidemiology, prevention, control and surveillance. Asian Pac J Trop Biomed. 2017;7(5):478-82.

[4] Selvamohan T, Sandhya V. Studies on bactericidal activity of different soaps against bacterial strains. J Microbiol Biotech. 2012;2:646-650.

[5] Friedman M, Wolf R. Chemistry of soaps and detergents various types of commercial products and their ingredient. Clin Dermatol. 1996;14:7–13. https://doi.org/10.1016/0738-081X(95)00102-L.

[6] Ikegbunam A, Fiss EM, Rule KL, Vikesland PJ. Formation of chloroform and other chlorinated byproducts by chlorination of triclosan-containing antibacterial products. Environ Sci Technol. 2013;41(7):2387–94.

[7] Oladosu P, Isu NR, Ibrahim K, Okolo P, Oladepo DK. Time kill-kinetics antibacterial study of Acacia nilotica. Afr J Microbiol Res. 2013;7(46):5248–52. DOI: 10.5897/ISSN 1996-0808.

[8] Richards MJ, Edwards JE, Culver DH, Gaynes RP. Nosocomial infections in medical intensive care units in the United States. Crit Care Med. 1999;27:887–92. https://doi.org/10.1097/00003246-199905000-00020.

[9] Antibacterial cleaning products [Internet]. Betterhealth.vic.gov.au. 2020 [cited 2020 Apr 28]. Available from: https://www.betterhealth.vic.gov.au/health/conditionsandtreatments/antibacterial-cleaning-products.

[10] Antibacterial cleaning products [Internet]. Betterhealth.vic.gov.au. 2020 [cited 3 May 2020]. Available from: https://www.betterhealth.vic.gov.au/health/conditionsandtreatments/antibacterial-cleaning-products.

[11] Khairatul Ayyun Mohd Ramli, Siti Nur Balqis Shamsuri, Nur Najihah Mohd Raslam, Nurul Huda Nabilah Halim, Nursyafiqah Samad, Mohamad Saifullah Sulaiman and

Mohd Fahmi Mastuki. Efficacy of Consumer Antibacterial and Non-antibacterial Body Washes on Skin Normal Flora and Pathogen. Malays J Med Health Sci. 2020;eISSN 2636-9346.

[12] Ikegbunam MN, Metuh RC, Anagu LO, Awah NS. Antimicrobial activity of some cleaning products against selected bacteria. Int Res J Pharm Appl Sci. 2013;3:133-135.

[13] Singh SR, Krishnamurthy NB, Mathew BB. A review on recent diseases caused by microbes. J Appl Environ Microbiol. 2014;2(4):106-115.

[14] Johnson SA, Goddard PA, Iliffe C, Timmins B, Rickard AH, Robson G, Handley PS. Comparative susceptibility of resident and transient hand bacteria to para-chloro-meta-xylenol and triclosan. J Appl Microbiol. 2002;93(2):336-344.

[15] Oladosu PO, Umar YA, Salawudeen A, Izebe K, Adamu MT, Aboh M. Antibacterial Activity of Soaps Indigenously Made in Gombe Metropolis, Nigeria. J Nat Remedies. 2018. DOI: 10.18311/jnr/22434.

[16] Ichor T, Aondoakaa EM, Ebah EE. Comparative Studies on the Antibacterial Activity of Alcohol-Based Hand Sanitizers Against Bacteria Isolates from the Hands of Undergraduate Students of University of Agriculture, Makurdi. J Clin Case Rep. 2018;8:1143. doi: 10.4172/2165-7920.10001143.

[17] Bachir Raho Ghalem. Sch Int J Tradit Complement Med. 2018;Vol-1, Iss-1: 18-21.

[18] Abbas SZ, Hussain K, Hussain Z, Ali R, Abbas T. Antibacterial Activity of Different Soaps Available in Local Market of Rawalpindi (Pakistan) against Daily Encountered Bacteria. Pharm Anal Acta. 2016;7:522. doi:10.4172/2153-2435.1000522.

Al-Kitab Journal for Pure Sciences (2024); 8(1):19-28.
https://doi.org/10.32441/kjps.08.01.p3

Al-Kitab Journal for Pure Sciences
ISSN: 2617-1260 (print), 2617-8141(online)

https://isnra.net/index.php/kjps

The protective role of ascorbic acid on the testis tissue damage induced by paracetamol in albino rats

Eda M. Alshailabi[1*], Ola A. Abdalally[2], Fatimah A. Mohammed[1]

[1]Zoology Department, Omar Al-Mukhtar University, El Beida, Libya
[2]Almahara institute for the medical and managerial sciences

*Corresponding Author: eda.muftah@omu.edu.ly

Citation: Alshailabi EM, Abdalally OA, Mohammed FA. The protective role of ascorbic acid on the testis tissue damage induced by paracetamol in albino rats. Al-Kitab J. Pure Sci. [Internet]. 2024 Feb 03 [cited 2024 Feb 03];8(1):19-28. Available from: https://doi.org/10.32441/kjps.08.01.p3.

Keywords: Testis tissues, Ascorbic acid, Histopathology, Paracetamol, Rats.

Article History
Received 15 Nov. 2023
Accepted 13 Jan. 2024
Available online 03 Feb. 2024

Abstract:

Ascorbic acid (AA) plays roles in many biological functions, such as participating in the production of collagen by taking a role in proline and lysine hydroxylation. AA works by removing the reactive oxygen species, thus removing the adhesion of neutrophils to endothelium. The present study investigates the protective effects of AA on the testis tissue damage induced by paracetamol in rats. Thirty-two male rats were equally divided into four groups, with eight rats in each. Group (1) regular control group, group (2) was received 500 mg/kg/b.w. of AA orally for two weeks, group (3) was received 500 mg/kg/b.w. of paracetamol orally for two weeks, group (4) was treated with the AA (500 mg/kg/b.w.) and paracetamol (500 mg/kg/b.w.) orally for two weeks. The histopathological investigations of the testis tissues from the paracetamol group showed atrophy and degeneration of seminiferous tubules with an absence of spermatozoa, presence of cell debris, and loss of the Sertoli cells in some seminiferous tubules when compared with control animals. The testis tissues from a protective group showed less damage in the tubules and germ cells when compared with the paracetamol group. This study indicates that AA protects against paracetamol-induced testis damage in adult male rats.

Keywords: Testis tissues, Ascorbic acid, Histopathology, Paracetamol, Rats.

الدور الوقائي لحمض الأسكوربيك على تلف أنسجة الخصية الناجم عن الباراسيتامول في الجرذان البيضاء

عيدة مفتاح الشيلابي[1*]، علا علي عبدالعالي[2] ، فاطمة العماري محمد[1]

[1]قسم علم الحيوان، جامعة عمر المختار، البيضاء، ليبيا.
[2]المعهد اسمه معهد المهارة للعلوم الطبيه والإدارية.

eda.muftah@omu.edu.ly, olaolysweet@gmail.com, fatima.alamari@omu.edu.ly

الخلاصة:

يلعب حمض الأسكوربيك أدوارًا مهمة في العديد من الوظائف الحيوية مثل المشاركة في إنتاج الكولاجين من خلال لعب دور في هيدروكسيل البرولين والليسين. يعمل حمض الأسكوربيك على إزالة أنواع الأكسجين التفاعلية عن طريق النقل السريع للإلكترون في المرحلة المائية، وبالتالي تقليل التصاق العدلات بالبطانة. تبحث الدراسة الحالية في التأثيرات الوقائية لحمض الأسكوربيك على تلف أنسجة الخصية الناجم عن الباراسيتامول في الجرذان. تم تقسيم ٣٢ من ذكور الجرذان بشكل متساوي إلى أربع مجاميع كل منها يحتوي على ثمانية. المجموعة الأولى (المجموعة الضابطة)، المجموعة الثانية تلقت (٥٠٠ مجم / كجم من وزن الجسم) من حمض الأسكوربيك عن طريق الفم لمدة أسبوعين، المجموعة الثالثة تلقت (٥٠٠ مجم / كجم من وزن الجسم) من الباراسيتامول عن طريق الفم لمدة أسبوعين، أما المجموعة الرابعة فقد تلقت حمض الأسكوربيك (٥٠٠ مجم / كجم من وزن الجسم) والباراسيتامول (٥٠٠ مجم / كجم من وزن الجسم) عن طريق الفم لمدة أسبوعين. أظهرت الفحوصات وجود تغيرات نسيجية مرضية في أنسجة الخصية لمجموعة الباراسيتامول كضمور وتنكس في الأنابيب المنوية مع غياب الحيوانات المنوية، ووجود حطام خلوي، وفقدان خلايا سيرتولي في بعض الأنابيب المنوية عند مقارنتها بالحيوانات الضابطة. بينما أظهرت أنسجة الخصية في المجموعة المكونة من حمض الأسكوربيك والباراسيتامول تلفًا أقل للأنابيب والخلايا الجرثومية مقارنة بمجموعة الباراسيتامول. تشير هذه الدراسة إلى أن حمض الأسكوربيك له تأثيرات وقائية ضد تلف الخصية الناجم عن الباراسيتامول في ذكور الجرذان البالغة.

الكلمات المفتاحية: أنسجة الخصية، حمض الأسكوربيك، أمراض الأنسجة، الباراسيتامول، الجرذان.

1. Introduction:

Antioxidants assist in guarding cells from damage produced by oxidative stress (OS) and improve the body's protection systems against degenerative illnesses. Thus, there is a pressing need to recognize more active and safe antiulcer mediators [1, 2]. The biologically essential antioxidants are vitamins B12, C, and E, giving electrons to free radicals, and the mechanism contains the deduction of initiators of nitrogen species or reactive oxygen [3].

Ascorbic acid (AA) naturally occurs for many biological roles in the body. It is the most antioxidant in plants and is used in agriculture to enhance plant oxidative stress confrontation [4, 5]. AA is an essential antioxidant in extracellular liquid; it protects plasma lipids from

peroxidative damage produced by peroxyl radicals [6]. Moreover, AA has the aptitude to counteract free radicals and defend the structure and function of DNA, proteins, and chromosomes against oxidation injury. They are the most influential in reducing the storage and harmfulness of reactive oxygen species (ROS) [7].

Paracetamol (PC) is usually known as acetaminophen. It is a commonly used antipyretic drug and painkilling [8]. PC is processed in the liver by cytochrome P450 (CYP450) enzymes to N-acetyl-benzoquinone imine (NAPQI), where NAPQI reacts with glutathione (GSH). So, the overdoses of PC may lead to a depletion of hepatocellular GSH [9, 2]. PC has an action similar to that of non-steroidal anti-inflammatory drugs (NSAIDs). Likewise, the cyclooxygenase type 2 (COX-2) selective inhibitors are weaker analgesics than NSAIDs or COX-2 selective inhibitors. [10, 11, 12]. Acute overdose of PC could be the reason for the toxicity of testis in men and male animals [13]. Furthermore, the long-term uses of PC cause toxicity effects in the organs, such as the liver, kidney, and testis, and it also affects the blood structures and reproductive hormones. [14,15], such as semen quality, particularly the sperm morphology and fertilizing ability [16]. Moreover, [14, 10] suggested that the long-term of PC caused an increased risk of OS, testicular tubules and blood cell damage, heart infarction, and high blood pressure. The present study investigates the protective effects of AA on the testis tissue damage induced by PC in male albino rats.

2. Material and Methods:

Drugs and chemicals: Ascorbic acid (AA) ($C_6H_8O_6$) (500 mg) and paracetamol (PC) ($C_8H_9NO_2$) (500 mg) were purchased from the local pharmacy.

Animals and treatments: For this study, thirty-two male albino rats (*Rattus norvegicus*) weight 200-250 g were taken from the Central Animal House, College of Veterinary, University of Omar Al-Mokhtar, El-Beida, Libya and were kept in cages at room temperature (22 ± 2°C). Rats were fed with diet and water ad libitum for free intake.

Rats were equally divided into four groups (eight rats):

Group (1): In the standard control group (NC), rats were kept under common laboratory conditions as normal control rats with no treatment.

Group (2): In the ascorbic acid-treated group (AA), rats were administrated AA at a dose of 500 mg/kg/b.w [17, 18] orally by gavage for two weeks.

Group (3): In the Paracetamol-treated group (PC), PC was administered to rats at 500 mg/kg/b.w. [19, 18] orally by gavage for two weeks.

Group (4): Protective group (PRO), rats were administered AA at a dose of 500 mg/kg/b.w., then they administered PC at a dose of 500 mg/kg/b.w. Orally by gavage for two weeks.

Rats were given the treatments six days a week [18], and at the end of the study, rats were sacrificed, and then the testes were detached.

Histopathological preparation:

Testis tissue samples were washed in normal saline, fixed in the buffered formalin (10%) for general histological examination, and studied under a light microscope [20]. The changes in the histopathological of the testis tissues were classified as follows: (–) shows regular, (+) shows mild, (++) shows moderate, and (+++) shows severe changes [21, 22].

3. Results:

The result of this research showed a typical structure of the seminiferous tubules in the testis tissues of the standard control group (**Figure 1**), where the seminiferous tubules had normal spermatogenic cells and Sertoli cells, and everyday interstitial spaces had normal Leydig cells (**Figure 2**). On the other hand, the testis tissues in the AA group revealed a standard histological structure, such as normal seminiferous tubules (**Figure 3**), having normal spermatogonial cells and Sertoli cells, as well as everyday interstitial spaces with normal cells of Leydig (**Figure 4**) as similar is the standard control group.

Whereas, histological examination of the testis section in the treated rats with PC showed different histopathological variations when compared with the standard control group, such as atrophy degeneration and necrosis of spermatogonial cells lining seminiferous tubules, with reduced diameter of seminiferous tubules as well as sloughing of germinal epithelium, congestion in testicular vessel. In addition, some tubules showed a marked reduction in the thickness of the germinal epithelium with loss of sperms in their lumen and focal tubular necrosis (**Figure 5**). Additionally, (**Figure 6**)showed that testicular atrophy degeneration appeared in most seminiferous tubules with fewer sperms in their lumen, and irregularly organized sperm cells with distortions of sperm cells as well as sloughing of germinal epithelium, degenerative changes like vacuoles of the interstitial tissue. So, the testis of the male adult rats, when given the PC at two weeks, showed severe damage in the testicular tissues.

Nevertheless, the testis sections of rats treated in the PRO group for two weeks showed minor damage in the testis tubules and germ cells compared to the PC group. Improve testicular arrangement with normal spermatozoa in their lumen, normal seminiferous epithelium with spermatogonia, reorganization of the germinal cells layer with some seminiferous tubules have a few intraepithelial empty spaces, normal Sertoli cells are seen with attached sperms, interstitial spaces were within a standard limit, and Leydig cells these were apparent in the (**Figure 7, 8**). Finally, in many parts of the testis tissues in PRO rats, they showed almost normal structures.

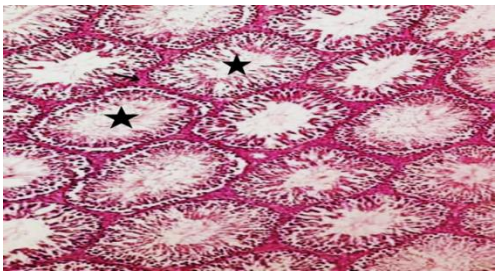

Figure 1: Microscopic image of the testis section of NC rats showing normal seminiferous tubules (stars). (H & E stain, X100).

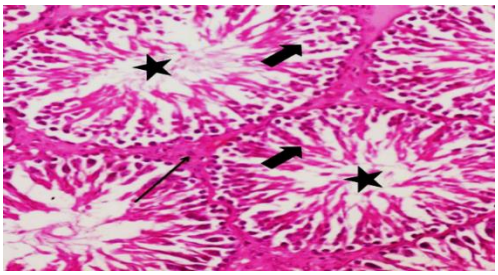

Figure 2: Microscopic image of the testis section of NC rats showing normal seminiferous tubule with standard germinal cell layer (thick arrow), spermatozoa (stars), and normal Leydig cells (arrow) (H & E, X400).

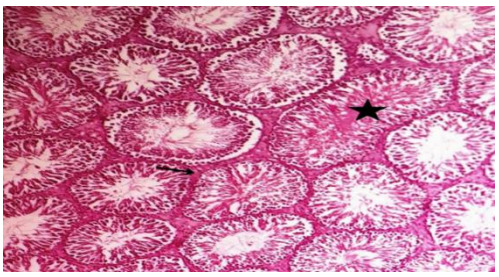

Figure 3: Microscopic image of the testis section of AA rats showing normal seminiferous tubules (star) and standard interstitial spaces (arrow). (H & E stain, X100).

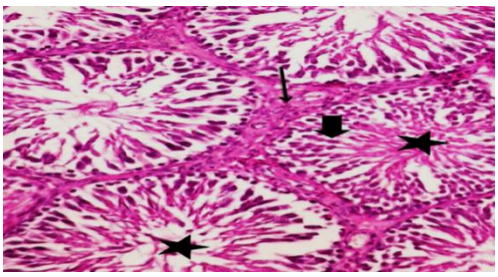

Figure 4: Microscopic image of the testis section of AA rats showing normal seminiferous tubule with standard germinal cell layer (thick arrow), sperms (stars), and everyday interstitial spaces with normal Leydig cells (arrow) (H & E, X400).

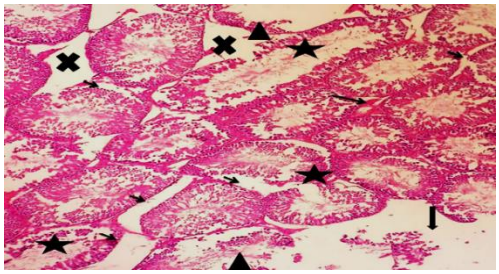

Figure 5: Microscopic image of the testis section of PC rats showing atrophy degeneration and necrosis of spermatogonial cells lining seminiferous tubules, with reduced diameter of seminiferous tubules (stars), widening of the interstitial tissue (X), as well as sloughing of germinal epithelium (small arrows), congestion in testicular vessel (thin arrows). Some tubules show a marked reduction in the thickness of the germinal epithelium with loss of sperms (head arrows) and focal tubular necrosis (thick arrows). (H & E, X100).

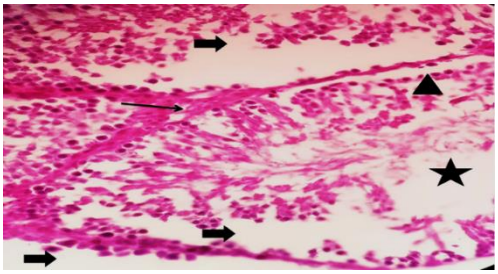

Figure 6: Microscopic image of the testis section of PC rats showing atrophy degeneration of the seminiferous epithelium (arrows) with fewer sperms in the lumen (stars) and irregularly organized sperm cells with alterations of sperm cells (head arrows) as well as sloughing of germinal epithelium (thick arrows), degenerative changes like vacuoles of the interstitial tissue (long arrow). (H & E, X400).

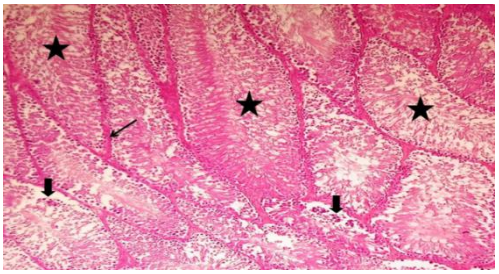

Figure 6: Microscopic image of the testis section of PRO rats showing improved testicular arrangement with normal tubules and germinal cells, repair of some seminiferous tubules with a few intraepithelial empty spaces (thick arrows), normal sperms in the lumen (stars), and standard interstitial spaces within normal Leydig cells (arrow) (H & E, X100).

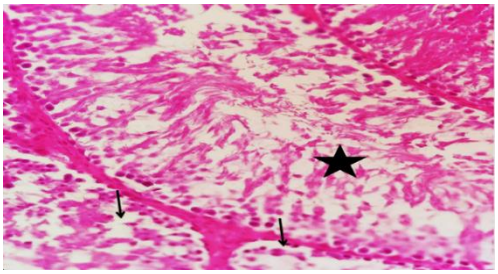

Figure 7: Microscopic image of the testis section of PRO rats showing normal spermatozoa in their lumen (star), seminiferous epithelium with spermatogonia (thick arrow), repair of some seminiferous tubules with a few intraepithelial empty spaces and reorganization of germinal cell layer (arrows). (H & E, X400).

Histopathological variations:

The histopathological variations of the testis tissues are given in (**Table. 1**). The testis tissues of the PRO rats showed a significant improvement in their tissue structure when compared with the PC group.

Table 1: Incidence of histopathological changes in the testis tissues in the normal control and experimental groups.

organs	Lesions	NC	AA	PC	PRO
Testis Tissues	Degeneration of seminiferous tubules	-	-	+++	-
	Widening of the interstitial tissue	-	-	++	-
	Reduction of spermatozoa	-	-	++	-
	Necrosis	-	-	++	-
	Absence of spermatogenesis	-	-	++	-
	Degeneration of germinal cells	-	-	+++	+
	Vacuolations	-	-	++	-
	Reduction of Sertoli cells	-	-	++	-
	Atrophy of seminiferous tubules	-	-	+++	-
	Absence of the spermatozoa	-	-	++	-
	Reduction of Leydig cells	-	-	++	-

*(–) shows normal, (+) shows mild, (++) shows moderate, (+++) shows severe changes.
*NC is the standard control group, AA is the ascorbic acid group, PC is the paracetamol group, and PRO is protective.

4. Discussion:

Results obtained in the present study showed histopathological changes in treated rats with PC for two weeks when compared with the NC rats, such as atrophy degeneration and necrosis of spermatogonial cells lining seminiferous tubules, with a reduced diameter of seminiferous tubules as well as a marked reduction in the thickness of the germinal epithelium with loss of sperms in their lumen, and irregularly arranged sperm cells with distortions of sperm cells as well as sloughing of germinal epithelium, degenerative changes like vacuoles of the interstitial tissue which is in agreement with other studies **[23]**, who found that the taken of the PC showed many histopathological variations in testes rats. They said that giving PC to the male rats' gnawers is mainly due to testicular degeneration and difficulty of spermatogenesis—these effects on the testis by prostaglandins on male maturity and spermatogenesis **[24]**. Moreover, the PC may cause impaired fertility by testicular toxicity. Also, the toxic effects of an overdose of PC on the reproductive organs of male animals may induce several changes and damagingly affect the tissue structure of the testis tubules **[25, 26, 13]**. So, the results showed that the PC

can potentially cause reproductive toxicity when high and long-term treatment. Research by [27] indicates that high doses of PC lead to unwanted side effects, such as the production of ROS that leads to OS. Furthermore, ROS may similarly affect the Sertoli cells, which impacts the protein mixture hardware required to depart the germ cells [28]. Besides that, the PC could pervade the blood of the testis barrier with alteration in the microenvironment of the seminiferous tubules, thus creating a different microenvironment in the testicular functions and the barrier of the seminiferous tubules [29].

Meanwhile, the testis tissues of the POR rats showed improved testicular structure with normal spermatozoa, seminiferous tubules, and typical structures of the Leydig cells compared to the PC group. AA protects against PC by removing the OS and reducing cell apoptosis [30, 31]. Moreover, it has been reported that AA inhibited OS. It reduced the lipid products and protein peroxidation [31]. Also, Heikal 2014 showed the protective properties of the AA in lowering the levels of biochemical changes and histopathological assessments.

Moreover, histopathological variations of the testis tissues in the albino rats showed that the AA was protective against PC-induced testis injury.

5. Conclusion:

The present results determine that histopathological variations in the testis tissues of the albino rats cause PC. In addition, the AA has protective roles against PC-induced testis injury in male rats.

6. References:

[1] De Lira Mota KS, Dias GEN, Pinto MEF, Luiz-Ferreira A, Souza-Brito ARM, Hiruma-Lima CA, Barbosa-Filho JM, Batista LM. Flavonoids with gastroprotective activity. Mole. 2009 Mar; 14(3): 979-1012. https://doi.org/10.3390/molecules14030979.

[2] Alshailabi EMA. The protective effects of indole-3-carbinol on stomach injury in rats. L J B S. 2021 Jul; 14 (1): 12-24. https://doi.org/10.36811/ljbs.2021.110070.

[3] Abdulkhaleq FM, Alhussainy TM, Badr MM, Khalil AA, Gammoh O, Ghanim BY, Qinna A. N. Antioxidative stress effects of vitamins C, E, and B12, and their combination can protect the liver against acetaminophen-induced hepatotoxicity in rats. Drug Des Devel Ther. 2018 Oct;18(12): 3525-3533. https://doi.org/10.2147/DDDT.S172487.

[4] Johnson M, Olufunmilayo LA, Anthony DO, Olusoji EO. Hepatoprotective effect of ethanolic leaf extract of *Vernonia amygdalina* and *Azadirachta indica* against acetaminophen-induced hepatotoxicity in Sprague-Dawley male albino rats. American J Pharmacol Sci. 2015Jul; 3(3): 79-86. https://doi.org/10.12691/ajps-3-3-5.

[5] Hassanin KMA, Hashem KSH, Samraa H, Abdel-Kawi SH. Hepatoprotective effects of vitamin C and micronized vitamin C against paracetamol induced hepatotoxicity in rats: A

comparative study. Int J Biochem Biotechnol. 2017 Jan; 6(4): 756-766. https://doi.org/10.21608/JVMR.2013.77678.

[6] Matić MM, Milošević1 MD, Paunović MG, Ognjanović BI, Štajn AS, Saičić ZS. Paracetamol-induced changes of haematobiochemical and oxidative stress parameters in rat blood: Protective role of vitamin C and ß-glucan. Kragujevac J. Sci. 2016 Mar; 38:135-146. https://doi.org/10.1080/01480545.2019.158745.

[7] Al-Eryani MAY, Shediwah FMH, Al-Awar MSA, Salih EMA, AL- Shaibani EAS. The ability of vitamin A, alone or in combination with vitamins C and E, in ameliorating the side effects of penicillin and streptomycin on hepatic damage in guinea pigs. JJBS. 2014 Jun; 7(2): 127-132. https://doi.org/10.12816/0008226.

[8] Olatosin TM, Akinduko DS, Uche CZ, Bardi J. Effects of *Moringa oleifera* seed oil on acetaminophen-induced oxidative stress and liver damage in Wistar albino rats. IOSR-JPBS. 2014 Jan; 9(2):53-59. https://doi.org/10.9790/3008-09215359.

[9] Blessing O, Frederick O. Effects of concurrent administration of paracetamol and aqueous extract of *Hibiscus sabdariffa* Linn calyx on paracetamol hepatotoxicity in Mice. J. Pharm Chem Biol Sci. 2017 Aug; 5(2):108-117.

[10] Ottani A, Leone S, Sandrini M, Ferrari A, Bertolini A. The analgesic activity of paracetamol is prevented by the blockade of cannabinoid CB1 receptors. Eur J Pharmacol. 2006 Feb; 15 (1-3):280-281. https://doi.org/10.1016/j.ejphar.2005.12.015.

[11] Graham GG, Davies MJ, Day RO, Mohamudally A, Scott KF. The modern pharmacology of paracetamol: Therapeutic actions, mechanism of action, metabolism, toxicity and recent pharmacological findings. Inflammopharmacol. 2013 Jun; 21(3):201-32. https://doi.org/10.1007/s10787-013-0172-x.

[12] Jóźwiak-Bebenista M, Nowak JZ. Paracetamol: Mechanism of action, applications and safety concern. Acta Pol Pharm. 2014 Feb; 71(1):11-23.

[13] Mohammed HU, Sabry RM. The possible role of curcumin against changes caused by paracetamol in testis of adult albino rat (histological, immunohistochemical and biochemical study). EJH. 2020 Sep; 43(3): 819-834. https://doi.org/10.21608/ejh.2019.18599.1189.

[14] Olaleye MT, Rocha BTJ. Acetaminophen induced liver damage in mice: Effect of some medicinal plants on the oxidative defense system. Exp Toxicol Pathol. 2008 Mar; 59(5):319-27. https://doi.org/10.1016/j.etp.2007.10.003.

[15] Khayyat LI. Evaluate of the efficacy of extra *Virgin* olive oil against paracetamol overdose induced renal toxicity in albino rats. Umm Al-Qura Univ J App Sci. 2018 Jun; 5(1): 1-13. https://doi.org/10.5053/ejobios.2016.10.0.4.

[16] Khayyat LI. Extra *Virgin* olive oil protects the testis and blood from the toxicity of paracetamol (overdose) in adult male rats. Biol. 2021 Oct; 10: 1-14. https://doi.org/10.3390/biology10101042.

[17] Adeneye AA, Olagunju JO. Protective effect of oral ascorbic acid (vitamin C) against acetaminophen-induced hepatic injury in rats. Afr. J. Biomed. Res. 2008 Ma; 11: 183-190. https://doi.org/10.4314/ajbr. v11i2.50704.

[18] Abdalally OA, Alshailabi, EMA, Ali MS. Effects of vitamin C on liver and kidney enzymes and some biochemical parameters against paracetamol induced hepato-nephrotoxicity in rats. Sirte U Sci J (Applied Sci.). 2021 Dec; 12(2): 59-72.

[19] Modo E, Okwandu N, Dongo B. Comparative effects of vitamin C and vitamin E pre-treatment in acute paracetamol induced toxicity on the liver of rats. World J Pharm Sc. 2015 Feb; 3(3): 407-412.

[20] Lillie RD. *Histopathological techniques and practical histochemistry*. Mc Graw-Hill U.S.A. 1954.

[21] Moshaie-Nezhad P, Bahari Z, Jangravi Z, Zarei SM, Iman MJ. The effect of *Descurainia sophia* seed extract on nephrotoxicity markers induced by acetaminophen in mice. J Adv Med Biomed Res. 2021 Apr; 29(134):139-144. https://doi.org/10.30699/jambs.29.134.139.

[22] Alshailabi EMA, Al- Zail NI, Abraheem RA. The effects of cigarette smoke on the epididymal tissues in adult male albino rats and the ameliorative effect of the Sidr honey. Libyan J Med Res.2023 Ma;16 (2B): 79-92.

[23] Haroun MR, Eldin AA, EL-Khouly SM, Mostafa IA. The protective effect of ascorbic acid and curcumin on the chronic toxicity of meloxicam on the testis of adult albino rats. BJAS. 2020 Aug; 5(5):189-207. https://doi.org/10.21608/bjas.2020.136691.

[24] Uzun B, Atli O, Perk BO. Evaluation of the reproductive toxicity of naproxen sodium and meloxicam in male rats. HET. 2015 Jul; 34(4):415-429. https://doi.org/10.1177/0960327114542886.

[25] Luangpirom A, Kourchampa W, Junaimuang T. Attenuating effect of *Allium ascalonicum* L. on paracetamol induced seminal quality impairment in mice. JMPR. 2012 Apr; 6: 2655–2659. https://doi.org/10.5897/JMPR11.1602.

[26] El-Maddawy ZK, El-Sayed YS. Comparative analysis of the protective effects of curcumin and N-acetyl cysteine against paracetamol-induced hepatic, renal, and testicular toxicity in Wistar rats. Environ Sci Pollut Res Int. 2018 Feb; 25(4):3468-3479. https://doi.org/10.1007/s11356-017-0750-3.

[27] James LP, Mayeux PR, Hinson JA. Acetaminophen-induced hepatotoxicity. Drug Metab Dispos. 2003 Dec; 31(12):1499-506. https://doi.org/10.1124/dmd.31.12.1499.

[28] Karaguzel E, Kadihasanoglu M, Kutlu O. Mechanisms of testicular torsion and potential protective agents. Nat Rev Urol. 2014 Jul;11(7):391-399. https://doi.org/10.1038/nrurol.2014.135.

[29] Olaniyi KS, Agunbiade TB. α-tocopherol attenuates acetaminophen-induced testicular dysfunction in adult male rats. Int J Health Allied Sci. 2018, 7(1):6-11. https://doi.org/10.4103/ijhas.IJHAS-100-17.

[30] Ghorbani-Taherdehi F, Nikravesh MR, Jalali M, Fazel AR, Gorji Valokola M. Evaluation of the antioxidant effect of ascorbic acid on apoptosis and proliferation of germinal epithelium cells of rat testis following malathion-induced toxicity. Iran J Basic Med Sci. 2020 Ma; 23:569-575. https://doi.org/10.22038/ ijbms.2020.35952.8608.

[31] Mohamed M, Mohamed A, Eldeen EA. The possible protective effect of vitamin C against sildenafil citrate affected liver of adult and senile male albino rats (Light and Electron Microscopic Study). AIMJ. 2022 Oct; 3(10): 8-14. https://doi.org/10.21608/aimj.2022.143240.1974.

[32] Heikal TM, Mossa ATH, Khalil WKB. Protective effects of vitamin C against methomyl-induced injures on the testicular antioxidant status and apoptosis-related gene expression in rat. J Environ Anal Toxicol. 2014 Mar; 5(2) 1-7: e1000255. https://doi.org/10.4172/2161-0525.1000255.

Al-Kitab Journal for Pure Sciences (2024); 8(1):29-39.
https://doi.org/10.32441/kjps.08.01.p4

Al-Kitab Journal for Pure Sciences
ISSN: 2617-1260 (print), 2617-8141(online)

https://isnra.net/index.php/kjps

Evaluating the Antimicrobial Efficacy of Apple Cider Vinegar on Bacteria and Fungi Isolated from Vaginitis

Shaymaa Jaber Hameed*

Kirkuk General Education Directorate, Kirkuk, Iraq

*Corresponding Author: Shymabio@gmail.com

Citation: Hameed SJ. Evaluating the Antimicrobial Efficacy of Apple Cider Vinegar on Bacteria and Fungi Isolated from Vaginitis. Al-Kitab J. Pure Sci. [Internet]. 2024 Mar 09 [cited 2024 Mar 09];8(1):29-39. Available from: https://doi.org/10.32441/kjps.08.01.p4.

Keywords: ACV, bacteria, fungi, Vaginitis.

Article History
Received 08 Jan. 2024
Accepted 03 Mar. 2024
Available online 09 Mar. 2024

Abstract:

Vaginitis is a prevalent medical illness that affects a substantial proportion of women, mostly attributed to the excessive proliferation of bacteria and fungi. The objective of this study was to assess the antimicrobial effectiveness of Apple Cider Vinegar against bacteria and fungi that were obtained from cases of vaginitis. 50 vaginal swabs were collected from vaginitis patients at private clinics in Kirkuk City, Iraq (10 pregnant women and 40 non-pregnant women). The research included the isolation and identification of bacterial and fungal isolates. All isolates performed the Minimum Inhibitory Concentration and disc diffusion techniques tests. Different concentrations of apple cider vinegar (20%, 30%, 40%, 50% and 100%) were tested against the isolates and Standard antibiotic drugs were used as positive controls. The results of 50 patients were examined, showing that 22 (44%) had bacterial vaginitis and 39 (78%) had fungal vaginitis. Vaginitis was more prevalent in pregnant women compared with non-pregnant. Staphylococcus aureus recorded 14 (24.9%) out of the 54 bacterial isolates, followed by Echerichia coli, Group B- Streptococcus, Klebsiella pneumoniae, Staphylococcus epidermidis and Pseudomonas aeruginosa respectively. whereas Candida albicans recorded 30 (61.2%) out of the 49 fungal isolates, followed by Candida tropicalis and Candida parapsilosis, respectively. The findings showed a range of sensitivity to apple cider vinegar among the isolated samples. The efficacy of apple cider vinegar was found to be greater against fungal isolates compared to bacterial isolates, with a higher effectiveness observed

against gram-negative bacteria in comparison to gram-positive bacteria. The highest MIC values were found for Gram-positive bacteria, which recorded 125 (µg/mL), followed by Gram-negative bacteria, 62.5 µg/ml. While the lowest MIC values for the isolated fungi were (31.25 µg/ml). A comparison to traditional antimicrobial drugs has highlighted ACV's potential as an alternative treatment for vaginitis. According to these findings, ACV may be an effective treatment choice for vaginitis.

Keywords: ACV, bacteria, fungi, Vaginitis.

تقييم الفعالية المضادة للميكروبات لخل التفاح على البكتريا والفطريات المعزولة من التهاب المهبل

شيماء جابر حميد*

المديرية العامة لتربية كركوك، كركوك، العراق

Shymabio@gmail.com

الخلاصة:

التهاب المهبل هو مرض طبي منتشر يصيب نسبة كبيرة من النساء، ويعزى معظمه إلى التكاثر المفرط للبكتريا والفطريات. الهدف من هذه الدراسة هو تقييم الفعالية المضادة للميكروبات لخل التفاح ضد البكتريا والفطريات التي تم الحصول عليها من حالات التهاب المهبل. تم جمع ٥٠ مسحة مهبلية من مريضات التهاب المهبل في العيادات الخاصة في مدينة كركوك، العراق، (١٠ نساء حوامل و٤٠ امرأة غير حامل). تضمن البحث عزل وتشخيص العزلات البكتيرية والفطرية. أجريت على جميع العزلات اختبارات التركيز المثبط الأدنى وتقنيات انتشار القرص. تم اختبار تراكيز مختلفة من خل التفاح (٢٠٪، ٣٠٪، ٤٠٪، ٥٠٪، ١٠٠٪) ضد العزلات وتم استخدام المضادات الحيوية القياسية كعناصر تحكم إيجابية. تم فحص نتائج ٥٠ مريضة، وأظهرت أن ٢٢ (٤٤٪) مصابات بالتهاب المهبل البكتيري و٣٩ (٧٨٪) مصابات بالتهاب المهبل الفطري. وكان التهاب المهبل أكثر انتشاراً عند النساء الحوامل مقارنة بغير الحوامل. سجلت بكتريا المكورات العنقودية ١٤ عزلة (٢٤,٩٪) من أصل ٥٤ عزلة بكتيرية، تلتها، *Group B- Streptococcus, Echerichia coli Klebsiella pneumonia, Staphylococcus, epidermidis* و *Pseudomonas aeruginosa* على التوالي. بينما سجلت المبيضة البيضاء ٣٠ عزلة (٦١,٢٪) من أصل ٤٩ عزلة فطرية، تلتها *Candida tropicalis* و *Candida parapsilosis* على التوالي. وأظهرت النتائج مدى الحساسية لخل التفاح بين العينات المعزولة. اذ سجلت خل التفاح فعالية أكبر ضد العزلات الفطرية مقارنة بالعزلات البكتيرية، مع ملاحظة فعالية أعلى ضد البكتريا سالبة الكرام مقارنة بالبكتريا موجبة الكرام. تم تسجيل أعلى قيم لل *MIC* للبكتريا موجبة الكرام، والتي بلغت ١٢٥ (ميكروجرام/مل)، تلتها البكتريا سالبة الكرام، ٦٢,٥ ميكروجرام/مل. في حين كانت أقل قيم لل *MIC* للفطريات المعزولة (٣١,٢٥ ميكروجرام/مل). وقد سلطت المقارنة مع الأدوية التقليدية المضادة للميكروبات الضوء على إمكانات استخدام خل التفاح كعلاج بديل لالتهاب المهبل. وفقا لهذه النتائج، قد يكون خل التفاح خيار علاج فعال لالتهاب المهبل.

الكلمات المفتاحية: خل التفاح، بكتريا، الفطريات، التهاب المهبل.

1. Introduction:

Vaginitis, often known as external genital inflammation, is an inflammation of the vaginal mucosa. Itching, burning, irritation, discharge, and discomfort are common side effects of the inflammation. It's one of the most common causes of doctor visits among females [1]. Many different things, including irritants, hormones, foreign bodies, sexually transmitted diseases, and infections, can cause vaginitis. All of these factors have the potential to cause discomfort for sick women [2]. Bacteria, fungi, parasites, and viruses can all contribute to the development of infected vaginitis, in addition to Chlamydia, Staph aureus, Group B streptococcus (GBS), E.coli, Klebsiella pneumonia, Listeria monocytogenes, Acinetobacter spp., and Neisseria gonorrhoea are the most common bacteria that cause vaginitis [3]. Candida albicans, an opportunistic polymorphic fungal species that is a leading cause of vulvovaginal candidiasis (VVC), which causes major quality-of-life issues for women around the world, can also cause vaginitis. VVC is characterized by burning, itching, and redness of the vulva and vaginal mucosa, often accompanied by a thick white vaginal discharge. About 75% of all women will experience VVC at some point in their life [4]. Antimicrobial drug resistance is an established and pervasive issue worldwide. There has been a rise in a variety of infections that are resistant to different kinds of antimicrobials [5]. Warns that the development of resistance to antimicrobial drugs could threaten our ability to treat many diseases that are currently treatable. Because of this, natural antimicrobials have attracted a lot of attention in recent years to be used for immune-compromised and high-risk patients [6]. Apple cider vinegar has been the subject of extensive research into its pharmacological qualities and applications as a natural product that is its growing usage in the pharmaceutical, food, and cosmetic industries, and its antimicrobial, antioxidant, anti-diabetic, anti-inflammatory, anti-hypertensive, immune-stimulating, and anticancer properties are only some of the many biological effects demonstrated by apple cider vinegar [7]. It has a long history of usage in alternative medicine. Numerous applications have been found for it due to the widespread acceptance of its purported antimicrobial, antiseptic, and antiviral properties [8]. The aim of this study is to evaluate the antibacterial and antifungal efficacy of apple cider vinegar for vaginitis isolates

2. Material and Methods:

1- Patients and Specimen Collection: 50 vaginal swabs have been obtained from vaginitis patients at private clinics in Kirkuk city, Iraq. Including 10 pregnant women and 40 non pregnant women. Each sample was inoculated onto blood agar plate, chocolate agar, nutrient

agar, McConkey agar and Sabouraud's Dextrose-Agar. The plates were incubated at 37°C for 24 hours, and Sabouraud's Dextrose agar plates were incubated at 27°C for 48 hours.

2- Identification of bacterial and fungal isolates: Colony morphology, Gram stain, and biochemical testing were used to diagnose bacteria in the patient's vaginal swabs, and the API 20 test was utilized for verifying the isolate's identity **[9]**. According to Murray *et al*., fungi were diagnosed using a series of tests based on their microscopic and cultural characteristics as well as biochemical tests **[10]**.

3- Preparation of Apple Cider Vinegar extract: The natural apple cider vinegar utilised in this research was acquired from a local supermarket. At 0.12 atm and -82 °C, the water content of a 1000 mL sample of vinegar was completely evaporated using a freeze dryer (Christ, Germany). After being freeze-dried, the sample of apple cider vinegar yielded 18 gm. A 1 mg/mL stock solution was prepared using distilled water, and then the solutions were sterilised by filtering them through a 0.45 µm filter **[11]**.

4- Inoculum Preparation: Candida spp. was incubated at 27°C for 48 hours, while all bacterial strains were incubated at 37°C for 24 hours **[12, 13]**. By transferring the bacteria and fungi in 0.9% sterile saline solution and adjusting to a 0.5 McFarland standard for each, the inoculum were standardised to contain around 10^8 cfu/mL for bacteria and 10^7 cfu/mL for Candida spp **[14, 15]**.

5- Minimum Inhibitory Concentration Test: The broth dilution method was used to determine the minimum inhibitory concentration (MIC) **[16, 17]**. The concentration range was obtained by making serial 2-fold dilutions, from (500 to 15.62) µg /mL. The (MIC) has been defined as the lowest concentration of extract required to inhibit the growth of bacteria and fungi. A tube without apple cider vinegar was considered as a positive control, while a tube with only broth was considered as a negative control. Triplicates of every test were done. Finally, the MIC for each isolated organism was recorded.

6- Preparation of concentrate solutions: Different concentrations of ACV extract (20%, 30%, 40%, 50% and 100%) were prepared **[18]**.

7- Disk diffusion method: Antibacterial and antifungal activity of ACV was measured using this method. In brief, sterile paper discs (6 mm) were saturated with 10 µl of each concentrate of ACV and then placed on inoculation plates (nutrient agar for bacteria and Sabouraud agar for fungus) that had already been prepared. Plates with bacteria were incubated at 37°C for 24

hours, while those with fungi were incubated at 27°C for 48 hours. Diameters of the microbial growth inhibitory zone were clearly measured in millimetres. However, fluconazole (25 µg/disc) and clindamycin (2µg /disc) have been employed as positive controls for fungi and bacteria, respectively. Every test was performed in triplicate [19].

8- Statistical analysis: Calculations of means, standard deviation and percentages were performed in SPSS version 18 and Microsoft excel 2013.

3. Results:

Numbers and percentages of bacteria and fungi isolated from vaginitis patients: 50 vaginitis specimens were cultured during the study period. 10 samples were of pregnant women and 40 samples were of non-pregnant women. Bacterial vaginitis included 22 (44%) samples, distributed among 15 (37.5%) non-pregnant women and 7 (70%) pregnant women. While fungal vaginitis included 39 (78%) samples, distributed among 31 (77.5%) non-pregnant women and 8 (80%) pregnant women. As shown in **Table (1).**

Table (1): Numbers and percentages of (bacterial and fungal) vaginitis in pregnant and non-pregnant women

Microorganisms	Non pregnant women (40)	Pregnant women (10)	Total no. (50)
Bacteria	15 37.5%	7 70%	22 44%
Fungi	31 77.5%	8 80%	39 78%

Vaginitis can be caused by a wide variety of microbes, including bacteria and fungi, and often results from an imbalance or interference between the types of organisms that cause inflammation and the normal vaginal flora [20]. Pregnant women had a higher rate of vaginitis (fungal and bacterial infections) than other women. Vaginitis is the most frequent genital infection in pregnant and breastfeeding women [21, 22], because estrogen stimulates and activates the growth and integration of the vaginal epithelial membrane, a normal level of estrogen is necessary to maintain the vaginal balance and its resistance to microbial infections. This is because estrogen is a potent anti-inflammatory [23]. According to Dybas *et al*., study most cases of vaginitis have been reported by pregnant women [24]. As for bacteria, 54 isolates were isolated from infected women: 14 (25.9%) *Staphylococcus aureus* isolates, 11(20.4%) *Echerichia coli*, 9 (16.7%) Group B- Streptococcus, 8 (14.8%) *Klebsiella pneumoniae*, 7 (13%) *Staphylococcus epidermidis*, and 5 (9.3%) *Pseudomonas aeruginosa* isolates. In addition, 49

fungal isolates were isolated from infected women, including 30 (61.2%) *Candida albicans*, 11(22.4%) *Candida tropicalis*, and 8 (16.3%) *Candida parapsilosis* isolates. As shown in **Table (2).**

Table (2): The percentage of bacteria and fungi that cause vaginitis

Bacteria	**No. (54 Isolates)**	**%**
Staphylococcus aureus	14	25.9%
Echerichia coli	11	20.4%
Group B- Streptococcus	9	16.7%
Klebsiella pneumoniae	8	14.8%
Staphylococcus epidermidis	7	13%
Pseudomonas aeruginosa	5	9.3%
Fungi	**No. (49 Isolates)**	**%**
Candida albicans	30	61.2%
Candida tropicalis	11	22.4%
Candida parapsilosis	8	16.3%

The results of the current study agreed with Razzak, *et al.'s*, study, as *Staphylococcus aureus*, *Pseudomonas aeruginosa*, *Staphylococcus epidermidis*, Group B- Streptococcus, *Klebsiella pneumonia*, and *Echerichia coli* were isolated, where they found that the presence of probiotics, which stimulated the production of defence components, correlated inversely with the organism that caused vaginitis **[25]**. Therefore, Antibiotics for vaginitis treatment must be carefully chosen so as not to eliminate the beneficial probiotics that play an essential role in keeping the vagina and its environment in a healthy order. The current study also agreed with the results of Hussein's study, *Candida albicans* that had the largest percentage of Candida species isolated from vaginitis, followed by *Candida tropicalis* and *Candida parapsilosis* **[26]**.

Minimum Inhibition Concentration value and antimicrobial activity of apple cider vinegar: The MIC test is commonly used to determine the minimum concentration of apple cider vinegar that inhibits isolates from vaginitis patients. The highest MIC values were found for gram positive bacteria (*Staphylococcus aureus*, *Staphylococcus epidermidis* and Group B-Streptococcus,), all of which were 125 (µg/mL).

Gram-negative bacteria recorded 62.5 (µg/mL) for (*Escherichia coli*, *Klebsiella pneumonia* and *Pseudomonas aeruginosa*). While the lowest MIC values were found for the isolated fungi (31.25 µg /mL) for (*Candida albicans*, *Candida parapsilosis*, and *Candida tropicalis*), as shown in **Table (3)**.

Table (3): MIC values for apple cider vinegar against isolates (µg/mL)

Isolates	500 (µg/mL)	250 (µg/mL)	125 (µg/mL)	62.5 (µg/mL)	31.25 (µg/mL)	15.62 (µg/mL)	+ve control	-ve control
Staphylococcus aureus	-	-	-	+	+	+	+	-
Echerichia coli	-	-	-	-	+	+		
Group B-Streptococcus	-	-	-	+	+	+		
Klebsiella pneumoniae	-	-	-	-	+	+		
Staphylococcus epidermidis	-	-	-	+	+	+		
Pseudomonas aeruginosa	-	-	-	-	+	+		
Candida albicans	-	-	-	-	-	+		
Candida tropicalis	-	-	-	-	-	+		
Candida parapsilosis	-	-	-	-	-	+		

The antimicrobial properties of apple cider vinegar were tested on all isolates, and the results are presented in **Table (4)**.

Table (4): The (Mean ± SD) of Diameter zones of inhibition (mm) at different concentrations of apple cider vinegar by the desk diffusion method.

Bacterial Isolates	20%	30%	40%	50%	100%	Control Clindamycin (2 µg/disc)
Staphylococcus aureus	-	-	3±1.6	6.5±1.4	8±2.4	20 ±9.1
Echerichia coli	-	0.5±0.4	2±1.2	9±5.1	14±3.4	14±3.5
Group B-Streptococcus	-	-	1.5±0.6	7±3.5	9±4.2	16±5.1
Klebsiella pneumoniae	-	3±1.4	6.5±2.3	10±3.2	13±4.1	14±3.4
Staphylococcus epidermidis	-	0.5±0.3	3±1.4	6±2.3	8.5±3.2	17±4.1
Pseudomonas aeruginosa	1±0.4	4±2.1	6.5±3.2	9±5.2	13±4.2	15±4.3
Fungi Isolates	**20%**	**30%**	**40%**	**50%**	**100%**	**Control fluconazole (25 µg/disc)**
Candida albicans	7±2.3	9±3.2	13±3.4	15±4.1	19±7.1	25±9.2
Candida tropicalis	8±2.3	10±3.3	13.5±4.1	15±4.2	17±4.3	23±7.2
Candida parapsilosis	6±2.1	8±2.4	12±3.4	13±4.1	16±4.4	20±5.1

*Values are the mean ± standard error of 5 replicates

In this study, apple vinegar was found to have significant antibacterial activity against the vaginitis isolates (as shown in Table 4). Apple cider vinegar acts on bacteria by penetrating their cell wall and destroying their DNA, which prevents them from reproducing **[27]**. Apple cider vinegar showed antibacterial activity from (13±4.1) – (14±3.4) mm in gram-negative bacteria and from (8±2.4) – (9±4.2) mm in gram-positive bacteria. Zones of inhibition were

found to be significantly larger for gram negative bacteria compared to gram positive bacteria, Peptidoglycan layers around Gram-positive bacteria were many times thicker than those surrounding Gram-negative bacteria. Long anionic polymers called teichoic acids made up primarily of repetitions of glycerophosphate, glucosyl phosphate, or ribitol phosphate, served as the threads between the peptidoglycan layers. Furthermore, Gram-positive microbes had a wide range of proteins on their surfaces, some of which were comparable to proteins found near Gram-negative species and might offer further antimicrobial action **[28]**. The current study agreed with the results of Kalaba *et al*.'s, study, which had reported an inhibitory zone of 11.33 mm for *Staphylococcus aureus* and of 13.00, 14.00, and 12.66 mm for *Enterobacter kobei*, *E. cloacae*, and *E. coli*, respectively **[7]**. Apple cider vinegar had been shown to be more effective against isolated fungi than against isolated bacteria. Inhibition zones at 100% concentration were between (16±4.4) and (19±7.1) mm in diameter. Some authors claimed that the widespread use of conventional antifungals for the treatment of systemic and superficial infections had contributed to the development of resistant strains among people at risk of contracting a disseminated Candida spp. Infection **[29]**. The objective of this study was not to ascertain the mechanism via which apple cider vinegar exerted its effects. However, according to other scientists, acetate had been shown to inhibit 14-lanosterol-demethylase, Toxic concentrations of acetic acid that could build up inside a cell because it could pass through intact cell membranes and reached its molecular target. As a result of this process, H+-ATPase got activated, consequently, the acidity of the medium increased, which was toxic to fungi **[30, 31]**. Flow cytometer was used in another study to show that prolonged exposure to high concentrations of acetic acid loss of cell integrity **[32]**. The results of the current study agreed with the findings of Ousaaid *et al*., and Patole *et al.'s*, Apple cider vinegar which recorded antibacterial and antifungal activity **[33, 34]**.

4. Conclusion:

This study found that Apple cider vinegar was efficient against vaginitis-causing bacteria and fungus. This finding suggests that ACV may be used as a safe and effective natural remedy for vaginitis. More research is needed to establish the mechanism by which ACV produces its antimicrobial properties and evaluate its therapeutic efficacy.

5. References:

[1] Egan ME, Lipsky MS. Diagnosis of vaginitis. American family physician. 2000; 62(5):1095-1104. https://www.scirp.org/reference/referencespapers?referenceid=1196881

[2] Joesoef M, Schmid G, Hillier S. Bacterial vaginosis: review of treatment options and potential clinical indications for therapy. Clinical Infectious Diseases. 1999; 28(Supplement_1):S57-S65. DOI: 10.1086/514725

[3] Stenchever MA. Comprehensive gynaecology .4th ed. Mosby Inc; 2001; (4):668–6678. https://www.amazon.com/Comprehensive-Gynecology-Mishell Herbst/dp/032301402X

[4] Sobel JD. Vaginitis. New England Journal of Medicine. 1997; 337(26):1896-1903. DOI: 10.1056/NEJM199712253372607

[5] Tacconelli E. Global Priority List of Antibiotic-Resistant Bacteria to Guide Research, Discovery, and Development. 2017. https://remed.org/wp-content/uploads/2017/03/lobal-priority-list-of-antibiotic-resistant-bacteria-2017.pdf

[6] Tan S. Vinegar fermentation [Master of Science thesis]. Louisiana State University, Department of Food Science, Baton Rouge p 101s. 2005.

[7] Kalaba V, Balaban Zm, Kalaba D. Antibacterial activity of domestic apple cider vinegar. Agrofor. 2019; 4(1). DOI:10.7251/AGRENG1901024K

[8] Darzi J, Frost G, Montaser R, Yap J, Robertson M. Influence of the tolerability of vinegar as an oral source of short-chain fatty acids on appetite control and food intake. International Journal of Obesity. 2014;38(5):675-681. DOI: 10.1038/ijo.2013.157

[9] Forbes BA, Sahm DF, Weissfeld AS. Diagnostic microbiology: Mosby St Louis; 2007.

[10] Murray, P. R., Baron, E. J., Pfaller, M. A., Tenover, F. C. & Yolken, R. H. Manual of clinical Microbiology.7th ed. ASM press. Wash- ington; 1999.

[11] Baladas B and Altuner Em. The antimicrobial activity of apple cider vinegar and grape vinegar, which are used as a traditional surface disinfectant for fruits and vegetables. Communications Faculty of Sciences University of Ankara Series C Biology. 2018;27(1):1-10. DOI:10.1501/commuc_0000000187

[12] Canli K, Yetgin A, Akata I, Altuner E. Antimicrobial activity and chemical composition screening of Epilobium montanum root. Indian Journal of Pharmaceutical Education and Research. 2017; 51(3). DOI:10.5530/ijper.51.3s.21

[13] Canli K, Altuner Em, Akata I. Antimicrobial screening of Mnium stellare. ||| Bangladesh Journal of Pharmacology. 2015; 10(2):321-325. DOI:10.3329/bjp.v10i2.22463

[14] Hameed SJ. Effect of Metformin on the Efficacy of Antibiotics (In Vitro). European Journal of Molecular and Clinical Medicine. 2022; 9:3235-3241. https://go.gale.com/ps/i.do?p=HRCA&u=googlescholar&id=GALE|A737509216&v=2.1&it=r&sid=googleScholar&asid=ab6763c7

[15] Altuner Em and Canli K. In vitro antimicrobial screening of Hypnum andoi AJE Sm. Kastamonu University Journal of Forestry Faculty. 2012; 12(1):97-101.

https://www.researchgate.net/publication/314044097_In_vitro_antimicrobial_screening_of_Hypnum_andoi_AJE_Sm

[16] Altuner E, Çetin B, Çökmüş C. Antimicrobial activity of Tortella tortulosa (Hedw.) Limpr. extracts. Kastamonu Üniversitesi Orman Fakültesi Dergisi. 2010; 10(2):111-116. https://www.researchgate.net/publication/314044097_In_vitro_antimicrobial_screening_of_Hypnum_andoi_AJE_Sm

[17] Altuner EM. Bazı karayosunu türlerinin antimikrobiyal aktivitesinin belirlenmesi. 2008. DOI: 10.26672.anatolianbryology.809057

[18] Hameed S. Effect of *Rosmarinus officinalis* L. extracts on bacteria isolated from conjunctivitis in Kirkuk City, Iraq. International Journal of Biology Sciences. 2023; 5:87-91. DOI:10.33545/26649926.2023.v5.i1b.150

[19] MA W. Methods for dilution antimicrobial susceptibility tests for bacteria that grow aerobically: approved standard. Clsi (Nccls). 2006; 26:M7-A. https://clsi.org/media/1928/m07ed11_sample.pdf

[20] Romanik M, Martirosian G. Frequency, diagnostic criteria and consequences of bacterial vaginosis in pregnant women. Przeglad epidemiologiczny. 2004; 58(3):547-553. https://pubmed.ncbi.nlm.nih.gov/15730019/

[21] Virginia,A.;Rauh,S.C.D.;Jennifer,F.;Culhane,P.H.D.;Vijaya,K.andHogan,D.R.P.H. Bacterial vaginosis :Apublic health problem for woman .J.JAWWA. 2002; 55 (4): 220- 224. https://pubmed.ncbi.nlm.nih.gov/10935356/

[22] Rex, J. H. ; Hwalsh, T. J. ; Sobel, S. G. ; filler, P. G. Pappas, W. E. ; Dismukes,T. W. & Edwards, J. E. Practice guide lines for the treatment of Candidiasis. Clin. Infect. Dis. 2000; 30: 662- 678. DOI: 10.1086/313749

[23] Reid G, Burton J, Hammond J-A, Bruce AW. Nucleic acid-based diagnosis of bacterial vaginosis and improved management using probiotic lactobacilli. Journal of medicinal food. 2004; 7(2):223-228. DOI: 10.1089/1096620041224166

[24] Dybaś I, Sidor-Wójtowicz A, Kozioł-Montewka M. Bacterial flora and mycosis of the vagina in women with symptoms of vaginal inflammation. Ginekologia Polska. 2005; 76(5):385-390. https://www.researchgate.net/publication/7615302_Bacterial_flora_and_mycosis_of_the_vagina_in_women_with_symptoms_of_vaginal_inflammation

[25] Razzak MSA, Al-Charrakh AH, Al-Greitty BH. Relationship between lactobacilli and opportunistic bacterial pathogens associated with vaginitis. North American Journal of Medical Sciences. 2011; 3(4):185. DOI:10.4297/najms.2011.3185

[26] Hussein, R. Comparison of biological and molecular parameters of some Candida species that are sensitive and resistant to some antifungals. Thesis. College of Science. University of Kufa. 2011.DOI: https://doi.org/10.36320/ajb/v15.i2.11882

[27] Yagnik D, Serafin V, J. Shah A. Antimicrobial activity of apple cider vinegar against Escherichia coli, Staphylococcus aureus and Candida albicans; downregulating cytokine and microbial protein expression. Scientific reports. 2018; 8(1):1732. https://www.nature.com/articles/s41598-017-18618-x.

[28] Kavanaugh NL, Ribbeck K. Selected antimicrobial essential oils eradicate Pseudomonas spp. and Staphylococcus aureus biofilms. Applied and environmental microbiology. 2012; 78(11):4057-4061. doi: 10.1128/AEM.07499-11

[29] Tobudic S, Kratzer C, Presterl E. Azole-resistant Candida spp.–emerging pathogens? Mycoses. 2012; 55:24-32. https://doi.org/10.1111/j.1439-0507.2011.02146.x

[30] Arneborg N, Jespersen L, Jakobsen M. Individual cells of Saccharomyces cerevisiae and Zygosaccharomyces bailii exhibit different short-term intracellular pH responses to acetic acid. Archives of microbiology. 2000; 174:125-128. https://doi.org/10.1007/s002030000185

[31] Guldfeldt LU, Arneborg N. Measurement of the effects of acetic acid and extracellular pH on intracellular pH of nonfermenting, individual Saccharomyces cerevisiae cells by fluorescence microscopy. Applied and environmental microbiology. 1998; 64(2):530-534. DOI: 10.1128/AEM.64.2.530-534.1998

[32] Prudêncio C, Sansonetty F, Côrte-Real M. Flow cytometric assessment of cell structural and functional changes induced by acetic acid in the yeasts Zygosaccharomyces bailii and Saccharomyces cerevisiae. Cytometry: The Journal of the International Society for Analytical Cytology. 1998; 31(4):307-313. DOI: 10.1002/(sici)1097-0320(19980401)31:4<307::aid-cyto11>3.0.co;2-u

[33] Ousaaid D, Laaroussi H, Bakour M, Ennaji H, Lyoussi B, El Arabi I. Antifungal and antibacterial activities of apple vinegar of different cultivars. International Journal of Microbiology. 2021; 2021. https://doi.org/10.1155/2021/6087671

[34] Patole V, Mahore J, Nandgude and T, Gutte A. Apple cider vinegar: Effective adjuvant treatment for aerobic vaginitis. Novel Research in Microbiology Journal. 2022; 6(4):1659-69. DOI: 10.21608/nrmj.2022.253697

Al-Kitab Journal for Pure Sciences (2024); 8(1):40-62.
https://doi.org/10.32441/kjps.08.01.p5

Al-Kitab Journal for Pure Sciences
ISSN: 2617-1260 (print), 2617-8141(online)
https://isnra.net/index.php/kjps

BANK OF PASSWORDS: a secure Android password manager implemented based on specific requirements

Hussein Abdulkhaleq Saleh*

Directorate General of Education in Dhi Qar., Iraq

*Corresponding Author: hussein.abd.alkhaliq@gmail.com

ORCID: 0009-0003-3426-7168

Citation: Saleh HA. BANK OF PASSWORDS: a secure Android password manager implemented based on specific requirements. Al-Kitab J. Pure Sci. [Internet]. 2024 Mar 12 [cited 2024 Mar 12];8(1):40-62. Available from: https://doi.org/10.32441/kjps.08.01.p5.

Keywords: Secure warehouse for passwords, Passwords vault, Passwords keeper app, Android application.

Article History

Received	16	Jan.	2024
Accepted	08	Mar.	2024
Available online	12	Mar.	2024

Abstract:

Passwords serve as a vital means to safeguard our digital accounts. Many individuals resort to conventional methods like writing down passwords on paper or storing them on cloud services, often overlooking security risks, forgetting, and divulging is the most notable, which leads to loss of access to accounts, or potential breaches. In this paper, we propose the development of an Android application named "BANK OF PASSWORD" to address this issue. Our work focuses on creating a lightweight app equipped with essential functionalities desired by users, including password addition, updating, copying, searching, and deletion. To ensure the security of stored passwords, our approach incorporates various protective measures, such as access restriction through a login process and the utilization of SHA256 hashing and AES256 encryption for password encryption, where stored passwords are securely encrypted and stored as ciphertexts within an SQLite database. A fingerprint authentication was implemented as a second login method. Extensive testing of the application demonstrates the successful functioning of all proposed features and requirements on devices running API level 26 or above.

Keywords: Secure warehouse for passwords, Passwords vault, Passwords keeper app, Android application.

بنك كلمات المرور: مدير كلمات مرور آمن لنظام *Android* تم تنفيذه بناءً على متطلبات محددة

حسين عبدالخالق صالح*

المديرية العامة للتربية في ذي قار، ذي قار، العراق

hussein.abd.alkhaliq@gmail.com

الخلاصة:

تعتبر كلمات المرور وسيلة أساسية لحماية حساباتنا الرقمية. يلجأ العديد من الأفراد إلى الطرق التقليدية مثل كتابة كلمات المرور على الورق أو تخزينها على الخدمات السحابية، وغالبًا ما يغفلون عن مخاطر الأمان، او النسيان، أو الكشف، وهو الأمر الأكثر بروزًا، والذي يؤدي إلى فقدان الوصول إلى الحسابات، أو خروقات محتملة. في هذه الورقة، نقترح تطوير تطبيق *Android* يسمى "بنك كلمات المرور" لمعالجة هذه المشكلة. يركز عملنا على إنشاء تطبيق خفيف يوفر الوظائف الأساسية التي يرغب بها المستخدمون، بما في ذلك إضافة كلمة المرور وتحديثها ونسخها والبحث عنها وحذفها. لضمان أمان كلمات المرور المخزنة، يتضمن نهجنا إجراءات حماية متنوعة، مثل تقييد الوصول من خلال عملية تسجيل الدخول، واستخدام تجزئة *SHA256* وتشفير *AES256* لتشفير كلمة المرور، حيث يتم تشفير كلمات المرور المخزنة بشكل آمن وتخزينها كنصوص مشفرة داخل قاعدة بيانات *SQLite*. كذلك، تم تنفيذ مصادقة بصمة الأصبع كوسيلة اخرى لتسجيل الدخول. يوضح الاختبار المكثف للتطبيق التشغيل الناجح لجميع الميزات والمتطلبات المقترحة على الأجهزة التي تعمل بنظام *API level* *26* أو إصدار أحدث من نظام Android.

الكلمات المفتاحية: مستودع آمن لكلمات المرور، خزانة كلمات المرور، تطبيق حفظ كلمات المرور، تطبيق Android.

1. INTRODUCTION:

In today's digital landscape, individuals possess multiple private accounts, including significant ones such as banking, social networks, websites, emails, and even Wi-Fi networks. These accounts are typically protected by private passwords, known only to the account holder, serving as a barrier against unauthorized access. However, the management of these passwords has become a significant challenge, leading to a pressing need for a secure and efficient solution. This paper is motivated by the desire to address this issue and enhance the security and convenience of password management for Android device users. It is worth noting that many users often tend to reuse the same password across multiple accounts for the sake of convenience. This practice poses a significant security risk, as a compromise of one password can lead to unauthorized access to several accounts **[1]**. Therefore, it is highly recommended to utilize unique and complex passwords for each user account **[2]**.

Managing multiple passwords can become a challenging task, potentially resulting in users forgetting their passwords and losing access to their accounts. Some individuals resort to writing down details of their passwords on paper, or storing them in a text file in cloud services

like Google Drive, or OneDrive, attempting to keep them secure. However, these traditional methods are still susceptible to security threats, including loss, damage, or unauthorized access to sensitive information.

Motivated by the need to provide a secure and user-friendly solution to these challenges, we propose developing a mobile application that provides a secure storage environment for user passwords. Given that most users employ devices powered by Android OS, which holds a significant market share of 67.72% [3], the proposed application will be tailored specifically for Android OS devices. The 'Bank of Passwords' app aims to provide a secure solution for Android users to manage their passwords, where, focuses on simplicity, usability, offline, free-cost, open-source, and available for most Android devices while still implementing robust security features. To ensure a satisfactory user experience, the application should offer convenient password management functionalities while prioritizing security. This necessitates a thorough determination of the requirements before the implementation process .

This paper aims to outline the application's design and implementation processes, demonstrating how it addresses the challenges of password management while enhancing user security. The paper is organized as follows: Section 2 covers user requirements and technical requirements for the app, Section 3 provides a brief implementation plan, Section 4 addresses the UI design processes, Section 5 covers the implementation of background processes, Section 6 is dedicated to test the application, and Section 7 concludes the paper.

2. CORE REQUIREMENTS:

For developing useful and usable applications, we have to understand user needs; and the techniques for implementing them, which means there are user requirements and technical requirements [4].

2.1 User Requirements: User requirements can be written from the perspective of what the users need to satisfy them [4]. In our approach, we will adopt the following requirements:

- The application offers users two login methods, either by entering a password or by using their fingerprint if supported.
- The user can assign a login password when the application launches for the first time for security purposes.
- The application forces the user to login every time he runs the application.
- For every new password to be added, the app must store a name and value.
- The application forces the user to use a unique name for every new password to be stored.
- The application can display all stored passwords as a scrollable list.

- The user should be able to copy any password value stored inside the application and paste it where needed.
- The application provides the user with the ability to edit any stored password easily (name or value or both).
- The application allows the user to delete any password stored inside the application.
- The user can search for any password stored inside the app.
- The application allows the user to change the login password.
- The user can erase (reset) all stored data inside the application with one click.
- The user can exit the application.
- The login-password length should be a minimum of eight characters.
- There is no need to get any access permissions from the user.
- The language of this application is English.
- The application Works offline.

2.2 Technical Requirements: To meet users' requirements in Sec. 2.1, and make it feasible, we need to define some technical requirements for describing how the application will be implemented practically **[4]**, plus illustrate how the background processes would be performed in this application. For such an application, our approach adopts the following technical requirements:

- For development, a reliable IDE should be used.
- A recommended Android API level must be used for development.
- The programming language that is used for development is preferred to be a popular and easy option for beginners and hobbyists.
- For storing the data of the user passwords, the application should use an efficient storage technic.
- The application must check and confirm that the new stored password has a unique name.
- The stored data (especially password values) must be secured by encrypting the plaintext of all stored passwords.
- The application must have the ability to decrypt all encrypted passwords to their plaintext again when needed to display them in the GUI.
- To assign a password for login, such an app must have the ability to store this kind of password and retrieve it when compared with the entered value in the login process.
- When a login password is assigned, the application must force the user to write this password twice in two different fields for more confirmation.

- For security level increase, the login password should be encrypted and stored as a ciphertext.
- The ciphertext of the login password should be used as a key for encrypting all stored passwords.

3. IMPLEMENTATION PLAN:

Before proceeding with designing and programming, it's essential to prepare an appropriate IDE, where we intend to use Android Studio because it's the official IDE for developing Android applications [5]. According to a Google announcement on 19 November 2020, Google Play Console will require all new apps to target API level 30 (Android 11) or above as reported by Android Developers [6].

For that reason, our app will be developed with API level 32 (Android 11) as a target, and API level 26 as minimum. For programming, there are many languages for developing Android apps such as Java, Kotlin, and C++. We plan to develop this app with Java, to produce a small apk file size [7], and as being the better option from the beginner's point of view [8]. Based on the common architectural principles mentioned by Android developers for best application development practices, each application should have at least two layers:

1. a UI layer.
2. a data layer.

The UI layer is accountable for presenting the application data on the screen, while the data layer encompasses the business logic, consisting of rules that govern the creation, storage, and manipulation of data within the application [8]. These processes occur independently of the user in the backend. Drawing from the aforementioned information, we can divide the implementation approach into two essential components:

1. UI Design.
2. Back-end Processes Implementation.

As we transition from the theoretical framework and requirements, it becomes pivotal to visualize the operational flow of the application to grasp its comprehensive functionality and user interaction dynamics, as described in **Figure 1**. This diagram will serve as a preliminary roadmap in the next phases, guiding the development process and ensuring that all user requirements are met effectively and efficiently.

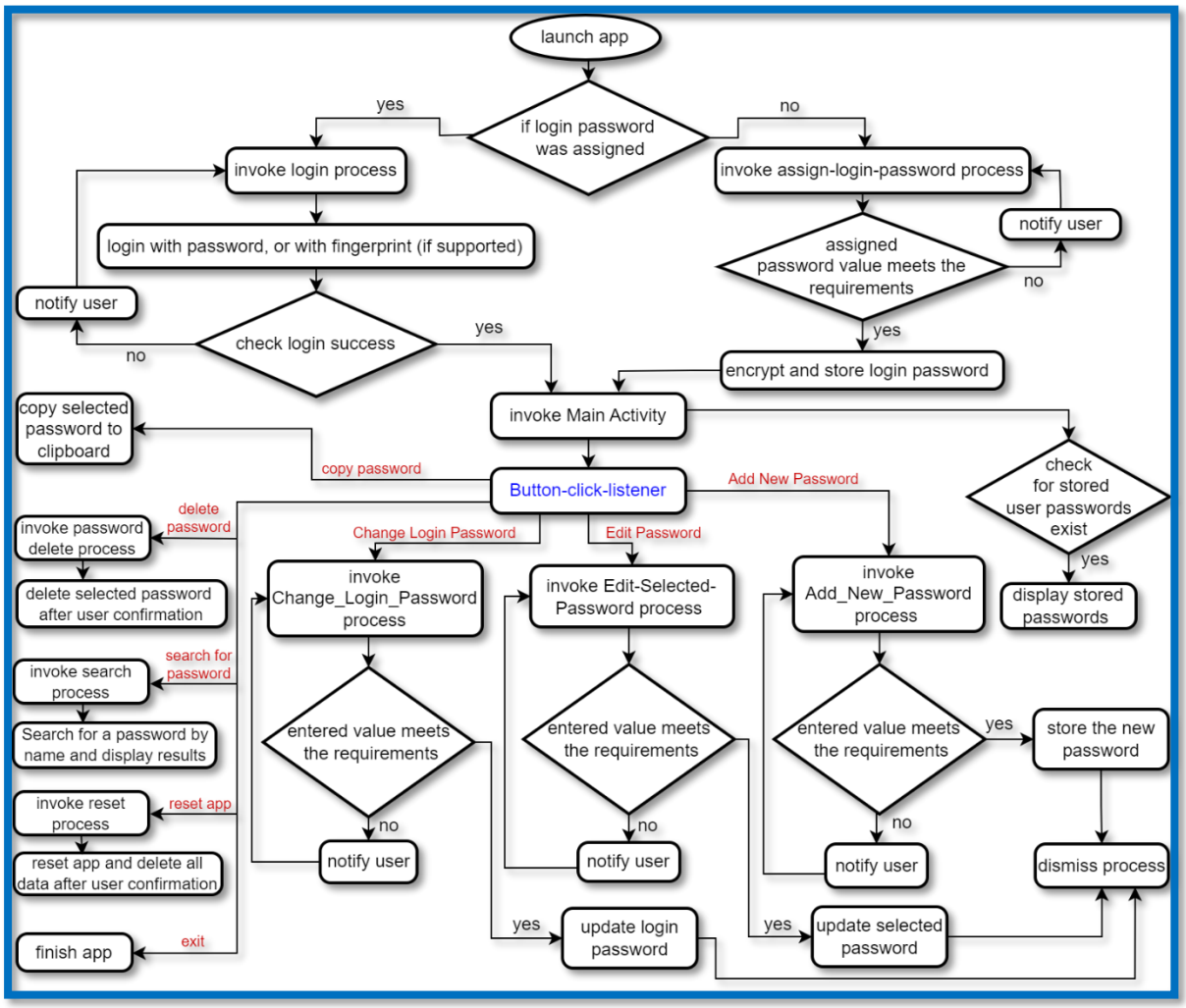

FIGURE 1: A Flowchart depicts the core functions and their processes in the 'Bank of Password' app.

4. UI DESIGN:

In this context, it is essential to gain a graphical design perspective to better comprehend the user requirements outlined in Section 2.1. This understanding allows us to visualize and create a feasible graphical user interface (GUI). Before embarking on the design phase, it is crucial to identify the primary tasks that the application will be carrying out based on the user requirements. Additionally, establishing the execution workflow, as depicted in **Figure 2**, helps to delineate the sequence of actions and interactions within the application.

4.1 Application's Main Tasks:

1. Assigning Login-password for the first time.
2. Login process.
3. Add a new password.
4. Display the stored passwords.
5. Delete password.

6. Copy password.
7. Update stored passwords.
8. Search for a password.
9. Change the login password.
10. Reset to default.
11. Exit.

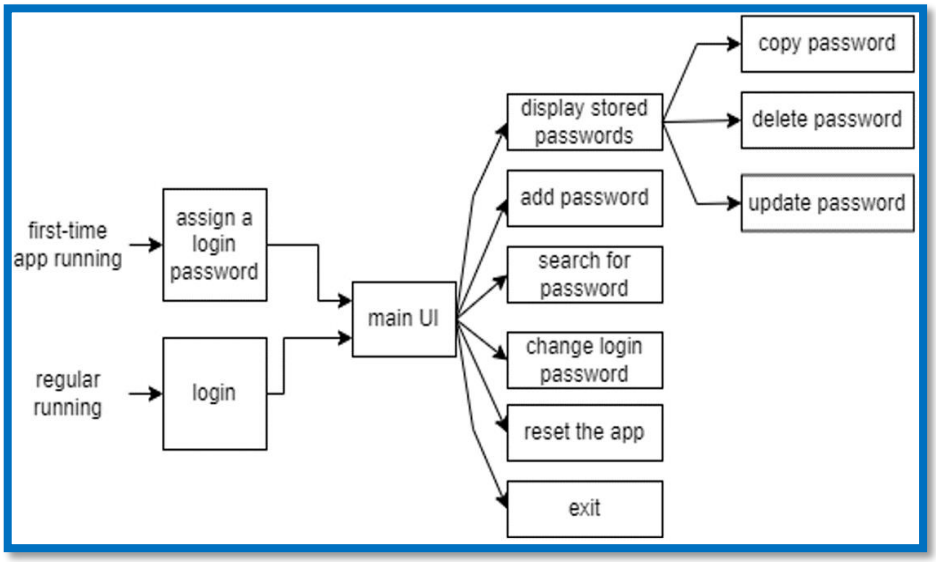

FIGURE 2: Diagram illustrating the workflow of UI functions execution.

Determining the main tasks and UI execution workflow provides a clear understanding and serves as a foundation for GUI building. These insights play a crucial role in shaping the background processes and programming logic required to implement all the application tasks. From a design perspective, each task can be visually represented on a single screen, and the most effective approach in Android development is to leverage the concept of activities. An Android activity represents a single screen that users see and interact with on their device **[9]**, serving as a window for the application to present its user interface.

Considering the nature of the tasks at hand, it becomes evident that certain tasks in our application necessitate dedicated activities, such as the login task and changing the login password. In contrast, others can be accommodated within the same activity, such as displaying the password list and performing a search. To address this situation, adopting a multiple-activity approach is recommended to ensure the appropriate graphical interface is built to cater to all tasks effectively.

4.2 Login-Password-Assigning Activity Design: Although this activity is not designated as the launch activity, it serves as the initial screen displayed to users after installing the application. The reason behind this design choice stems from the user requirements outlined in Section 2.1. Our application necessitates a login process to gain access, which, in turn, requires

a login password. Therefore, it is crucial to prompt the user to assign a login password before proceeding with any other actions within the application. The suggested layout components for this activity are depicted in **Figure 3**.

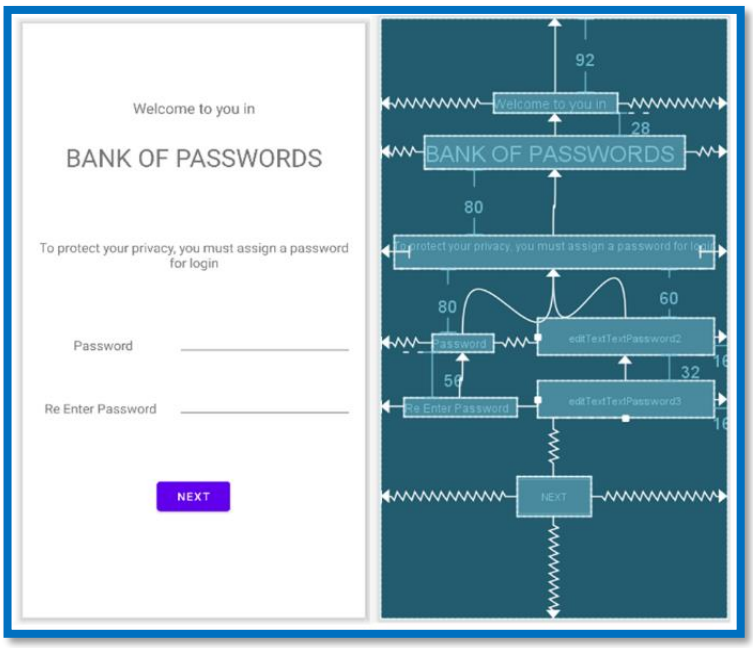

FIGURE 3: Layout design of the login-password-assigning activity.

(This layout consists of five TextViews for labeling, two EditText for getting login-password values, and a Button for executing.)

4.3 Login Activity Design: Once the user has been assigned a login password during the initial launch of the application, our app ensures user access verification in subsequent runs by initiating a login process. The user is granted entry only when the login password matches the correct value, as specified in the user requirements outlined in Section 2.1. Therefore, in regular app launches, it is imperative to display this activity as the first screen. The layout components for this activity are visually depicted in **Figure 4**.

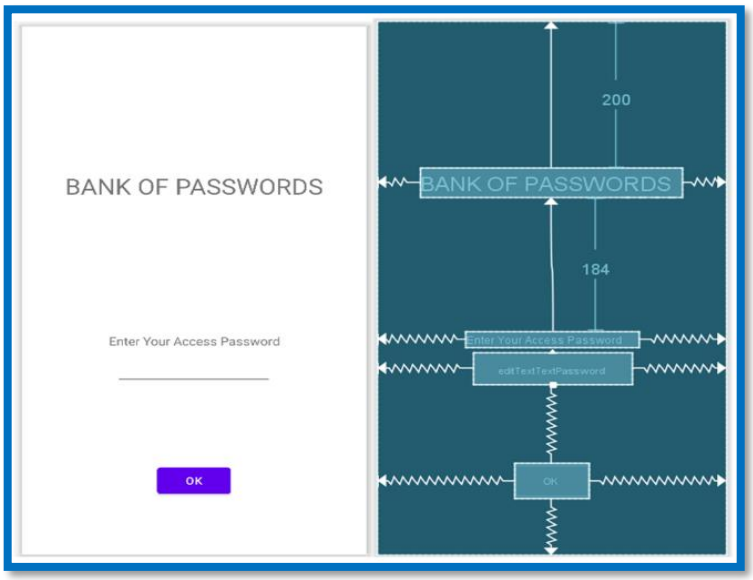

FIGURE 4: Layout design of the Login Activity

(This layout consists of five TextViews for labeling, two EditText for getting the values, on a Button for executing.)

4.4 Main Activity Design: The main activity is the central hub where the primary operations of the app take place, aligning with the execution workflow illustrated in **Figure 2**. The final UI layout design for this activity can be observed in **Figure 7**. The layout of this activity incorporates the following components:

- A constraint layout is utilized as the container for organizing all the elements.
- A TextView is positioned in the top left corner, dedicated to displaying the application name.
- An ImageView, clickable and located in the top right corner, features a settings icon. When clicked, it triggers the emergence of a Popup Menu, as demonstrated in **Figure 5**.
- A RecyclerView is situated in the middle of the screen, serving as a list to showcase the stored passwords. The proper functioning of this element requires the creation of a ViewHolder and an Adapter. The ViewHolder allows for customization of the appearance and behavior of each list element (list rows), while the Adapter is responsible for associating the data with the ViewHolder views. In our context, we recommend designing a custom ViewHolder layout that presents the information of each stored password (including the name and value), along with the relevant operations (update, copy, delete) for each list element, as depicted in **Figure 6**.
- A FloatingButton is included to facilitate the addition of new passwords.
- At the bottom of the screen, a SearchView is provided to enable password searching functionality.

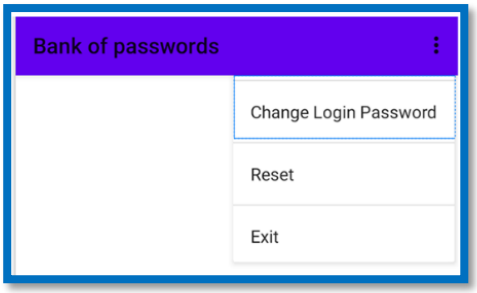

FIGURE 5: Layout design of the Setting Menu and its items.

(This layout consists of three items: change the login password, reset the application, and exit.)

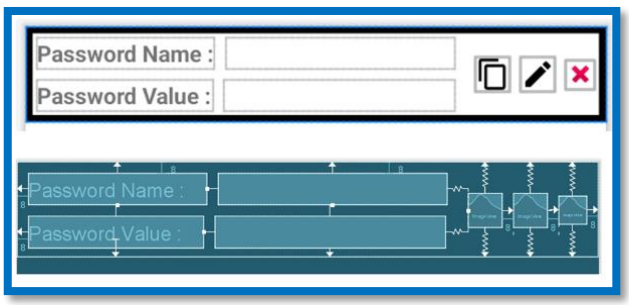

FIGURE 6: Layout design of the ViewHolder

(This layout contains: a constraint layout to hold all components; two TextViews for labeling; two TextViews for displaying password info; three clickable ImageViews for operations (copy, edit, delete)

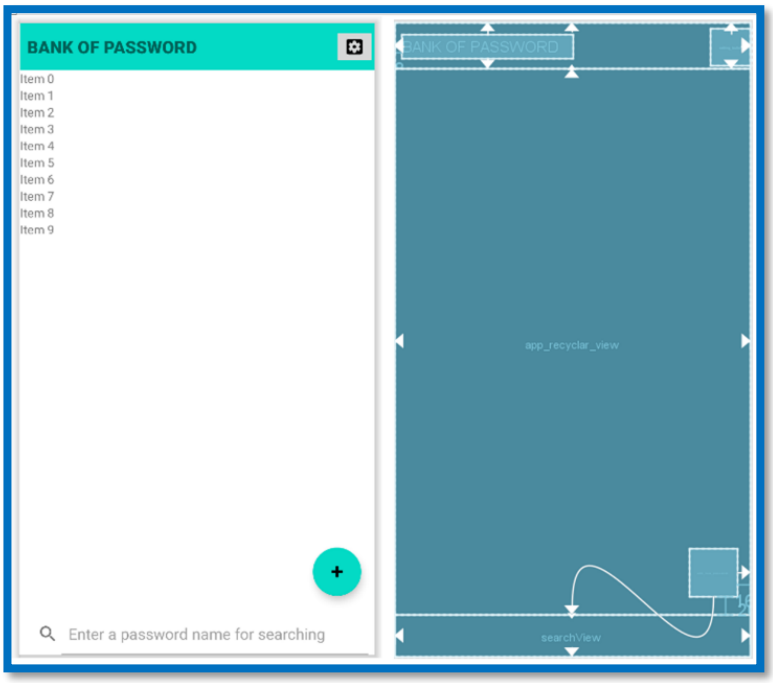

FIGURE 7. - Final layout design of the Main Activity.

4.5 Store-New-Password Dialog Design: When the user clicks on the floating button '+' in the main activity, depicted in **Figure 7**, a dialog containing a custom layout will be displayed. This dialog enables the user to add a new password. As per the user requirements mentioned in Section 2.1, each stored password should include two essential pieces of information: the name and the value. The layout design for this dialog is illustrated in **Figure 8**.

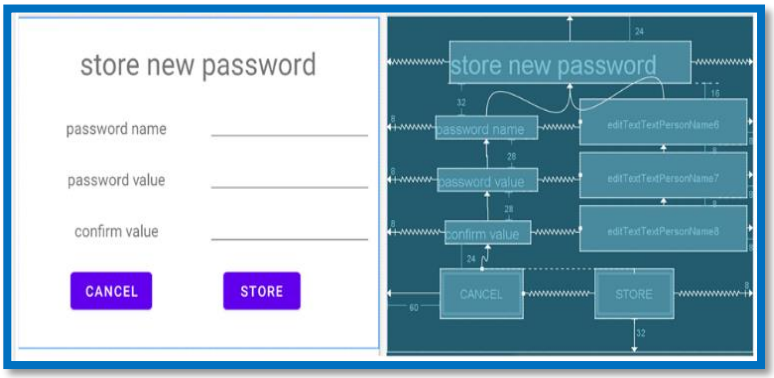

FIGURE 8: Layout design of the Store-New-Password Dialog

(This layout consists of a constraint layout for holding all components; four TextViews for labeling; three EditTexts to get the values; two buttons for actions (one for cancel and the other for adding)

4.6 Edit-Selected-Password Dialog Design: As depicted in **Figure 6**, the application provides the user with the capability to update the stored information (name or value) of any password listed by selecting the corresponding update button (pen icon) associated with that specific password. To accomplish this process, we need to design a suitable dialog that allows the user to enter the new values. The design of this dialog is presented in **Figure 9**.

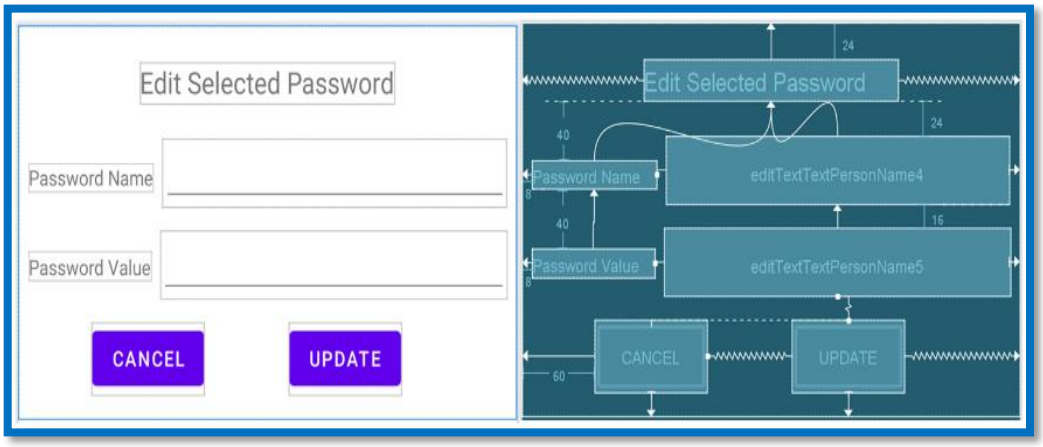

FIGURE 9: Layout design of the Edit-Selected-Password Dialog.

(This layout consists of a constant layout for containing all components; three TextView for labeling; two EditText to display the current values and edit them at the same time; two buttons one for cancellation, and the other for updating.)

4.7 Change-Login-Password Dialog Design: To enable the user to change the login password, a dialog should appear on the screen when the user selects the corresponding item in the setting menu (labeled as 'change login password' as shown in **Figure 5**). The design details of this dialog can be found in **Figure 10**.

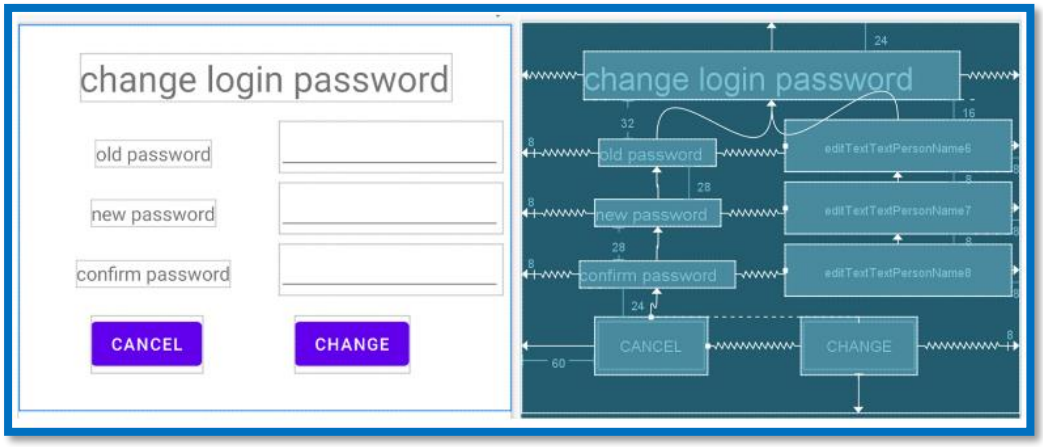

FIGURE 10: Layout design of the Change-Login-Password dialog.

(This dialog layout consists of a constant layout for containing all components; four TextView for labeling; three EditText to get the values; two buttons one for cancellation, and the other to change.)

4.8 The Rest of The Tasks: Upon revisiting the user requirements (in Sec.2.1), it becomes evident that the remaining tasks in our app (copying a password, deleting a password, resetting) do not necessitate the use of activities to fulfill their functions. These tasks no longer require data input or output. Instead, they may involve confirming or notifying dialogs (such as AlertDialog or Toast) to inform the user about their actions. The handling of these processes will be discussed in detail during the implementation of the back-end processes.

5. BACKGROUND PROCESSES IMPLEMENTATION:

Once the UI designing phase is finished, it is essential to establish the necessary connection between all application UI components and the corresponding programming logic to ensure their functionality aligns with user and technical requirements. To create a feasible roadmap for implementing the back-end processes, we propose defining a sequential flow for the execution of the application UI, starting from launch until exit. This planned sequence will serve as a guide for the implementation phase, as illustrated in **Figure 11**.

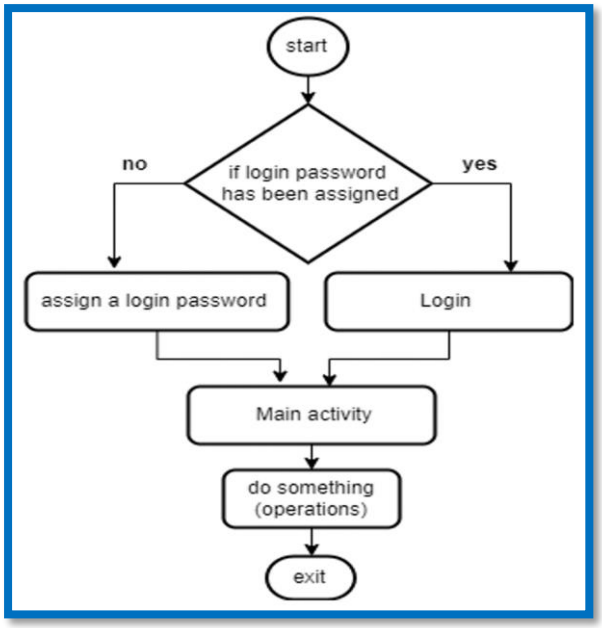

FIGURE 11: Sequential flow of application UI execution processes.

By examining the processing sequence depicted in **Figure 11**, we can deduce that the initial logic in our application involves verifying the state of the login password to determine the appropriate activity to launch. This situation encompasses two possible states: either the login password has been assigned or it hasn't. To accomplish this straightforwardly, we can create an empty activity (referred to as the Launch activity in Section 5.1) that solely performs the check to determine the true case, and subsequently deploys the corresponding activity accordingly.

5.1 Launch Activity: The Launch Activity serves as an empty activity running in a background thread. Its primary purpose is to check whether a login password has been previously saved or not, without the need for displaying any graphical user interface (GUI). This involves retrieving the stored login password, which requires determining the appropriate method of storing it within the application. In our case, the recommended approach is utilizing the SharedPreferences APIs, as suggested by the Android developers' website, as it is suitable for storing a small collection of data within our app **[10]**. Assuming the SharedPreferences APIs are employed, the role of this activity is to search the SharedPreferences for a previously stored

login password, allowing it to make the necessary decision, as illustrated in **Figure 12**. Consequently, this activity is designated as the default launch activity in our application, requiring modifications to be made to the manifest file.

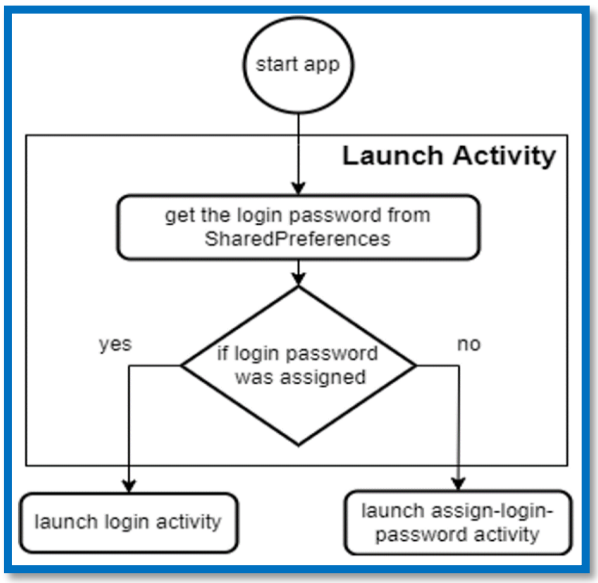

FIGURE 12: Flowchart illustrating the logic of the Launch Activity.

5.2 Login-Password Assigning Process: When the Login-password-assigning activity (in Sec. 6.2) is triggered (as depicted in **Figure 3**), the user is prompted to enter his password and proceed by tapping the 'NEXT' button. At this point, in accordance with the technical requirements (detailed in Sec. 2.2), the subsequent procedures should be sequentially executed in a background thread of the invoked activity:

1. Get password value: where two fields are holding the passwords that must be obtained (One for the password, and the other for confirming as shown in **Figure 3**).
2. Verify password value: checking the identically and length of the two values, where the length is a minimum of eight characters according to the user requirements (see Sec. 2.1). If those conditions are true, then the application can take any one of the two values as a login password.
3. Encrypt password value: In general, one-way hashing is one of the best security options in cryptography, where there are a lot of functions in this field such as MD5 and SHA256 **[11]**. In Android, the MessageDigest class provides the functionality of a message digest algorithm. Based on some recommendations to improve the security of the login process **[12]**, we intend to use the SHA-256 Hash function to generate a digest from the login password.
4. Store the generated digest: The generated digest will be stored as a Hex string in the SharedPreferences, as described clearly in **Figure 13**.

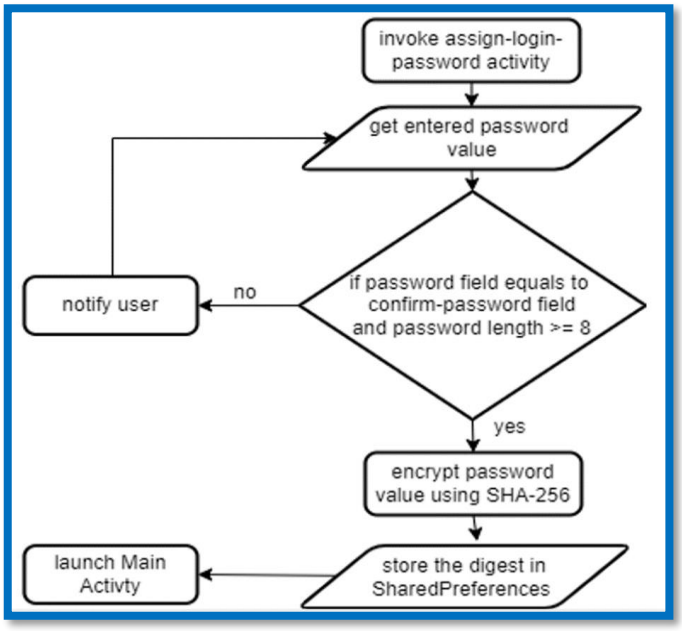

FIGURE 13: A flowchart illustrating the Login-password Assigning Process.

5.3 Login Process: Upon invocation of the login activity (as depicted in **Figure 3**), the user is prompted to enter his login password. Our objective in this stage is to generate a digest using SHA-256 from the entered value. This is achieved by converting the entered value to a Hex String as the initial step. Subsequently, the generated digest is compared with the stored digest. If the two digests are found to be identical, the login process is deemed successful, allowing the user to proceed to the main activity as outlined in the steps illustrated in **Figure 14**.

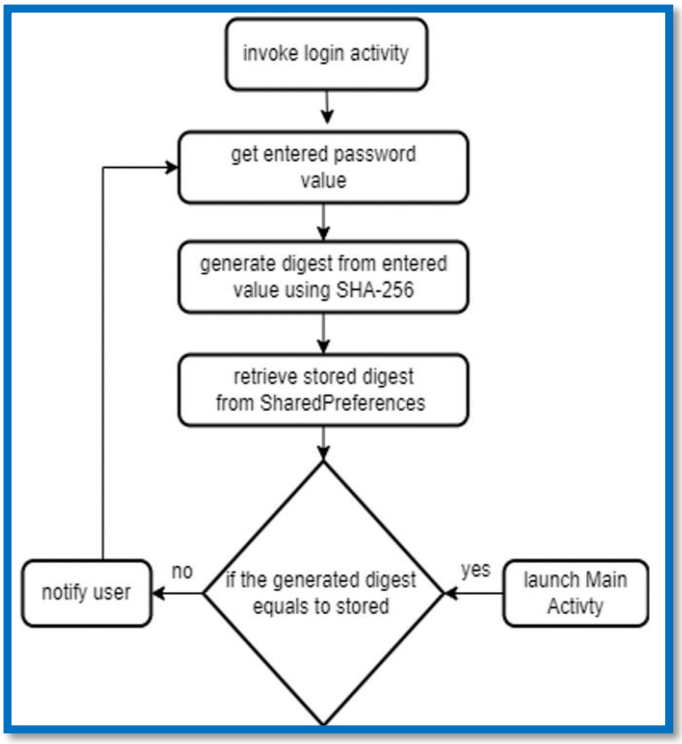

FIGURE 14: A Flowchart illustrating the login process.

5.4 Additional Login Method: In several cases, login using the traditional password method is not enough to provide the security level required to protect the data, because the login password is exposed to disclosure, which means we should employ other techniques and methods to increase the security level to protect user data (passwords). In this section, we will explore another technic that will be included with our app to enable login securely relying on user biometrics.

5.4.1 Login with fingerprint: Fingerprint technology in Android has become increasingly popular for authentication and authorization purposes, particularly in securing smartphones and protecting security-sensitive operations. It refers to biometric-based authentication and authorization using the fingerprint API. This API allows mobile apps to recognize and authenticate users based on fingerprints, providing better security for security-sensitive operations **[17]**.

To implement this feature in our app, first add the required dependencies, then get the necessary permissions:

- <uses-permission android:name="android.permission.USE_BIOMETRIC"/>
- <uses-permission android:name="android.permission.USE_FINGERPRINT"/>

To check if the user device can authenticate using fingerprint, android includes a class called `BiometricManager` which provides access to the biometric hardware and software on the device. If the checking process is complete with success (there is a sensor and stored fingerprint), it means that the device is ready for biometric authentication and waiting for the user to put his finger on the sensor. To execute the authentication task on a specific thread, we can use the 'Executor' class.

To handle the biometric authentication process, we can use the 'BiometricPrompt' class. To hold the information for the biometric prompt such as the title, the description, and the negative button text, we can use 'PromptInfo' class. Also, it is necessary to call 'onAuthenticationError' method for handling errors that occur during the authentication process, which is a useful process, especially for displaying the error message to the user. For checking the success or failure of authentication, the 'onAuthenticationSuccess' and "onAuthenticationFailed' methods are called to handle the two situations. Finally, If the fingerprint matches, the app will directly switch to the main activity, as explained clearly in **Figure 15**.

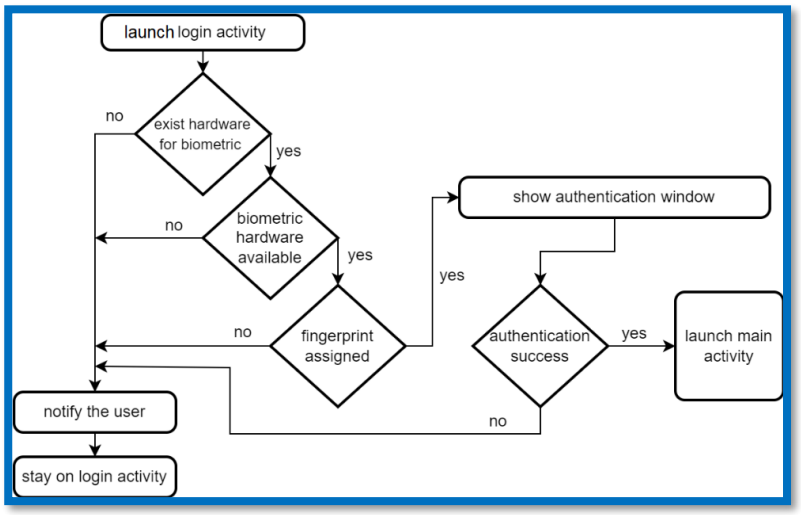

FIGURE 15: A flowchart describes the process of login using the fingerprint technique

5.5 Main Activity Processes: The main activity serves as the central component of our app, responsible for implementing the majority of its functions. The workflow within this activity starts by retrieving any stored passwords, if available, and preparing the RecyclerView to display them. To accomplish these tasks, it is crucial to establish an efficient storage mechanism for managing user passwords.

5.5.1 Passwords Storing Mechanism: To efficiently save data, the database concept is widely recognized, and in the context of Android OS, the SQLite database offers an ideal solution for managing repeated or structured data **[13]**. In our case, utilizing an SQLite database to store password information is highly suitable. Android treats the SQLite database as files stored in the device's internal storage. The necessary APIs for creating such a database can be found in the android.database.sqlite package. To construct the database, we can extend the SQLiteOpenHelper class and implement its methods. As stated in the user requirements (in Sec.2.1), each stored password consists of a name and a value. Therefore, a single table with two columns is sufficient for our needs, as depicted in **Figure 16**.

Once the implementation of the SQLite database is completed, the next step is to create an instance, either readable or writable, in the main activity. This instance will be responsible for building the database in a background thread to prevent any long-running operations. With the database successfully created, we gain the flexibility to perform various operations such as reading, inserting, deleting, or updating the database from any part of our application code.

Password_table	
Password Name *	TEXT
Password value	TEXT

FIGURE 16. – SQLite database schema for password storage

5.5.2 Storing New Passwords: When the user clicks on the '+' button as illustrated in **Figure 7**, the main activity should launch the corresponding dialog to enable the user to add new passwords as shown in **Figure 8**. Adhering to the technical requirements outlined in Section 2.2, the following procedures are performed in the background to facilitate the addition of new passwords:

1. Get and Confirm: First, get the entered name and check if other stored passwords have the same name by searching the database, then notify the user. Second, get the two entered passwords' values; and verify their identically, where this process is critical in case of users' mistype. If identical is approved, one of the values will be adopted.
2. Displaying: Add the new passwords to the RecyclerView.
3. Encrypting: For encrypting new passwords, we intend to use AES in CBC mode with 256-bit keys to provide a higher level of security and robustness against attacks. Using AES in CBC mode with a 256-bit key will ensure the data's confidentiality and integrity, making it suitable for applications requiring high-security levels **[14]**. The CBC mode has been modified to enhance the security of encrypted data by protecting against bit-flipping attacks and adding an integrity approach using the keyed-hash function **[15] [16]**. Also, using a 256-bit key in AES further strengthens the security of the encryption, making it more resistant to brute-force attacks and Grover's quantum search algorithm **[14]**. To meet technical requirements (in Sec. 2.2), the digest of the login password will be used for encrypting with this algorithm as a key, noting that the algorithm and the digest have the same length.
4. Storing: Store generated bytes from the encrypted password value with its corresponding name in the SQLite database, then dismiss the dialog (shown in **Figure 8**). Moreover, executing the encryption and storing processes in a separate thread would avoid hanging the UI thread. The sequence of the entire process is shown clearly in **Figure 17**.

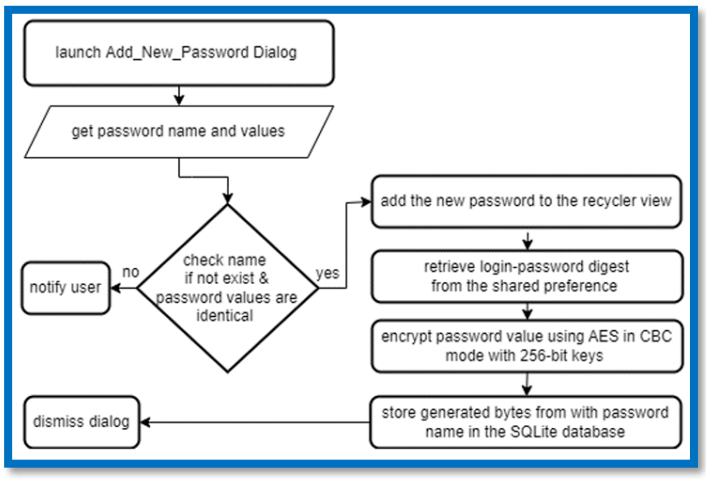

FIGURE 17: A flowchart describes the Storing-New-Passwords process

5.5.3 Displaying stored passwords: Upon launching the main activity, a checking process is initiated to verify the presence of any stored passwords within the SQLite database. If passwords are found, they are retrieved as a List containing password information such as names and values. Subsequently, the password values in the list are decrypted using a reversed encryption approach. Finally, the resulting list is utilized to populate the RecyclerView, ensuring the display of the stored passwords. The sequential workflow for this process is depicted in **Figure 18**.

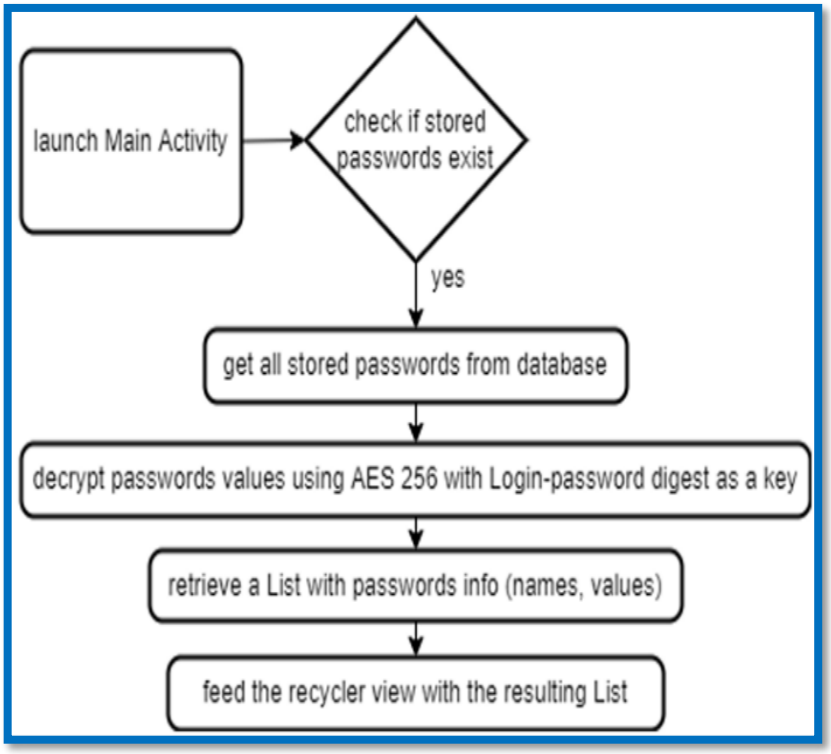

FIGURE 18A: flowchart depicts the execution process of displaying stored passwords.

Let us recall that each stored password will be accompanied by three buttons (icons) - delete, edit, and copy - as depicted in **Figure 6**. The implementation of those procedures should be incorporated within the RecyclerView adapter class, specifically in the onBindViewHolder method, as outlined below:

- Delete password: Remove the selected password from the database after receiving user confirmation, and then update the RecyclerView to reflect the changes.
- Edit password: Launch the Edit-Selected-Password Dialog (as depicted in **Figure 10**) to obtain new values from the user. Encrypt the password value and store it, along with its name, in the SQLite database. Finally, update the information of the respective password, as illustrated in **Figure 19**.
- Copy password: Copy the value of the selected password to the clipboard.

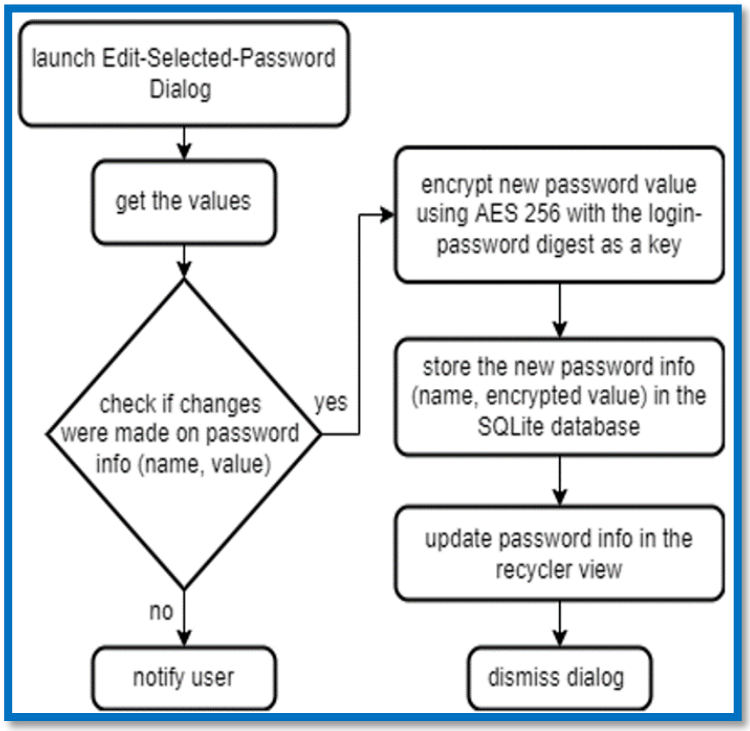

FIGURE 19: A flowchart outlining the Edit-Stored-Passwords process

5.5.4 Search for Passwords: To enable users to search for a stored password within the application, we have incorporated a SearchView widget. The SearchView located at the bottom of the main activity layout as depicted in **Figure 7**, allows users to enter a password name and view suggestions or results. When the user enters a password name in the search view, the RecyclerView is filtered based on the input text to display matching passwords, ensuring relevant results are displayed.

5.5.5 Setting Menu Items: As depicted in **Figure 5**, the setting menu consists of three items: "Change login password," "Reset," and "Exit." When the user selects any of these items, the corresponding functionality is executed in the background of the Main Activity. The implementation logic for each setting menu item is as follows:

- Change login password: To change the login password, the associated dialog (as shown in **Figure 10**) is displayed. The user must enter the valid old password along with the new password values, ensuring that the new password fields match and meet the required length conditions. The next step involves generating a new SHA256 digest from the new password value and replacing the old stored digest (in shared preference) with the new one. However, the process doesn't end here. After changing the login password and relaunching the application, the Main Activity (as shown in **Figure 18**) attempts to decrypt all password values (in the SQLite database) using the old digest as a key, resulting in incorrect plaintext. Therefore, it becomes necessary to retrieve and

re-encrypt all stored passwords with the new digest using the same AES 256 encryption approach, as described in detail in **Figure 20**.

- Reset: Resetting the app involves dropping the passwords table in the SQLite database, removing the stored login-password digest from shared preference, and returning the application to the Launch Activity, as demonstrated in **Figure 21**.
- Exit: This task entails finishing all activities and exiting the application.

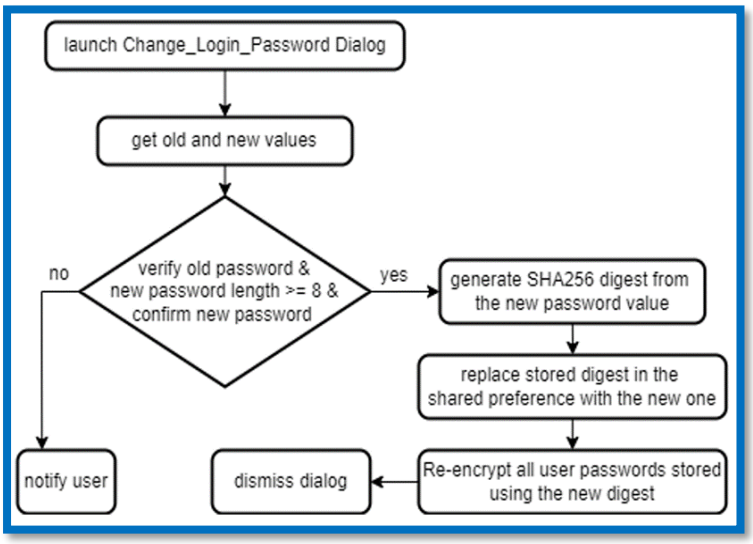

FIGURE 20: A Flowchart illustrating the Change-Login-Password process

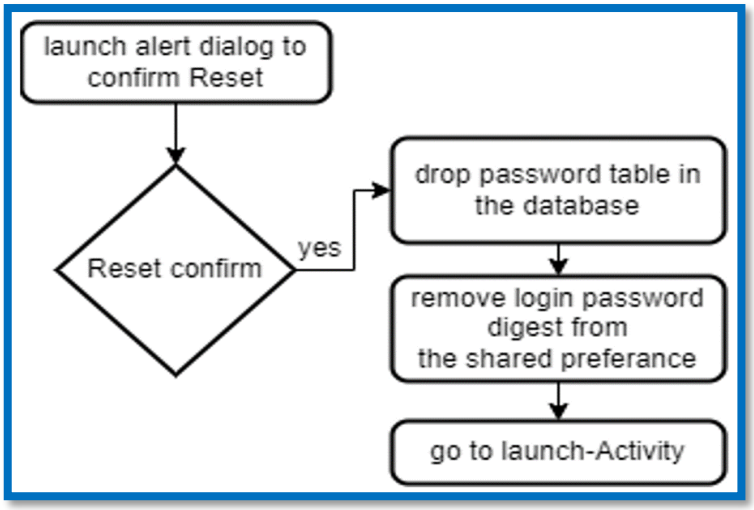

FIGURE 21: A flowchart describes how the reset process will be executed

6. TEST THE APP:

After generating the APK file, the app size was 3.91 MB. When testing the app on Android devices running with API levels 26 to 32, all the required functions worked correctly. The testing began with the first launch, where a login password needed to be assigned. Assuming the login password value was set to '12345678', the generated digest was stored directly in the SharedPreferences after encoding its bytes with Base64, resulting in the value

'73l8gRjwLftklgfdXT+MdiMEjJwGPVMsyVxe16iYpk8='. Also, The user can login using his fingerprint if it was assigned to the device, where this feature works perfectly on devices with Android 7.1 (Nougat1) and above.

During the testing of adding a new password, the password value was encrypted correctly using the stored digest as a key for the AES algorithm. For example, if a new password with the value 'pass1234' was added, the encrypted value to be stored after encoding its bytes with Base64 would be '6m0edekTY3MSbe+2OVhdaQ==='. When relaunching the app, the login procedure had to be followed by entering the correct login password. The app was then able to decrypt and display all the stored passwords in the SQLite database correctly.

In the testing phase, the login password was changed to 'computer'. The old digest was replaced directly with the new one, resulting in the value 'qpcwIVD86BFCXNhFNwKKWvvjfj8TYq1FpR1Gfhev3Jw='. The value of the previously added password "pass1234" was re-encrypted using the newly generated digest, resulting in the value 'jTf9UOE7BE/MIRpQt2oD/Q==='. However, when attempting to run the application on older devices with API level 25 or lower, it failed to launch due to the minSdk version used during development.

7. CONCLUSIONS:

As individuals, we often encounter difficulties in managing and remembering multiple passwords. The more passwords we have, the greater the risk of forgetting them and losing access to our accounts, which is a common scenario. To address this challenge, some people resort to traditional methods such as writing passwords on paper or storing them in cloud services like Google Drive. However, these approaches are flawed and can easily lead to unauthorized access by attackers or malicious individuals.

Instead of relying on traditional methods, developing an Android application specifically designed for users with Android OS devices can provide a convenient and portable solution. However, implementing such an application requires careful consideration of security aspects and usability. To ensure secure access, a login process must be enforced, requiring users to verify their identity with a password.

Storing passwords in their raw form within the device is not advisable as it poses the same risks as traditional methods. The passwords' values would be easily accessible in the database, making them vulnerable to inspection or cracking attempts. Therefore, it is crucial to store

passwords securely, and encryption is a reliable solution. Similarly, the login password should not be stored in plaintext. Hashing is an appropriate approach to make the login password unreadable.

Using the SHA256 algorithm for hashing the login password and AES for encrypting the user's stored passwords is recommended to increase the security level. Utilizing the generated digest from the login password as a key for AES encryption further strengthens the overall encryption process. By adopting these measures, users can benefit from a more secure and robust password management solution.

- **FUNDING:** None
- **ACKNOWLEDGEMENT:** None
- **CONFLICTS OF INTEREST:** The author declares no conflict of interest.

- **AVAILABILITY OF PROJECT AND CODES**
  - Our application project 'Bank of Passwords' is available on GitHub and can be accessed via: https://github.com/Hussein-abd-alkhaleq/Bank-of-Passwords
  - DOI of the project: 10.5281/zenodo.8017281

8. REFERENCES

[1] Gaw S, Felten EW. Password Management Strategies for Online Accounts. Proceedings of the Second Symposium on Usable Privacy and Security. 2006;44–55. https://doi.org/10.1145/1143120.1143127.

[2] Florêncio D, Herley C, van Oorschot PC. Password Portfolios and the Finite-Effort User: Sustainably Managing Large Numbers of Accounts. In: 23rd USENIX Security Symposium (USENIX Security 14). Aug. 2014;575–590. [Online]. Available: https://www.usenix.org/conference/usenixsecurity14/technical-sessions/presentation/florencio.

[3] Mobile Operating System Market Share Worldwide. Statcounter GlobalStats, Sep. 03, 2023. Available: https://gs.statcounter.com/os-market-share/mobile/worldwide . [Accessed: Sep. 03, 2023].

[4] Kujala S, Kauppinen M, Rekola S. Bridging the gap between user needs and user requirements. In: Advances in Human-Computer Interaction I (Proceedings of the Panhellenic Conference with International Participation in Human-Computer Interaction PC-HCI 2001). Typorama Publications, 2001;45–50.

[5] Wihidayat ES. Pengembangan Aplikasi Android Menggunakan Integrated Development Environment (Ide) App Inventor-2. 2017.

[6] New Android App Bundle and target API level requirements in 2021. Android Developers, Nov. 19, 2020. Available: https://android-developers.googleblog.com/2020/11/new-android-app-bundle-and-target-api.html . [Accessed: Sep. 04, 2023].

[7] Putranto BP, Saptoto R, Jakaria OC, Andriyani W. A Comparative Study of Java and Kotlin for Android Mobile Application Development. 2020 3rd International Seminar on Research of Information Technology and Intelligent Systems (ISRITI). 2020;383–388.

[8] Bose S, Mukherjee M, Kundu A, Banerjee M. A comparative study: java vs kotlin programming in Android application development. Int J Adv Res Comput Sci. 2018;9(3):41–45.

[9] Gargenta M. Main building blocks. In: Learning Android. Sebastopol, California, O'Reilly Media, Inc., 2011;28–29.

[10] Iamnitchi A, Ripeanu M, Santos-Neto E, Foster IT. The Small World of File Sharing. IEEE Transactions on Parallel and Distributed Systems. 2011;22:1120–1134.

[11] Rachmawati D, Tarigan J, Ginting A. A comparative study of Message Digest 5 (MD5) and SHA256 algorithm. Journal of Physics: Conference Series. 2018;978:012116.

[12] Ebanesar T, Suganthi G. Improving Login Process by Salted Hashing Password Using SHA-256 Algorithm in Web Applications. International Journal of Computer Sciences and Engineering. 2019.

[13] Liu H, Yang L, Wu H. Design of Embedded Data Acquisition and Management System Based on SQLite Database. 2022 11th International Conference of Information and Communication Technology (ICTech). 2022;335–338.

[14] Alslman YS, Ahmad A, AbuHour Y. Enhanced and authenticated cipher block chaining mode. Bulletin of Electrical Engineering and Informatics. 2023.

[15] Wade S. Description of Image Encryption Using AES-256 bits. International Journal for Research in Applied Science and Engineering Technology. 2023.

[16] Nugrahantoro A, Fadlil A, Riadi I. Optimasi Keamanan Informasi Menggunakan Algoritma Advanced Encryption Standard (AES) Mode Chiper Block Chaining (CBC). Jurnal Ilmiah FIFO. 2020.

[17] ElMouatez B, Karbab M, Mourad D, Debbabi A, Abdelouahid Derhab D, Djedjiga Mouheb. Fingerprinting Android Malware Packages. 2021. doi: 10.1007/978-3-030-74664-3_3.

Al-Kitab Journal for Pure Sciences (2024); 8(1):63-70.
https://doi.org/10.32441/kjps.08.01.p6

Al-Kitab Journal for Pure Sciences
ISSN: 2617-1260 (print), 2617-8141(online)
https://isnra.net/index.php/kjps

Apricot addition for Enrichment Yogurt with Amygdalin

Hagar F. Forsan[1*], Monier M. El Abd[2], Wafaa B. Elsabie[1], Hassan M. Sobhy[3]

[1] Dairy Chemistry Research Department, Animal Production Research Institute (APRI), Agricultural Research Center (ARC), Giza, Egypt
[2] Dairy Science Department, Faculty of Agriculture, Cairo University, Giza, Egypt
[3] Department of Natural Resources, Faculty of African Post Graduated Studies, Cairo University, Giza, Egypt

*Corresponding Author: hagarfathy@pg.cu.edu.eg

Citation: Forsan HF, El-Abd MM, Elsabie WB, Sobhy HM. Apricot addition for Enrichment Yogurt with Amygdalin. Al-Kitab J. Pure Sci. [Internet]. 2024 Apr. 02 [cited 2024 Apr. 01];8(1):63-70. Available from: https://doi.org/10.32441/kjps.08.01.p6.

Keywords: Yogurt, Apricot, Apricot kernel, Amygdalin, nutritive value.

Article History
Received 05 Feb. 2024
Accepted 23 Mar. 2024
Available online 02 Apr. 2024

Abstract:

The objective of the present research was to enrich yogurt with amygdalin (vitamin B17) and increase the nutritional value of yogurt using apricot and a by-product of apricot fruit kernels. Amygdalin was considered an antibacterial, hepatic protecting, anti-tumor, antifungal, anti-inflammatory, anti-coagulant, anticancer, antiaging, antidiabetic, anti-atherosclerotic, anti-angina, and antioxidant. Apricots that were mixed in a blinder for 3 min and filtered were used as a source of dietary fiber, lipids, proteins, minerals, and vitamins. Apricot kernels that were heated for 2 minutes at 120 ˚C. then cold and grind in a blender were used as a source of amygdalin (B17). Obtained results showed that the incorporation of apricot and apricot kernel is considerably impacted by the addition of apricot and apricot kernel 5% Apricot pulp + 1% Apricot kernel and 10% Apricot pulp + 2% Apricot kernel 1.42, 2,92 mg/100gm respectively.

Keywords: Yogurt, Apricot, Apricot kernel, Amygdalin, nutritive value.

اضافة المشمش لتدعيم الزبادى بالاميغدالين

هاجر فتحى فرسان[1*]، منير محمود العبد[2]، وفاء بديع السبع[1]، حسن محمد صبحى[3]

[1]قسم بحوث كيمياء الالبان، معهد بحوث الانتاج الحيوانى، مركز البحوث الزراعية، الجيزة، مصر

[2]قسم تكنولوجيا الالبان، كلية الزراعة، جامعة القاهرة، الجيزة، مصر

[3]قسم الموارد الطبيعية، كلية الدراسات الافريقية العليا، جامعة القاهرة، الجيزة، مصر

hassansobhy20@yahoo.com, wafa.elsabie@arc.sci.eg, Moniur.Ibrahim@agr.cu.edu.eg, hagarfathy@pg.cu.edu.eg

الخلاصة:

تهدف الدراسه الحالية الى تدعيم الزبادى بالاميجدالين (فيتامين ب ١٧) و زيادة القيمة الغذائية للزيادة عن طريق اضافة المشمش و نواة المشش كمنتج ثانوى. يعتبر الاميغدالين مضاد للبكتريا و حماية الكبد و ،مضاد للاورام و الفطريات و الالتهابات و التخثر و السرطان و الذبحة الصدرية و تصلب الشرايين و الشيخوخه. تم عصر المشمش فالخلاط لمدة ٣ دقائق و تصفيته حيث يستخدم كمصدر للالياف الغذائية و الدهون و البروتين و الفيتامينات و الاملاح المعدنية. تم تسخين نواة المشمش ١٢٠ درجة مئوية لمدة دقيقتين ثم تركه ليبرد و طحنه فالمطحنة حيث يستخدم كمصدر للاميغدالين (فيتامين ب ١٧). تم استخدام المشمش الذي تم خلطه في الخلاط لمدة ٣ دقائق وتصفيته وذلك كمصدر للألياف الغذائية والدهون والبروتينات والمعادن والفيتامينات. تم تسخين حبات المشمش لمدة دقيقتين عند ١٢٠ درجة مئوية. ثم تركها لتبرد و تخلط في الخلاط. أظهرت النتائج الى ان محتوى الأميغدالين فالزبادى الطازج المعد من ٥٪ مشمش + ١٪ نواة المشمش كان ١,٤ ملجم/١٠٠ جرام و المعد من ١٠٪ مشمش + ٢٪ نواة المشمش ٢,٩ ملجم/ ١٠٠ جرام على التوالى.

الكلمات المفتاحية: الزبادى، المشمش، نواة المشمش، الأميغدالين، القيمة الغذائية.

1. Introduction:

Each person's eating habits determine how they should be fed, although all humans eat to maintain their health by consuming the nutrients found in food, particularly in fruits and vegetables [1, 2]. One of the most well-known fruits is apricot, which holds significant value due to its composition, which allows it to have a significant role in human nutrition and be utilized in a variety of non-food products. In terms of proteins (8%), sugars (more than 60%), crude fat (2%), crude fibers (11.50%), total minerals (4%), vitamins (vitamins A, C, K, and B), and reasonable levels of organic acids (malic and citric acids) [3]. Apricots are a fruit with a high nutritional richness [4, 5]. The apricot kernel contains exceptional nutritional value, much like the fruit. Particularly high in fat, protein, and dietary fiber overall, apricot kernels may be beneficial for human nutrition. Numerous research organizations have extensively examined the chemical and nutritional properties of apricot kernels [6].

Rosaceae nuclei are the source of the naturally occurring chemical amygdalin (D-mandelonitrile-b-D-glucoside-6 b-glucoside) [7]. It's a cyanogenic glycoside present in several

fruits, including apricots. Amygdalin views it as a natural cancer treatment [8], antibacterial, hepatic protecting, anti-tumor, antifungal, anti-inflammatory, anti-coagulant, anticancer, antiaging, antidiabetic, anti-atherosclerotic, anti-angina, and antioxidant are only a few of the pharmacological properties of apricot kernels that have been documented [9, 12]. Additionally, apricot kernels have a significant role in both the management and prevention of chronic illnesses [5, 13].

These advantageous health effects are brought about by the presence of bioactive ingrediens such as cyanogenic glycosides, Carotenoids, fatty acids, volatile substances, and polyphenols [5- 14]. Algeria is one of the world's top producers of apricots [15]. The majority of the country's apricot crop is used for fresh or dried fruit, as well as for making jam and juice. Apricot kernels have long been regarded as trash in all these applications. Because agricultural wastes are readily available, biodegradable, and most importantly, less expensive, there has been an increased focus on their utilization in recent times [16, 17]. Because of this, researchers have invested in the value-adding of apricot fruits by recovering and using their seeds [18, 19]. Nevertheless, because apricot kernels contain amygdalin (cyanogenic glycoside, commonly referred to as laetrile or vitamin B17), which is hazardous when ingested in quantities higher than recommended, their usage in food is restricted. Despite this, considering their advantageous health effects, researchers have suggested that apricot kernels can be added to specific meal preparations [10-20].

This study focuses on increasing Amygdalin and the nutritional value of yogurt by using apricots and apricot kernels supplement, as they represent some of the waste resulting from the manufacture of juice, jam, etc. The Purpose for apricot juices is also to mask apricot kernel taste.

2. Materials:

The Ministry of Agriculture's Animal Production Research Institute herd provided fresh cow's milk. Apricots and sucrose sugar were acquired from a local marketplace. The laboratories of Chr. Hansen in Copenhagen, Denmark. CMC. provided a yogurt culture including Streptococcus thermophiles and Lactobacillus delbrueckii subsp. bulgaricus. Sigma-Aldrich was the source of amygdalin (98% purity), diethyl ether (98%), methanol, and HPLC-grade ethanol (98%).

3. Methods:

3.1 Preparation of apricot yogurt:

To make apricot pulp, mix in a blinder for three minutes, then filter. The apricot kernel was heated for 2 minutes at 120 ˚C., then let it cool after that grind it in a blinder. For 20 minutes,

fresh cow milk and 5% sugar were heated to 80°C. This milk was split into three identical portions. The 1st considered as control, 5 % Apricot juice + 1 % apricot kernel and 10 % Apricot juice + 2 % apricot kernel were added to the 2nd and the 3rd portions respectively. The three portions were inoculated with 3% yogurt culture. The chemical properties of the made apricot yogurt and its control were evaluated both during its fresh state and after a week of refrigeration at 6± 1˚C**.**

3.2 Chemical analysis:

Total protein, fiber and Total lipids, Cyanide content and acidity were determined **[21]**. Total flavonoids were determined **[22]**. Total phenolics were determined **[23]**. Mg, K, and Ca: An innovative microwave digestion system was used to determine the values of Mg, K, and Ca. Thermo Scientific's Icap6000 series inductively coupled plasma (ICP-AES) is used to determine calcium, magnesium, and potassium. Argon gas excites an elemental atom. For every element, the sample values assumed the blank values. potassium calculated using the formula **[24]**. Amygdalin calibration curve: A stock 1, solution of 100 µg ml -1 was created by dissolving the amygdalin standard in water, and it was kept at 20 C until analysis. Six standard solutions containing 1, 5, 10, 20, 40, and 50 µg ml -1 of amygdalin were used to create a calibration curve **[25]**. Amygdalin extraction: Five grams of apricot kernels were blended, and two grams were weighed into a 200-milliliter conical flask. After adding 50 ml of water, the flask was put in a water bath with shaking at 37 °C. The extraction of amygdalin used 40,80,100,120, and 180 minutes. After filtering via Whatman No. 1 filter paper, the extracts were put into 50 ml plastic polypropylene tubes. Three times fat extractions were made by vortexing (20 ml) of n-hexane for one minute. The tubes were spun for 10 minutes at 3250 g using a benchtop Eppendorf 5810R centrifuge. Supernatants were combined and thrown away. The remaining hexane was removed from the sample using a rotary evaporator operating at low pressure, 35 degrees Celsius, and 7 millibars **[25].**

Sensory evaluation: All samples were evaluated as the organoleptic properties included flavor (20 points); body & texture (10 points) and Color and appearance (10 points) **[7]**.

4. Statistical analysis:

Differences between samples were tested using a one-way analysis of variance using the COSTAT program and Standard deviation (SD) was calculated by Excel program**.**

4.1 The functional properties and chemical composition of apricot and apricot kernel:

Table 1 illustrates the chemical composition of apricot pulp and kernel while the Total protein was 6.4, 14.04 g/100 gm. These results are in accordance with the findings of **[26]**. Chemical composition results are in accordance with the findings of **[5]**. Amygdalin is not

detected in Apricot pulp. Apricot pulp contains 0.001 ± 0.10 HCN mg/gm on the other wise Apricot kernel contains 0.005 ± 0.001 gm/100 gm. Given that the lethal dose of HCN for an adult is 0.54 mg/kg of body weight, this is safe [27].

Table 1. Chemical composition of Apricot pulp and Apricot kernel

	Apricot pul (g/100gm)	Apricot kernel (g/100gm)
Total phenols	0.072 ± 0.001	0.18 ± 0.001
Total flavonoids	0.012 ± 0.001	0.05 ± 0.000
Total protein	06.41 ± 0.02	14.04 ± 0.02
Total lipid	01.40 ± 0.01	08.34 ± 0.01
Total fiber	14.04 ± 0.02	30.54 ± 0.01
Ca	0.17 ± 0.001	0.20 ± 0.001
K	2.94 ± 0.001	0.65 ± 0.001
Fe	0.0031 ± 0.002	0.0004 ± 0.000
Amygdalin	Not Detected	0.16 ± 0.01
HCN	0.001 ± 0.001	0.005 ± 0.001

4.2 Chemical composition of apricot yogurt:

The chemical composition of the control and yogurt supplemented with different treatments of Apricot and apricot kernel is presented in **Table 2** for fresh and stored yogurt. The data show that Amygdalin that is not detected in control and treatment 10% Apricot pulp + 2% Apricot kernel yogurt had a higher total protein, Total lipid, and Amygdalin contents being 4.32, 4.73, and 2.92 respectively **.**

The mean average of total protein, total lipid, and amygdalin contents of 5% Apricot pulp + 1% Apricot kernel yogurt and 10% Apricot pulp + 2% Apricot kernel yogurt samples increased with the advancing storage period at 6 ± 1 ˚C for 7 days which may be due to the evaporation of water and loss of moisture during the storage period.

Table 2. Chemical composition of apricot yogurt

Treatments	Control	5% Apricot pulp + 1% Apricot kernel yogurt	10% Apricot pulp + 2% Apricot kernel yogurt
Fresh Yogurt			
Total protein	3.41 ± 0.01c**	3.86 ± 0.01b**	4.32 ± 0.01a*
Total lipid	3.9 ± 0.01c*	4.36 ± 0.01b*	4.73 ± 0.01a*
Amygdalin	Not Detected	1.42 ± 0.01b*	2.92 ± 0.01a*
Stored yogurt (After 7 days			
Total protein	3.44 ± 0.01c*	3.95 ± b*	4.34 ± 0.01a*
Total lipid	3.93 ± 0.01c*	4.36 ± 0.01b*	4.9 ± 0.01a**
Amygdalin	Not Detected	1.44 ± 0.02b*	2.93 ± 0.01a*

Each value represents the mean ± S.E (Standard Error) and mean of three replicates. Values in the same column with the same letter are not significant at p≤0.05**.**

4.3 The acidity of apricot yogurt:

Table 3 indicated that significant increase in acidity with added 5 and 10 % apricot pulp and 1 + 2 % apricot kernel in fresh. The acidity percentage of 5% Apricot pulp + 1% Apricot kernel yogurt and 10% Apricot pulp + 2% Apricot kernel yogurt samples increased with the advancing storage period at 6 ± 1 ˚C for 7 days which may be due to the Production of lactic acid by yogurt culture during the storage period for 7 days at 6 ± 1 ˚C.

Table 3. The acidity of apricot yogurt

Treatments	Control	5% Apricot pulp + 1% Apricot kernel yogurt	10% Apricot pulp + 2% Apricot kernel yogurt
Fresh Yogurt			
Acidity %	0.6 ± 0.1a**	0.8 ± 0.1b**	0.9 ± 0.1a**
Stored yogurt (After 7 days)			
Acidity %	0.7 ± 0.1a*	0.9 ± 0.1b*	1.0 ± 0.1a*

Each value represents the mean ± S.E (Standard Error) and mean of three replicates. Values in the same column with the same letter are not significant at p≤0.05.

4.4 Sensory evaluation of apricot yogurt:

Scores of sensory properties of yogurt are given in **Table 4**. Sensory properties were evaluated in fresh and after 7 days of storage period. Higher values were given by the panelists for the flavor, texture, and appearance of fresh control yogurt than stored yogurt. At fresh yogurt, 5% Apricot pulp + 1% Apricot kernel recorded the highest total scores (37 and 37) followed by treatment 10% Apricot pulp + 2% Apricot kernel. The same trend was also recorded after the storage period (7 days). Fresh control yogurt and fresh 5% Apricot pulp + 1% Apricot kernel are the best values than other treatments after storage.

Table 4. sensory evaluation of adding apricot kernels and pulp on yogurt

Treatments	Flavor (20)	Body and texture (10)	Color and appearance (10)	Total scores (40)
Fresh yogurt				
Control	19 ± 1	8 ± 1	9 ± 1	37
5% Apricot pulp + 1% Apricot kernel	19 ± 1	9 ± 1	9 ± 1	37
10% Apricot pulp + 2% Apricot kernel	17± 1	8 ± 1	8 ± 1	33
Stored yogurt (After 7 days)				
Control	19 ± 1	8 ± 1	9 ± 1	36
5% Apricot pulp + 1% Apricot kernel	17 ± 1	8 ± 1	8 ± 1	33
10% Apricot pulp + 2% Apricot kernel	16 ± 1	7 ± 1	7 ± 1	30

5. Conclusion

It could be concluded through this study, that it is possible to produce yogurt supplemented with apricot and apricot kernel rich in many important nutritional components such as vitamins such as amygdalin, minerals, protein, fat, and fibers.

6. References

[1] Forsan HF, Hassan RS. Novel Nutraceutical Milk Compound in Alzheimer's Prevention. In: Mohamed E, editor. Handbook of Neurodegenerative Disorders. Singapore: Springer; 2023.

[2] M.Sobhy H, Abd ME, Elsabie W, Forsan HF. Study of high nutritive value of almond milk milk beverage. Plant archives 2021;21:2493-6.

[3] Forsan HF, Awad SS. Cyanidin: Advances on Resources, Biosynthetic Pathway, Bioavailability, Bioactivity, and Pharmacology. In: Xiao J, editor. Handbook of Dietary Flavonoids. Cham: Springer International Publishing; 2023. p. 1-50.

[4] Sarıdaş MA, Ağçam E, Ünal N, Akyıldız A, Kargı SP. Comprehensive quality analyses of important apricot varieties produced in Türkiye. Journal of Food Composition and Analysis. 2024;125:105791.

[5] Fatima T, Bashir O, Gani G, Bhat T, Jan N. Nutritional and health benefits of apricots. International Journal of Unani and Integrative Medicine. 2018;2(2):5-9.

[6] Makrygiannis I, Athanasiadis V, Chatzimitakos T, Mantiniotou M, Bozinou E, Lalas SI, editors. Unveiling the Potential of Apricot Residues: From Nutraceuticals to Bioenergy. Waste; 2024: MDPI.

[7] Clark S, Costello M, Drake M, Bodyfelt F. The sensory evaluation of dairy products: Springer; 2009.

[8] Kožich V, Ditrói T, Sokolová J, Křížková M, Krijt J, Ješina P, et al. Metabolism of sulfur compounds in homocystinurias. British journal of pharmacology. 2019;176(4):594-606.

[9] Jaafar HJ. Effects of apricot and apricot kernels on human health and nutrition: a review of recent human research. Technium BioChemMed. 2021;2(2):139-62.

[10] Aziz M, Yasmin I, Batool R, Khan W, Naz S, Ashraf F, et al. Exploring the effect of apricot addition on nutritional, antioxidant, textural and sensory characteristics of cookies apricot supplemented functional cookies. Italian Journal of Food Science. 2020;32(4).

[11] Gupta S, Chhajed M, Arora S, Thakur G, Gupta R. Medicinal Value of Apricot: A Review. Indian Journal of Pharmaceutical Sciences. 2018;80(5).

[12] Ramadan A, Kamel G, Awad NE, Shokry AA, Fayed HM. The pharmacological effect of apricot seeds extracts and amygdalin in experimentally induced liver damage and hepatocellular carcinoma. Journal of Herbmed Pharmacology. 2020;9(4):400-7.

[13] Chen Y, Al-Ghamdi AA, Elshikh MS, Shah MH, Al-Dosary MA, Abbasi AM. Phytochemical profiling, antioxidant and HepG2 cancer cells' antiproliferation potential

in the kernels of apricot cultivars. Saudi Journal of Biological Sciences. 2020;27(1):163-72.

[14] Siddiqui SA, Anwar S, Yunusa BM, Nayik GA, Khaneghah AM. The potential of apricot seed and oil as functional food: Composition, biological properties, health benefits & safety. Food Bioscience. 2023;51:102336.

[15] Data FFA. Available online: http://www. fao. org/faostat/en/# data. QC (accessed on 26 March 2021). 2020.

[16] Benmeziane-Derradji F, Derradji E-F, Djermoune-Arkoub L. Antioxidant activities and beneficial health effects of some dried fruits commonly consumed in Algeria: A review. Euro-Mediterranean Journal for Environmental Integration. 2019;4(1):28.

[17] Melini V, Melini F, Luziatelli F, Ruzzi M. Functional ingredients from agri-food waste: Effect of inclusion thereof on phenolic compound content and bioaccessibility in bakery products. Antioxidants. 2020;9(12):1216.

[18] Augustin M, Sanguansri L, Fox E, Cobiac L, Cole M. Recovery of wasted fruit and vegetables for improving sustainable diets. Trends in Food Science & Technology. 2020;95:75-85.

[19] Sajjad Hussain SH, Ejaz Hussain EH, Uma Partap UP. Strategies for apricot value chain development in Chitral, Pakistan. 2017.

[20] Dhen N, Rejeb IB, Boukhris H, Damergi C, Gargouri M. Physicochemical and sensory properties of wheat-Apricot kernels composite bread. Lwt. 2018;95:262-7.

[21] Lindler L, Appler J, Ballin J, Bauer T, Beck L, Boylan J, et al. AOAC SMPR® 2016.008. Journal of AOAC International. 2016;99(4):1095-100.

[22] Zhishen J, Mengcheng T, Jianming W. The determination of flavonoid contents in mulberry and their scavenging effects on superoxide radicals. Food chemistry. 1999;64(4):555-9.

[23] Azeem SMA, Al Mohesen IA, Ibrahim AM. Analysis of total phenolic compounds in tea and fruits using diazotized aminobenzenes colorimetric spots. Food chemistry. 2020;332:127392.

[24] Lajunen LH, Perämäki P. Spectrochemical analysis by atomic absorption and emission: Royal Society of Chemistry; 2004.

[25] Bolarinwa IF, Orfila C, Morgan MR. Amygdalin content of seeds, kernels and food products commercially-available in the UK. Food chemistry. 2014;152:133-9.

[26] Pala M, Mahmutoğlu T, Saygi B. Effects of pretreatments on the quality of open-air and solar dried apricots. Food/Nahrung. 1996;40(3):137-41.

[27] Cereda M, Mattos M. Linamarin: the toxic compound of cassava. Journal of Venomous Animals and Toxins. 1996;2:06-12.

Al-Kitab Journal for Pure Sciences (2024); 8(1):71-80.
https://doi.org/10.32441/kjps.08.01.p7

Al-Kitab Journal for Pure Sciences
ISSN: 2617-1260 (print), 2617-8141(online)

https://isnra.net/index.php/kjps

HEAVY METALS DETECTION IN SOME TYPES OF HERBS USED IN MEDICAL TREATMENTS

Wedad Hamad Al-Dahhan[1], Muataz Adnan Ali[1], Amer Adnan Hasan[1], Hassan Nasir Hashim[2], Baqir Abdualatif Altimmime[3], Yudhisman Ismail Imran[4], Ali Hadi Jawad[5] and Emad Abdul-Hussain Yousif*[1]

[1]Department of Chemistry, College of Science, Al-Nahrain University, Baghdad, Iraq
[2]Department of Physics, College of Science, Al-Nahrain University, Baghdad, Iraq
[3]College of Pharmacy, Al-Nahrain University, Baghdad, Iraq
[4]Department of Neurology, Universitas Tri Sakti, Indonesia
[5]Faculty of Applied Sciences, University Technology MARA, 40450 Shah Alam, Selangor, Malaysia

*Corresponding Author: emad.yousif@nahrainuniv.edu.iq

Citation: Al-Dahhan WH, Ali MA, Hasan AA, Hashim HN, Altimmime BA, Imran YI, Jawad AH, Yousif EA. HEAVY METALS DETECTION IN SOME TYPES OF HERBS USED IN MEDICAL TREATMENTS. Al-Kitab J. Pure Sci. [Internet]. 2024 Apr. 07 [cited 2024 Apr. 07];8(1):71-80. Available from: https://doi.org/10.32441/kjps.08.01.p7 .

Keywords: Heavy metals, Herbs, Toxicity, Corona pandemic.

Article History

Received	15	Feb.	2024
Accepted	27	Mar.	2024
Available online	07	Apr.	2024

Abstract:

Given the backdrop of the Corona pandemic, the objective of this study was to identify some of the heavy metal presence in specific herbs collected from local markets in Iraq. Eight samples were selected, with four (Chamomile, Laurus nobilis, Artemisia, and Borage) used for COVID-19 prevention and the remaining four (Quince, Clove, Thyme, and Propolis) for treating COVID-19 patients. For the detection of metals in the selected specimens, EDX (energy-dispersive X-ray spectroscopy) was employed. The results revealed the existence of (Ca), (K), (S), (Si), (Al), (Mg), and (Zn) in Chamomile; (K), (Si), (Al), and (Zn) in Laurus nobilis; (Ca), (K), (S), (Si), (Al), (Mg), and (Zn) in Artemisia; (Ca), (K), (P), (Si), (Al), (Mg), and (Zn) in Borage; (Ca), (K), (S), (Si), (Mg), and zinc (Zn) in Quince; (Ca), (K), (Mg), and zinc (Zn) in Clove; (Ca), (K), (Si), (Al), and (Zn) in Thyme; and (Si) in Propolis. All the detected elements are considered essential metals, which are crucial for living biological systems and needed in relatively low concentrations. It is worth mentioning that the selected samples did not contain toxic heavy metals such as (Cd), (Pb), and (Hg), which are regarded as biochemically nonessential. Further analysis for heavy metal content, starting from acid digestion. This process aimed to liberate heavy metals from organic components

in the herb samples. The results obtained through atomic absorption confirmed the absence of toxic heavy elements (Cd, Pb, and Hg). This is considered a positive thing as far as these toxic elements are concerned.

Keywords: Heavy metals, Herbs, Toxicity, Corona pandemic.

الكشف عن المعادن الثقيلة في بعض أنواع الأعشاب المستخدمة في العلاجات الطبية

وداد حمد الدهان[١]، معتز عدنان علي[١]، عامر عدنان حسن[١]، حسن ناصر هاشم[٢]، باقر عبد اللطيف التميمي[٣]، يوديسمان إسماعيل عمران[٤]، علي هادي جواد[٥]، عماد عبد الحسين يوسف[١]

[١]قسم الكيمياء، كلية العلوم، جامعة النهرين، بغداد، العراق

[٢]قسم الفيزياء، كلية العلوم، جامعة النهرين، بغداد، العراق

[٣]كلية الصيدلة، جامعة النهرين، بغداد، العراق

[٤]قسم طب الأعصاب، جامعة تريساكتي، إندونيسيا

[٥]كلية العلوم التطبيقية، جامعة مارا التكنولوجية، ٤٠٤٥٠ شاه علم، سيلانجور، ماليزيا

wedad.aldahhan@nahrainuniv.edu.iq, muataz.ali@nahrainuniv.edu.iq, amer.adnanh@nahrainuniv.edu.iq, hassan.hashim@nahrainuniv.edu.iq, baqer.mchs22@ced.nahrainuniv.edu.iq, yudhisman.imran@trisakti.ac.id, ali288@uitm.edu.my, emad.yousif@nahrainuniv.edu.iq

الخلاصة:

على خلفية جائحة كورونا، كان الهدف من هذه الدراسة هو التعرف على وجود المعادن الثقيلة في أعشاب معينة تم جمعها من الأسواق المحلية في العراق. تم اختيار ثماني عينات، أربع منها (البابونج، لوروس نوبيليس، الشيح، ولسان الثور) تستخدم للوقاية من كوفيد-١٩ والأربعة المتبقية (السفرجل، القرنفل، الزعتر، والعنج) لعلاج مرضى كوفيد-١٩. للكشف عن المعادن في العينات المختارة، تم استخدام (*EDX*)(التحليل الطيفي للأشعة السينية المشتتة). أظهرت النتائج وجود *(Ca)*، *(K)*، *(S)*، *(Si)*، *(Al)*، *(Mg)*، و (*Zn*) في البابونج. *(K)*، *(Si)*، *(Al)*، و (*Zn*) في لوروس نوبيليس ؛ *(Ca)*، *(K)*، *(S)*، *(Si)*، *(Al)*، *(Mg)*، و (*Zn*) في الشيح؛ *(Ca)*، *(K)*، *(P)*، *(Si)*، *(Al)*، *(Mg)*، و (*Zn*) في لسان الثور؛ *(Ca)*، *(K)*، *(S)*، *(Si)*، *(Mg)*، والزنك (*Zn*) في السفرجل؛ *(Ca)*، *(K)*، *(Mg)*، والزنك (*Zn*) في القرنفل؛ و(*Ca*)، و(*K*)، و(*Si*)، و(*Al*)، و(*Zn*) في الزعتر؛ و (*Si*) في العنج. وتعتبر جميع العناصر المكتشفة معادن أساسية، وهي ضرورية للأنظمة البيولوجية الحية وتحتاج إليها بتركيزات منخفضة نسبيًا. ومن الجدير بالذكر أن العينات المختارة لم تحتو على معادن ثقيلة سامة مثل (*Cd*) و(*Pb*) و(*Hg*) والتي تعتبر غير ضرورية من الناحية البيوكيميائية. مزيد من التحليل لمحتوى المعادن الثقيلة تم تنفيذه بدءاً من الهضم الحمضي. تهدف هذه العملية إلى تحرير المعادن الثقيلة من المكونات العضوية في عينات الأعشاب. أكدت النتائج التي تم الحصول عليها من خلال الامتصاص الذري عدم وجود العناصر الثقيلة السامة (الكادميوم والرصاص والزئبق). ويعتبر هذا أمرا إيجابيا فيما يتعلق بهذه العناصر السامة.

الكلمات المفتاحية: المعادن الثقيلة، الأعشاب، السمية، جائحة كورونا.

1. Introduction:

Heavy metals are distinguished by their relatively high density (leastwise 5g /cm^3) and their relatively high atomic mass (greater the 23) [1]. In biochemical systems, metals might be classified as essential like (Mn, Fe, Cu, and Zn) because they are significant for living organisms and are needed in the body in very low quantities and nonessential such as (Cd, Pb, and Hg) which up to now, have not been proven to have known essential biological role in living organisms and considered toxic elements [2]. Excess or deficiency of metals in the human body may lead to abnormal conditions or diseases [3]. Accumulation of metals especially heavy ones in plants is highly dependent on the availability or concentration in the soil, also from the air pollution as in excused of cars or factory [4] in other words, there is an increased chance of the metal to accumulate in plant tissues as the concentration of heavy metals in the soil is bigger [5]. Also, heavy metals percentages are wastewater treatment will be increasing because of the contaminated soil, they interfere with the plant roots and eventually end up in the food chain, when consumed by living things [6]. Heavy metal usually absorbed from soil by plants and piloe up in the roots and migrates in small portions to all other parts [7]. Several factors affect element migration to plants such as: soil chemistry, plant type, kinds of fertilizer used, and climate changes on the earth surface, but eventually, the most dominant element is metal concentrations and types in soil. The availability of the metals can also be directly affected by the plant independently [8]. Plants which considered medicinal and their sub-products (distillates, extracts, mixtures, etc.) are defined as herbal medicines; at the present time herbs in various species are extensively used as raw materials in the pharmaceutical preparations and widely used as in home remedies [9].

Currently, herbal medicines usage has been always in increase mainly because of the popular belief that the herbal remedies are natural and consequently, inherently safer if compared to synthetic medicines [10]. Aromatic herbs and volatile oils are known for their antifungal and antibacterial properties. Also, herbal based medicine is originated purely from nature, so its known to provoke fewer side effects [11]. Herbal medicines and other known natural products have long history in treatment of respiratory infections and are deemed as drugs. Mostly, those plant-based medicines have acceptable safety profiles due to their low toxicity in addition; some toxicity of herbal-based plants may be back in relation to contaminants that came from microbes, pesticides, adulterants, and chemical toxins [12].

The main known symptoms of COVID-19 might include cough, fever, and sometimes shortness of breath. Thyme can be one of the remedies for simple lung issues like coughs because, backed by the fact that it contains volatile oils that stimulate tissues inside the lungs, ease up congestion, struggle against viruses and bacteria, in addition to stimulating

expectoration [13]. Essential oils might be used in different ways like using a diffuser or directly inhaled or used to thin mucus by steam, resulting in better fighting against microbes, expectoration boosting, and increase the response of immune system. Plants like Laurus Nobilis, have been pleasing smelling oil and might be used specifically for boosting immune cells and exhilarating lymph drainage. Also, Chamomile as an herb is known for its calming abilities that can be consumed to ease pain and reduce inflammations. It is usually marvelous for treating children especially those who are sensitive, irritable, and anxious to pain. Moving towards Borage which has seeds oil known as a plant source of GLA, which might actively reduce inflammation. Artemisia oils besides its antioxidant abilities inhibits growth of bacteria, dermatophytes, yeast, and microspore [14].

Cooling and anti-inflammatory effects are also reported in Clove oil, which is also used to clear the breathing passages. This expectorant is useful in many disorders in the respiratory system like asthma, coughs, colds, sinusitis, bronchitis, and tuberculosis. As illustrated in countless studies, Propolis have an exceptional capability to destroy bacteria instantly, not to mention other abilities in fighting against viruses, fungi, and even against penicillin-resistant staphylococcus. Researchers have been even looking recently at the abilities of bee propolis for stimulating immune system. They used a different dose of propolis measure the response in the immune systems., 3 g/kg of propolis in the daily diet showed a significant boost in antibody levels which otherwise stated increased immune activity [15]. Further looking toward zinc which has been to have the ability to stimulate immunity system during a virus infection. Moreover, Zn supplements are favored in terms of COVID-19 treatment protocols. The abilities of Zn might be improved by using chloroquine as an ionophore, while Zn if reached inside the infected cell would be able to stop replications of SARS-CoV-2 [16]. Cadmium on the other hand, accumulate in human body which develops many problems includes for instance; nervous, kidney, cardiovascular and bone problem have extra portions might severely irritates stomach, which might lead to severe side effects like diarrhea and vomiting, while long-term exposure to fewer amounts might lead to metal accumulations in liver and kidneys. Eventually possible liver, kidney, and obstructive lung disease, and has been also likened to more serious diseases like lung cancer, and osteoporosis in living subjects [17].

2. Aim of the study:

This study aims to determine heavy metals in some types of herbs used in medical treatments. Experimental & Sampling. Eight samples of common herbs that use d through covid-19 period from local Iraqi markets in Baghdad include: Chamomile, Laurus nobilis, Artemisia, borage, Quince, clove, Thyme and propolis. The first four samples (Chamomile,

Laurus nobilis, Artemisia and borage) have been chosen on the basis that they were used for preventive purposes from the Corona virus, while the other four (Quince, clove, Thyme and propolis) were chosen on the basis that they were used as medicinal herbs for Corona virus patients.

Table 1: The selected samples with its origin

Sample No.	Herb Type	Country
1	Chamomile	India
2	Laurus nobilis	India
3	Artemisia	Thailand
4	Borage	Thailand
5	Quince	Iran
6	Clove	Iraq
7	Thyme	Iraq
8	Propolis	Iraq

Figures 1 to 14 illustrate the herbs used in this project and their original plants while **Figures 15 and 16** show the beehive and propolis which extracted from it.

Figure 1: Chamomile herb

Figure 3: Laurus Nobilis herb

Figure 5: Artemisia herb

Figure 7: Borage herb

Figure 2: Chamomile flowers

Figure 4: Laurus Nobilis plant

Figure 6: Artemisia flowers

Figure 8: Borage flowers

Figure 9: Quince herb

Figure 11: Clove herb

Figure 13: Thyme herb

Figure 15: Propolis

Figure 10: Quince Seeds

Figure 12: Clove flowers

Figure 14: Thyme plant

Figure 16: Propolis in the beehive

3. Reagents and Chemicals:

Nitric acid (Analytical grade, 65%, Sigma Aldrich) and HCl (Analytical grade, 37%, Sigma Aldrich) were deployed to prepare samples. All the solutions were prepared using deionized water**.** Reference solutions (Mg, Zn, K, Cu, Cr, Ni, Co, Cd, Pb and Fe) were prepared from 1000 mg/l in deionized water from Standard Stock Solution of GFS Fishers' (AAS Reference Standard for calibration). Dilution correction as required was implemented for samples during analysis**.**

3.1 Samples Drying

One gram of each sample was dried from water by putting them separately in a watch glasses, then further dried by putting them an electrical oven at 100 °C and later weighed, then the samples marked with numbers 1, 2, 3, 5, 6, 7, 8 in the same time 0.5g of sample 4 were prepared separately in the same procedure**.**

3.2 Grinding and Sieving

To increase the surface area for more efficient acid digestion, an electric grinder was used to grind the dried plants. Afterward sieving was implemented for the grinded samples to separate the preferred size of particles for digestion **.**

3.3 Acid Digestion

A sample of 1g of 1,2,3,5,6,7,8 and 0.5g of 4 of the selected dry samples were placed separately into 200ml beakers. A 15ml of 65% HNO3 with 10ml of 37% HCL was added. The contents were placed in a beaker and stirred thoroughly on a hot plate surface. The process was ongoing until the contents were mostly dissolved. The digested solution was filtered using Whatman filter paper No.41. After cooling filtrate solutions were later diluted with deionized water to 100ml. The prepared solution was used as samples for spectrophotometric determination of various metal analyses. According to laboratory safety regulations, this procedure was entirely accomplished in fume hood**.**

3.4 Energy-Dispersive X-Ray Spectroscopy (EDX) Analysis

Energy-dispersive X-ray spectroscopy (EDS, EDX, or XEDS) Bruker model XFlash6I10, is the analytical technique employed for the elemental characterization of the samples. The tests were conducted at Al-Nahrain University.

4. Result and Discussion:

4.1 EDX Analysis

Chamomile**,** Laurus nobilis**,** Artemisia**,** Borage**,** Quince**,** Clove**,** Thyme and Propolis herb samples were tested in an EDX instrument to determine elements of interest. Results obtained for this test shown in the figures 17, 18, 19, 20, 21, 22, 23 and 24 respectively.

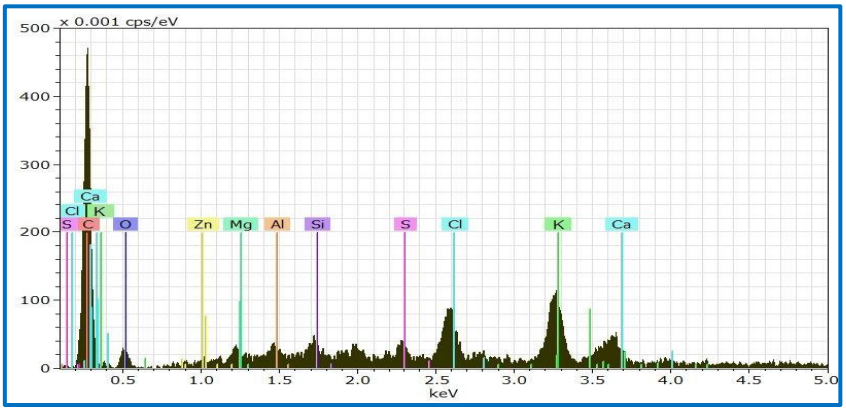

Figure 17. EDX, spectrum for Chamomile herb sample

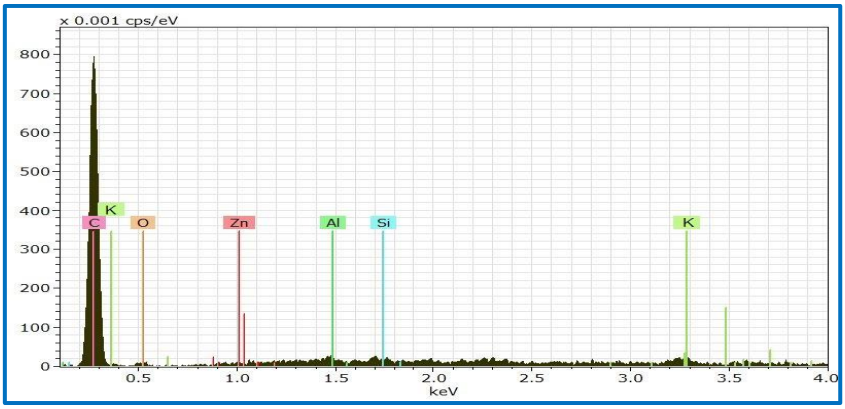

Figure 18. EDX, spectrum for Laurus nobilis herb sample

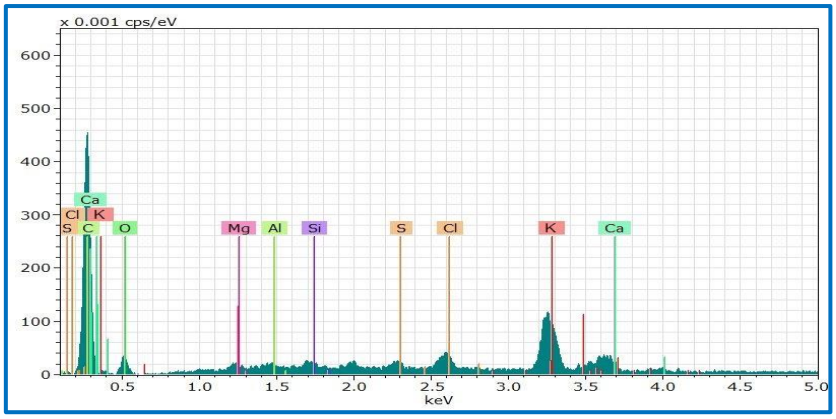

Figure 19. EDX, spectrum for Artemisia herb sample

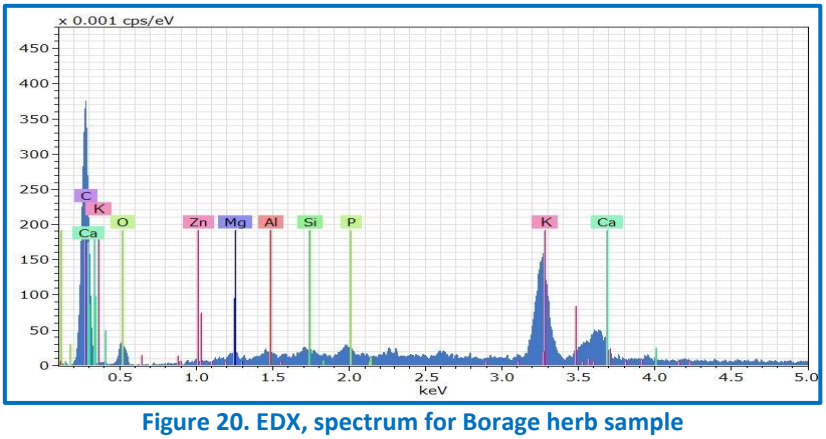

Figure 20. EDX, spectrum for Borage herb sample

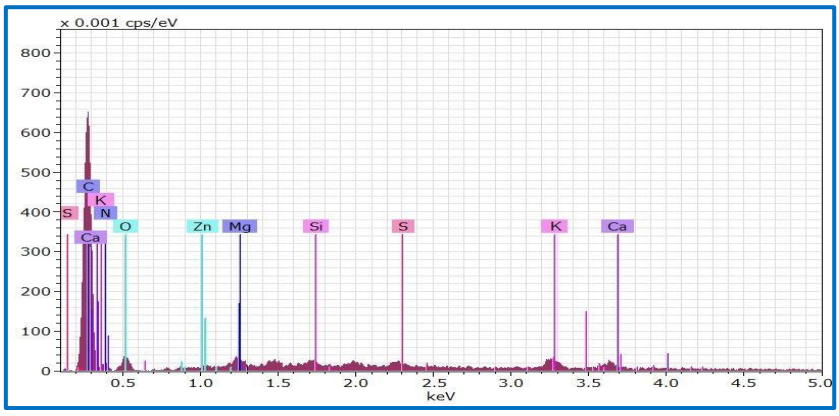

Figure 21.EDX, spectrum for Quince herb sample

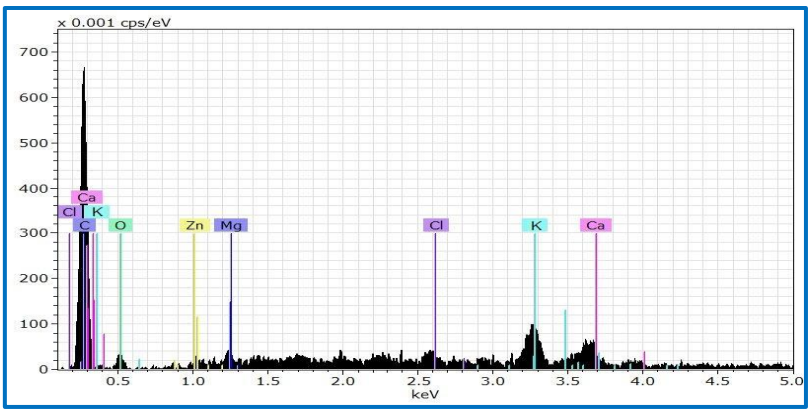

Figure 22.EDX, spectrum for Clove herb sample

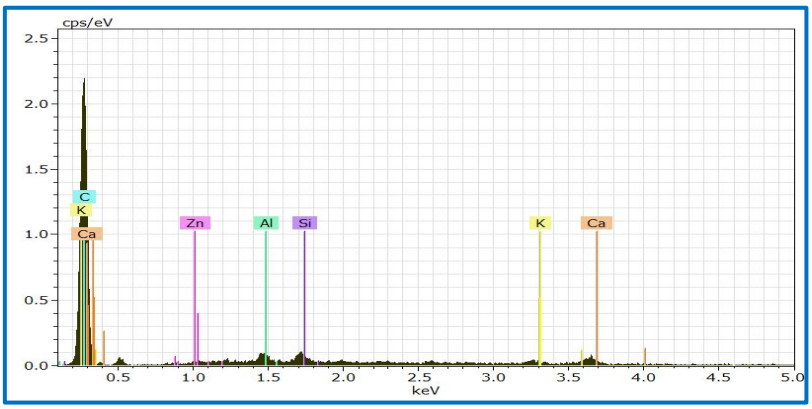

Figure 23. EDX, spectrum for Thyme herb sample

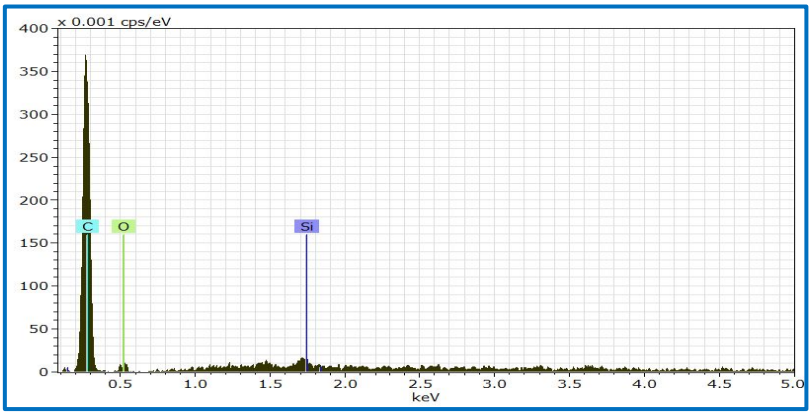

Figure 24. EDX, spectrum for Propolis sample

EDX analysis shows the presence of (Ca, K, S, Si, Al, Mg and Zn) in Chamomile, (K, Si, Al and Zn) in Laurus nobilis, (Ca, K, S, Si, Al, and Mg) in Artemisia, (Ca, K, P, Si, Al, Mg and Zn) in Borage, (Ca, K, S, Si, Mg and Zn) in Quince, (Ca, K, Mg and Zn) in Clove, (Ca, K, Si, Al and Zn) in Thyme and (Si) in Propolis. All the elements that were detected were considered as essential heavy metals which are crucial for living bodies and required in bodies in very low concentrations.

It is very important to notice that the selected samples did not content heavy metals like (Cd, Pb, and Hg) which are poisonous and are regarded as biochemically nonessential.

The clarification here that the concentrations of zinc in some herb samples are very simple, while the other samples lack zinc element. In both cases, all herbs used as preventive from the Corona virus or curative for Corona patients require the use of zinc separately in a dose estimated by the doctor.

To find out the exact concentrations of the elements that were diagnosed in the EDX device with others that research and studies indicated their presence and may be in low concentrations that were not detected by the EDX due to their concentrations may be outside the sensitivity limits of the device, a digestion process was carried out for the selected samples. Acid digestion with a mixture of (65% HNO_3 with 37% HCL) was carried out to free metals from the organic constituents in herb samples to be tested in atomic absorption instrument for metal detection and concentration determination. Atomic absorption results confirmed the absence of toxic heavy elements (Cd, Pb, and Hg) in the concentration level of mg/Kg as in EDX results.

5. Conclusion:

The eight herb samples which were selected from Iraqi markets were researched using Energy-dispersive X-ray spectroscopy (EDX). EDX data shows the existence of (Ca, K, S, Si, Al, Mg and Zn) in Chamomile, (K, Si, Al and Zn) in Laurus nobilis, (Ca, K, S, Si, Al, and Mg) in Artemisia, (Ca, K, P, Si, Al, Mg and Zn) in Borage, (Ca, K, S, Si, Mg and Zn) in Quince, (Ca, K, Mg and Zn) in Clove, (Ca, K, Si, Al and Zn) in Thyme and (Si) in Propolis. All the elements detected are considered essential metals which are crucial for living organisms' activities nevertheless in specifically low concentrations. It is very important to notice that the selected samples did not contain heavy metals like (Cd, Pb, and Hg) which even at these low levels are considered very toxic and are categorized as biologically nonessential. Atomic absorption results confirmed the unavailability of the toxic heavy elements (Cd, Pb, and Hg) at the concentration level of mg/Kg as in EDX results.

Acknowledgments: The authors would like to thank the Department of Chemistry, College of Science, Al-Nahrain University for their support.

6. References:

[1]Duffus J, Heavy metals, a meaningless term?(IUPAC Technical Report). Pure and applied chemistry. 2002;74(5): 793-807.

[2]Jovic M, Onjia A, Stankovi S. Toxic metal health risk by mussel consumption. Environmental Chemistry Letters. 2012; (10)1: 69–77.

[3]Chalkiadaki O, Dassenakis M, Lydakis-Simantiris M. Bioconcentration of Cd and Ni in various tissues of two marine bivalves living in different habitats and exposed to heavily polluted seawater. Chemistry and Ecology 2014, 308, 726-742.

[4] Cheng S. Heavy metals in plants and phytoremediation: a state-of-the-art report with special reference to literature published in Chinese journals, Environmental Science and Pollution Research. 2003;(10)335-340.

[5] Annan, K, et al.The heavy metal contents of some selected medicinal plants sampled from different geographical locations, Pharmacognosy research. 2013;(5)2:103.

[6] Vaikosen E, Alade G. Evaluation of pharmacognostical parameters and heavy metals in some locally manufactured herbal drugs, J Chem Pharm Res. 2011; (3)2: 88-97.

[7] Singh A, et al. Health risk assessment of heavy metals via dietary intake of foodstuffs from the wastewater irrigated site of a dry tropical area of India, Food and chemical toxicology. 2009; 48(2): 611-619.

[8]Zhang F, Romheld V, Marschner H. Release of zinc mobilizing root exudates in different plant species as affected by zinc nutritional status. Journal of Plant Nutrition. 1991; 14(7): 675-686.

[9] Ciriminna R, et al. Industrial feasibility of natural products extraction with microwave technology, ChemistrySelect. 2016; 1(3):549-555.

[10]Clemens S, Ma, J. Toxic heavy metal and metalloid accumulation in crop plants and foods, Annual review of plant biology. 2016;67: 489-512.

[11]Li X, et al. Network bioinformatics analysis provides insight into drug repurposing for COVID-19, Medicine in Drug Discovery. 2021;10: 100090.

[12]Huang, J, et al. Current prevention of COVID-19: natural products and herbal medicine. Frontiers in Pharmacology. 2020; 11:588508.

[13]Lai C, et al. Severe acute respiratory syndrome coronavirus 2 (SARS-CoV-2) and coronavirus disease-2019 (COVID-19): The epidemic and the challenges. International journal of antimicrobial agents. 2020; 55(3): 105924.

[14]Kaliannan, K, et al. A host-microbiome interaction mediates the opposing effects of omega-6 and omega-3 fatty acids on metabolic endotoxemia. Scientific reports. 2015; 5(1) :11276.

[15]Bankova V, et al. Propolis produced in Bulgaria and Mongolia: phenolic compounds and plant origin. Apidologie. 1992; 23(1): 79-85.

[16]Chen, C, et al. Sambucus nigra extracts inhibit infectious bronchitis virus at an early point during replication. BMC veterinary research. 2014; 10(1): 1-12.

[17]Martin S, Griswold W. Human health effects of heavy metals. Environmental Science and Technology briefs for citizens. 2009; (15)5.

Al-Kitab Journal for Pure Sciences (2024); 8(1):81-91.
https://doi.org/10.32441/kjps.08.01.p8

Al-Kitab Journal for Pure Sciences
ISSN: 2617-1260 (print), 2617-8141(online)

https://isnra.net/index.php/kjps

Study of the Effect of Thin Layer Thickness on the Structural Properties of Copper Phthalocyanine (CuPc) Films Prepared by Vacuum Thermal Evaporation Method

Laith S. Alhiti [*1], Rafal A. Jawad[2], Rafaa A. Abd Alwaahed[1], Hala M. Sobhi[3]

[1]Medical Physics Department, College of Applied Sciences-Heet, University of Anbar, Iraq
[2]Department of Physics, College of Science, University of Babylon, Hilla, Iraq
[3]Optic Techniques Department, College of Health and Medical Techniques, Al-Mustaqbal University, Iraq

*Corresponding Author: laith2011alhiti@uoanbar.edu.iq

Citation: Alhiti LS, Jawad RA, Abd Alwaahed RA, Alhassan HM. Study of the Effect of Thin Layer Thickness on the Structural Properties of Copper Phthalocyanine (CuPc) Films Prepared by Vacuum Thermal Evaporation Method. Al-Kitab J. Pure Sci. [Internet]. 2024 Apr. 07 [cited 2024 Apr. 07];8(1):81-91. Available from: https://doi.org/10.32441/kjps.08.01.p8.

Keywords: CuPc thin films, vacuum thermal evaporation technique (PVD), atomic force microscope (AFM), thickness, root mean square (R.M.S.), structural characteristics.

Article History
Received 03 Feb. 2024
Accepted 25 Mar. 2024
Available online 07 Apr. 2024

Abstract:

The structural properties of thin films prepared with different thicknesses before and after the annealing process and at different temperatures were studied. X-ray diffraction (XRD), atomic force microscopy (AFM), and emission scanning electron microscopy (FESEM) were used to study the structural properties. X-ray diffraction analysis revealed that the thin films prepared with different thicknesses, as well as those annealed at temperatures of 300 and 373 K, were composed of the β-phase, which is widely known as the most stable phase. The analysis also showed that the material has a polycrystalline structure characterized by a monoclinic crystal system. The density shows a constant increase in all thin films, with the dominant trend being (312) for all films. Atomic force microscopy (AFM) measurement results indicated that there was an increase in roughness with a change in the thickness of the thin films. In addition, there was an increase in the crystalline size of the thin films that underwent annealing at 300 and 373 K. However, there was a decrease in crystallite size at the annealing temperature of 473 K due to the phase change of the thin film material.

Keywords: CuPc thin films, vacuum thermal evaporation technique (PVD), atomic force microscope (AFM), thickness, root mean square (R.M.S.), structural characteristics.

دراسة تأثير سمك الأغشية الرقيقة على الخواص الهيكلية لأغشية فثالوسيانين النحاس المحضرة بطريقة التبخير الحراري الفراغ (*CUPC*)

ليث صالح محمد*[١]، رفل علي جواد[٢]، رفاء عبدالكريم عبدالواحد[١]، هالة محمد صبحي[٣]

[١]* قسم الفيزياء الطبية،كلية العلوم التطبيقية-هيت،جامعة الانبار،هيت،العراق

[٢]قسم الفيزياء،كلية العلوم،جامعة بابل،حله،العراق

[٣]قسم التقنيات البصرية، كلية التقنيات الصحية والطبية، جامعة المستقبل، العراق

laith2011alhiti@uoanbar.edu.iq, sci.rafal.jawad@uobabylon.edu.iq, Rafaa1987abd@uoanbar.edu.iq, hala.mohammed.subhi@uomus.edu.iq

الخلاصة:

تم دراسة الخصائص الهيكلية للأغشية الرقيقة المحضرة بسماكات مختلفة قبل وبعد عملية التلدين وبدرجات حرارة مختلفة. استخدمت الدراسة حيود الأشعة السينية (*XRD*) ومجهر القوة الذرية (*AFM*) والمجهر الالكتروني الماسح للانبعاث (*FESEM*) لدراسة الخصائص الهيكلية. كشف تحليل حيود الأشعة السينية بأن الأغشية الرقيقة المحضرة بسماكات مختلفة وكذلك التي تم تلدينها عند درجات حرارة ٣٠٠ و٣٧٣ كلفن كلفن، كانت تتكون من الطور بيتا (*β-phase*) والذي يعرف على نطاق واسع بأنه الطور الأكثر استقرار. كذلك بينت التحاليل ان المادة لها بنية متعددة البلورات والتي تتميز بنظام بلوري احادي الميل. تظهر الكثافة زيادة ثابتة في جميع الاغشية الرقيقة، مع كون الاتجاه السائد (٣١٢) ولجميع الاغشية. أشارت نتائج القياس لمجهر القوة الذرية (*AFM*) ان هناك زيادة في الخشونة مع تغير سمك الاغشية الرقيقة. بالإضافة إلى ذلك، كان هناك زيادة في الحجم البلوري للأغشية الرقيقة التي خضعت للتلدين عند ٣٠٠ و٣٧٣ كلفن. ومع ذلك، كان هناك انخفاض في الحجم البلوري عند درجة حرارة التلدين ٤٧٣ كلفن نتيجة لتغير الطور لمادة الاغشية الرقيقة.

الكلمات المفتاحية: الأغشية الرقيقة CuPc، تقنية التبخر الحراري الفراغي (PVD)، مجهر القوة الذرية (AFM)، السمك، متوسط الجذر التربيع (R.M.S.)، الخصائص الهيكلية.

1. Introduction:

Phthalocyanine polymers, a type of organic material with highly functional properties, have made them the subject of intense study in the fields of chemistry and physics. The prominent feature of these materials is their great stability in the face of thermal changes and chemical reactions, which makes them excellent candidates for diverse applications, especially in fields requiring highly stable materials [1]. Phthalocyanine can take several crystalline forms, and these different forms are known as polymorphic forms. The most common forms are α-, β-, and γ-. Each of these forms has unique properties that affect how the material is used in practical applications [2]. The differences between these shapes are due to the arrangement of atoms within the crystal, which in turn affects the physical and chemical properties of the material [3]. The research highlights the structure properties of metal-modified or metal-free phthalocyanine

polymers. Examples cited, such as MnPc (manganese phthalocyanine) [4], CuPc (copper phthalocyanine) [5], NiPc (nickel phthalocyanine) [6], FePc (iron phthalocyanine) [7], and CoPc (cobalt phthalocyanine) [8], reflect the diversity in the compositions of these polymers and the resulting applications. One important use of these materials is in gas sensors, where they take advantage of their high sensitivity to chemical changes. They are also used in optical logic displays and in solar energy conversion applications, such as solar cells, due to their ability to absorb and convert light efficiently. In addition, they are used in the manufacture of color filters and as materials for organic lasers, where they provide unique optical properties [9].

The chemical nature of these materials makes them p-type semiconductors, which means they contain electrical holes that facilitate the flow of electricity. The ability to easily evaporate these materials allows the production of high-purity thin films without degradation, enhancing the quality and efficiency of downstream applications [10].

Thermal evaporation was used to create thin film coatings of copper phthalocyanine on quartz substrates in the work that is being presented here [11]. In this work, structural elements were found and addressed. These characteristics include statements about considerations made during research or analysis that are relevant to the study of thin films. X-ray diffraction is an important method for analyzing the crystalline structure of thin films, as X-ray radiation can be used to study the atomic and crystalline structure of materials [12]. Also, advanced techniques like atomic force electron microscopy (AFM), which can show very clear, very small pictures of thin film surfaces, and field scanning electron microscopy (FESEM), which can show very fine details about the structure of surfaces at very high resolution, have been looked at and reviewed [13].In this way, it is demonstrated that analytical aspects have been taken care of using multiple techniques to understand and evaluate the structural and surface properties of the studied thin films.

2. Experimental work:

2.1 Thin film deposition system:

The deposition method used a vacuum thermal evaporation technique, where copper phthalocyanine is heated until it evaporates and then condenses on a colder surface, forming a thin film [14]. Equipment used: An Edwards (E 306 A coating unit) was used, which is known for its ability to achieve high-level vacuums of up to (2×10-5) Torr. The dimensions of the basin used in the deposition process are arranged in a symmetrical and geometric manner with respect to the target or foundation. This arrangement helps in achieving uniformity in the distribution of the evaporated particles of copper phthalocyanine on the substrate. The main goal is to

produce a homogeneous and even film of copper phthalocyanine. Achieving homogeneity in the deposited film is essential to obtaining the desired properties and specifications in the final film. Careful regulation of the bed and substrate contributes to ensuring the quality and consistency of the deposited film [15].

2.2 Preparation of copper phthalocyanine films:

Copper phthalocyanine films with a thickness of 200, 215, 235, and 255 nanometers were formed in a molybdenum metal boat when the evaporation chamber pressure reached 2.2 × 10-5 Torr using a unit. The E306 Coating Unit deposits material on glass 18 cm from the evaporation tank at a rate of 2.078813 nm sec-1 at normal temperature. A current transformer sends a high current for deposition. After cooling in the evaporation chamber, the samples are ready for thickness measurement. Subsequently, the lab tests these membranes for their structural, optical, and electrical characteristics.

2.3 Measuring the thickness of thin films:

The researchers use the indirect gravimetric approach to measure the thickness of thin films through mass measurement. Several steps were involved in this process. In this research, a sensitive scale is used to weigh the substrate before applying the film, and a vacuum thermal evaporation is also used to deposit the thin layer onto the substrate. The substrate is weighed again on the sensitive balance after film deposition. This time, the substrate and thin films will be weighed. To determine the mass of thin films, the researchers subtract the weight of the substrate before deposition from its weight after deposition, and also use film density and mass to calculate the volume of the thin film. The volume divided by the surface area of the film deposit yields the film thickness [16].

This approach is precise and efficient for thin films. Measurement tools like scales must be reliable and calibrated to produce accurate findings. Repeating measurements helps confirm findings and decrease mistakes.

3. Results and discussion:

3.1 X-ray diffraction:

The results of X-ray diffraction (XRD) examinations of CuPc thin films deposited using the thermal evaporation technique in vacuum on glass substrates with different thicknesses (200, 215, 235 and 255) nanometers show that it is a polycrystalline structure of the monoclinic type [17], and compared with the standard values in the card (JCPDS: 00-037-1846), the $(2\bar{1}5)$, and (213), respectively.

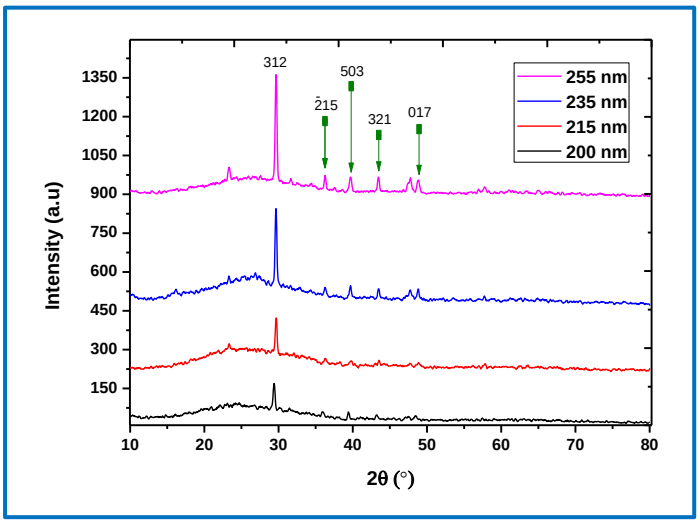

Figure 1: X-ray diffraction pattern (XRD) of copper phthalocyanine CuPc films.

The characteristic and dominant direction was (312), as shown in **Figure 1**. The results also had a good match between the calculated and measured surface area values and the crystal diffraction angles, as shown in **Table 1**.

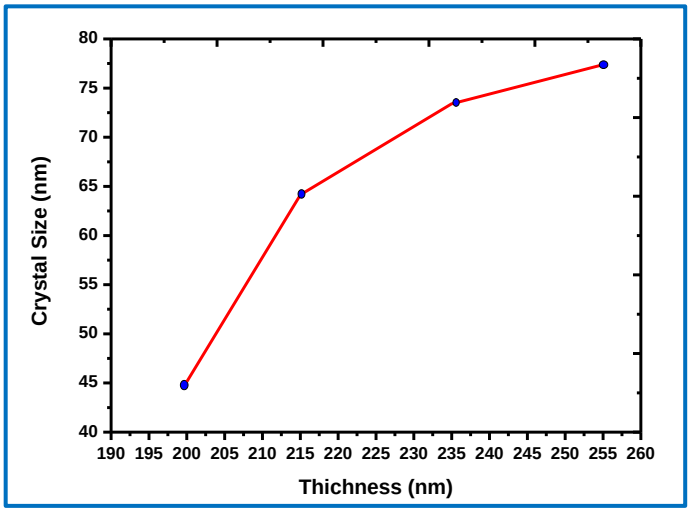

Figure 2: illustrates the relationship between crystal size and the thickness of CuPc thin films.

Table 1 shows the structural parameters of CuPc films, where the results show that as the thickness of the thin films increases, there will be an increase in crystal size due to columnar growth with increasing film thickness, as shown in **Figure 2**, and an increase in density.

The average crystallite size was calculated, which agrees well with the estimated value obtained from FESEM images.

A copper phthalocyanine (CuPc) film, measuring 255 nm in thickness, underwent annealing at temperatures of 300, 373, and 473 Kelvin. The outcomes of X-ray diffraction (XRD) analyses for these thin CuPc films are presented in **Figure 3**. By examining the XRD results, structural

parameters for the CuPc films in the direction of the crystal peak (312) at varying annealing temperatures can be inferred, as detailed in **Table 1**.

As the annealing temperatures rise, the full width at half maximum (FWHM) in the primary orientation decreases significantly. This shows that the lattice quality has improved, as explained in **[18]**.

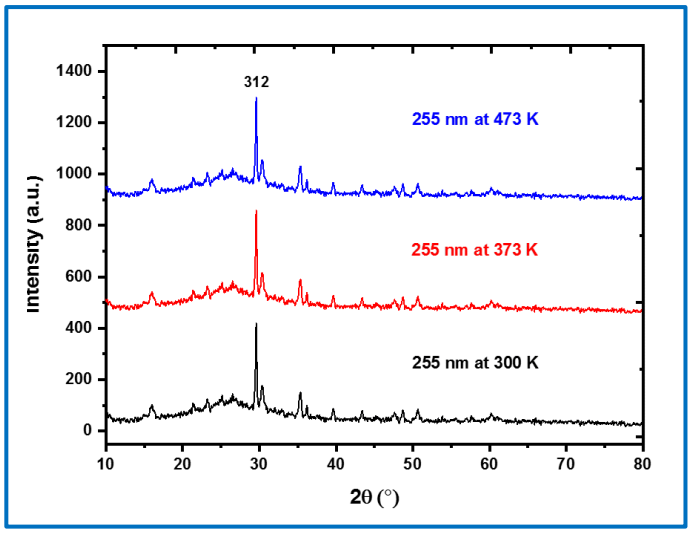

Figure 3: displays the X-ray diffraction (XRD) patterns of copper phthalocyanine (CuPc) films that have been annealed at various temperatures.

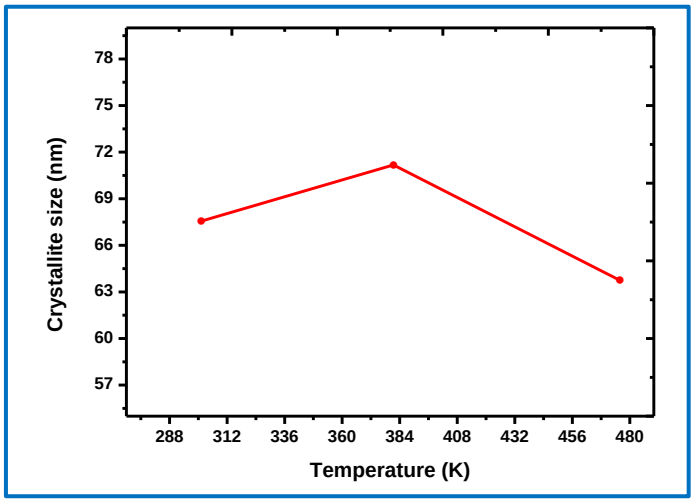

Figure 4: depicts the variation in crystal size as a function of the annealing temperature for copper phthalocyanine (CuPc) thin films.

This improvement allowed for the estimation of crystallite size using the Scherer equation. According to the data in **Table 1**, there is an observable increase in crystal size at annealing temperatures of 300 and 373 Kelvin. This increase can be attributed to regrowth involving phthalocyanine, as the crystallization process of the films is temperature-dependent. However, at a higher temperature of 473 Kelvin, a decrease in crystal size is observed, likely due to a phase change. This pattern aligns with findings from previous research, as noted in **[19]**.

Table 1: Results obtained from XRD for CuPc films and different thicknesses.

Thickn. (nm)	2θ(std.) (°)	2θ(Exp.) (°)	I (a.u)	d_{hkl}(std.) (Å)	d_{hkl}(Exp.) (Å)	FWHM (°)	C.S. (nm)	hkl
200	29.47	29.563	169.34	3.027	3.015	0.23	37.12	**312**
	36.07	36.18	60.26	2.488	2.480	0.20	54.13	2̲15
	39.47	39.63	59.50	2.281	2.272	0.18	50.99	**503**
215	29.47	29.575	299.28	3.027	3.014	0.21	43.52	**312**
	36.07	36.19	73.14	2.488	2.479	0.22	61.17	2̲15
	39.47	39.65	63.74	2.281	2.271	0.23	71.38	**503**
235	29.47	29.614	397.89	3.027	3.012	0.205	62.24	**312**
	36.07	36.24	92.80	2.488	2.478	0.24	69.16	2̲15
	39.47	39.66	98.74	2.281	2.270	0.28	73.94	**503**
255	29.47	29.62	493.96	3.027	3.011	0.184	66.91	**312**
	36.07	36.27	103.96	2.488	2.475	0.141	88.07	2̲15
	39.47	39.60	96.60	2.281	2.270	0.29	74.91	**503**

3.2 Results of atomic force microscopy (AFM) examinations:

The surface relief and topography of CuPc thin films with different thicknesses (200, 215, 235, (and) 255) nm were studied using atomic force microscopy (AFM). This microscope is characterized by its high resolving power, which reaches (0.1–1.0) nanometers, and a magnification power estimated at ($5 * 10^2$ - 10^8), which enables the nature of the surface to be examined accurately.

Table 2: displays the average grain size, surface roughness, and root mean square values for CuPc films with different thicknesses, including 200, 215, 235, and 255 nanometers.

Thickness (nm)	D (nm)	Roughness Average (nm)	R.M.S (nm)
200	62.80	3.26	3.9
215	73.01	4.28	4.95
235	80.98	5.25	6.29
255	88.80	7.75	8.99

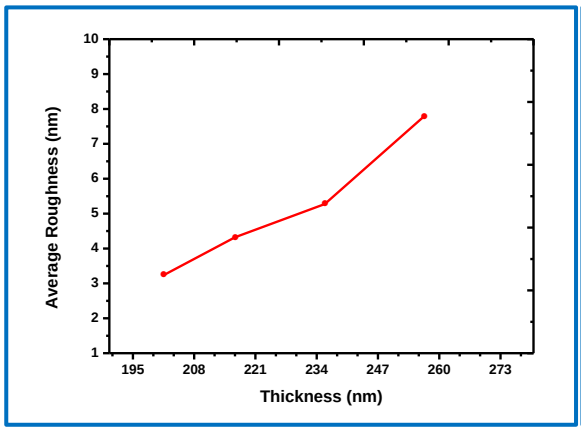

Figure 6: shows the roughness rate as a function of varying thickness for CuPc thin films.

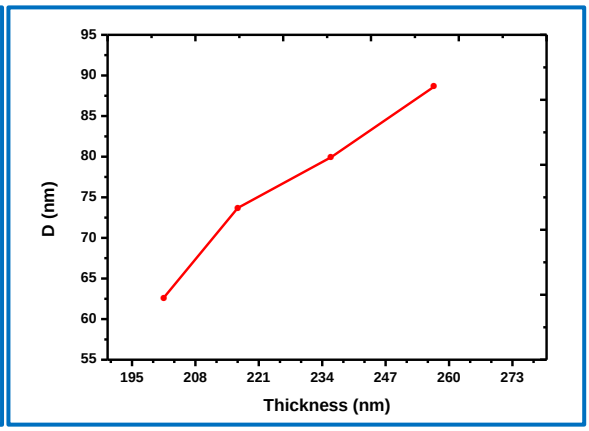

Figure 5: shows grain size as a function of varying thickness for CuPc thin films.

The AFM provides statistical values for the average grain size and distribution on the surface, in addition to the degree of surface roughness using the root mean square of roughness (RMS). This also allows 2D and 3D images to be displayed for comprehensive surface inspection. The grain size and average roughness were determined as a function of thickness, as shown in **Figures 5 and 6**. The results showed an increase in grain size, which is consistent with the results of XRD analysis, as well as an increase in average roughness with increasing thickness.

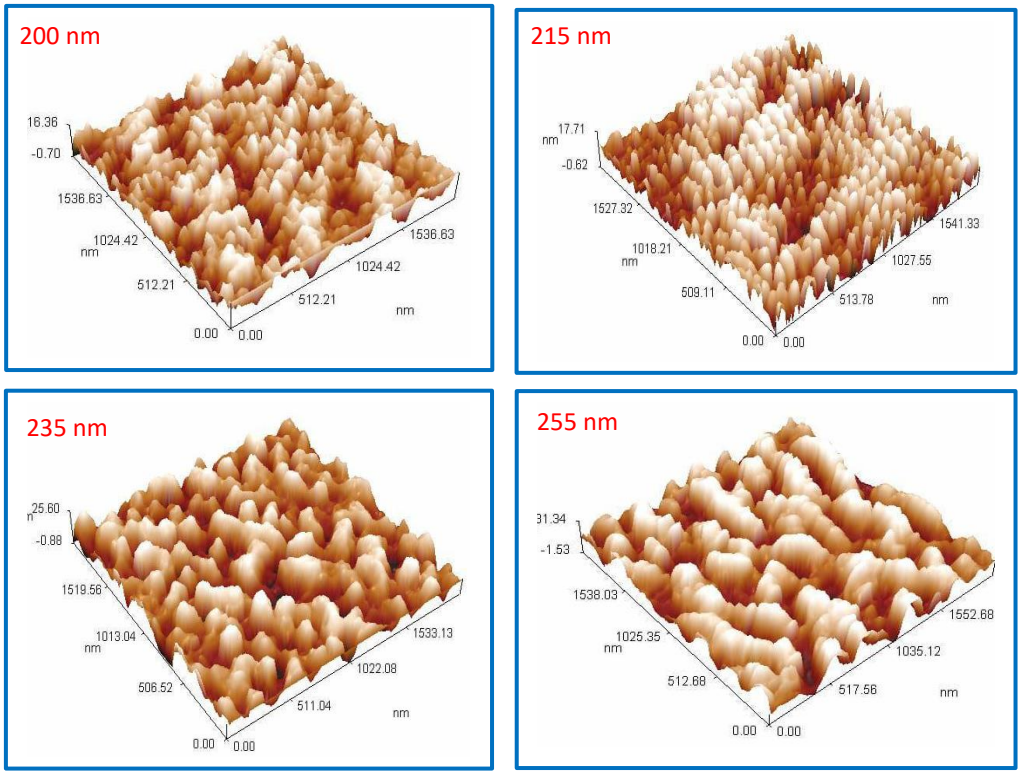

Figure 7: shows three-dimensional atomic force microscopy (AFM) images of thin films of copper phthalocyanine (CuPc) with different thicknesses.

Figures 7 A, B, and D show two-dimensional images from atomic force microscopy (AFM) as well as grain distribution diagrams of the surface of CuPc thin films, which are 200, 215, 235, and 255 nm thick, respectively. The images taken at 25 °C, show the presence of a large number of tubular-shaped CuPc grains. This pattern indicates a crystalline nature resulting from the high active content of the expelled species, as described in ref **[20]**.

3.3 Results of field emission scanning electron microscopy (FESEM)

Field emission scanning electron microscopy (FESEM) provides topographical and elemental information at magnifications between 10X and 300,000X, with an almost unlimited depth of field. Compared to scanning electron microscopy (SEM), FESEM produces sharper images and less electrostatic distortion. All films prepared and deposited on glass substrates

were examined using this technique to obtain a clear image of the features, which helps in identifying the surface nature of the films and observing changes in grain size based on the change in thickness.

The FESEM image shown in **Figure 8** of the prepared film reveals particles of larger size, ranging from 15 to 30 nm. There is a noticeable increase in particle size in parallel with the increase in the thickness of the thin film, and this is consistent with the measurements extracted from XRD and AFM analyses. It is noted that the granular size is larger than the existing crystalline size.

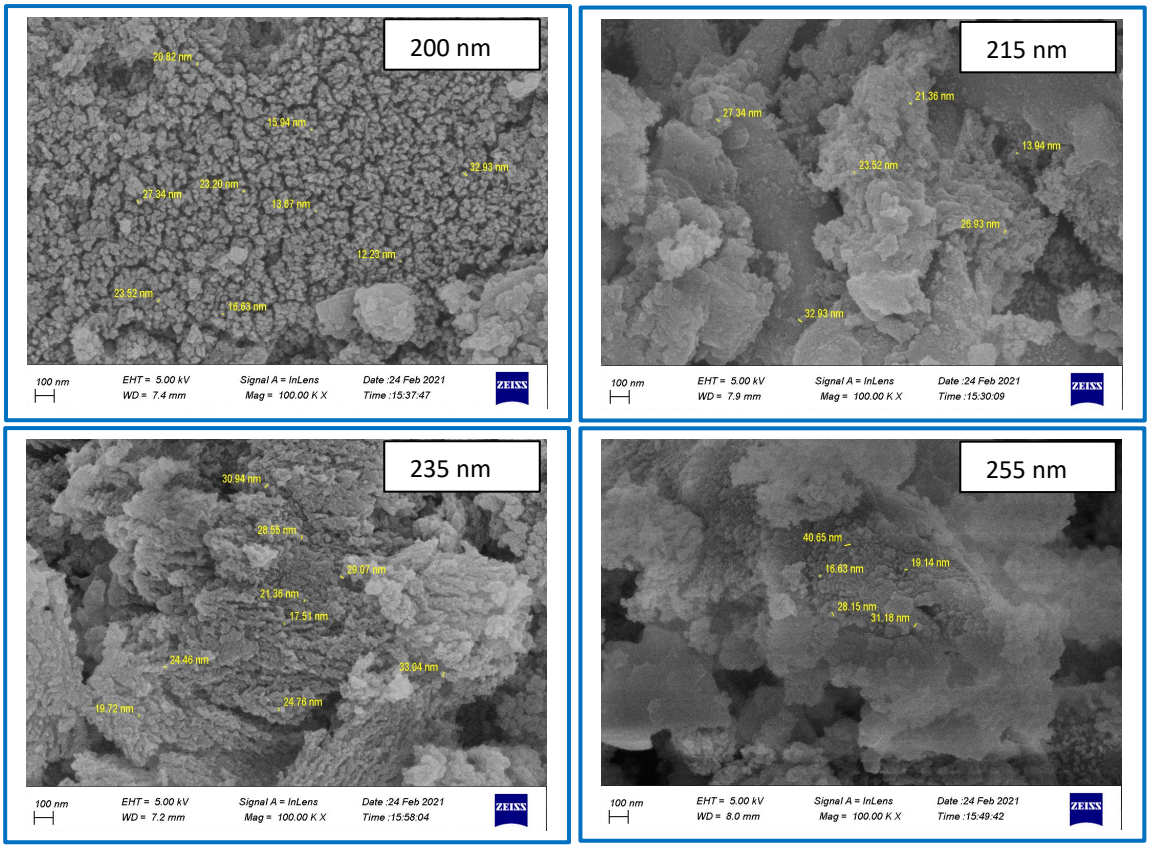

Figure 8: displays field emission scanning electron microscope (FESEM) images of copper phthalocyanine (CuPC) films with varying thicknesses.

4. Conclusion:

The research revealed the effect of thin film thickness on the structural properties of copper phthalocyanine (CuPc) films. It was found that there is a relationship between the structural properties and the thickness of the thin films, as the best properties that were reached, were for the thin films with a thickness of 255 nanometers. X-ray diffraction (XRD) analysis also indicates changes in the size of crystalline grains with a change in the thickness of the prepared thin films, which is a crucial factor that affects the structural integrity of the material. Atomic force microscopy (AFM) has revealed valuable information on the evolution of surface features, providing a comprehensive understanding of structural modifications whereby this tuning can

be exploited to customize the material for specific applications in organic electronics and optoelectronic devices.

5. References:

[1] Awni RA, Song Z, Chen C, Li C, Wang C, Razooqi MA, et al. Influence of Charge Transport Layers on Capacitance Measured in Halide Perovskite Solar Cells. Joule. 2020;4(3):644–57. Available from: https://doi.org/10.1016/j.joule.2020.01.012.

[2] Schechtman BH, Spicer WE. Near infrared to vacuum ultraviolet absorption spectra and the optical constants of phthalocyanine and porphyrin films. J Mol Spectrosc. 1970;33(1):28-48. Available from: https://doi.org/10.1016/0022-2852(70)90050-0.

[3] Asha AB, Narain R. Nanomaterials properties. In: Polymer science and nanotechnology. Elsevier; 2020. p. 343-59. Available from: https://doi.org/10.1016/B978-0-12-816806-6.00015-7.

[4] Nie Z, Wang C, Xue R, Xie G, Xiong H. Two-dimensional FePc and MnPc monolayers as promising materials for SF6 decomposition gases detection: Insights from DFT calculations. Appl Surf Sci. 2023;608:155119. Available from: https://doi.org/10.1016/j.apsusc.2022.155119.

[5] Pindolia G, Pandya J, Shinde S, Jha PK. Fluorinated copper phthalocyanine as an electron transport material in perovskite solar cell. Int J Energy Res. 2022;46(11):15127–42. Available from: https://doi.org/10.1002/er.8211.

[6] Xu J, Wang H, Wang X, Liao J, Song J, Zhao Z, et al. Photoresponse and Noise Characteristics of In-Situ Fabricated Nipc Nanowire Photodetectors. Available from: https://doi.org/10.2139/ssrn.4464236.

[7] de Oliveira MAC, Ficca VCA, Gokhale R, Santoro C, Mecheri B, D'Epifanio A, et al. Iron(II) phthalocyanine (FePc) over carbon support for oxygen reduction reaction electrocatalysts operating in alkaline electrolyte. J Solid State Electrochem. 2020;25(1):93–104. Available from: https://doi.org/10.1007/s10008-020-04537-x.

[8] Balogun SA, Fayemi OE. Recent Advances in the Use of CoPc-MWCNTs Nanocomposites as Electrochemical Sensing Materials. Biosensors. 2022;12(10):850. Available from: https://doi.org/10.3390/bios12100850.

[9] Yu L, Wang Y, Wang J, Zhao X, Xing W, Rodrigues LA, et al. CuPc nanowires PVD preparation and its extra high gas sensitivity to chlorine. Sens Actuators A Phys. 2022;334:113362. Available from: https://doi.org/10.1016/j.sna.2021.113362.

[10] You Z, Chang J, Li Z, Lu T, Wang S, Wang F, et al. High-performance triboelectric nanogenerators based on the organic semiconductor copper phthalocyanine. Nanoscale. 2021;13(47):20197–204. Available from: https://doi.org/10.1039/d1nr03649a.

[11] Schwieger T, Peisert H, Golden MS, Knupfer M, Fink J. Electronic structure of the organic semiconductor copper phthalocyanine and K-CuPc studied using photoemission spectroscopy. Phys Rev B. 2002;66(15). Available from: https://doi.org/10.1103/physrevb.66.155207.

[12] Sukhikh A, Bonegardt D, Klyamer D, Krasnov P, Basova T. Chlorosubstituted Copper Phthalocyanines: Spectral Study and Structure of Thin Films. Molecules. 2020;25(7):1620. Available from: https://doi.org/10.3390/molecules25071620.

[13] Klyamer DD, Basova TV. EFFECT OF THE STRUCTURAL FEATURES OF METAL PHTHALOCYANINE FILMS ON THEIR ELECTROPHYSICAL PROPERTIES. J Struct Chem. 2022;63(7):997–1018. Available from: https://doi.org/10.1134/s0022476622070010.

[14] Sukhikh A, Bonegardt D, Klyamer D, Krasnov P, Basova T. Chlorosubstituted Copper Phthalocyanines: Spectral Study and Structure of Thin Films. Molecules. 2020;25(7):1620. Available from: https://doi.org/10.3390/molecules25071620.

[15] Torimtubun AAA, Follana-Berná J, Sánchez JG, Pallarès J, Sastre-Santos Á, Marsal LF. Fluorinated Zinc and Copper Phthalocyanines as Efficient Third Components in Ternary Bulk Heterojunction Solar Cells. ACS Appl Energy Mater. 2021;4(5):5201–11. Available from: https://doi.org/10.1021/acsaem.1c00734.

[16] Ubale AU, Belkhedkar MR. Size Dependent Physical Properties of Nanostructured α-Fe2O3 Thin Films Grown by Successive Ionic Layer Adsorption and Reaction Method for Antibacterial Application. J Mater Sci Technol. 2015;31(1):1–9. Available from: https://doi.org/10.1016/j.jmst.2014.11.011.

[17] Darwish AAA, Alharbi SR, Hawamdeh MM, Alsharari AM, Qashou SI. Dielectric Properties and AC Conductivity of Organic Films of Copper(II) 2,9,16,23-Tetra-tert-butyl-29H,31H-phthalocyanine. J Electron Mater. 2019;49(3):1787–93. Available from: https://doi.org/10.1007/s11664-019-07869-1.

[18] Hussein MT, Aadim KA, Hassan EK. Structural and Surface Morphology Analysis of Copper Phthalocyanine Thin Film Prepared by Pulsed Laser Deposition and Thermal Evaporation Techniques. Adv Mater Phys Chem. 2016;06(04):85–97. Available from: https://doi.org/10.4236/ampc.2016.64009.

[19] Structural and Transport Properties of Copper Phthalocyanine (CuPc) Thin Films. Egyptian J Solids. 2002;

[20] Caplins BW, Mullenbach TK, Holmes RJ, Blank DA. Femtosecond to nanosecond excited state dynamics of vapor deposited copper phthalocyanine thin films. Phys Chem Chem Phys. 2016;18(16):11454-11459. Available from: https://doi.org/10.1039/c6cp00958a.

Al-Kitab Journal for Pure Sciences (2024); 8(1):92-103.
https://doi.org/10.32441/kjps.08.01.p9

Al-Kitab Journal for Pure Sciences
ISSN: 2617-1260 (print), 2617-8141(online)

https://isnra.net/index.php/kjps

Rainfall Repercussions: Assessing Climate Change Influence on Iraq Precipitation Patterns

Abdul Haleem A. Al-Muhyi*, Faez Younis Aleedani, Munaf Qasim Albattat, Jamila Mohammed Badr

Marine physics Department, Marine Science center, University of Basrah, Iraq

*Corresponding Author: abdulhaleem.hussien@uobasrah.edu.iq

Citation: Al-Muhyi AH, Aleedani FY, Albattat MQ, Badr JM. Rainfall Repercussions: Assessing Climate Change Influence on Iraq Precipitation Patterns. Al-Kitab J. Pure Sci. [Internet]. 2024 Apr. 08 [cited 2024 Apr. 08];8(1):92-103. Available from: https://doi.org/10.32441/kjps.08.01.p9 .

Keywords: Rainfall variability, drier years, deforestation, heterogeneity, temporal.

Article History

Received	01	Feb.	2024
Accepted	15	Mar.	2024
Available online	08	Apr.	2024

Abstract:

The unequal spatial and temporal distribution of precipitation, exacerbated by climate change, has received significant attention. Rainfall is pivotal for crop growth and environmental health, crucial in the water cycle, and essential to replenishing surface water sources vital for drinking water supplies. Consequently, understanding this phenomenon is critical for future planning. Evaluating spatial and temporal variations in rainfall is essential for the effective management of water resources. This study employs a statistical analysis of rainfall data from 16 rain gauge stations to identify annual rainfall trends, Linear Regression Equations, Coefficients of Determination (R^2), Precipitation Concentration Index (PCI), and Rainfall Variability Index (RVI). The findings of the study show that the PCI has indicated strongly irregular rainfall concentration in Iraq. RVI identifies 2017 and 1983 as notably dry years, while 2018 stands out as a particularly wet year within the 40 years from 1980 to 2019. RVI also highlights that normal rainfall years predominate, with very dry years ranging from 2 to 13, dry years from 3 to 11, wet years from 1 to 7, and very wet years from 6 to 10 within the study period.

Keywords: Rainfall variability, drier years, deforestation, heterogeneity, temporal.

تقييم أثر تغير المناخ على توزيع الأمطار في العراق

عبد الحليم علي المحيي*، فايز يونس خليل العيداني، مناف قاسم البطاط، جميلة محمد بدر

جامعة البصرة، مركز علوم البحار، قسم الفيزياء البحرية

abdulhaleem.hussien@uobasrah.edu.iq, faez.khalil@uobasrah.edu.iq, munaf.jaber@uobasrah.edu.iq, alfoutimalmhdoya@gmail.com

الخلاصة:

لقد حظي التوزيع المكاني والزماني غير المتكافئ لهطول الأمطار والذي تفاقم بسبب تغير المناخ باهتمام كبير. يعد هطول الأمطار أمرًا محوريًا لنمو المحاصيل والصحة البيئية، وهو أمر بالغ الأهمية في دورة المياه، وضروري لتجديد مصادر المياه السطحية الحيوية لإمدادات مياه الشرب. وبالتالي، فإن فهم هذه الظاهرة أمر بالغ الأهمية للتخطيط المستقبلي. يعد تقييم الاختلافات المكانية والزمانية في هطول الأمطار أمرًا ضروريًا للإدارة الفعالة للموارد المائية، تستخدم هذه الدراسة التحليل الإحصائي لبيانات هطول الأمطار من ١٦ محطة قياس المطر لتحديد اتجاهات هطول الأمطار السنوية، ومعادلات الانحدار الخطي، ومعاملات التحديد (R^2)، ومؤشر تركيز هطول الأمطار (PCI)، ومؤشر تقلب هطول الأمطار (RVI).

تكشف النتائج عن اتجاه الانحدار سلبي في هطول الأمطار السنوي. ويشير PCI إلى عدم انتظام تركز الأمطار بشكل كبير في العراق. ويحدد RVI عامي ٢٠١٧ و١٩٨٣ على أنهما سنوات جافة بشكل ملحوظ، في حين يبرز عام ٢٠١٨ باعتباره عامًا ممطرًا بشكل خاص خلال فترة ٤٠ عامًا (١٩٨٠-٢٠١٩). يسلط RVI الضوء أيضًا على أن سنوات هطول الأمطار العادية هي السائدة، حيث تتراوح سنوات الجفاف الشديد من ٢ إلى ١٣، وسنوات الجفاف من ٣ إلى ١١، وسنوات الرطب من ١ إلى ٧، والسنوات الرطبة جدًا من ٦ إلى ١٠ خلال فترة الدراسة.

الكلمات المفتاحية: تقلب هطول الأمطار، سنوات الجفاف، إزالة الغابات، عدم التجانس، الزمانية.

1. Introduction:

Climate change is caused by a variety of human activities such as burning fossil fuels, deforestation, and agricultural practices. These activities have led to an increase of carbon dioxide and other greenhouse gases in the atmosphere, trapping more heat and causing an increase in global temperatures. This has led to several changes in the earth's climate, such as more frequent and intense storms, floods, droughts, and heat waves. It can also lead to significant changes in weather patterns .The unequal spatial and temporal distribution of precipitation, which is exacerbated by climate change, has received a lot of attention recently [1]. This is because climate change will alter all aspects of the hydrological cycle ranging from evaporation through precipitation, run-off, and discharge [2].

Rain is considered one of the most critical components of weather and climate. Changes in precipitation, including its decrease, can lead to climatic drought, which in turn causes hydrological and agricultural droughts. These impacts affect the nation's environmental system,

economic growth, and food security. Moreover, extreme rainfall events, such as floods, highlight the importance of understanding rainfall variability and intensity [3].

Rain also plays a significant role in the hydrologic cycle, Both science and socioeconomics place great emphasis on its fluctuation through time and geography. Although the annual total rainfall may not change, a change in seasonal rainfall significantly impacts runoff, evapotranspiration, and infiltration, which affects ecosystem management, stream flow, and flood forecast [4].

Research into this phenomenon is a top priority when making plans for the future. Evaluation of spatial and temporal variations in rainfall is crucial for the effective management of water resources. The present study aims to examine the rainfall distribution characteristics of the Iraq area, by utilizing time series data from 1980 to 2019. The study will analyze trends in annual rainfall, which may show either decreasing or increasing patterns. The study will analyze trends in annual rainfall, which may show either decreasing or increasing patterns. Additionally, the research will use the rainfall concentration index to estimate the monthly heterogeneity of rainfall, and the rainfall variability index, which is typically computed as the standardized precipitation departure.

The findings of this study could help inform decision-making and water resource management plans in Iraq. For instance, they could provide insights into the spatial and temporal variations in rainfall, enabling adjustments to water management plans. Furthermore, the findings could enhance preparations for and management of floods, as well as inform drought management strategies.

2. Location and Extent of Studied Area:

The Republic of Iraq is located in Southwest Asia, northeast of the Arab homeland. It is bordered by Turkey to the north, Iran to the east, Syria, Jordan, and Saudi Arabia to the west, and the Arab Gulf, Kuwait, and Saudi Arabia to the south. Iraq is divided into 18 governorates, situated between latitudes 29˚ 5′ and 37˚ 22′ north, and longitudes 38˚ 45′ and 48˚ 45′ east, covering an area of 435,052 square kilometers. Iraq's climate is located within the northern temperate region, but it is characterized as subtropical continental. Its rainfall pattern is similar to that of the Mediterranean, with most rain falling in winter, autumn, and spring, and little to none in summer. Data from the country's 16 weather stations were used to create a GIS database, as shown in **Figure 1**.

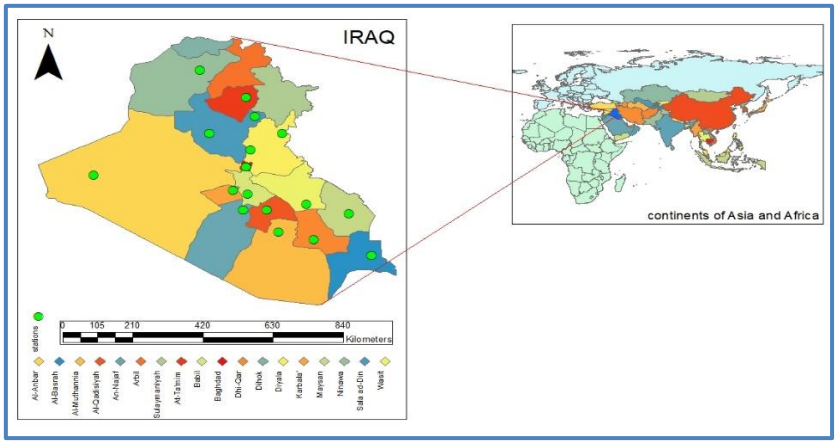

Figure 1: The Study area

3. Data and Methodology:

The Iraqi Meteorological Organization and Seismology Department provided monthly rainfall data for the period 1980-2019 from 16 rain gauge sites. Missing data in climate time series can be addressed using the Inverse Distance Weighting (IDW) strategy, as described in references **[5]** and **[6]**.

$$P_k = \frac{\sum_{k=1}^{n} \frac{R_k}{d_k^2}}{\sum_{k=1}^{n} \frac{1}{d_k^2}}$$

Where, P_k = missing rainfall value, R_k = rainfall value at k surrounding rainfall stations, n = number of observations of surrounding stations, and d_k = Distance from missing rainfall station to k^{th} surrounding rainfall stations. The technique of examining historical rainfall data to identify long-term trends in precipitation is known as rainfall trend analysis. Statistical methods such as regression analysis and the coefficient of determination (R2) are used to determine the significance of rainfall trends. The monthly rainfall heterogeneity was analyzed using the rainfall concentration index, originally proposed by **[7]** and modified by **[8]**.

$$PCI = 100 * \frac{\sum_{k=1}^{12} P_k^2}{\sum_{k=1}^{12} P_k} \quad \text{----------(1)}$$

Where P_i is the amount of rainfall in the i^{th} month. The index was calculated for each rain gauge and for each year over the study period. The annual PCI values describe in the **Table 1**.

Table 1: classification of (PCI) [9,10]

Rang of precipitation concentration index (PCI) Value			
PCI < 10	PCI >11 and < 15	PCI >16 and < 20	PCI >20
Uniform rainfall concentration	Moderate rainfall concentration	Irregular rainfall concentration	Strongly irregular rainfall concentration

The available rainfall time series can be divided into different climatic regimes such as "very dry climatic year," "normal climatic year," "wet climatic year," "very wet climatic year," etc. using the rainfall variability index **Eq. (2)**.

$$V_i = \frac{(R_i - m)}{\sigma} \quad ------(2)$$

Where, V_i is the rainfall variability index for a year i, R_i is the annual rainfall for year i, and m and σ are the yearly precipitation series' mean and standard deviation for the given duration of study station respectively**[6]**. The range of rainfall variability index is described in **Table 2.**

Table 2: Rang of rainfall variability index

$V_i > 1$	$V_i \geq 0.5$ *and* ≤ 1	$V_i \leq 0.5$ *and* ≥ -0.5	$V_i \geq -0.5$ *and* ≤ -1	$V_i > -1$
very wet year	*wet year*	*normal year*	*dry year*	*very dry year*

3. Results and discussion:

Using Excel software, a statistical analysis of rainfall was conducted for each of the sixteen stations to identify any trends or persistence in the data. A linear regression test was performed, revealing a rising tendency in all stations toward shortfall and sparse rainfall. The values of R2 ranged from 0.00004 to 0.0946, except for four stations (Baghdad, Samawa, Hilla, and Missan), which showed a weak coefficient of determination and a positive trend (see **Table 3**). The table also presents the linear regression equations for each station.

Table 3: Rainfall Trend

stations	location		Regression equation	R^2 coefficient of determination	Trend sign
	Latitude	Longitude			
Mosul	36.32°	43.15°	y = -1.7782x +398.43	0.0247	Negative
Kirkuk	35.47°	44.40°	y = -2.7581x + 401.51	0.0706	Negative
Tuz	34.88°	44.65°	y = -1.3032x + 300.71	0.0248	Negative
Khanaqin	34.35°	45.38°	y = -1.799x + 334.72	0.0498	Negative
Tikrit	34.34°	43.42°	y = -1.6888x + 218.96	0.0816	Negative
Alkhalls	33.83°	44.53°	y = -0.6662x + 189.81	0.0181	Negative
Baghdad	33.30°	44.40°	y = 0.7979x + 103.92	0.0278	Positive
Rutba	33.03°	40.28°	y = -0.9179x + 130.82	0.0409	Negative
Hilla	32.45°	44.45°	y = 0.4636x + 96.698	0.0172	Positive
Al- hai	32.13°	46.03°	y = -0.03x + 135.29	0.00004	Negative
Najaf	31.95°	44.32°	y = -0.6501x + 108.79	0.0291	Negative
Diwaniya	31.95°	4.95°	y = -0.2284x + 108.69	0.0037	Negative
Samawa	31.27°	45.27°	y = 0.4431x + 89.533	0.0115	Positive
Nasiriya	31.02°	46.23°	y = -0.3453x + 130.48	0.0051	Negative
Missan	31.83°	47.17°	y = 1.008x + 154.13	0.0221	Positive
Basra	30.52°	47.78°	y = -1.5156x + 160.62	0.0946	Negative

The average annual total rainfall for all of Iraq from 1980 to 2019 is represented by contour lines in **Figure 2**. The highest amount of rainfall, 308 mm, was recorded in the north, while the lowest, 95 mm, was in the southwest. The average rainfall amount, of 120 mm, was observed in the west.

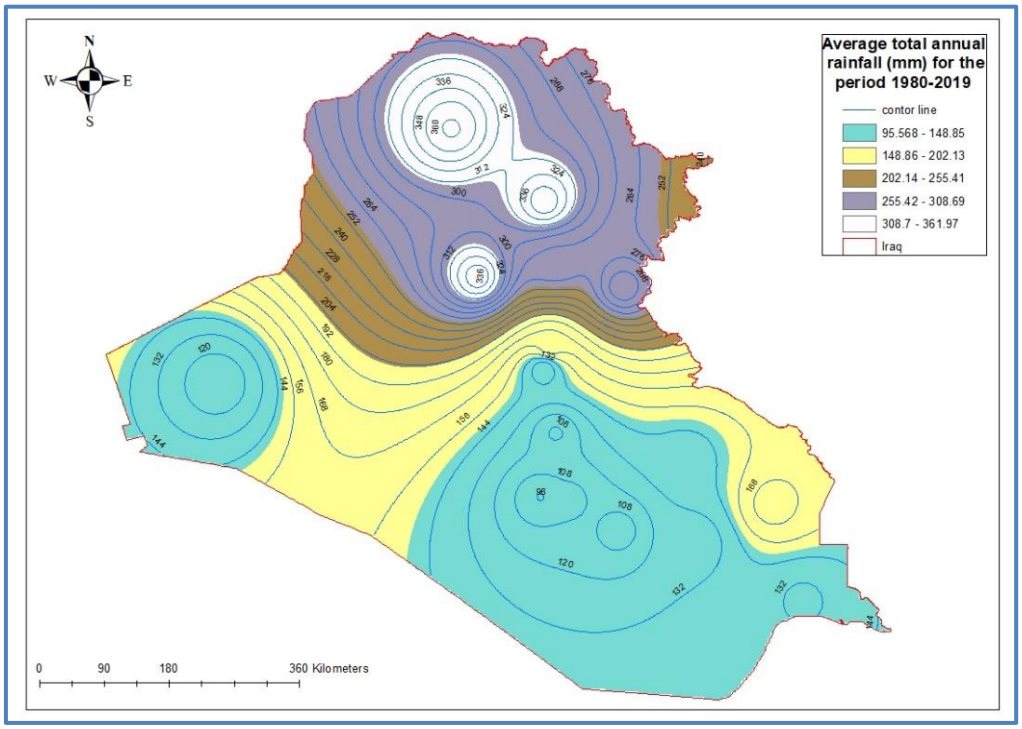

Figure 2: Average total annual rainfall (mm) for the period 1980-2019

Oliver's definition of the Precipitation Concentration Index (PCI) describes it as a potent measure of the temporal distribution of precipitation (7). **Eq. (1)** is used to calculate the yearly PCI for all stations (see **Table 4**). The number of years for each PCI class is determined based on the PCI value, as shown in **Table 5**. It is observed that no years have a PCI value less than 10. Kirkuk and Baghdad fall into the PCI class >11 and <15, with one and two years of moderate rainfall concentration, respectively. All stations have the number of years in the class PCI >16 and <20, indicating irregular rainfall concentration. The largest number of years is located in the PCI class larger than 20, indicating strongly irregular rainfall concentration.

From **Figure 2**, we observe that the average annual PCI values in Iraq range from 22.4 to 31.4. The highest PCI values are concentrated in the southern region, specifically in the governorates of Samawa and Nasiriya, while the lowest values are in the northern region, particularly in the governorates of Mosul and Kirkuk. This indicates that the majority of rainy years in Iraq between 1980 and 2019 are characterized by strong irregularity.

Table 4: PCI level of precipitation concentration measured on an annual scale for a specific year

Year	Mosul	Kirkuk	Tuz	Khanaqin	Tikrit	Alkhalls	Baghdad	Rutba	Hilla	Alhai	Najaf	Diwaniya	Samawa	Nasiriya	Missan	Basra
1980	20.3	17.0	18.4	19.7	18.7	18.4	21.2	22.0	39.6	52.0	45.1	45.5	57.3	47.2	46.6	40.8
1981	16.3	16.9	17.1	18.8	18.1	17.0	21.5	20.4	20.2	35.9	27.8	25.2	42.4	31.2	34.6	27.2
1982	17.2	15.8	15.1	16.8	16.6	16.0	14.5	15.6	23.6	29.4	17.7	22.5	23.9	29.0	34.3	24.0
1983	16.0	15.6	15.8	20.9	18.0	18.6	19.0	17.9	18.4	22.8	28.1	25.6	36.7	26.5	28.0	29.1
1984	25.4	30.1	29.4	31.0	37.2	30.3	25.7	19.1	20.4	32.8	31.2	24.2	29.9	38.8	30.4	33.2
1985	18.0	19.7	18.9	21.6	24.8	24.7	26.2	19.5	18.0	23.9	27.8	18.7	64.0	31.9	31.6	38.1
1986	18.2	23.2	20.0	18.9	20.7	21.4	22.3	16.1	28.4	19.5	26.2	22.1	29.1	23.5	19.1	18.8
1987	23.9	26.1	27.8	25.3	22.4	21.7	26.3	46.8	31.7	24.0	33.8	21.5	20.6	27.1	25.3	27.0
1988	21.5	19.5	19.4	18.5	24.7	18.6	20.7	18.8	22.7	19.9	22.2	20.2	22.4	26.1	20.7	21.7
1989	28.0	25.7	21.6	25.9	35.4	21.6	28.7	27.8	28.4	24.8	41.7	28.1	35.6	25.8	24.2	24.0
1990	20.5	26.8	24.2	28.7	33.2	18.0	23.0	45.1	32.1	33.6	45.4	35.4	38.1	29.9	18.3	23.0
1991	32.4	14.5	19.0	22.1	19.0	30.8	16.2	34.1	25.6	29.4	19.2	20.0	23.3	18.5	15.2	22.0
1992	17.7	18.6	17.5	20.0	19.4	19.9	20.3	18.9	30.0	24.8	24.3	38.9	23.4	23.1	28.4	22.2
1993	17.6	13.5	23.7	15.9	17.9	28.1	38.6	16.4	25.1	27.7	34.6	27.7	21.3	20.6	20.2	24.7
1994	15.9	17.1	19.2	19.7	21.5	18.9	19.1	35.8	27.7	28.5	25.6	35.8	25.3	25.1	29.9	20.4
1995	22.0	24.7	21.1	20.3	25.7	20.9	32.9	52.3	39.7	21.4	24.5	30.3	25.3	19.1	21.9	26.6
1996	22.7	23.8	22.1	26.4	29.5	22.6	25.2	20.1	26.2	28.0	29.7	23.9	27.1	28.0	25.7	23.6
1997	16.9	15.9	20.1	19.2	21.3	26.1	26.5	27.2	32.8	29.3	24.6	21.0	21.8	20.6	24.6	22.3
1998	22.7	26.7	33.9	35.3	48.8	38.1	26.0	23.2	31.4	51.4	35.3	34.4	49.9	42.0	34.1	47.8
1999	19.0	30.1	30.9	36.1	28.8	33.6	37.2	27.5	28.8	25.4	26.3	22.8	37.4	27.8	31.0	22.5
2000	19.0	25.1	21.6	35.7	23.5	35.5	30.6	23.6	30.5	29.5	30.2	26.2	22.9	43.3	38.6	39.3
2001	18.9	19.7	23.5	20.7	17.6	17.8	20.0	32.4	19.3	22.4	23.1	22.7	19.5	48.6	31.9	33.4
2002	22.1	24.5	22.9	18.2	16.6	22.0	24.3	19.6	26.7	28.6	21.2	37.9	25.1	50.8	26.5	20.0
2003	18.9	18.7	18.2	20.3	23.7	18.6	17.8	16.8	38.1	26.1	23.7	33.3	18.1	33.4	19.7	22.2
2004	20.7	24.2	23.9	25.8	30.1	19.5	21.2	16.4	35.7	31.8	30.8	34.9	19.2	25.3	30.2	22.9
2005	21.8	23.8	26.4	25.4	29.1	27.4	36.8	21.0	29.5	26.7	24.1	27.9	21.9	32.8	34.5	37.5
2006	19.9	25.7	22.2	22.6	27.1	27.2	23.9	19.9	17.0	19.3	18.4	19.1	32.1	20.8	23.0	26.0
2007	23.5	24.7	26.7	27.7	31.0	31.7	22.8	16.7	38.8	27.6	30.4	25.6	26.0	50.1	24.1	25.3
2008	19.3	23.1	26.4	21.3	23.1	27.4	28.1	19.5	33.1	20.6	20.7	20.5	36.3	35.7	36.3	44.4
2009	24.2	18.6	18.2	17.4	17.5	22.5	16.4	22.4	20.0	27.3	21.0	23.9	19.4	28.4	36.7	28.3
2010	17.6	18.6	18.9	18.5	18.0	20.1	24.8	25.5	19.9	22.9	21.3	22.9	25.2	34.3	36.3	23.7
2011	25.7	22.3	24.4	21.6	23.5	23.3	22.8	37.5	35.2	26.8	27.0	26.5	31.6	18.7	31.1	23.7
2012	19.0	19.9	22.9	36.2	26.2	20.8	35.8	27.3	44.2	32.8	31.8	40.9	28.0	32.2	44.7	29.3
2013	20.1	22.0	29.9	33.8	23.2	31.6	40.7	27.6	62.6	25.5	48.6	35.2	50.5	56.5	39.4	34.2
2014	19.1	17.5	17.7	17.2	20.7	16.7	21.3	16.5	26.2	19.1	25.5	27.9	23.0	29.2	23.1	46.1
2015	18.4	16.8	18.4	23.7	19.4	33.7	27.0	20.3	21.7	26.6	24.7	33.5	26.1	25.7	18.6	25.6
2016	17.7	21.2	18.6	17.7	24.1	23.6	23.5	21.3	29.3	25.6	26.1	23.7	39.0	27.4	19.7	19.8
2017	25.7	29.4	35.2	29.7	39.6	46.8	39.5	35.9	25.6	57.9	25.3	45.2	48.1	44.1	36.2	56.0
2018	18.9	22.4	21.3	23.9	20.5	23.9	23.5	21.8	22.3	30.7	18.7	21.2	33.8	38.8	28.1	23.1
2019	21.9	19.1	20.1	18.2	23.4	18.7	22.5	15.4	26.1	20.0	22.3	17.5	22.6	18.6	27.2	19.8

Table 5: Number of years for each class of Precipitation Concentration Index (PCI)

	Number of years			
Stations	PCI≤10	PCI >10 and ≤15	PCI >15 and ≤ 20	PCI>20
Mosul	0	0	0	40
Kirkuk	0	2	3	35
Tuz	0	0	20	20
Khanaqin	0	0	15	25
Tikrit	0	0	12	28
Alkhalls	0	0	14	26
Baghdad	0	1	6	33
Rutba	0	0	19	21
Hilla	0	0	6	34
Al- hai	0	0	5	35
Najaf	0	0	4	36
Diwaniya	0	0	5	35
Samawa	0	0	4	36
Nasiriya	0	0	4	36
Missan	0	0	7	33
Basra	0	0	4	36

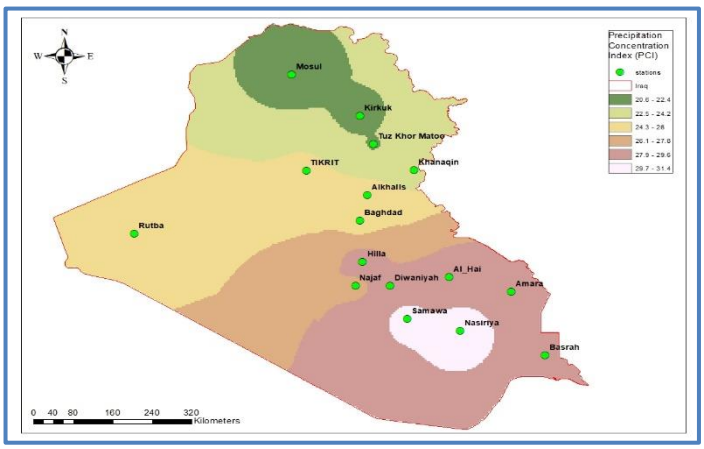

Figure 3: Annually Average Precipitation Concentration Index (PCI)

The Rainfall Variability Index (RVI) **Eq. (2)** is used to classify the climatic systems of the 40-year data series for Iraq. Based on the RVI values, the periods are classified as shown in the table in the data and methodology section. The rainfall variability index plots for each station are presented in **Figures 4, 5, and 6**. In these plots, values above the positive red dashed line represent very wet years, values between the solid red line and the dashed red line represent wet years, values between the solid red line and the solid green line represent normal years, and negative values between the solid green line and the dashed green line represent dry years. Negative values below -1 indicate very dry years.

It has been observed that the years 2017 and 1983 were the driest years, while the year 2018 was the wettest during the 40-year period. **Table 5** shows the number of years for each classification and for each station. It is clear from the table that the number of normal years is prevalent during the study period, ranging from 10 to 21 years. The number of very dry years ranged from 2 to 13 years, dry years from 3 to 11 years, wet years from 1 to 7 years, and very wet years from 6 to 10 years. The variability in rainfall patterns for the entire Iraq, as determined by applying RVI, is shown in **Figure 7**. It can be seen that normal rainfall occurred 36.1% of the time, dry years occurred 19.5% of the time, very wet years occurred 15.8% of the time, very dry years occurred 14.4% of the time, and wet periods were experienced 9% of the time.

Table 6: Number of years for each class of Rainfall Variability Index (RVI)

stations	Number of years				
	$V_i > +1$	V_i between +0.5 to +1	V_i is within ±0.5	V_i between -0.5 to -1	$V_i < -1$
Mosul	8	2	16	8	6
Kirkuk	7	3	17	8	5
Tuz	10	1	12	11	6
Khanaqin	9	6	10	9	6
Tikrit	7	3	17	8	5
Alkhalls	6	7	14	7	6
Baghdad	6	4	18	6	6
Rutba	5	3	19	11	2
Hilla	6	5	14	9	6
Al-hai	4	7	14	9	6
Najaf	9	2	12	10	7
Diwaniya	4	4	21	3	8
Samawa	6	3	16	11	4
Nasiriya	7	5	15	5	13
Missan	7	1	16	10	6
Basra	5	11	9	10	5

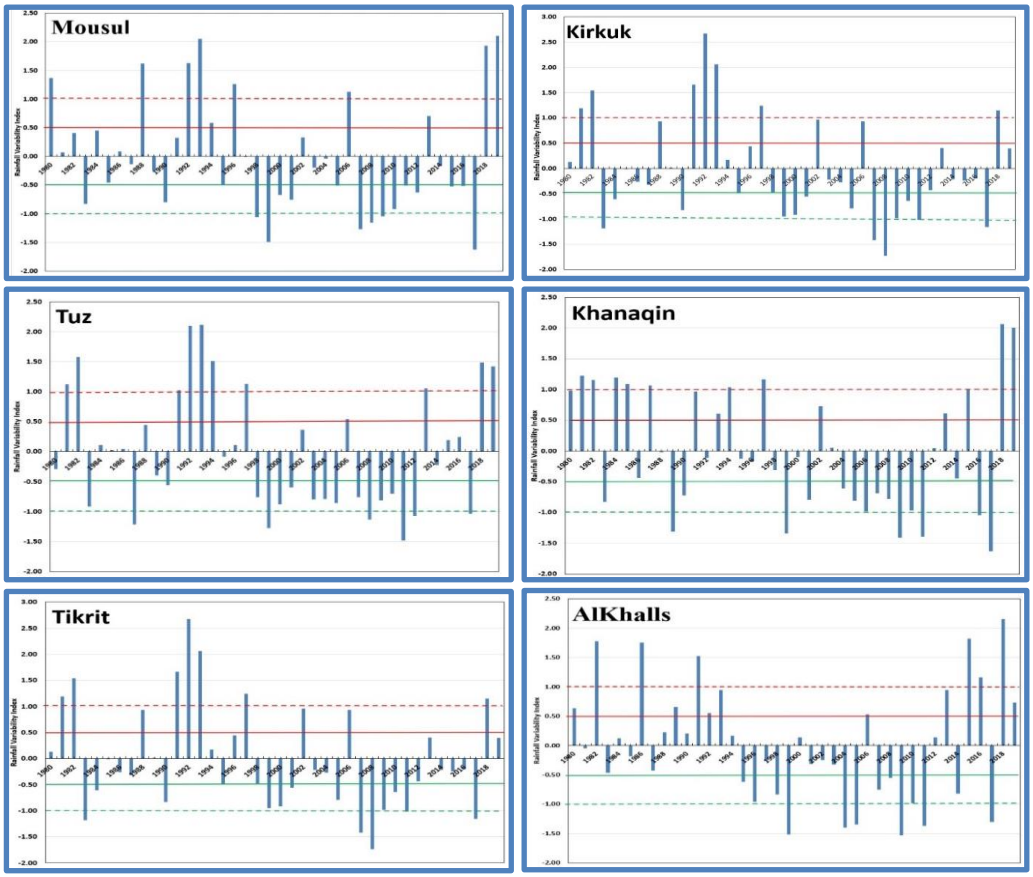

Figure 4:Rainfall variability index plots for stations of (Mosul, Kirkuk,Tuz, Khanaqin,Tikrit, Alkhalls).

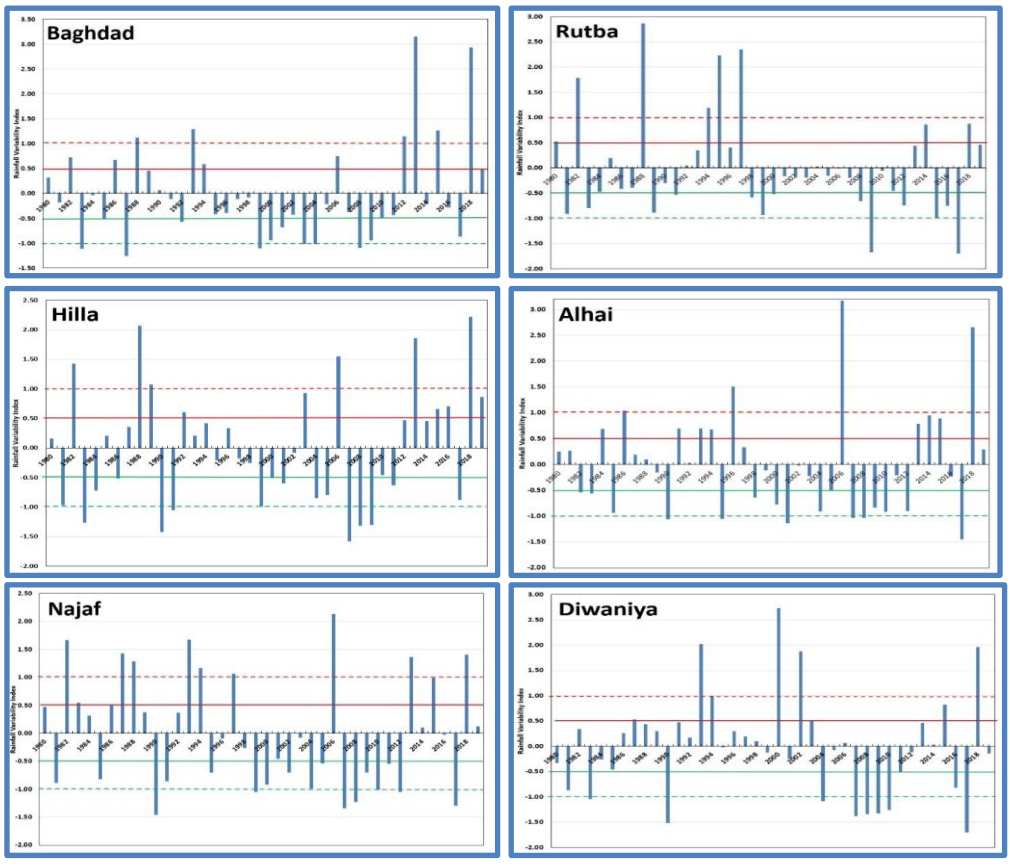

Figure 5: Rainfall variability index plots for stations of (Baghdad, Rutba, Hilla, Al-hai , Najaf, Diwaniya).

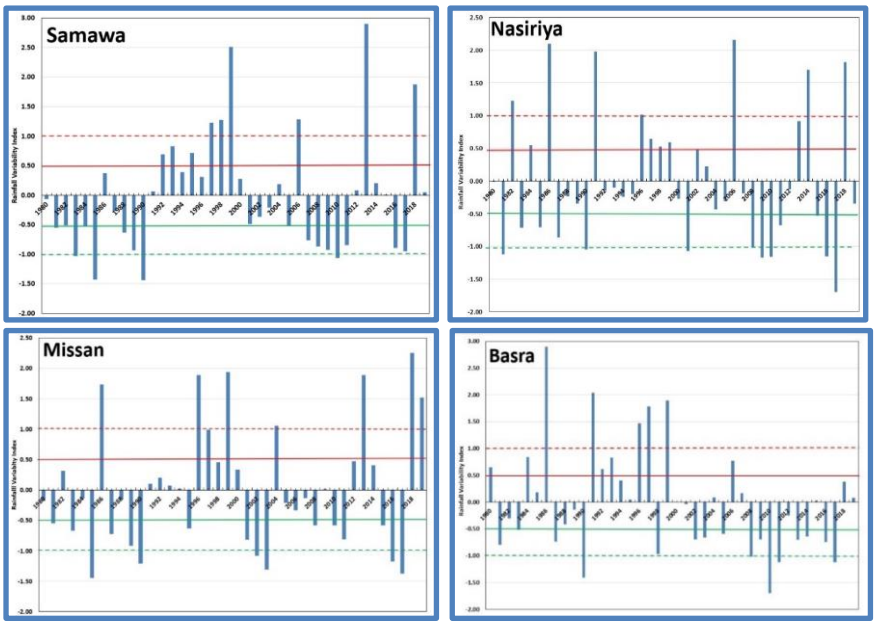

Figure 6: Rainfall variability index plots for stations of (Samawa, Nasiriya, Missan and Basrah)

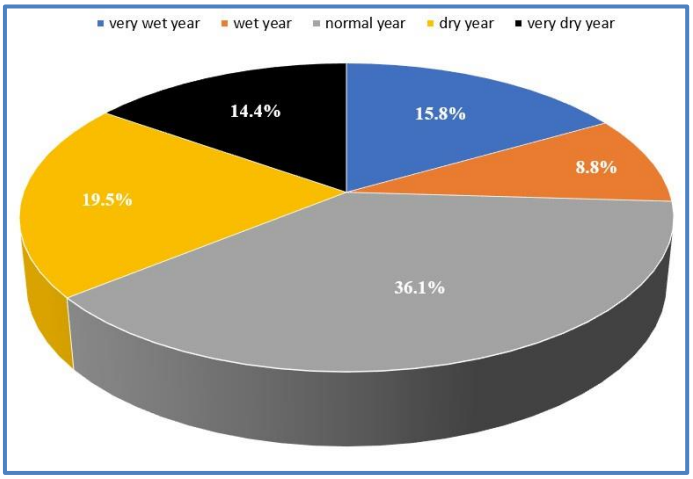

Figure 7: IRAQ's rainfall variability index distribution over time (1980-2019)

4. Conclusion:

Climate change is a global phenomenon that affects many aspects of Earth's climate, including rainfall distribution in Iraq. While the effects of climate change on rainfall in Iraq are not yet fully understood, there is evidence to suggest that the amount and intensity of rainfall are changing. Despite the impact of climatic changes on rainfall in Iraq, as evidenced by the negative linear regression trend of annual average rainfall for the period 1980-2019, the geographical distribution of rainfall remains variable from one place to another, depending on the factors causing precipitation. It is found that the annual average rainfall in northern regions is high, while in central and western regions, it is moderate, and in southern regions, it is low. The concentration indicator suggests strongly irregular rainfall concentration, while the RVI indicator shows that rainfall in Iraq fluctuates between normal, dry, and very dry years, with

very few wet years confined to the northern region. This variation in rainfall distribution is due to several factors, including the astronomical location of Iraq cities.

Terrain plays a significant role in heavy rainfall situations, with topographic features impacting rainfall fluctuation. Rainfall depth increases with elevation (known as the orographic effect), while depressions in the Mediterranean Sea, the Red Sea, and the Arabian Gulf cause light to medium intensity rain.

5. References:

[1] Li C, Zhang H, Singh VP, Fan J, Wei X, Yang J, et al. Investigating variations of precipitation concentration in the transitional zone between Qinling Mountains and Loess Plateau in China: Implications for regional impacts of AO and WPSH. Plos one. 2020;15(11):e0238709. https://journals.plos.org/plosone/article?id=10.1371/journal.pone.0238709.

[2] Solomon Zi W, Hyacinth M D. Climate Change, Rainfall Trends and Variability in Jos Plateau. Journal of Applied Sciences. 2020;20(2):76-82. https://scialert.net/fulltext/?doi=jas.2020.76.82.

[3] Oloruntade AJ, Mogaji KO, Imoukhuede OB. Rainfall Trends and Variability over Onitsha, Nigeria. Ruhuna Journal of Science. 2018;9. https://paravi.ruh.ac.lk/rjs/index.php/rjs/article/view/221.

[4] Small D, Islam S, Vogel RM. Trends in precipitation and streamflow in the eastern US: Paradox or perception? Geophysical research letters. 2006;33. https://agupubs.onlinelibrary.wiley.com/doi/full/10.1029/2005GL024995.

[5] Chen F-W, Liu C-W. Estimation of the spatial rainfall distribution using inverse distance weighting (IDW) in the middle of Taiwan. Paddy and Water Environment. 2012;10(3):209-22. https://link.springer.com/article/10.1007/s10333-012-0319-1.

[6] Vinay MD, Sharma PJ, Timbadiya P, Patel P, editors. Analysis of Rainfall Variability For Middle Tapi Basin, India. National Conference on Water Resources & Flood Management with Special Reference to Flood Modelling Presented at the National Conference on Water Resources & Flood Management with special reference to Flood Modelling, October; 2016.

[7] Oliver JE. Monthly precipitation distribution: a comparative index. The Professional Geographer. 1980;32(3):300-9. https://www.tandfonline.com/doi/abs/10.1111/j.0033-0124.1980.00300.x.

[8] De Luis M, Gonzalez-Hidalgo J, Brunetti M, Longares L. Precipitation concentration changes in Spain 1946–2005. Natural Hazards and Earth System Sciences. 2011;11(5):1259-65. https://nhess.copernicus.org/articles/11/1259/2011/.

[9] Valli M, Sree KS, Krishna IVM. Analysis of precipitation concentration index and rainfall prediction in various agro-climatic zones of Andhra Pradesh, India. Int Res J

Environ Sci. 2013;2(5):53-61. https://www.isca.me/IJENS/Archive/v2/i5/8.ISCA-IRJEvS-2013-078.pdf.

[10] Nery JT, Carfan AC, Martin-Vide J. Analysis of rain variability using the daily and monthly concentration indexes in southeastern Brazil. Atmospheric and Climate Sciences. 2017;7(02):176. https://www.scirp.org/journal/paperinformation?paperid=74841.

[11] Bahrawi J. RAINFALL DISTRIBUTION AND ITS CHARACTERISTICS IN MAKKAH AL-MUKARRAMAH REGION, SAUDI ARABIA. Applied Ecology and Environmental Research. 2018;16(4):4129-44. https://www.aloki.hu/indvol16_4.htm.

Al-Kitab Journal for Pure Sciences (2024); 8(1):104-124.
https://doi.org/10.32441/kjps.08.01.p10

Al-Kitab Journal for Pure Sciences
ISSN: 2617-1260 (print), 2617-8141(online)

https://isnra.net/index.php/kjps

The Fifth Section, the Semi Parabolic Curves, when the Focus equals the Vertex

Laith H. M. Al-Ossmi
https://orcid.org/0000-0002-6145-9478

Department of Civil Engineering, College of Engineering, University of Thi-Qar, Thi-Qar, IRAQ.

Corresponding Author: laithhady@utq.edu.iq

Citation: Al-Ossmi LH. The Fifth Section, the Semi Parabolic Curves, when the Focus equals the Vertex. Al-Kitab J. Pure Sci. [Internet]. 2024 May. 27 [cited 2024 May. 27];8(1):104-124. Available from: https://doi.org/10.32441/kjps.08.01.p10.

Keywords: Circles, Parabolic Curves, Secants, Parabola, Vertex.

Article History
Received 17 Jan. 2024
Accepted 26 Apr. 2024
Available online 27 May. 2024

Abstract:

This article introduces a unique case study involving open curves of parabolic form situated within two-dimensional spaces. It presents a new form of a two-dimensional curve achieved by repositioning the focal point to coincide with the vertex position, resulting in what is termed a Semi-Parabolic Curve (SPC) where the focal point acts as the vertex referred to as the SPC head point. In essence, the SPC represents the path traced by a point on a plane, where its distance from a fixed point (the focus), is always greater than or equal to its distance from a fixed straight line (the directrix). Furthermore, the article provides the coordinate equations that govern the points along these curves. With the potential to pave the way for exploring additional geometric aspects relevant to this class of curves, and to enabling comparative analyses across diverse mathematical and geometric domains, particularly in three-dimensional contexts in the future.

Keywords: Circles, Parabolic Curves, Secants, Parabola, Vertex.

القطع الخامس، منحنيات الشبيهة بالقطع المكافئ، عندما تتساوى نقطة البؤرة مع نقطة الرأس

ليث هادي منشد العصامي

كلية الهندسة / جامعة ذي قار/ محافظة ذي قار / العراق

Email: hardmanquanny@gmail.com

الخلاصة:

يدرس هذا البحث حالة جديدة تضم منحنيات مفتوحة في فضاء ثنائي الأبعاد ويقدم شكلًا جديدًا من المنحنيات ثنائية الأبعاد متحققا من إعادة توضيب نقطة التركيز لتتزامن مع موضع الرأس مما يؤدي إلى ما يُعرف بالمنحنى شبه القطع المكافئ (*SPC*) حيث تعمل نقطة التركيز عمل الرأس ويُشار إليها باسم نقطة الرأس. وتأسيسا، يمثل *SPC* المسار الذي ترسمه نقطة على مستوى، حيث تكون مسافتها عن نقطة ثابتة (البؤرة) دائمًا أكبر من أو تساوي مسافتها عن خط مستقيم ثابت (المستقيم الموجه).

علاوة على ذلك، فقد قدم البحث المعادلات الإحداثية التي تحكم النقاط على هذا النوع من المنحنيات ووفر القدرة لتمهيد الطريق لاستكشاف جوانب هندسية إضافية ذات صلة بهذا النوع من المنحنيات بما يؤمن مستقبلا إجراء تحليلات مقارنة عبر مجموعات متنوعة من المجالات الرياضية والهندسية، خصوصًا في سياقات ثلاثية الأبعاد في المستقبل.

الكلمات المفتاحية: دوائر، منحني القطع المكافئ، خطوط قاطعة، قطع مكافئ، رأس القطعة.

1. Introduction:

The parabola stands out as one of the easiest conic sections to understand, alongside the circle. Initially, Menaechmus used it to replicate the volume of a cube **[1-5]**. Apollonius, in naming and unraveling numerous crucial attributes, made significant contributions to its study. The parabola earned mentions in the works of Archimedes concerning the calculation of areas under parabolic arcs, found its place in Euclid's writings, and was subjected to scrutiny by Pappus, who delved into the concepts of focus and directrix. Galileo's investigations revealed that projectiles trace graceful parabolic paths through the air **[2]**.

The phenomenon of reflection by parabolic surfaces was analyzed by notable figures such as Gregory and Newton. In modern times, these ideas are employed successfully to find applications in diverse fields, from automotive headlight design to solar cookers, telescopes, astronomical radio dishes, the trajectories of comets, architectural design, and whenever a relationship between two variables involves one being proportional to the square of the other **[3].** A parabola is the set of all points in a plane that are equidistant from a fixed line (directrix) and a fixed point (focus) not on the line. The midpoint between the focus and the directrix is called the vertex, and the line passing through the focus and the vertex is called the axis of the parabola. It has a single focus and a directrix, which is a fixed line perpendicular to the axis of symmetry. The distance from any point on the parabola to the focus is equal to its distance to the directrix. Historically, conics have a long history that started with Menaechmus (ca 380- 320 BCE), continued with Euclid and Archimedes, and reached its peak with Apollonius **[3-4]**. Born about 380 BC in Alopeconnesus, Menaechmus called a parabola a section of a right-angled cone, and hyperbola a section of an obtuse-angle cone **[4-5]**. In mathematics, a parabola is indicated as a plane curve which is mirror-symmetrical and is approximately U

shaped. On the other hand, classical geometry indeed regards the parabola as a fundamental element within the realm of Euclidean geometry, typically within the framework of real numbers. Numerous treatises and mathematical works have been dedicated to exploring and establishing various properties of the parabola within this mathematical context. Euler made contributions to the study of parabolas and their equations, providing insights into their geometric and algebraic properties **[6-7]**. Laplace made advancements in applying algebraic methods to the study of conic sections, including parabolas **[8-9]**. They have significantly contributed to our understanding of this geometric shape and its properties over the real number field, making the parabola a fundamental concept in Euclidean geometry. In general, there are many methods in which the parabola features are constructed. For example, Eccentricity method, rectangular method, Parallelogram method, Tangent method and Offset method **[10]**. These methods are explained through various examples for drawing a parabola **[11].** Nevertheless, geometric constructing methods of parabola are very interesting when using the concentric circles. In parabola, the vertex point, i.e. the parabola head point, is equidistant from a point, the focus, and a line, the directrix. There are several geometric construction methods for drawing a parabola. But here are two commonly used methods: Focus-Directrix Method **[11-12]**, and Vertex-Focus Method **[11-13]**, as geometric construction methods, provide a visual representation of the parabolic curve based on the properties of the focus, directrix, and vertex. By following these steps and constructing multiple points, a parabola can be accurately drawn. Focus-Directrix Method **[14]** is based on the fundamental definition of a parabola, which states that a parabola is the locus of points equidistant from a fixed point (focus) and a fixed line (directrix). While Vertex-Focus Method focuses on constructing the parabola using the vertex and the focus of the parabola. In Focus-Directrix Method **[14-15]**, the construction process involves drawing the directrix perpendicular to the given line and finding points on the parabola equidistant from the focus and the directrix, whereas Vertex-Focus Method **[16]** as this method begins with marking the vertex and the focus, followed by constructing points on the parabola equidistant from the vertex and the line connecting the vertex and the midpoint between the focus and the vertex **[17-18]**. In general, both methods yield accurate representations of the parabola and are widely used in different contexts. The choice between the methods depends on the given information, preferences, and the specific requirements of the problem at hand **[19-20].**

In this part of the article, a new form of two-dimensional curve is produced by shifting the focus point along the equilibrium axis to be located at the vertex position which means a Semi Parabolic Curve (SPC) whose focus is the vertex point (the SPC's head point). An SPC is the

locus of a point which moves in a plane such that its distance from a fixed point, called the focus, is greater than or equal to the distance from a fixed straight line, called the directrix. An SPC's axis is a straight line passes through the focus and perpendicular to the directrix is called the axis of PSC while the point of intersection of an SPC and its axis is called the vertex of the SPC.

Furthermore, a geometric method in this paper simply flattened the picture and put the series of tangent circles in the same plane as the curve, where one of the segments is held constant. these techniques will be applied to the proposed model of SPC as a special form curve which has a geometric means; hence, its single point simultaneously lies at focus and vertex, and it extends in infinity at both directions of x and y-axis. This paper developed a geometric method and investigated the proportions of this new form of curve, SPC. To draw SPC, let a distance from (F) along the x-axis be a given constant (a), then let the y-axis pass perpendicularly on the symmetrical-axis from the point (F), the origin point (0,0). Let be given a point (F) sets as a vertex point (the PSC head point) at a given constant (AF) on the symmetrical-axis, then on the y-axis construct a line segment (AA1) with angle (u). Then draw a perpendicular on (AA1) intersects the x-axis at point (B1), the midpoint of line segment (AA1) is point B, which is a point of SPC. These segments are then plotted against the series of geometric means A1, A2, A3, to give a set of the points of B1, B2, B3, all of which lie along y-axis and x-axis respectively. This new curve is named as the SPC.

The vertex is the point of the focus which is the point of intersection of axis and directrix. Besides, if B be a point on the SPC and Bn and BF are the distance from the directrix and focus F point respectively, then the ratio (BF / BA) is called the eccentricity of the SPC, which is denoted by (e). By the parabola definition, the SPC ratio of e is; ($e \geq a$), **Figure 1**.

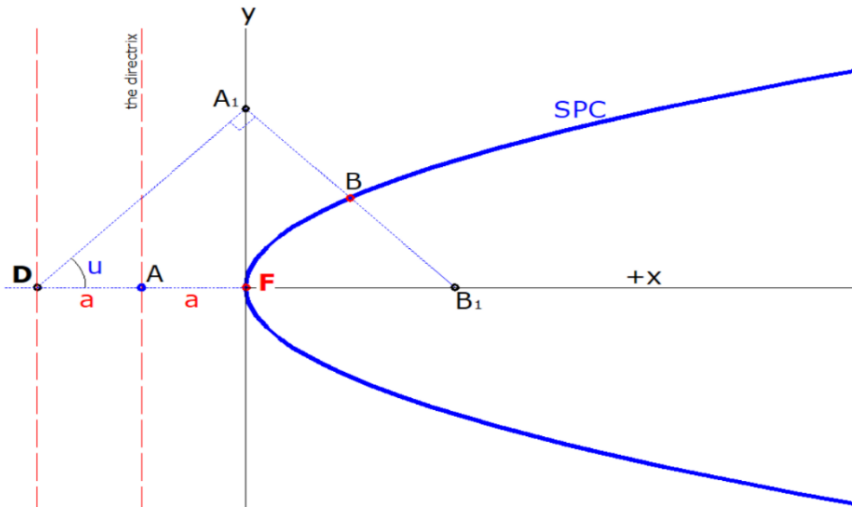

Figure 1. plot the SPC by a set of points in the plane that are equidistant from a SPC's point of *B* (the midpoint of line segment A_1B_1) which is a perpendicular on a line segment (DA_1) drawn from *D* with angle (*u*).

1. SPC's CONSTRUCTION METHODS

A set of geometric methods are produced in this paper to determine points and then to draw the SPC. These three methods are listed as follows:

2.1 Tangents and Circles Centers Method (TCCM):

The TCCM is built according to the proportion of the SPC. The particular principle of TCCM is depending on letting a given distance from the point (*A*), and the Focus point (the vertex) which is a constant of the SPC, determining the directrix of the SPC on the symmetrical-axis. In addition, the TCCM is applied to the construction of SPC by changing the meanings of tangents and perpendiculars at both side of y and x-axis, then the midpoints of obtained points help to construct the SPC points. The following procedures are presenting the TCCM:

- Let a horizontal distance from (*A*) to (*F*) along the x-axis be a given constant, (*a*), then let the y-axis be the symmetrical-axis from the origin point (*F*).
- Let be given a point (*F*) sets as a vertex point, the PSC head point, at a given constant (*AF=a*) on the symmetrical-axis.
- By angle (*u*), construct line segments from point (*D*) at a distance of (2*a*), these line segments intersect the y-axis at points (A_n).
- Then draw a perpendicular on (A_nD) from point (A_n), which intersect the x-axis at point (B_n).

By drawing a perpendicular on (A_nD) from point (A_n), a line segment (A_nE_n) is intersecting the y-axis at (*An*) and the x-axis at (E_n). From the midpoint of (A_nB_n), draw a circle that passes through intersection points; (A_n), and (E_n). As a result, the midpoint (*B*) is a center of the drawing circle, and also it is a point of SPC. Also, the generation method of TCCM benefits to determine as many as possible of points of SPC, and with a help from the French curves the pure curve is precisely drawn, as it is illustrated in **Figure 2**.

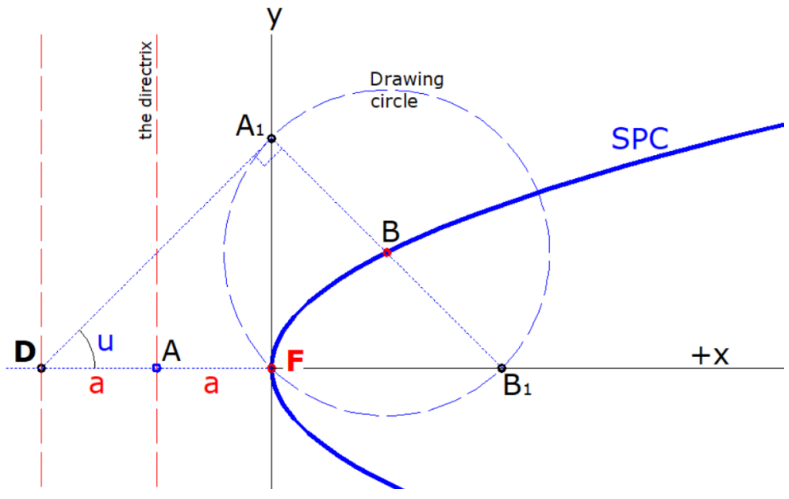

Figure 2.- plot the SPC according to TCSM, where the distance (*AF=a*) is a constant.

TCCM's theorem (1): This theorem states that the SPC's point is the midpoint of the line segment which is drawn from the intersection points with the y-axis and the x-axis, if the line segment is a perpendicular at the y-axis with the line which is drawn from the directrix point on the symmetrical-axis. TCCM generation method ia applied to the construction of SPC by the first theorem. To determine the position of a point on the SPC, let (AF) be a given distance where (F) is the origin point. Construct a segment line from (D) to intersect the y-axis at a point (let it be A_1), then from (A_1) draw a perpendicular on (AA_1) which is extended passing through x-axis at (B_1). Point (B) is the midpoint of the segment (A_1B_1), which is a point of the SPC, **Figure 2**.

***Proof*:** To proof this theorem, let the segment line (DF) be a given distance on the symmetrical-axis where (F) is the SPC focus which is located on the origin point. Construct a segment line from (D) to intersect the y-axis at point (let it be A_n), then from (A_n) draw a perpendicular on (DA_n) which is the secant passing through coordinate x-axis at (B_n), then let the point (B) be the midpoint of this segment (A_nB_n). the triangle (A_nFB_n) is a right-angled triangle. Thus, the circle drawn from the midpoint of the segment (A_nB_n) is passing through three points (F), (A_n), and (B_n); this means ($A_nB = BB_n$). Hence, points in the plane that are equidistant from a point B, the midpoint of line segment A_nB_n, is a perpendicular on line (DA_n) with angle (u). And then, according to the SPC definition, Figure 1, the point of the SPC is the midpoint of the segment (A_nB_n), **Figure 3**. Hence, points in the plane that are equidistant from a point B, the midpoint of line segment A_nB_n, is a perpendicular on line (DA_n) with angle (u). And then, according to the SPC definition, Figure 1, the point of the SPC is the midpoint of the segment (A_nB_n), **Figure 3**.

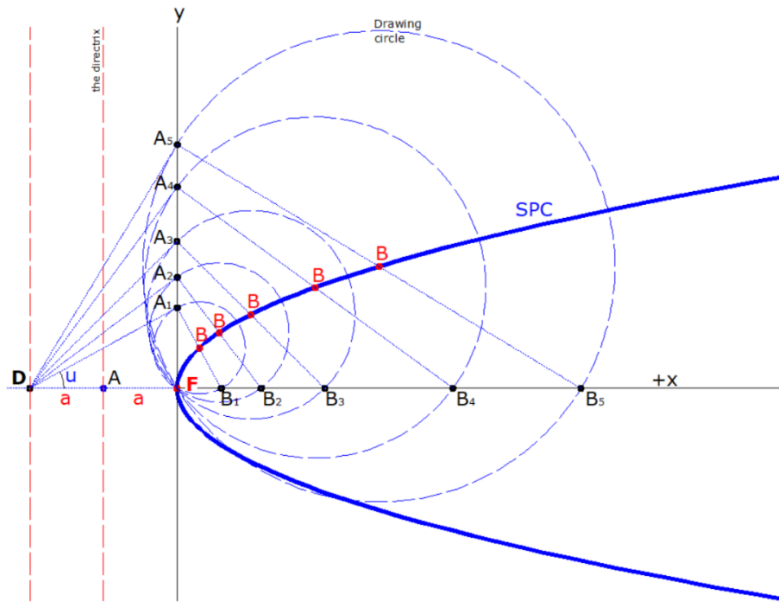

Figure 3.- The plot of the SPC according to TCCM's theorem (1), where; (F) is the focus- vertex point.

It is noticeable that the SPC has a single drawing circle whose center point is the vertex point of the SPC. Therefore, any shared point at the SPC and the parabola segment passes through a single point which is the SPC's vertex and the parabola focus, (F).

TCCM's theorem (2): states that at any segment whose midpoint is a point of SPC, the line length from the focus to the SPC point or that from the SPC point to either the top or end point of the segment is a constant.

***Proof*:** To proof this theorem, let (*AF*) be a given distance where (*F*) is the SPC focus located on the origin point (0,0). Then let (*DF*) be a segment line of (2*a*) located on x-axis. From theorem 1, the SPC' drawing circle whose diameter is the segment (A_nB_n), thus the drawing circle passes throught 3 points: (*F*), (A_n) and (B_n). Then, from drawing a circle defination, the diameter (A_nB_n) is divided into two equal parts: ($A_nB = BB_n$), then from these three points, the $\Delta(A_nB_nF)$ is a right angled triangle at the focus- vertex point (*F*) **, Figure 4**.

Accordingly, the segments;

$$(A_1F) \llcorner (FBn),$$

then from the drawing circle defination;

$$(A_1B = BF = BB_1),$$

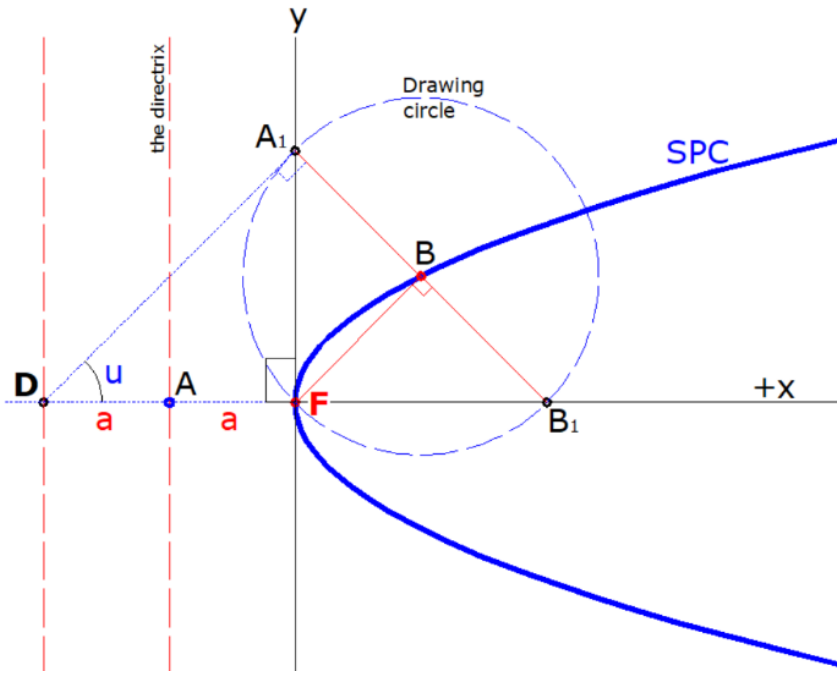

Figure 4.- plot the SPC according to TCCM's theorem (2), where; (*F*) is the focus- vertex point and Segments ($A_1B = BF = BB_1$) .

TCCM's theorem (3): states that for any SPC, all secants are intersected at a single point lies on the x-axis at a distance of (2*a*), from the focus- vertex point.

***Proof*:** To proof this theorem, let (*AF*) be a given distance where (*F*) is the SPC focus located on the origin point (0,0). Then let (*DF*) be a segment line of (2*a*) located on x-axis. From theorems 1 and 2, the right-angled triangles $\Delta(DFA_n)$ are adjacent triangles shared angle (*AnFD*) and they are said to be adjacent to each other along a common side (*DF*), which is the horizontal distance from the focus- vertex point; thus, *DF*=2*a*, , **Figure 3**.

It is noticeable from theorem (3) that the SPC is extended into the infinity along the symmetrical-axis where (*F*) is the SPC focus located on the origin point (0,0). However, it is a succinct way to say that the length of SPC segment is varied according to constance value of (*a*), the horizontal distance from the focus- vertex point (*F*) and (*DF*). Furthermore, any point of SPC is a center of a single circle which is passing through the focus point. Biulding on the theorem one, all circles whose center point is a point of SPC are passing through 3 points (*F*), (A_1) and (B_1), where (*B*) is the center point and a point of the SPC.

TCCM's theorem (4): states that from any drawing circle, (whose center is a point of SPC), the horizontal line from its center point parallel to the x-axis and intersects the tangent of the drawing circle at a midpoint which from it the perpendicular is drawn from the focus on the line segment that is constructing the focus and the center point of the drawing circle.

***Proof*:** To proof this theorem, let (*B*) be a point on SPC, and the drawing circle of SPC whose center point is (*B*) intersects the y and x-axis at (A_n) and (E_n) respectively. From point (*B*) construct a line segment parallel to x-axis and perpendicular on (DA_n), hence line segment (BN_n) intersects (DA_n) at a point (N_n) which lies on the directrix. Then, from SPC definition, ($DA = AF=a$). From the right-angled triangles $\Delta(DFA_n)$, line segments (N_nA) parallel to y-axis, and divides (DF); then,

($DA= AF = N_nA = a$), thus; ($DN_n = N_nA_n$),

This theorem indicates that the triangle whose sides are (N_nB), (BF), and (FN_n) is a right angled- triangle, hence the line segment (N_nF) is perpendicular on (FB), **Figure 5**. Similarly, it indicates that the line segment constructed from any point on SPC and the focus is perpendicular on that line segment constructed from the horizontal line from the SPC focus- vertex point, which intersects the directrix, hence; angle ($BFN_n = 90^o$).

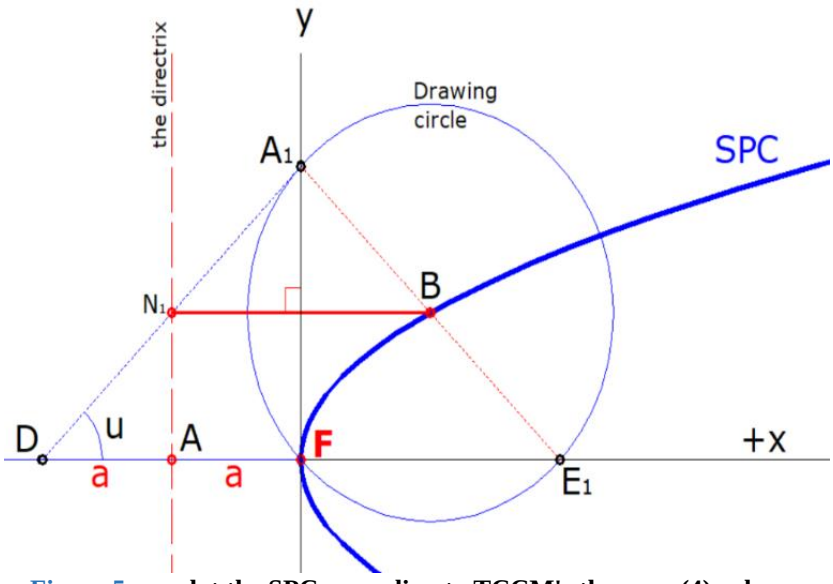

Figure 5.a. - plot the SPC according to TCCM's theorem (4), where;

($DN_1 = N_1A_1$) *and;* ($DN_2 = N_2A_2$),

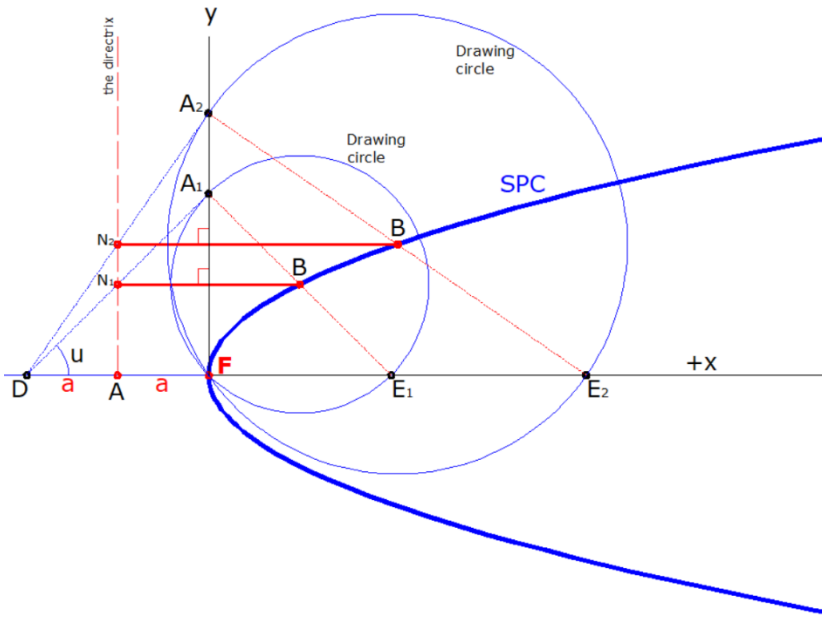

Figure 5.b. - plot the SPC according to TCCM's theorem (4), where; ($DN_1 = N_1A_1$) *and;* ($DN_2 = N_2A_2$),

TCCM's theorem (5): states that the tangent of latus rectum point of SPC is a perpendicular on the line segment drawn from the center point of the drawing circle, whose center is a point of SPC, passing through the x-axis at a point that made by the vertical tangent of this circle.

Proof: To proof this theorem, let (B) be a point on SPC, which is the center point of the drawing circle of SPC and its circumference intersects the y and x-axis at (A_n) and (E_n) respectively. From point (B) and (E_n) draw vertical segment intersect SPC at point (T) and (T_n), which are SPC latus rectum. Then, link between (A) and (T), and between (D) and (T_n) , **Figure 6**.

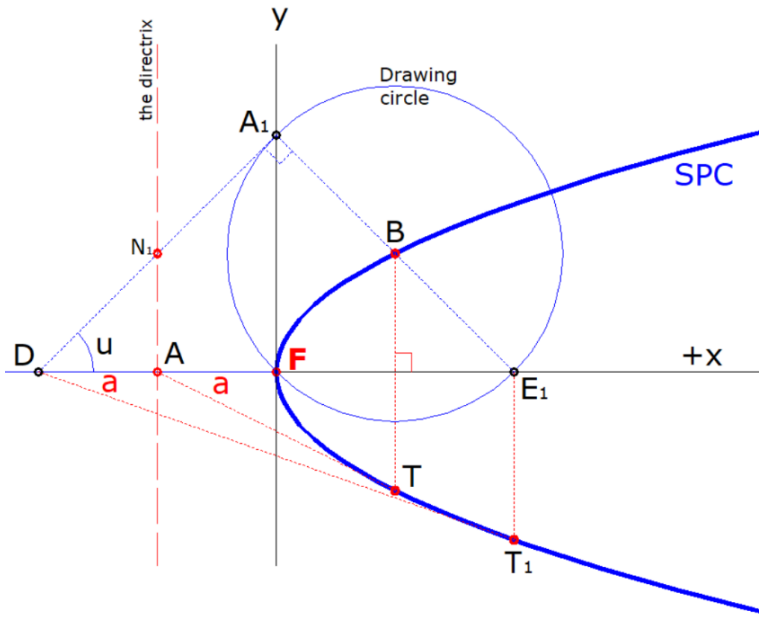

Figure 6. - plot the SPC according to TCCM's theorem (°), latus rectum

Where segments; *AT* and T_nD are tangents on the SPC from points; *T* and T_n respectivelly.

TCCM's theorem (6): states that eccentricity of SPC is $e \geq a$:

***Proof*:** To proof this theorem, let (B_n) be a point on SPC, and *A* and *F* are the distance from the SPC directrix and focus respectively. From the previous theorem (5), the three points (N_n), (*Bn*) and (*F*) made up a right angled- triangle $\Delta(N_nFB_n)$, where angle $u = \left(\frac{\pi}{2}\right)$. Note that when ($FB_n=0$), formerly ($e= a$). Besides, the line segment (FB_n) is the radius of the drawing circle of SPC, then the ratio:

$e= (r/ N_nB_n)$, see **Figure 7**.

Then, the ratio $e= (BF/ N_nB_n)$ is called the eccentricity of the SPC, which is denoted by *e*. By the definition for the SPC, $e \geq a$.

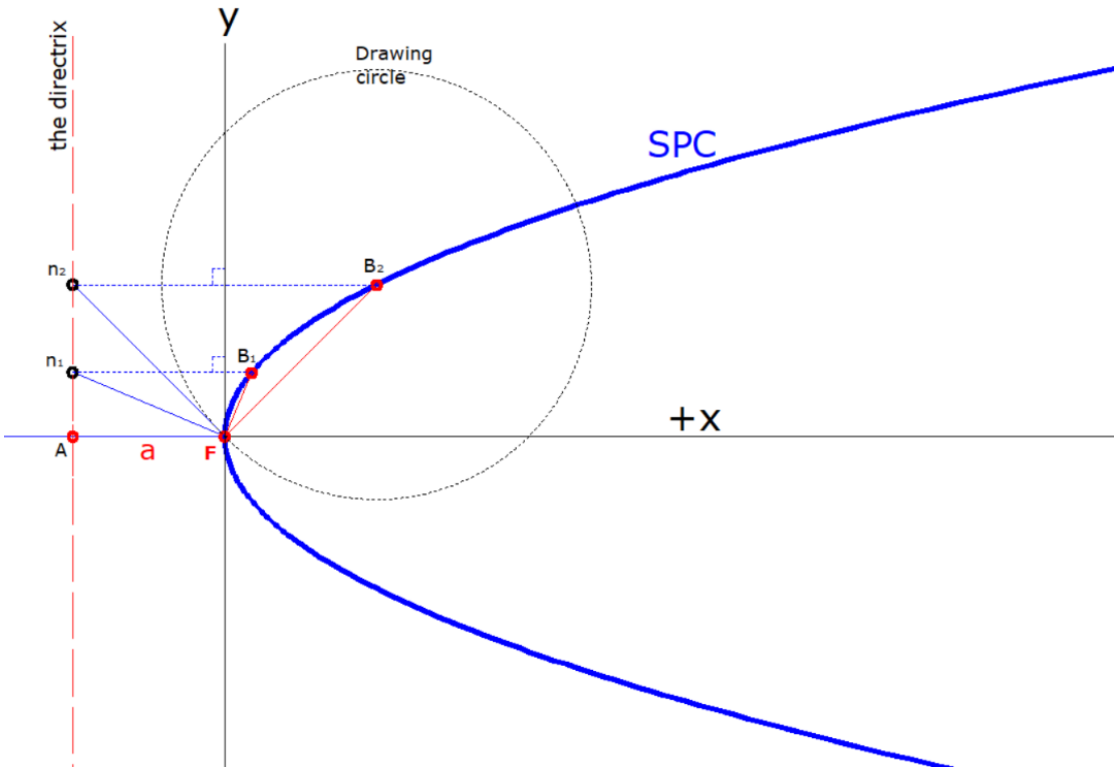

Figure 7. - Eccentricity of the SPC, $e \geq a$

Regarding the parabola segment whose focus is the vertex of SPC, eccentricity of the parabola is (e =1) which is less than that of SPC. From the origin point (0,0), there is only one tangent which touch SPC from the latus rectum at point ($\pm 2a$, $\pm a$), and its length can be determined by the following formula: $\sqrt{3a^2}$, since the SPC drawing circle, whose center is the tangent point (*B*) has a radius of ($\sqrt{a}$), which lies at ($\pm 2a$, $\pm a$), whereas the origin circle of SPC

whose center point is (*A*), it has radius of (*a*) and it tangent the vertex-focus point of the SPC, **Figure 7**.

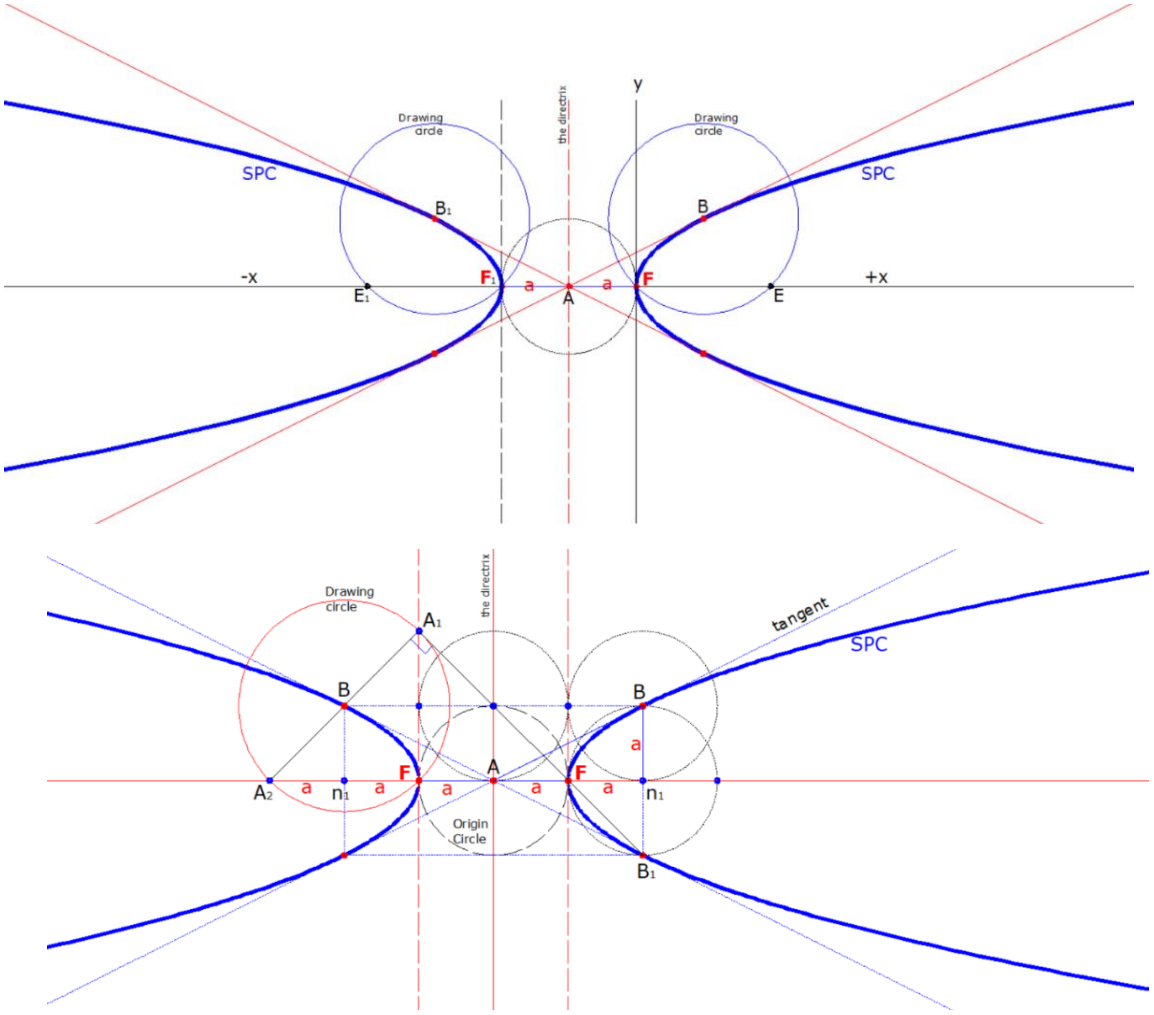

Figure 8. - plot tangents related to SPC latus rectum' point.

Figure 8 illustrates that from the intersection point of the directrix and the x-axis, point (*A*), is only one tangent to the SPC from the latus rectum' point (*B*). Hence, the SPC tangent point lies at ($\pm a$,$\pm$ $2a$), since the SPC tangent from the latus rectum' point has a constant slop with a precisely value of (u = 26.56512º), where:

$$A_1B=BA_2=\sqrt{a}\,, \tag{1}$$

$$A_1B_1=3\sqrt{a}\,, \tag{2}$$

2.2 Tangent Circles & Secant Midpoints (TCSM) construction method:

The TCSM method is built according to the proportion of the SPC. The particular principle of TCSM method is depending on letting a given distance from the point (*A*), and the Focus point (the vertex) is a constant of the SPC, determining the directrix of the SPC and the vertex point (*B*) set on the symmetrical-axis. In addition, the TCSM method is applied to the construction of SPC by changing the meanings of tangent circles on the midpoint of their

secants. In this paper, given the focus (F) and the directrix at a constant distance of (a) from point (A), and letting (F) be the origin point of y and x-axis, the TCSM method can construct any number of points on the SPC. The following procedures are presenting the TCSM:

- Let a horizontal distance from (A) to (F) along the x-axis be a given constant, (a), then let the y-axis be the symmetrical-axis from the origin point (F).
- Let be given a point (F) sets as a PSC vertex point, the head point, at a given constant ($DF= 2a$) on the symmetrical-axis, and then from point (D) construct a set of tangent circles at the symmetrical axis starting by the first circle with radius (a), so that the next circles are drawn with increased radius gradually, each circle intersect the y-axis and x-axis at points (A_1) and (E_1) respectively.
- Construct secants from point (A_1) at y-axis to link that point (E_1) at the x-axis.
- From the midpoint of secants (A_nE_1), the midpoint of the secant (B_1) is a point of the SPC, **Figure 9**.

In order to obtain the other points of the SPC across the symmetrical axis, repeat the previous steps at the symmetrical axis to determine these opposite points. Besides, the generation method of TCSM benefits to determine as many as possible points of SPC, and with the help from the French curves, the pure curve is precisely drawn, as it is illustrated in **Figure 9**.

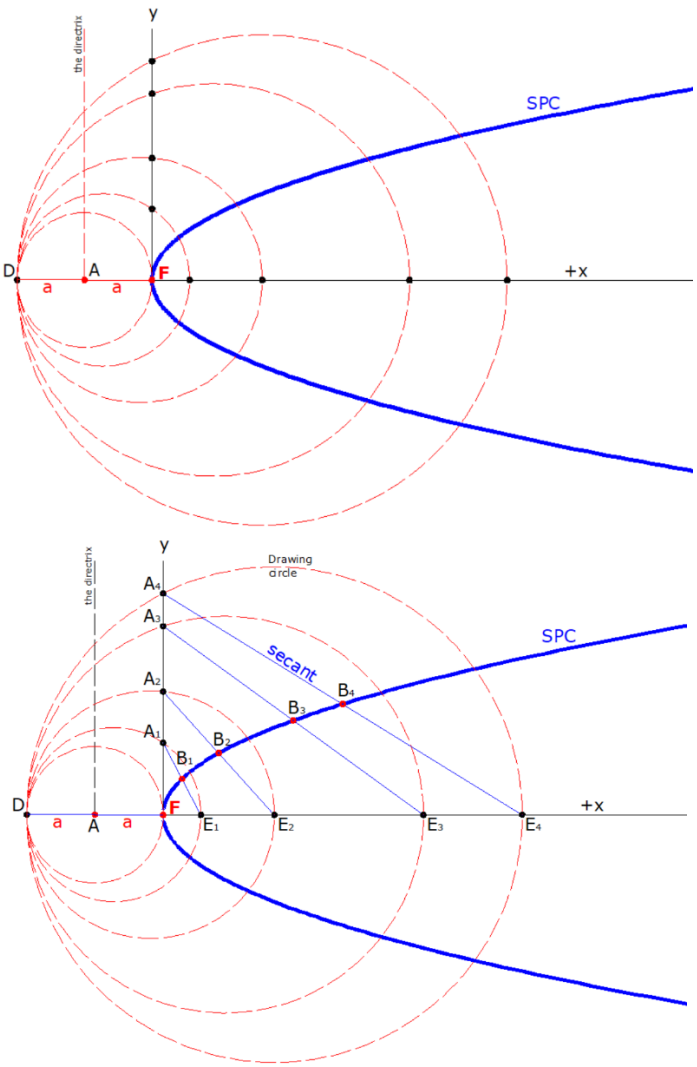

Figure 9. - plot the SPC according to TCSM, where the SPC vertex- focus is (*F*), and (*DF*= 2*a*).

It is perceptible that both methods, (TCSM) and (TCCM), can work together to produce SPC points; hence, drawing procedures of both methods are built on a set of circles. However, all points of SPC can be obtained without drawing circles since PSC points lie on the midpoints of secants, (in TCSM), or by a set of perpendiculars midpoints at these segments drawn from y-axis and point (*D*), (in TCCM), **Figure 10**. Correspondingly, the SPC points can be determined according to two constants: the first constant is (*a*), and then the distance between (*D*) and (*F*), (*2a*). The second constant is angle (*u*) which determines all secants lengths and then its midpoints which are the SPC points. Additionally, value of (*a*) determine the case in which the SPC is a concave up curve or a concave down.

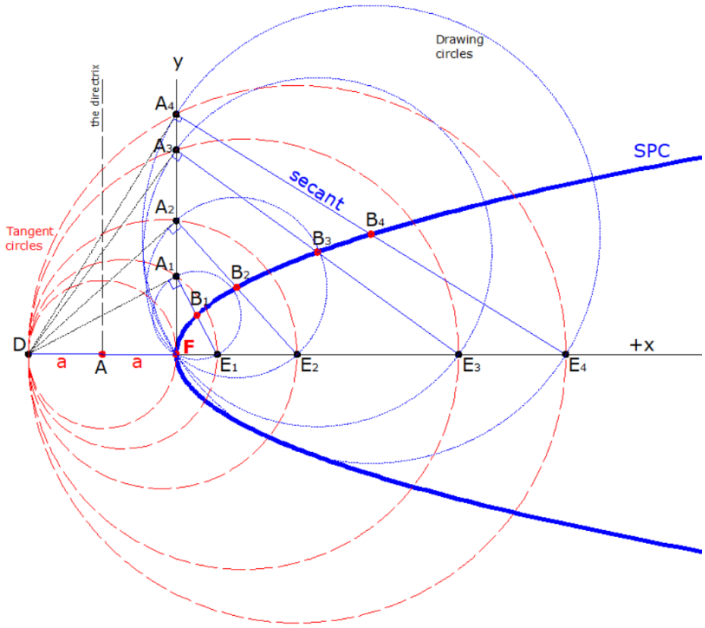

Figure 10. - plot the SPC by both TCSM & TCCM's theorems.

3. Relationships between SPC and Parabola

In general, SPC is a curve whose vertex lies at the focus point of a parabola segment. Furthermore, the parabola directrix lies at ($2a$); hence, the SPC's vertex point is the parabola focus, (F). Similar to the parabola, the SPC has two orientations, concave up and concave down. The orientation of an SPC can be found from its equation.

- The SPC is concave up if ($a > 0$)and concave down if ($a < 0$).
- The y-intercept is where the SPC meets the y-axis.
- The x-intercepts are where the SPC meets the x-axis.

Also, there will be either;

- two x-intercepts.
- exactly one intercept.
- no intercepts.

A reflection of a geometric figure is a transformation that results in a mirror image of it. For example, the SPC is reflected across the x-axis. Each point (x, y) on the original SPC is reflected to ($x, –y$) on the reflected parabola. When the parabola directrix lies at (a) then the SPC's vertex point is the parabola focus, (F). Also, when the parabola segment and the SPC share the same point of the vertex, then the midpoints of all these vertical perpendiculars from any points of parabola and the x-axis are SPC' points. This means that the midpoint (B_n) of a vertical segment (P_nD_n) drawn from any point of parabola segment (P_n) to x-axis is a point of SPC, **Figure 11**.

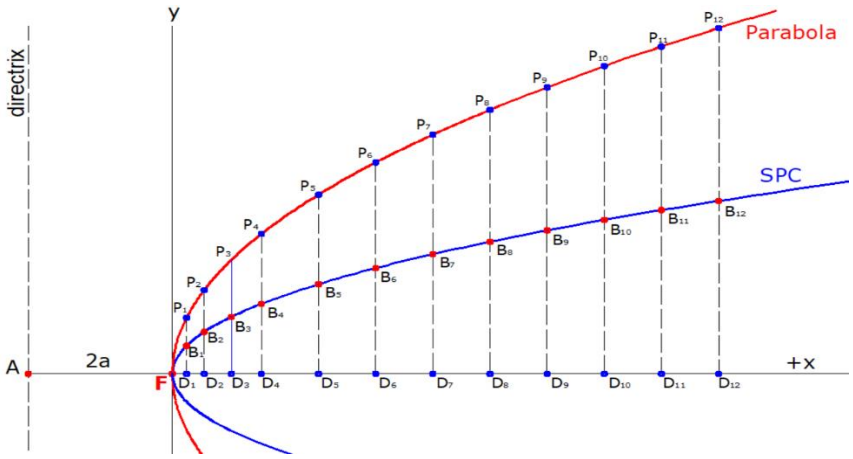

Figure 11. - plot the SPC by a midpoint of perpendicular drawn from any point on parabola to the x-axis, where; ($P_nB_n = B_nD_n$), if the parabola segment and SPC share the same point of the vertex.

The SPC is a curve whose vertex lies at the focus point in 2-dimentional plane. In general, SPC key proportions are listed in **Table 1**.

Table 1. - Key standard forms of the SPC.

SPC's Standard Equation.	$y=x\tan(90-u)$, where; ($a > 0$)			
Shape of SPC.	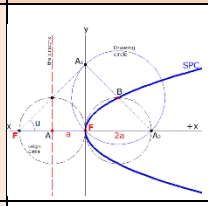	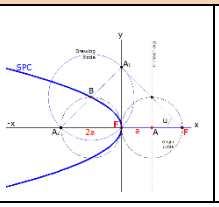	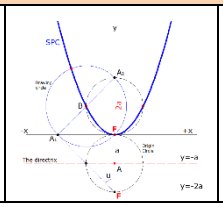	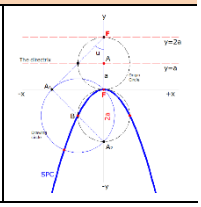
Vertex point.	*A (0,0)*	*A (0,0)*	*A (0,0)*	*A (0,0)*
Focus point.	*F (0,0)*	*F (0,0)*	*F (0,0)*	*F (0,0)*
Equation of directrix.	$x= -a$	$x= a$	$y= -a$	$y= a$
Equation of axis.	$y= 0$	$y= 0$	$x= 0$	$x= 0$
Length of latus rectum.	$2a$	$2a$	$2a$	$2a$
Extremities of latus rectum.	$(a , \pm a)$	$(-a , \pm a)$	$(\pm a , \pm a)$	$(a , - a)$
Equation of latus rectum.	$x=a$	$x=-a$	$y=a$	$y=-a$
Equation of tangents at vertex.	$x=0$	$x=0$	$y=0$	$y=0$
Focal distance of $B(x,y)$	$x+a$	$x-a$	$y+a$	$y-a$
Eccentricity (e).	$\geq a$	$\geq a$	$\geq a$	$\geq a$

4. SPC's Standard Equation

By drawing the SPC according to the TCCM, let (a) be the distance of the directrix and the SPC's vertex point (F) along the symmetry axis, where a $\neq 0$, as it is illustrated in **Figure 12**. Then, from the right-angled triangles: (DA_1F), (A_1FE_1), and (DA_1E_1):

$$\cos u = 2a / DA_1, \qquad (3)$$

And defined by;

$$DE_1 = 2a + FE_1, \quad (4)$$

Where;

$$\cos u = \left(\frac{\left(\frac{2a}{\cos u}\right)}{2a+FE1}\right), \quad (5)$$

And we denoted this relation as;

$$2a \cos u + FE_1 \cos u = (2a/\cos u), \quad (6)$$

$$FE_1 \cos u = (2a / \cos u) - 2a \cos u, \quad (7)$$

$$FE_1 \cos u = 2a - 2a \cos^2 u/(\cos u), \quad (8)$$

$$FE_1 \cos u = 2a\,(1 - \cos^2 u)/(\cos u), \quad (9)$$

Then by equations 1 and 9 we find;

$$FE_1 = 2a\,(1 - \cos^2 u)\,/(\cos^2 u), \quad (10)$$

hence SPC' points (x,y) given as follows;

$$x = FE_1 / 2, \quad (11)$$

where; ($a > 0$), then; $\tan(90-u) = (y/x)$,

Then, all points of SPC can be determined by the following formulae:

$$x = \left(\frac{1}{2}\right)\left(\frac{2a\,(1 - \cos^2 u)}{\cos^2 u}\right), \quad (12)$$

$$\boldsymbol{y} = \left(\left(\frac{1}{2}\right)\left(\frac{2a\,(1 - \cos^2 u)}{\cos^2 u}\right)\right)\tan(90 - u)\,, \quad (13)$$

The standard equation of SPC's point (x,y) is given as follows:

$$y = x \tan(90 - u), \quad (14)$$

$$x = y/\tan(90 - u), \quad (15)$$

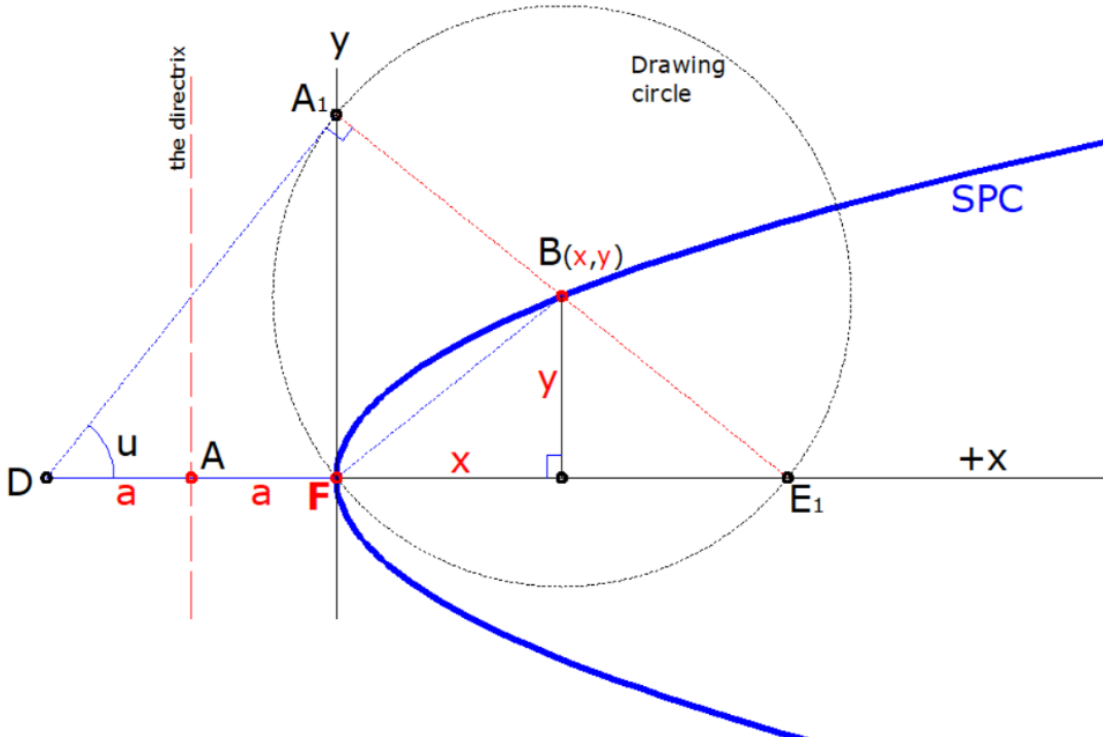

Figure 12. - plot the SPC according to the TCCM to determine position of B(*x,y*).

5. APPENDIX A: SPECIAL CASES OF SPC

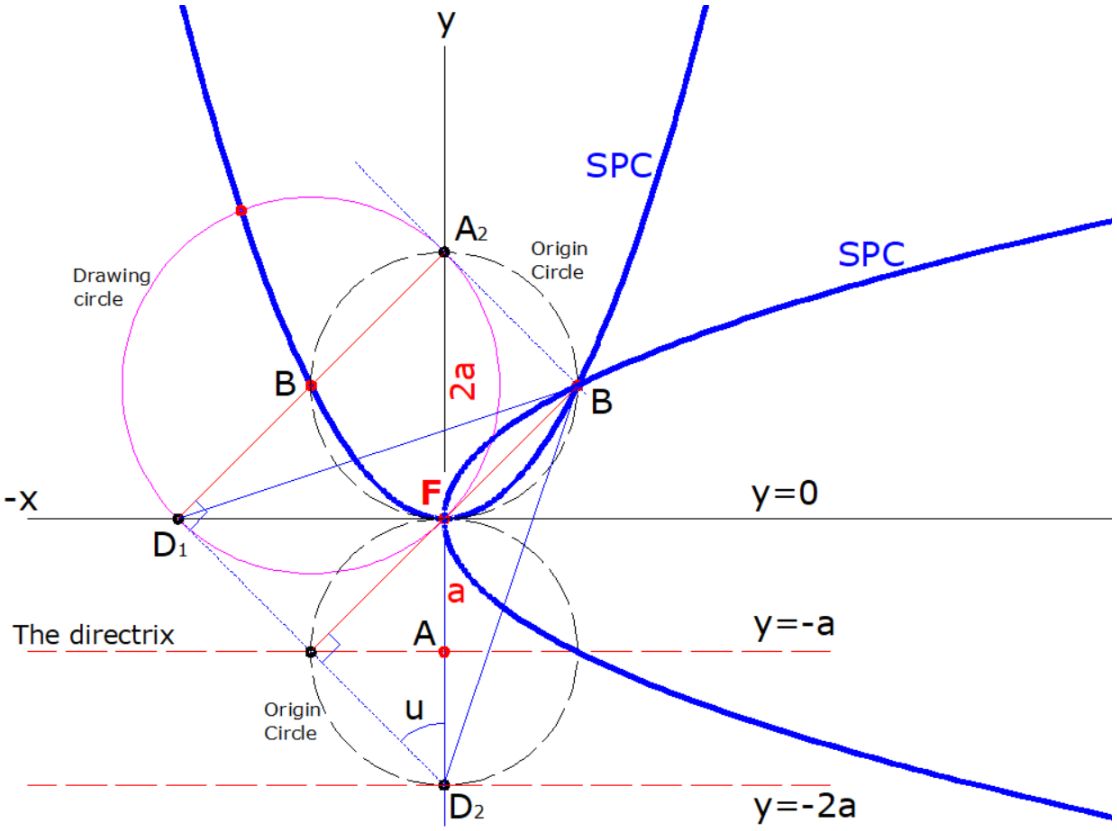

Figure 13: intersection two SPC, when *AF= a, FB = BA₂, & BA₂* parallel and equal to *D₁D₂/₂*.

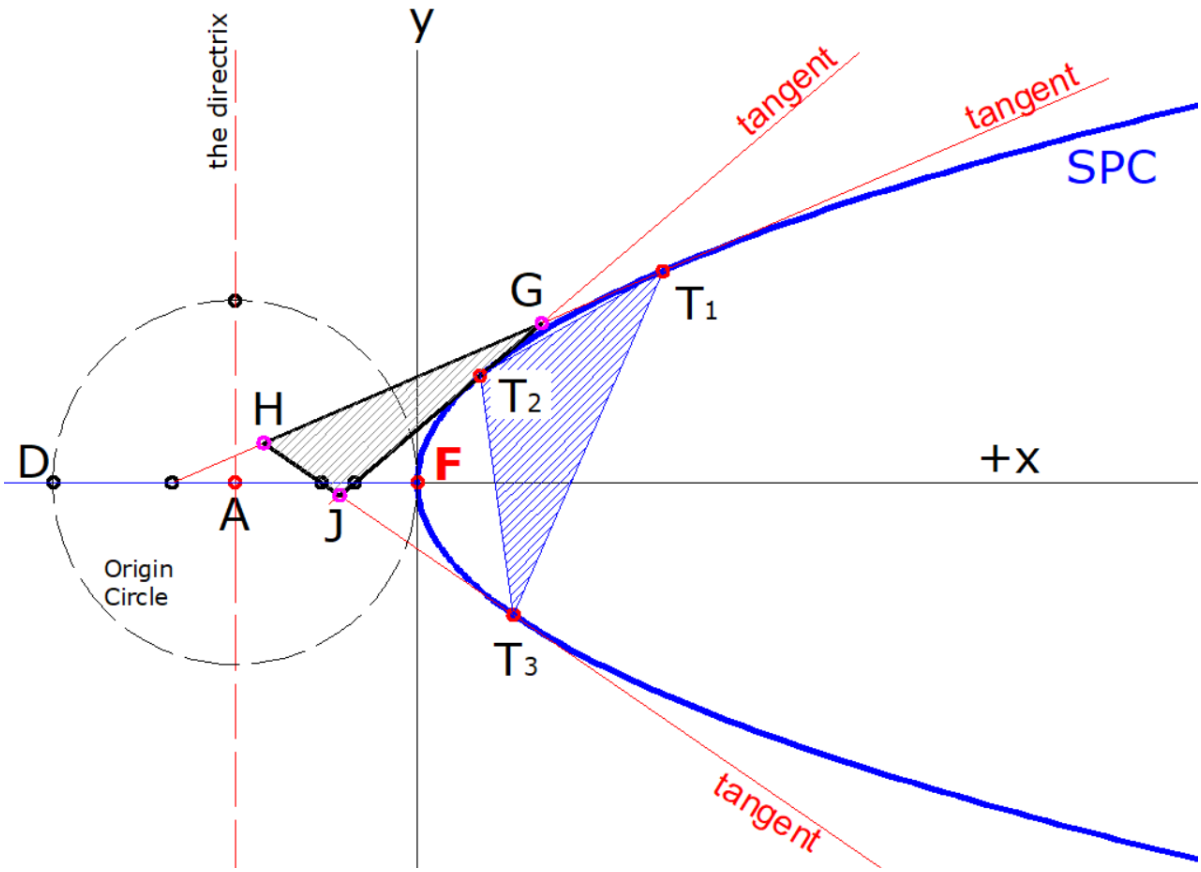

Figure 14: If all three points lie on the SPC, then we have SPC's triangle.

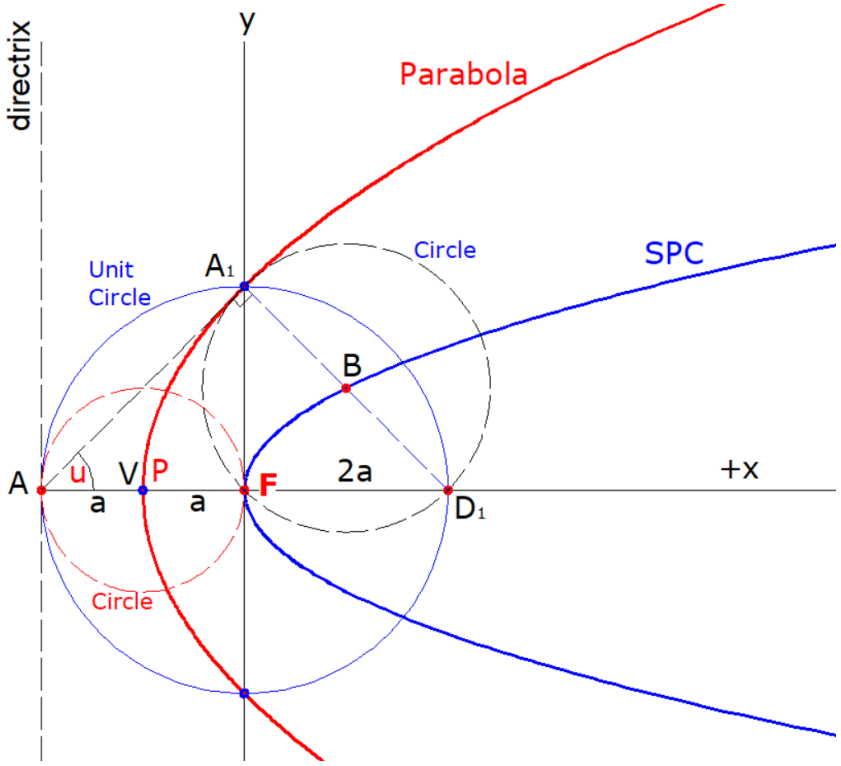

Figure 15 : when both parabola and SPC shared the drawing circle radius, (circle1= circle2).

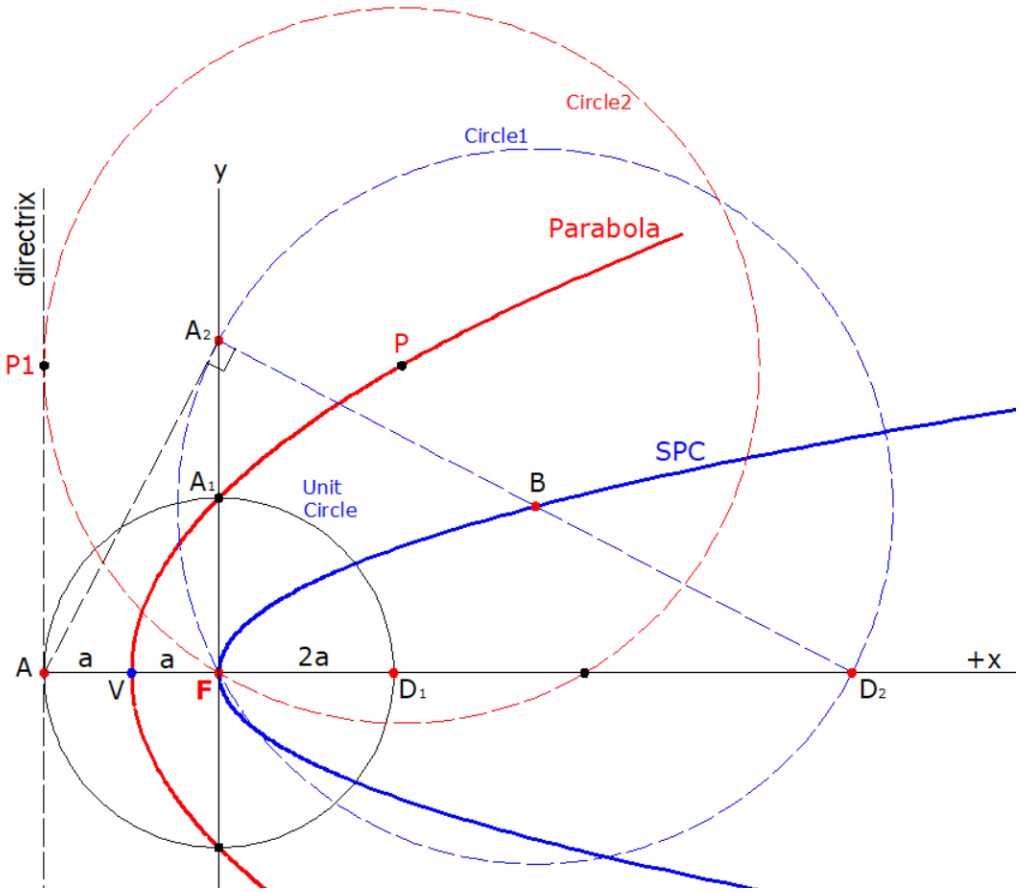

Figure 16: when both parabola and SPC shared the drawing circle radius, (circle1= circle2).

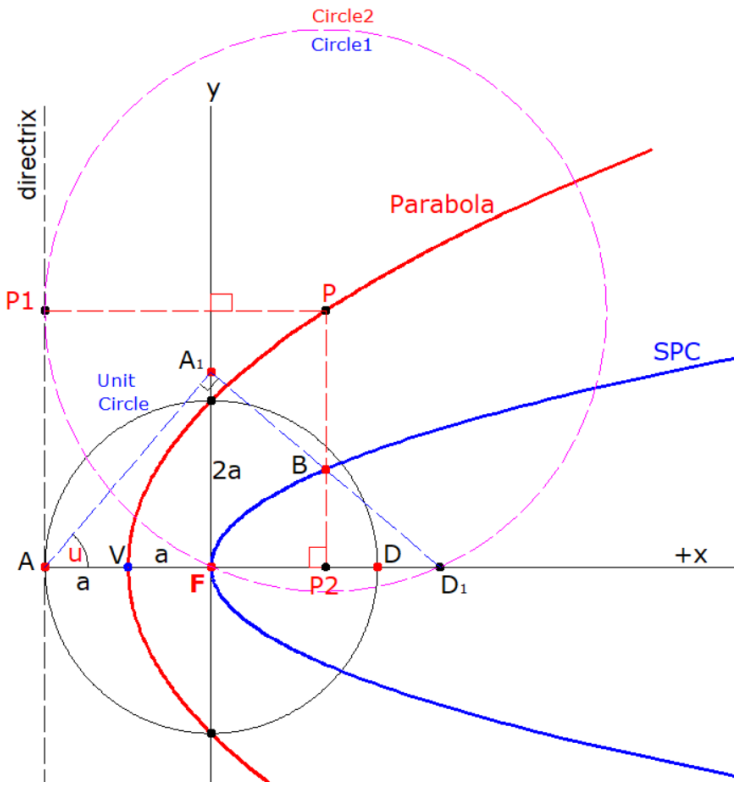

Figure 17 : when the SPC' vertex = parabola's focus

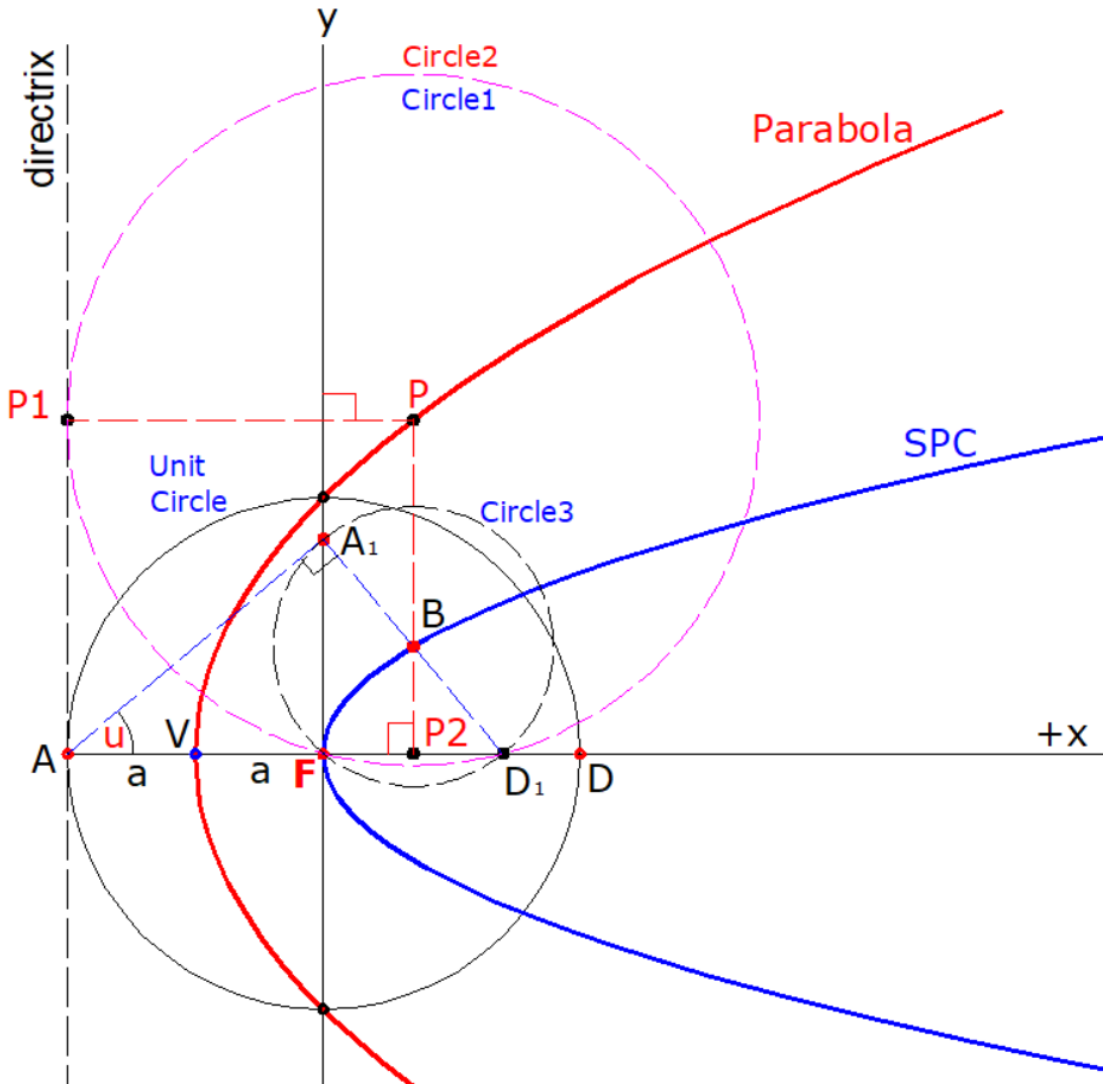

Figure 18: when the SPC' vertex = parabola's focus

6. Conclusion

This paper has dealt with a novel form of an open curve named SPC, whose focus point lies on its vertex. Two geometric construction methos, (TCSM) and (TCCM) are produced to determine the points of SPC. The SPC is a symmetric and open curve, and it extends into infinity alone its symmetrical axis. The SPC shared some geometric and algebraic proportions, but the key difference is that the SPC's focus lies on its vertex point, a set of SPC key proportions are investigated and listed in **Table 1**.

This article has shown that this new curve has a focus, in which all drawing circles whose center is located on the SPC are passing through the SPC focus and intersecting the x-axis and y-axis respectively. The distance along the symmetry line between the SPC focus and the directrix point is varied (a) in which the shape of SPC is concaved up (if $a > 0$) ,or concaved

down (if $a < 0$) while from any point at SPC, the drawing circle is intersecting the symmetrical axis at a constant of ($2x$). Additionally, the radius of any drawing circle equals to $\left(\sqrt{x^2 + y^2}\right)$, correlated to any point of SPC. In general, there is a couple of key integers [a, u] for generating and describing the SPC proportions.

There are several known proofs that have not been introduced in this article, but even though a lot of proofs are known. There is no doubt that there are a lot of undiscovered proofs, and they are worth discussing, sharing and presenting.

Future researches may deeply deal other proportions of this curve, and a list of these proportions are illustrated and listed in **Appendix of special cases of SPC,** for those interested in studying them and applying the result to a generalization of some geometrical theorems related to this form of curve.

FUNDING : None.

ACKNOWLEDGEMENT: It gives vast pleasure to thank all those who extended their honest support, guidance and fortified to reach the publication of the article. Thanks go to my family members for their complete support and co-ordination; my wife Angham Mehdi, daughters; Noor, Nada, Fatima and Omneya.

Authors' declaration: - Conflicts of Interest: None. - I hereby confirm that all the Figures, Tables, and measurements in the manuscript are mine.

7. References:

[1] Sanchez WB, Glassmeyer DM. Connecting Parabolas and Quadratic Functions. Math Teach. 2016/2017;110(5):380-386.

[2] Choi SC. The Universal Parabola. KoG. 2018 Jan; DOI: 10.31896/k.22.4.

[3] Alkhaldi, Wildberger NJ. The Parabola in Universal Hyperbolic Geometry I. KoG. 2013; pp.14–41.

[4] Choi SC, Wildberger N. Parabolic Triangles, Poles and Centroid Relations. KoG. 2020; DOI: 10.31896/k.24.1.

[5] Todhunter I. A treatise on plane co-ordinate geometry as applied to the straight line and the conic section. JO. 2020; Available from: info:edu-jhu-library/collection/brittlebooks/id/barcode/31151007555125.

[6] Ibragimov NH. CRC Handbook of Lie Group Analysis of Differential Equations Volume I: Symmetries, Exact Solutions, and Conservation Laws. CRC Press; 2018.

[7] Chindamo R, Ellis J, Peck R. The Mathematics of Parabolas: Focusing on the Vertex Form. Int J Math Teach Learn. 2021;22(3).

[8] Icon DV, Fulier J, Icon O, R Lucia. Note on Archimedes' quadrature of the parabola. Int J Math Educ Sci. 2020; Available from: https://doi.org/10.1080/0020739X.2021.1889700.

[9] Al-Ossmi LHM. Elementary Treatise on Melted-like Curves Derived from Center Ellipse and Circle. Iraqi J Comput Sci Math. 2023;4(1):114-129. DOI: 10.52866/ijcsm.2023.01.01.009.

[10] Williams K. Leonhard Euler: life, work and legacy. Math Intelligencer. 2018;30:66-69. DOI: 10.1007/BF02985741.

[11] Wen X. Parabolic higgs bundles on the projective line, quiver varieties and deligne-simpson problem. Algebraic Geometry (math.AG). 2020; Available from: https://doi.org/10.48550/arXiv.2101.01913.

[12] Wen X. Parabolic higgs bundles on the projective line, quiver varieties and deligne-simpson problem. Algebraic Geometry (math.AG). 2021; Available from: https://doi.org/10.48550/arXiv.2101.01913.

[13] Jianping W, Wen X. On the moduli spaces of parabolic symplectic/orthogonal bundles on curves. Algebraic Geometry (math.AG). 2021 Jan 7; Available from: https://doi.org/10.48550/arXiv.2101.02383.

[14] Björn J, La SB, López-M J, L Francesco, Z Myrka. Perceptual judgments of duration of parabolic motions. Sci Rep. 2021;11:7108.

[15] Lyachek Y. An Efficient Method for Forming Parabolic Curves and Surfaces. Mathematics. 2020;8(4):592. DOI: 10.3390/math8040592.

[16] Bialy M. β-Function for ellipses and rigidity. Entropy. 2022;24(11):1600. DOI: 10.3390/e24111600.

[17] Da Silva J, Ramos R. The Lambert-Kaniadakis wκ function. Phys Lett A. 2020;38(4):126175.

[18] Haiming L, Jiajing M. Geometric invariants and focal surfaces of spacelike curves in de Sitter space from a caustic viewpoint. AIMS Math. 2021;6(4):3177-3204. DOI: 10.3934/math.2021192.

[19] Sareh M, Gilani S, Gilani N, Abazari Y. Characterizations of dual curves and dual focal curves in dual Lorentzian space D{3}_{1}. Turk J Math. 2020;44:1561-1577. DOI: 10.3906/mat-1909-6.

[20] Yücesan GÖ, Tükel J. A new characterization of dual general helices. ICOM 2020 Conf Proc Book. 2020; Available from: http://raims.org/files/final_proceedings.pdf.

Al-Kitab Journal for Pure Sciences (2024); 8(1):125-135.
https://doi.org/10.32441/kjps.08.01.p11

Al-Kitab Journal for Pure Sciences
ISSN: 2617-1260 (print), 2617-8141(online)

https://isnra.net/index.php/kjps

Bayesian prediction of the stock price rate in the Iraq stock market based on the symmetric heavy tails regression model

Sarmad A. Salih*, Raed Sabeeh Karyakos, Ilham M. Yacoob, Sarah Ghanim Mahmood

Dep. of Mathematics, (E.P.S.) College, University of Al – Hamdaniya, Iraq.

Corresponding Author: sarmadsalih@uohamdaniya.edu.iq

Citation: Salih SA, Karyakos RS, Yacoob IM, Mahmood SG. Bayesian prediction of the stock price rate in the Iraq stock market based on the symmetric heavy tails regression model. Al-Kitab J. Pure Sci. [Internet]. 2024 May. 28 [cited 2024 May. 28];8(1):125-135. Available from: https://doi.org/10.32441/kjps.08.01.p11 .

Keywords: Bayesian prediction, Regression model, generalized multivariate modified Bessel distribution.

Article History

Received	11	Apr.	2024
Accepted	21	May.	2024
Available online	28	May.	2024

Abstract:

In this paper, we investigate the estimation of generalized modified Bessel regression model by using the Bayesian techniques under the assumption that the scale parameter and shape parameters are known. We use the informative priors for estimating of model. Then we derive a prediction distribution of the future response variable _Y_f by using informative priors for predictive future.

Our work applied our results to real data which represent the Iraqi market for securities having taken monthly data for the services sector and of Baghdad sector of Iraq for public transport for the year 2018, as the stock variable rate response variables affecting it are closing price variable, the stock turnover variable. Through the study shows that the explanatory variables are the most important influence on the stock price rate variables through variance inflation factor, the estimated model was appropriate for the data studied.

Keywords: Bayesian prediction, Regression model, generalized multivariate modified Bessel distribution.

التنبؤ البيزي لمعدل سعر السهم في سوق العراق للاوراق المالية بالاعتماد على نموذج الانحدار ذات النهايات الثقيلة

سرمد عبدالخالق صالح*، رائد صبيح قرياقوس، الهام متي يعقوب، سارة غانم محمود

قسم الرياضيات ، كلية التربية للعلوم الصرفة، جامعة الحمدانية ، العراق

sarmadsalih@uohamdaniya.edu.iq, raed_sabeeh@uohamdaniya.edu.iq, ilhammatta@uohamdaniya.edu.iq, sarahghanim@uohamdaniya.edu.iq

الخلاصة:

يهدف البحث الى تقدير نموذج انحدار بسل المحور المعمم بالأسلوب البيزي تحت افتراض ان تكون معلمة القياس ومَعلمات الشكل معلومة. إذ تم استعمال المعلومات السابقة الخبرية لتقدير النموذج. ومن ثم قمنا باشتقاق التوزيع التنبؤي لمتجه مشاهدات متغير الاستجابة المستقبلية Y_f بالاعتماد على معلومات سابقة خبرية لغرض التنبؤ بالمستقبل.

وطبقت النتائج التي تم التوصل إليها على بيانات حقيقية تتعلق بسوق العراق للأوراق المالية إذ اخذت بيانات شهرية مدرجة ضمن قطاع الخدمات والمتمثلة بقطاع بغداد العراق للنقل العام لسنة ٢٠١٨، إذ كان متغير الاستجابة هو معدل سعر السهم والمتغيرات المؤثرة عليه هي متغير سعر الاغلاق ، متغير معدل دوران السهم. ومن خلال الدراسة تبين بان المتغيرات التوضيحية هي من اهم المتغيرات المؤثرة على معدل سعر السهم من خلال عامل تضخم التباين وان النموذج المقدر كان ملائماً للبيانات المدروسة.

الكلمات المفتاحية: التنبؤ البيزي، نموذج الانحدار ، توزيع بسل متعدد المتغيرات المحور المعمم.

1. Introduction:

The concept of the Iraq stock market is economic market enjoy financial and administrative independence that is not related to a set party. It is managed a council consisting of (9) members representing the different economic segments the investment sector, named a council of governors. The market had placed where investors meet, as stock markets dealt with in buying and selling. It constitutes one of the channels through which money flows between individuals, institutions and different sectors, which helps in mobilizing and developing and mobilizing and preparing savings for different investment range. Trading in the market takes place according to the manual method and based on the public bidding system written on boards. A plastic board has been allocated to each listed joint stock company, arranged according to the following sectors: banking sector, insurance sector, investment sector, services sector, industrial sector, hotels sector, tourism, and agriculture sector. Sometimes a multiple regression models are estimated when random errors follow a normal distribution (ND).However, there are cases in which the (ND) of errors is not suitable. Therefore, mixture distributions are more suitable, one of these distributions use such as Generalised Multivariate Modified Bessel (GMMB) distribution. This distribution has applications in variety regions that included displaying stock market data.

The researchers [1] estimated parameters of the multivariate semi-parametric regression model when the error follows a matrix-variate (GMB) distribution using the Bayes method when previous information is not available, in addition to testing hypotheses for the model parameters through the Bayes factor criterion. The theoretical results were applied to experimental data and they concluded that the sample that was used was drawn from a population does not belong to the (GMB) community. The researchers [2] tested statistical hypotheses about the population means of a (GMMB), as well as statistical tests related to the equality of the population means, and they concluded the probability distribution of the statistics (Hotelling-T2) and (Scheffe-T2) for the two tests above respectively and when they have the same covariance matrix. The researchers [3] studied Bayes prediction of a multiple linear regression model in case of equal correlations, as it was assumed that the prior probability function of the variance parameter of the general regression model follows a Generalised Inverse Gaussian (GIG) distribution, predictive distribution was obtained that follows a (GMMB) distribution. This result differs inversely with the t-distribution obtained using the inverse chi-square distribution the prior probability function of the variance parameter, where the predictive distribution was based on interclass correlation. The research covered several sections, where the first section was a general introduction to stock market, and the (GMBR) model was described in the second section, as well as Bayesian estimation and Bayesian prediction. The third section included the application of real data related to the Iraq stock market for the purpose of Bayesian prediction based on the best Bayesian estimator. In the fourth and fifth sections, the most prominent conclusions reached by the research and future studies were presented.edings.pdf.

2. Theoretical side:

2.1 Description of the Generalized Modified Bessel Regression (GMBR) model:

The multiple linear regression models are described by the following linear equation: [4]

$$\underline{Y} = X\underline{\beta} + \underline{u} \qquad (1)$$

Where:

$\underline{Y}$: Response variable with dimension (n× 1).

X: Non-random matrix of explanatory variables with dimension (n× p), where p is number of explanatory variables.

$\underline{\beta}$: A vector of regression model parameters with dimension (p× 1).

$\underline{u}$: Vector of random errors has amplitude (n×1), which has a (GMMB) distribution, the probability function for $\underline{u}$ is defined to the following equation: [4]

$$f(\underline{u}) = \frac{\left(\frac{\lambda}{\psi}\right)^{\frac{n}{4}}}{(2\pi\,\sigma^2)^{\frac{n}{2}} K_v\left(\sqrt{\lambda\psi}\right)} \left[1 + \frac{\underline{u}'\underline{u}}{\psi\sigma^2}\right]^{\frac{2v-n}{4}}$$

$$\times\ K_{\frac{2v-n}{2}}\left(\sqrt{\lambda\psi\left(1 + \frac{\underline{u}'\underline{u}}{\psi\sigma^2}\right)}\right) \quad -\infty < u < \infty\ , \sigma^2 > 0 \qquad (2)$$

As (λ, ψ, v) it represents the shape parameters, and the field of its parameters is defined as follows: [5]

$$\left.\begin{array}{ll} \psi > 0\ ;\ \lambda \geq 0 & if\ and\ only\ if\ \ v < 0 \\ \psi > 0\ ;\ \lambda > 0 & if\ and\ only\ if\ \ v = 0 \\ \psi \geq 0\ ;\ \lambda > 0 & if\ and\ only\ if\ \ v > 0 \end{array}\right\} \qquad (3)$$

$K_v\,(x)$: Modified Bessel function of the third type to order (v), and is defined according to the following equation: [6]

$$K_v(x) = \frac{1}{2}\int_0^{\infty} t^{v-1} e^{\frac{-x}{2}(t+t^{-1})}\, dt \qquad (4)$$

The probability distribution of $\underline{u}$ is expressed descriptively by:

$$\underline{u} \sim GMMBD_n(\underline{0}, \sigma^2 I_n, \lambda, \psi, v) \qquad (5)$$

Equation (1) represents a combination in vector $\underline{u}$, which follows a (GMMB) distribution. Therefore, [7] deduced the probability distribution of the random vector Y, which follows a (GMMB) distribution. The probability function for the random response Y, is as follows:

$$f(\underline{Y}) = \frac{\left(\frac{\lambda}{\psi}\right)^{\frac{n}{4}}}{(2\pi\,\sigma^2)^{\frac{n}{2}} K_v\left(\sqrt{\lambda\psi}\right)} \left[1 + \frac{\left(\underline{Y} - X\underline{\beta}\right)'\left(\underline{Y} - X\underline{\beta}\right)}{\psi\sigma^2}\right]^{\frac{2v-n}{4}}$$

$$\times K_{\frac{2v-n}{2}}\left(\sqrt{\lambda\psi\left(1 + \frac{\left(\underline{Y} - X\underline{\beta}\right)'\left(\underline{Y} - X\underline{\beta}\right)}{\psi\sigma^2}\right)}\right) \qquad (6)$$

Descriptively expresses this distribution $\underline{Y} \sim GMBD_n\left(X\underline{\beta}, \sigma^2 I_n, \lambda, \psi, v\right)$, for more details see [7].

2.2 Bayesian estimation of a location parameter for the (GMBR) model:

Location parameter of the (GMBR) model was estimated based on informative prior. In this section, we also find on the predictive distribution when an additional sample is available for the response variable Y and the explanatory variables that sample have no relationship to the sample that was used in the estimation process. The Bayesian prediction properties of the future response variable were also studied.

2.2.1 Estimating the location parameter using informative prior:

In this study, **[7]** concluded the estimation of the location parameter for a (GMBR) model and it was as follows:

$$\underline{\hat{\beta}}_B = \underline{\beta}_0 + \left(X'X + {P_0}^{-1}\right)^{-1} X'X \left(\left(X'X\right)^{-1} X'Y - \underline{\beta}_0\right) \tag{7}$$

This estimator is biased and the amount of bias is equal to:

$$bias\left(\underline{\hat{\beta}}_B\right) = \left(X'X + {P_0}^{-1}\right)^{-1} {P_0}^{-1} \left(\underline{\beta}_0 - \underline{\beta}\right) \tag{8}$$

Therefore, the mean square error matrix for $\underline{\hat{\beta}}_B$ is as follows:

$$M\left(\underline{\hat{\beta}}_B\right) = \text{tr}(E\left(\underline{\hat{\beta}}_B - E\underline{\hat{\beta}}_B\right)\left(\underline{\hat{\beta}}_B - E\underline{\hat{\beta}}_B\right)' + \left(bias\left(\underline{\hat{\beta}}_B\right)\right)\left(bias\left(\underline{\hat{\beta}}_B\right)\right)')$$

$$= \text{tr}\,(\sigma^2 D \times \frac{K_{v+1}\left(\sqrt{\lambda\psi}\right)}{K_v\left(\sqrt{\lambda\psi}\right)} \left(\frac{\lambda}{\psi}\right)^{\frac{-1}{2}} + \left(bias\left(\underline{\hat{\beta}}_B\right)\right)\left(bias\left(\underline{\hat{\beta}}_B\right)\right)') \tag{9}$$

$$D = \left(X'X + {P_0}^{-1}\right)^{-1} X'X \left(X'X + {P_0}^{-1}\right)^{-1} \tag{10}$$

2.2.2 Predictive distribution:

Predictive distribution is an important issue in predictive inference applied in many real-life domains. It represents the probability density function of future observations $\underline{Y_f}$ conditional on a set of current observations Y. **[8] [9]**

After merging the complete posterior distribution of $\underline{\beta}$ conditional on σ^2, τ, determined by the following equation:

$$P\left(\underline{\beta}\middle|\underline{Y}, \sigma^2, \tau\right) = \frac{\left|X'X + {P_0}^{-1}\right|^{\frac{1}{2}}}{(2\pi\sigma^2\tau)^{\frac{P}{2}}} e^{-\frac{1}{2\sigma^2\tau}\left[\left(\underline{\beta}-\underline{\hat{\beta}}_B\right)'\left(X'X+{P_0}^{-1}\right)\left(\underline{\beta}-\underline{\hat{\beta}}_B\right)\right]} \tag{11}$$

With the probability density function of $\underline{Y_f}$ conditional by the random variable τ and defined according to the following equation:

$$f\left(\underline{Y}_f\middle|\underline{\beta},\sigma^2,\tau\right)=\frac{1}{(2\pi\sigma^2\tau)^{\frac{n_f}{2}}}\ e^{-\frac{1}{2\sigma^2\tau}\left[\left(\underline{Y}_f-X_f\underline{\beta}\right)'\left(\underline{Y}_f-X_f\underline{\beta}\right)\right]} \tag{12}$$

We obtain that the predictive distribution of $\left(\underline{Y}_f\middle|\underline{Y},\tau\right)$ is as follows:

$$f\left(\underline{Y}_f\middle|\underline{Y},\tau\right)=\int_{\underline{\beta}}^{\square} f\left(\underline{Y}_f\middle|\underline{\beta},\sigma^2,\tau\right)\times P\left(\underline{\beta}\middle|\underline{Y},\tau,\sigma^2\right)\ d\underline{\beta} \tag{13}$$

$$f\left(\underline{Y}_f\middle|\underline{Y},\tau\right)=\frac{\left|X'X+{P_0}^{-1}\right|^{\frac{1}{2}}\ e^{-\frac{\left(\underline{Y}_f-X_f\underline{\hat{\beta}}_B\right)'\left(\underline{Y}_f-X_f\underline{\hat{\beta}}_B\right)}{2\sigma^2\tau}}}{(2\pi\sigma^2\tau)^{\frac{n_f}{2}}\left|X'X+{P_0}^{-1}+{X'}_fX_f\right|^{\frac{1}{2}}} \tag{14}$$

Since $\underline{\hat{\beta}}_B$ was previously defined in equation (7), and integrating equation (14) relative to the random variable τ, the predictive distribution of $\underline{Y}_f$ as follows:

$$f\left(\underline{Y}_f\middle|\underline{Y}\right)=\frac{\left|X'X+{P_0}^{-1}\right|^{\frac{1}{2}}\left(\frac{\lambda}{\psi}\right)^{\frac{n_f}{4}}}{\left|X'X+{P_0}^{-1}+{X'}_fX_f\right|^{\frac{1}{2}}(2\pi\sigma^2)^{\frac{n_f}{2}}\ K_v\left(\sqrt{\lambda\psi}\right)}\left[1+\frac{\Re}{\psi\sigma^2}\right]^{\frac{2v-n_f}{4}}$$

$$\mathbf{x}\ K_{\frac{2v-n_f}{2}}\left(\sqrt{\lambda\psi\left(1+\frac{\Re}{\psi\sigma^2}\right)}\right) \tag{15}$$

Where $\Re=\left(\underline{Y}_f-X_f\underline{\hat{\beta}}_B\right)'\left(\underline{Y}_f-X_f\underline{\hat{\beta}}_B\right)$.

Since the predictive distribution of $\underline{Y}_f$ is not a common probability distribution, the Bayesian prediction for the response variable Y is found by the following formula:

$$E\left(\underline{Y}_f\middle|\underline{Y}\right)=\int_0^{\infty}\int_{\underline{\beta}}^{\square} E\left(\underline{Y}_f\middle|\underline{\beta},\sigma^2,\tau\right)\times\ P\left(\underline{\beta}\middle|\underline{Y},\tau,\sigma^2\right)P(\tau)\ d\underline{\beta}\ d\tau$$

$$E\left(\underline{Y}_f\middle|\underline{Y}\right)=X_f\left(\underline{\beta}_0+\left(X'X+{P_0}^{-1}\right)^{-1}X'X\left(\left(X'X\right)^{-1}X'Y-\underline{\beta}_0\right)\right) \tag{16}$$

3. Applied side:

The Iraqi market during the period between 1992 and 2003 was known as the Baghdad stock market. It was instituted according to Law (24) for the year 1991. This market was a government exchange that was able to list 113 companies (Iraqi and mixed stock), and was able to attract in the last year It has an annual trading rate of over (17,500,000) dollars. The Iraq Stock market was established on (18 April 2004). Temporary Law (74) was issued to establish two important institutions in the capital sector, which Iraq Stock market and Iraq stock Commission. **[10]**

3.1 Determine basic variables and preparing data:

In this side, practical application will be made on data related to the Iraq Stock market, as monthly data related to the services sector, represented by the Iraq Baghdad for General Transportation sector for the year 2018, will be studied, as the effect of both (Stock turnover rate X1, Closing price X2) which represents the explanatory variables on (Stock price rate Y) which represents the response variable, and **Table 1** shows the measurements for the study variables measured in Iraqi dinars.

Table 1: Measurements of the variables of closing price and stock turnover rate affecting the stock price rate for the year 2018

		.Response V	Elanatory V.'sxp	
No.	Month	Stock price rate	Stock turnover rate	Closing price
1	January	56.710	0.66	51.000
2	February	58.920	0.59	54.100
3	March	55.480	0.45	52.800
4	April	43.460	0.80	42.850
5	May	45.170	0.31	48.000
6	June	40.920	0.08	42.000
7	July	41.320	0.05	41.750
8	August	43.430	0.08	47.000
9	September	45.860	0.02	44.010
10	October	52.210	0.34	57.050
11	November	54.470	0.24	51.380
12	December	43.300	0.76	41.000

Source: http://www.isx-iq.net/isxportal/portal/homePage.html

Before using the (GMBR) model to represent the relationship between variables, the data is time series or not. This was done by drawing Auto-correlation function for stock price rate; it became clear from the drawing that the data is white noise. **Figure 1** shows a plot auto-correlation function for stock price rate variable:

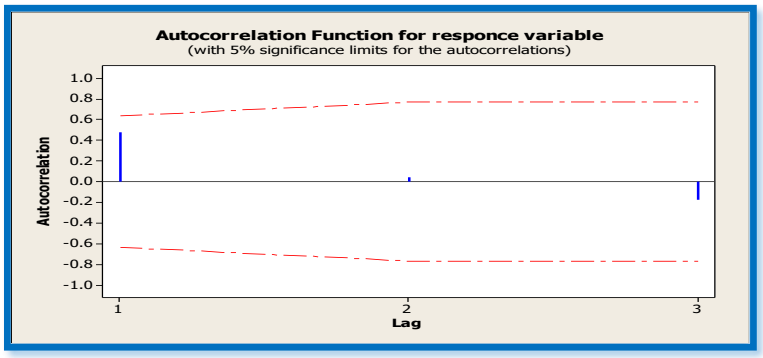

Figure 1: Plot of Auto-correlation function for stock price rate variable

In order to determine the suitability of the data to the model used, the study data was tested through goodness of fit and based on the default shape parameters (λ = 5, ψ = 2, v = 3). The value of the Kolmogorov-Smirnov test extracted (0.2140) for this model was lowerhan the tabulate value $D_{tab}(0.05,12) = 0.2420$, which indicates that the data fit to model used.

Multicollinearity between explanatory (independent) variables was tested based on criterion called the Variance Inflation Factor (VIF). Where both values were less than 10, which indicates that there is no problem of multicollinearity, as shown in the following **Table 2**:

Table 2: Variance inflation factor values for explanatory variables

Variables	VIF
Stock turnover rate	1.0081
Closing price	1.0081

The sample data was divided into two parts, the first consisting of a random sample of size (n=10). This data was used for estimation and the last two observations were used for the purpose of prediction. The parameter vector β was estimated for the sample data with a size of (n=10) by the classical method to choose the initial values, these values were as follows:

$$\underline{\beta}_0 = \begin{bmatrix} 5.9985 \\ 0.9921 \end{bmatrix}, \quad {\sigma_0}^2 = 6.0151, \quad a_0 = 25 \ , \ b_0 = 120 \quad , P_0 = \begin{bmatrix} 1 & 0 \\ 0 & 1 \end{bmatrix}, P_0 = \begin{bmatrix} 2 & 1 \\ 1 & 3 \end{bmatrix}$$

In this aspect, the location parameter for the (GMBR) model will be estimated based on the shape parameters (λ=5, ψ=2, v=3) and future values will be predicted. The following **Table 3** shows the location parameter estimation using the Bayesian method.

Table 3: Location parameter estimation for the generalized modified Bessel regression model using Bayesian method

Estimator	Bayesian method	
	Informative prior	
	$P_0 = \begin{bmatrix} 1 & 0 \\ 0 & 1 \end{bmatrix}$	$P_0 = \begin{bmatrix} 2 & 1 \\ 1 & 3 \end{bmatrix}$
$\underline{\hat{\beta}}$	$\begin{bmatrix} 6.0024 \\ 0.9752 \end{bmatrix}$	$\begin{bmatrix} 6.2739 \\ 0.9581 \end{bmatrix}$
$MSE(\underline{\hat{\beta}})$	2.6571	4.6210

Table 4 shows the real and estimated values of the stock price rate by using the Bayesian estimator based on informative prior.

Table 4: Real and estimated values for the stock price rate

	Real values	Estimated values
1	56.710	52.5637
2	58.920	54.7972
3	55.480	53.7163
4	43.460	47.3048
5	45.170	47.3010
6	40.920	39.8218
7	41.320	40.9038
8	43.430	42.9570
9	45.860	41.9761
10	52.210	55.9836

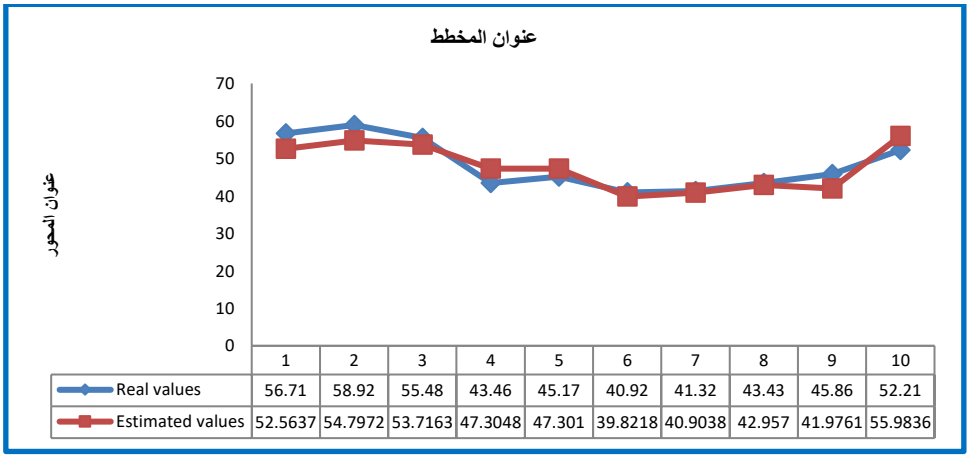

Figure 2: Behavior of the real and estimated values of the stock price rate

Figure 2 shows the real estimated values for **Table 4**. We note from the above figure that the estimated values of the response variable vector have the same pattern as the real values, which indicates that the estimated model was appropriate to the study data.

3.2 Bayesian prediction:

In this study, future values will be predicted based on the best Bayesian estimator. The predictive value represents the predictive mean defined in equation (16).

Table 5: Real and Predictive Values

No.	Real values	Predictive values
1	54.470	50.0124
2	43.300	46.2560

Figure 3 shows the behavior of the real values of the stock price rate variable that was not used in the estimation process and the predictive values.

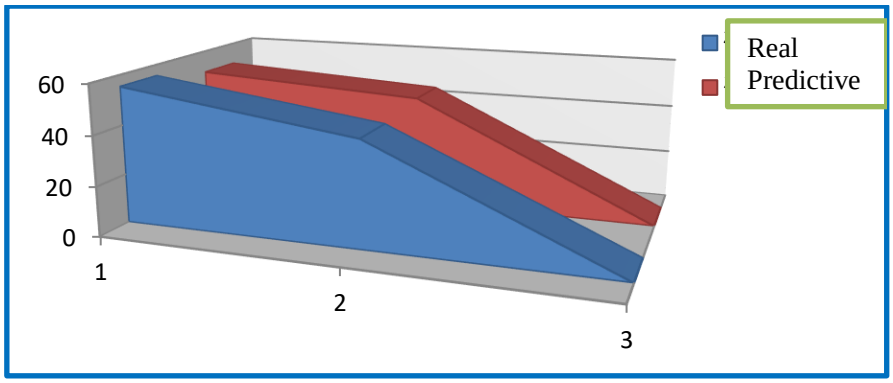

Figure 3: Behavior of the real and predictive values of the stock price rate variable

4. Conclusions:

The researchers arrived at the most important theoretical and practical conclusions, including:

1. The property of linearity is achieved in the (GMB) distribution, and this property similar to case the (ND) and the student-t distribution.
2. When estimating the location parameter using the Bayesian method, the best estimator was the assumed identity matrix.
3. From **Figure 2**, the estimated generalized modified Bessel regression model was appropriate to the study data.
4. Based on the best Bayesian estimator, there is a correspondence between the behavior of the real and predicted values through the (R^2) criterion, the value of which reached (0.91).

5. Recommendations:

1. We recommend expanding the generalized modified Bessel regression model to a multivariate regression model, as this model can be used in principal components analysis and non-normal factor analysis models.
2. We recommend analyzing the generalized modified Bessel regression model when the scale and shape parameters are unknown.
3. We recommend using one of the modern artificial intelligence algorithms and comparing it with the Bayesian method of the generalized modified Bessel regression model.

6. References:

[1] Salih SA., Aboudi EH. Bayesian Inference of a Non normal Multivariate Partial Linear Regression Model. Iraqi Journal of Statistical Sciences. 2021;18(2):51-64.

[2] Thabane L, Drekic S. Testing linear Hypothesis with a generalized multivariate modified Bessel error variable. IIQP Research Report. 2002.

[3] Thabane L, Kibria B. M. Bayesian Prediction for the linear model with Equi-Correlated Responses: An Application of the generalized multivariate modified Bessel distribution. Journal of Applied Statistical Science. 2007:328-335.

[4] Thabane L, Drekic S. Hypothesis testing for the generalized multivariate modified Bessel model. Journal of Multivariate Analysis. 2003 Aug 1; 86(2):360-374.

[5] Butler RW. Generalized inverse Gaussian distributions and their Wishart connections. Scandinavian journal of statistics. 1998 Mar; 25(1):69-75.

[6] Hu W. Calibration of multivariate generalized hyperbolic distribution using the EM algorithm, With applications in risk management, Portfolio optimization and portfolio credit risk. The Florida State University; 2005.

[7] Saieed HA, Salih SA. Estimation and Statistical tests For the Parameters of Multiple Linear Generalized Modified Bessel Regression Model**.** Iraqi Journal of Statistical Sciences. 2013; 13 (25):257-274.

[8] Jefferys H. The Theory of probability. OuP Oxford; 1998 Aug 6.

[9] Saieed HA, Alobedi SAS**.** Bayesian analysis of multiple linear generalized modified Bessel regression model**.** Iraqi Journal of Statistical Sciences. 2014; 14 (26):98-116.

[10] Hamza HK, Abdulhamid GR. The Iraq stock market, its inception- analysis and evaluated of its indicators**.** Kufa Studies Center Journal. 2012; 1 (24): 255-284.

Al-Kitab Journal for Pure Sciences (2024); 8(1):136-144.
https://doi.org/10.32441/kjps.08.01.p12

Al-Kitab Journal for Pure Sciences
ISSN: 2617-1260 (print), 2617-8141(online)

https://isnra.net/index.php/kjps

Application of Coding Theory in Field 5

Hajir Hayder Abdullah[*1], Nada Yassen Kasm [2], Noor Hussain Abdullah[1]

[1]Department of Mathematics, College of Education for Pure Science, University of Hamdaniya
[2]Department of Mathematics, College of Education for Pure Science, University of Mosul

Corresponding Author: hajarhayder@uohamdaniya.edu.iq

Citation: Abdullah HH, Kasm NY, Abdullah NH. Application of Coding Theory in Field 5. Al-Kitab J. Pure Sci. [Internet]. 2024 May. 31 [cited 2024 May. 31];8(1):136-144. Available from: https://doi.org/10.32441/kjps.08.01.p12.

Keywords: projective plane, coding theory, incidence matrix, distance, perfect code.

Article History
Received 12 Apr. 2024
Accepted 04 May. 2024
Available online 31 May. 2024

Abstract:

The main aim of this paper introduce the relationship between the topic of coding theory and the projective plane of order five where special points were found in field 5, which is 31 points, in addition to 31 straight lines, and by applying the theorem that gives the number 1 for the point that lies on the straight line and the number 0 for the point that does not lie on the straight line, we get the code n = 31, d = 6, e = 2, from which we get the table m, v, n. ,n,h, and based on these tables, the distance difference between the code elements was found, where the minimum distance was 6 and the largest distance was 31. These values were used to test the optimality of the code. We can generalize this theorem and apply it to larger fields such as 21 or 23 and others, test their ideality, and find the difference between field 5 and the rest of the fields. M is the maximum value of the size of code over the finite field of order five and an incidence matrix with the parameters, n (length of code), d(minimum distance of code), and e (error-correcting of code)have been constructed some example and theorem have been given.

Keywords: projective plane, coding theory, incidence matrix, distance, perfect code.

تطبيق نظرية الترميز في الحقل٥

هاجر حيدر عبد الله*[١]، ندى ياسين قاسم[٢]، نور حسين عبدالله[١]

[١] قسم الرياضيات ، كلية التربية للعلوم الصرفة ، جامعة الحمدانية

[٢] قسم الرياضيات ، كلية التربية للعلوم الصرفة ، جامعة الموصل

hajarhayder@uohamdaniya.edu.iq, drnadaqasim3@uomosul.edu.iq, noorhussain@uohamdaniya.edu.iq

الخلاصة:

الهدف الرئيسي لهذا البحث هو تقديم العلاقة بين نظرية الترميز والمستوي الإسقاطي من الرتبة الخامسة حيث تم إيجاد النقاط الخاصة بالحقل ٥ وهي ٣١ نقطة إضافة الى ٣١ مستقيم وبتطبيق المبرهنة التي تعطي الرقم ١ للنقطة الواقعة على المستقيم والرقم ٠ للنقطة التي لا تقع على المستقيم نحصل على الكود $n=31,d=6,e=2$, ومنها نحصل على جدول $m\ ,v$ $n\ ,h$, وبالاعتماد على هذه الجداول تم إيجاد فرق المسافة بين عناصر الكود حيث كانت اقل مسافة تساوي ٦ واكبر مسافة ٣١وان هذه القيم تمت الاستفادة منها في اختبار مثالية الكود .ونستطيع تعميم هذه المبرهنة وتطبيقها على حقول اكبر مثل ٢١ أو ٢٣ وغيرها واختبار مثليتها وإيجاد الفرق بين الحقل ٥ وبقية الحقول. M القيمة العظمى لحجم الرمز حول الحقل المنتهي من الرتبة الخامسة . d اقل مسافة للرمز e. تصحيح رمز الأخطاء وأيضا بعض الأمثلة والنظريات.

الكلمات المفتاحية: المستوي الإسقاطي ، نظرية الترميز، مصفوفة الوقوع.

1. Introduction:

This section tackles an explanation of the coding theory in PG(2,5). Coding theory is defined as the study of the properties of symbols and their strengths for specific applications and the polynomial function is also defined as a mathematical structure consisting of one or more constants and variables **[1]**, which are functions whose base algebraic terms or expression While the projective plane is defined as a plan homogeneous space, just as it a plane in space in which plane geometry is achieved, in the research, we have linked them and The theory of coding was presented in the fifth field, which contains the elements (0,1,2,3,4) i.e., they are five in number **[2] [3]**. By multiplying the first point by (1,0,0) by the matrix of its elements from an equation of a certain degree, we obtain the rest of the points that we rely on to obtain the straight lines, and the number of straight lines was 31 **[4] [5]**.

Likewise, by relying on the theorem that gives the value 1 when the point lies on a straight line and gives the value 0 when the point does not belong, thus we obtain the incidence matrix whose elements are 0 and 1. Then we find the distance between each straight line of the projective plane of the fifth order, and from the results, we get different values, where the lowest value is relied upon to test the optimality of the code **[6] [7]**. The results obtained can be relied upon and used in applying a theorem that shows the ideality of the code. These results are considered important because they show us the values of the distance between the code elements and the straight lines. The value of M was also obtained because of its importance in testing the optimality of the code. The motivation for studying the theory of coding was to encode certain elements belonging to a certain field, regardless of the field's rank in the projective plane, to transform the elements of the field into points that differ in the formula, to find the lines and expressions in the plane, and to test the ideality of those elements if they were converted into a code. The motivation for studying the theory of coding was to encode certain elements belonging to a certain field, regardless of the field's rank in the projective plane, to

transform the elements of the field into points that differ in the formula, to find the lines and expressions in the plane, and to test the ideality of those elements if they were converted into a code.

2. Preliminaries:

2.1 Definition: the plane π =$\pi_z$has order q if some line contains exactly z+1 points in the case it follows that π has .[8]

(1 z^2+ z +1 points

(2) z^2+ z +1 lines

(3) z+1 points on a line

(4) z+1 lines through a points

Here is the unique plane =PG(2,z)

2.2 Definition: companion matrix

Let f(x) = x^{n+1}-$a_n x^n$-$a_{n-1}x^n$ …….. a_0 be any manic polynomial then it is companion matrix c(F) is given by (n+1)× (n+1) matrix .[9]

$$C(F)=\begin{bmatrix} 0 & 1 & 0 & . & . & . & 0 \\ 0 & 0 & 1 & . & . & . & . \\ a_0 & a_1 & a_2 & . & . & . & a_n \end{bmatrix}$$

2.3 Theorem: A z- ary (n , M ,2e +1)-code c satisfies.

$$M\left\{\binom{n}{0}+\binom{n}{1}(z-1)+\ldots\ldots\ldots\ldots\ldots+\binom{n}{e}(z-1)^e\right\}\leq z^n.$$ [10][11]

2.4 Corollary: z- ary (n , M ,2e +1)-code c is perfect if and only if equality holds in theorem 2.3. [12] [13]

3. The classification of cubic over a finite field of order five

The polynomial of degree five $f_2(x)$ =x^3-$2x^2$-x +1 is primitive f_5 ={0,1,2,3,4} since $f_2(0)$=1,$f_2(1)$ =4,$f_2(2)$=4,$f_2(3)$=2 ,$f_2(4)$ =4 and we have by **definition 1** z^2+ z +1 points and z^2+ z +1 lines and z+1 points on a line d q+1 lines through a points t he companion matrix of $f_2(x)$ =x^3-$2x^2$-x +1 in $f_5(x)$ generated the points and lines PG (2,5) as follows. [14] [15]

$$P(k)=[1,0,0]c(g)^{k-1}=[1,0,0]\begin{bmatrix} 0 & 1 & 0 \\ 0 & 0 & 1 \\ -1 & 1 & 2 \end{bmatrix}$$

The points of PG(2,5) are:

{ p_1=[1,0,0] , p_2=[0,1,0] , …., p_{30}=[1,2,3] , p_{31}=[1,2,4]} With selecting the point of PG(2,5) which is the third coordinate equal to zero we obtain l_1={1,2,5,7,14,22} and l_kWith selecting the point of PG(2,5) which are the third coordinate[1] equal to zero we obtain l_1={1,2,5,7,14,22} and $l_k = l_1 c(g)^{k-1}=l_1\begin{bmatrix} 0 & 1 & 0 \\ 0 & 0 & 1 \\ -1 & 1 & 2 \end{bmatrix}$,k= 1,2,…..,31.

Table 1: The line of PG (2,5)

l_1	1	2	5	7	14	22
l_2	2	3	6	8	15	23
l_3	3	4	7	9	16	24
l_4	4	5	8	10	17	25
.	.	.	.	.	.	.
.	.	.	.	.	.	.
.	.	.	.	.	.	.
l_{29}	29	30	2	4	12	19
l_{30}	30	31	3	5	13	20
l_{31}	31	1	4	6	14	21

3.1Theorem: the projective plane of order five is a code with a parameter [n = 31 ,d= 6 ,e =2 , $m=5^{28}$].[16]

***proof*:** the plan $\pi_5$has an incidence matrix A=(aij),where

$a_{ij} = 1$ if $p_i \in l_i$ And also condition $a_{ij} = 0$ if $p_i \notin l_i$

Table 2: Incidence matrix

	p_1	p_2	p_3	p_4	p_5	p_6	p_7	p_8	p_9	p_{10}	p_{11}	p_{12}	p_{13}	p_{14}	p_{15}	p_{16}	p_{17}	p_{18}	p_{19}	p_{20}	p_{21}	p_{22}	p_{23}	p_{24}	p_{25}	p_{26}	p_{27}	p_{28}	p_{29}	p_{30}	p_{31}
l_1	1	1	0	0	1	0	1	0	0	0	0	0	0	1	0	0	0	0	0	0	0	1	0	0	0	0	0	0	0	0	0
l_2	0	1	1	0	0	1	0	1	0	0	0	0	0	0	1	0	0	0	0	0	0	0	1	0	0	0	0	0	0	0	0
l_3	0	0	1	1	0	0	1	0	1	0	0	0	0	0	0	1	0	0	0	0	0	0	0	1	0	0	0	0	0	0	0
l_4	0	0	0	1	1	0	0	1	0	1	0	0	0	0	0	0	1	0	0	0	0	0	0	0	1	0	0	0	0	0	0
l_5	0	0	0	0	1	1	0	0	1	0	1	0	0	0	0	0	0	1	0	0	0	0	0	0	0	1	0	0	0	0	0
l_6	0	0	0	0	0	1	1	0	0	1	0	1	0	0	0	0	0	0	1	0	0	0	0	0	0	0	1	0	0	0	0
l_7	0	0	0	0	0	0	1	1	0	0	1	0	1	0	0	0	0	0	0	1	0	0	0	0	0	0	0	1	0	0	0
l_8	0	0	0	0	0	0	0	1	1	0	0	1	0	1	0	0	0	0	0	0	1	0	0	0	0	0	0	0	1	0	0
l_9	0	0	0	0	0	0	0	0	1	1	0	0	1	0	1	0	0	0	0	0	0	1	0	0	0	0	0	0	0	1	0
l_{10}	0	0	0	0	0	0	0	0	0	1	1	0	0	1	0	1	0	0	0	0	0	0	1	0	0	0	0	0	0	0	1
l_{11}	1	0	0	0	0	0	0	0	0	0	1	1	0	0	1	0	1	0	0	0	0	0	0	1	0	0	0	0	0	0	0
l_{12}	0	1	0	0	0	0	0	0	0	0	0	1	1	0	0	1	0	1	0	0	0	0	0	0	1	0	0	0	0	0	0
l_{13}	0	0	1	0	0	0	0	0	0	0	0	0	1	1	0	0	1	0	1	0	0	0	0	0	0	1	0	0	0	0	0
l_{14}	0	0	0	1	0	0	0	0	0	0	0	0	0	1	1	0	0	1	0	1	0	0	0	0	0	0	1	0	0	0	0
l_{15}	0	0	0	0	1	0	0	0	0	0	0	0	0	0	1	1	0	0	1	0	1	0	0	0	0	0	0	1	0	0	0
l_{16}	0	0	0	0	0	1	0	0	0	0	0	0	0	0	0	1	1	0	0	1	0	1	0	0	0	0	0	0	1	0	0
l_{17}	0	0	0	0	0	0	1	0	0	0	0	0	0	0	0	0	1	1	0	0	1	0	1	0	0	0	0	0	0	1	0
l_{18}	0	0	0	0	0	0	0	1	0	0	0	0	0	0	0	0	0	1	1	0	0	1	0	1	0	0	0	0	0	0	1
l_{19}	1	0	0	0	0	0	0	0	1	0	0	0	0	0	0	0	0	0	1	1	0	0	1	0	1	0	0	0	0	0	0
l_{20}	0	1	0	0	0	0	0	0	0	1	0	0	0	0	0	0	0	0	0	1	1	0	0	1	0	1	0	0	0	0	0
l_{21}	0	0	1	0	0	0	0	0	0	0	1	0	0	0	0	0	0	0	0	0	1	1	0	0	1	0	1	0	0	0	0
l_{22}	0	0	0	1	0	0	0	0	0	0	0	1	0	0	0	0	0	0	0	0	0	1	1	0	0	1	0	1	0	0	0
l_{23}	0	0	0	0	1	0	0	0	0	0	0	0	1	0	0	0	0	0	0	0	0	0	1	1	0	0	1	0	1	0	0
l_{24}	0	0	0	0	0	1	0	0	0	0	0	0	0	1	0	0	0	0	0	0	0	0	0	1	1	0	0	1	0	1	0
l_{25}	0	0	0	0	0	0	1	0	0	0	0	0	0	0	1	0	0	0	0	0	0	0	0	0	1	1	0	0	1	0	1
l_{26}	1	0	0	0	0	0	0	1	0	0	0	0	0	0	0	1	0	0	0	0	0	0	0	0	0	1	1	0	0	1	0
l_{27}	0	1	0	0	0	0	0	0	1	0	0	0	0	0	0	0	1	0	0	0	0	0	0	0	0	0	1	1	0	0	1
l_{28}	1	0	1	0	0	0	0	0	0	1	0	0	0	0	0	0	0	1	0	0	0	0	0	0	0	0	0	1	1	0	0
l_{29}	0	1	0	1	0	0	0	0	0	0	1	0	0	0	0	0	0	0	1	0	0	0	0	0	0	0	0	0	1	1	0
l_{30}	0	0	1	0	1	0	0	0	0	0	0	1	0	0	0	0	0	0	0	1	0	0	0	0	0	0	0	0	0	1	1
l_{31}	1	0	0	1	0	1	0	0	0	0	0	0	1	0	0	0	0	0	0	0	1	0	0	0	0	0	0	0	0	0	1

Let,

z={ 0,0,0,0,0,0,0,0,0,0,0,0,0,0,0,0,0,0,0,0,0,0,0,0,0,0,0,0,0,0,0,}

u={1,1,1,1,1,1,1,1,1,1,1,1,1,1,1,1,1,1,1,1,1,1,1,1,1,1,1,1,1,1,1}

w={2,2,2,2,2,2,2,2,2,2,2,2,2,2,2,2,2,2,2,2,2,2,2,2,2,2,2,2,2,2,2}

f={3,3,3,3,3,3,3,3,3,3,3,3,3,3,3,3,3,3,3,3,3,3,3,3,3,3,3,3,3,3,3,}

g={4,4,4,4,4,4,4,4,4,4,4,4,4,4,4,4,4,4,4,4,4,4,4,4,4,4,4,4,4,4,4} we have

$\mathbf{m_{i=u+l_i}}$

Where

i={1,2,3,4,5,6,7,8,9,10,11,12,13,14,15,16,17,18,19,20,21,22,23,24,25,26,27,28,29,30,31}

That is:

Table 3: The first element is with the incidence matrix

m_1	2	2	1	1	2	1	2	1	1	1	1	1	1	2	1	1	1	1	1	1	1	2	1	1	1	1	1	1	1	1	1
m_2	1	2	2	1	1	2	1	2	1	1	1	1	1	1	2	1	1	1	1	1	1	1	2	1	1	1	1	1	1	1	1
m_3	1	1	2	2	1	1	2	1	2	1	1	1	1	1	1	2	1	1	1	1	1	1	1	2	1	1	1	1	1	1	1
m_4	1	1	1	2	2	1	1	2	1	2	1	1	1	1	1	1	2	1	1	1	1	1	1	1	2	1	1	1	1	1	1
m_5	1	1	1	1	2	2	1	1	2	1	2	1	1	1	1	1	1	2	1	1	1	1	1	1	1	2	1	1	1	1	1
m_6	1	1	1	1	1	2	2	1	1	2	1	2	1	1	1	1	1	1	2	1	1	1	1	1	1	1	2	1	1	1	1
m_7	1	1	1	1	1	1	2	2	1	1	2	1	2	1	1	1	1	1	1	2	1	1	1	1	1	1	1	2	1	1	1
m_8	1	1	1	1	1	1	1	2	2	1	1	2	1	2	1	1	1	1	1	1	2	1	1	1	1	1	1	1	2	1	1
m_9	1	1	1	1	1	1	1	1	2	2	1	1	2	1	2	1	1	1	1	1	1	2	1	1	1	1	1	1	1	2	1
m_{10}	1	1	1	1	1	1	1	1	1	2	2	1	1	2	1	2	1	1	1	1	1	1	2	1	1	1	1	1	1	1	2
m_{11}	2	1	1	1	1	1	1	1	1	1	2	2	1	1	2	1	2	1	1	1	1	1	1	2	1	1	1	1	1	1	1
m_{12}	1	2	1	1	1	1	1	1	1	1	1	2	2	1	1	2	1	2	1	1	1	1	1	1	2	1	1	1	1	1	1
m_{13}	1	1	2	1	1	1	1	1	1	1	1	1	2	2	1	1	2	1	2	1	1	1	1	1	1	2	1	1	1	1	1
m_{14}	1	1	1	2	1	1	1	1	1	1	1	1	1	2	2	1	1	2	1	2	1	1	1	1	1	1	2	1	1	1	1
m_{15}	1	1	1	1	2	1	1	1	1	1	1	1	1	1	2	2	1	1	2	1	2	1	1	1	1	1	1	2	1	1	1
m_{16}	1	1	1	1	1	2	1	1	1	1	1	1	1	1	1	2	2	1	1	2	1	2	1	1	1	1	1	1	2	1	1
m_{17}	1	1	1	1	1	1	2	1	1	1	1	1	1	1	1	1	2	2	1	1	2	1	2	1	1	1	1	1	1	2	1
m_{18}	1	1	1	1	1	1	1	2	1	1	1	1	1	1	1	1	1	2	2	1	1	2	1	2	1	1	1	1	1	1	2
m_{19}	2	1	1	1	1	1	1	1	2	1	1	1	1	1	1	1	1	1	2	2	1	1	2	1	2	1	1	1	1	1	1
m_{20}	1	2	1	1	1	1	1	1	1	2	1	1	1	1	1	1	1	1	1	2	2	1	1	2	1	2	1	1	1	1	1
m_{21}	1	1	2	1	1	1	1	1	1	1	2	1	1	1	1	1	1	1	1	1	2	2	1	1	2	1	2	1	1	1	1
m_{22}	1	1	1	2	1	1	1	1	1	1	1	2	1	1	1	1	1	1	1	1	1	2	2	1	1	2	1	2	1	1	1
m_{23}	1	1	1	1	2	1	1	1	1	1	1	1	2	1	1	1	1	1	1	1	1	1	2	2	1	1	2	1	2	1	1
m_{24}	1	1	1	1	1	2	1	1	1	1	1	1	1	2	1	1	1	1	1	1	1	1	1	2	2	1	1	2	1	2	1
m_{25}	1	1	1	1	1	1	2	1	1	1	1	1	1	1	2	1	1	1	1	1	1	1	1	1	2	2	1	1	2	1	2
m_{26}	2	1	1	1	1	1	1	2	1	1	1	1	1	1	1	2	1	1	1	1	1	1	1	1	1	2	2	1	1	2	1
m_{27}	1	2	1	1	1	1	1	1	2	1	1	1	1	1	1	1	2	1	1	1	1	1	1	1	1	1	2	2	1	1	2
m_{28}	2	1	2	1	1	1	1	1	1	2	1	1	1	1	1	1	1	2	1	1	1	1	1	1	1	1	1	2	2	1	1
m_{29}	1	2	1	2	1	1	1	1	1	1	2	1	1	1	1	1	1	1	2	1	1	1	1	1	1	1	1	1	2	2	1
m_{30}	1	1	2	1	2	1	1	1	1	1	1	2	1	1	1	1	1	1	1	2	1	1	1	1	1	1	1	1	1	2	2
m_{31}	2	1	1	2	1	2	1	1	1	1	1	1	2	1	1	1	1	1	1	1	2	1	1	1	1	1	1	1	1	1	2

W={2,2,2,2,2,2,2,2,2,2,2,2,2,2,2,2,2,2,2,2,2,2,2,2,2,2,2,2,2,2,2}

$\mathbf{v_{i=w+l_i}}$

Where

i={1,2,3,4,5,6,7,8,9,10,11,12,13,14,15,16,17,18,19,20,21,22,23,24,25,26,27,28,29,30,31}

Table 4: The second element is with the incidence matrix

v_1	3	3	2	2	3	2	3	2	2	2	2	2	3	2	2	2	2	2	2	3	2	2	2	2	2	2	2	2
v_2	2	3	3	2	2	3	2	3	2	2	2	2	2	3	2	2	2	2	2	2	3	2	2	2	2	2	2	2
v_3	2	2	3	3	2	2	3	2	3	2	2	2	2	2	3	2	2	2	2	2	2	3	2	2	2	2	2	2
v_4	2	2	2	3	3	2	2	3	2	3	2	2	2	2	2	3	2	2	2	2	2	2	3	2	2	2	2	2
v_5	2	2	2	2	3	3	2	2	3	2	3	2	2	2	2	2	3	2	2	2	2	2	2	3	2	2	2	2
v_6	2	2	2	2	2	3	3	2	2	3	2	3	2	2	2	2	2	2	3	2	2	2	2	2	2	3	2	2	2
v_7	2	2	2	2	2	2	3	3	2	2	3	2	3	2	2	2	2	2	2	3	2	2	2	2	2	2	3	2	2
v_8	2	2	2	2	2	2	2	3	3	2	2	3	2	3	2	2	2	2	2	2	3	2	2	2	2	2	2	3	2	2
v_9	2	2	2	2	2	2	2	2	3	3	2	2	3	2	3	2	2	2	2	2	2	3	2	2	2	2	2	2	3	2
v_{10}	2	2	2	2	2	2	2	2	2	3	3	2	2	3	2	3	2	2	2	2	2	2	3	2	2	2	2	2	2	3
v_{11}	3	2	2	2	2	2	2	2	2	2	3	3	2	2	3	2	3	2	2	2	2	2	2	3	2	2	2	2	2	2
v_{12}	2	3	2	2	2	2	2	2	2	2	2	3	3	2	2	3	2	3	2	2	2	2	2	2	3	2	2	2	2	2
v_{13}	2	2	3	2	2	2	2	2	2	2	2	2	3	3	2	2	3	2	3	2	2	2	2	2	2	3	2	2	2	2
v_{14}	2	2	2	3	2	2	2	2	2	2	2	2	2	3	3	2	2	3	2	3	2	2	2	2	2	2	3	2	2	2
v_{15}	2	2	2	2	3	2	2	2	2	2	2	2	2	2	3	3	2	2	3	2	3	2	2	2	2	2	2	3	2	2
v_{16}	2	2	2	2	2	3	2	2	2	2	2	2	2	2	2	3	3	2	2	3	2	3	2	2	2	2	2	2	3	2
v_{17}	2	2	2	2	2	2	3	2	2	2	2	2	2	2	2	2	3	3	2	2	3	2	3	2	2	2	2	2	2	3	2
v_{18}	2	2	2	2	2	2	2	3	2	2	2	2	2	2	2	2	2	3	3	2	2	3	2	3	2	2	2	2	2	2	3
v_{19}	3	2	2	2	2	2	2	2	3	2	2	2	2	2	2	2	2	2	3	3	2	2	3	2	3	2	2	2	2	2	2
v_{20}	2	3	2	2	2	2	2	2	2	3	2	2	2	2	2	2	2	2	2	3	3	2	2	3	2	3	2	2	2	2	2
v_{21}	2	2	3	2	2	2	2	2	2	2	3	2	2	2	2	2	2	2	2	2	3	3	2	2	3	2	3	2	2	2	2
v_{22}	2	2	2	3	2	2	2	2	2	2	2	3	2	2	2	2	2	2	2	2	2	3	3	2	2	3	2	3	2	2	2
v_{23}	2	2	2	2	3	2	2	2	2	2	2	2	3	2	2	2	2	2	2	2	2	2	3	3	2	2	3	2	3	2	2
v_{24}	2	2	2	2	2	3	2	2	2	2	2	2	2	3	2	2	2	2	2	2	2	2	2	3	3	2	2	3	2	3	2
v_{25}	2	2	2	2	2	2	3	2	2	2	2	2	2	2	3	2	2	2	2	2	2	2	2	2	3	3	2	2	3	2	3
v_{26}	3	2	2	2	2	2	2	3	2	2	2	2	2	2	2	3	2	2	2	2	2	2	2	2	2	3	3	2	2	3	2
v_{27}	2	3	2	2	2	2	2	2	3	2	2	2	2	2	2	2	3	2	2	2	2	2	2	2	2	2	3	3	2	2	3
v_{28}	3	2	3	2	2	2	2	2	2	3	2	2	2	2	2	2	2	3	2	2	2	2	2	2	2	2	2	3	3	2	2
v_{29}	2	3	2	3	2	2	2	2	2	2	3	2	2	2	2	2	2	2	3	2	2	2	2	2	2	2	2	2	3	3	2
v_{30}	2	2	3	2	3	2	2	2	2	2	2	3	2	2	2	2	2	2	2	3	2	2	2	2	2	2	2	2	2	3	3
v_{31}	3	2	2	3	2	3	2	2	2	2	2	2	3	2	2	2	2	2	2	2	3	2	2	2	2	2	2	2	2	2	3

F={3,3,3,3,3,3,3,3,3,3,3,3,3,3,3,3,3,3,3,3,3,3,3,3,3,3,3,3,3,3,3,3,3,3,3}, $\mathbf{n_{i=f+l_i}}$,Where:
i={1,2,3,4,5,6,7,8,9,10,11,12,13,14,15,16,17,18,19,20,21,22,23,24,25,26,27,28,29,30,31}

Table 5:The third element is with the incidence matrix

n_1	4	4	3	3	4	3	4	3	3	3	3	3	4	3	3	3	3	3	3	4	3	3	3	3	3	3	3	3
n_2	3	4	4	3	3	4	3	4	3	3	3	3	3	3	4	3	3	3	3	3	3	3	4	3	3	3	3	3	3	3
n_3	3	3	4	4	3	3	4	3	4	3	3	3	3	3	3	4	3	3	3	3	3	3	3	4	3	3	3	3	3	3
n_4	3	3	3	4	4	3	3	4	3	4	3	3	3	3	3	3	4	3	3	3	3	3	3	3	4	3	3	3	3	3
n_5	3	3	3	3	4	4	3	3	4	3	4	3	3	3	3	3	3	4	3	3	3	3	3	3	3	4	3	3	3	3
n_6	3	3	3	3	3	4	4	3	3	4	3	4	3	3	3	3	3	3	4	3	3	3	3	3	3	3	4	3	3	3
n_7	3	3	3	3	3	3	4	4	3	3	4	3	4	3	3	3	3	3	3	4	3	3	3	3	3	3	3	4	3	3	3
n_8	3	3	3	3	3	3	3	4	4	3	3	4	3	4	3	3	3	3	3	3	4	3	3	3	3	3	3	3	4	3	3
n_9	3	3	3	3	3	3	3	3	4	4	3	3	4	3	4	3	3	3	3	3	3	4	3	3	3	3	3	3	3	4	3
n_{10}	3	3	3	3	3	3	3	3	3	4	4	3	3	4	3	4	3	3	3	3	3	3	4	3	3	3	3	3	3	3	4
n_{11}	4	3	3	3	3	3	3	3	3	3	4	4	3	3	4	3	4	3	3	3	3	3	3	4	3	3	3	3	3	3	3
n_{12}	3	4	3	3	3	3	3	3	3	3	3	4	4	3	3	4	3	4	3	3	3	3	3	3	4	3	3	3	3	3	3
n_{13}	3	3	4	3	3	3	3	3	3	3	3	3	4	4	3	3	4	3	4	3	3	3	3	3	3	4	3	3	3	3	3
n_{14}	3	3	3	4	3	3	3	3	3	3	3	3	3	4	4	3	3	4	3	4	3	3	3	3	3	3	4	3	3	3	3
n_{15}	3	3	3	3	4	3	3	3	3	3	3	3	3	3	4	4	3	3	4	3	4	3	3	3	3	3	3	4	3	3	3
n_{16}	3	3	3	3	3	4	3	3	3	3	3	3	3	3	3	4	4	3	3	4	3	4	3	3	3	3	3	3	4	3	3
n_{17}	3	3	3	3	3	3	4	3	3	3	3	3	3	3	3	3	4	4	3	3	4	3	4	3	3	3	3	3	3	4	3
n_{18}	3	3	3	3	3	3	3	4	3	3	3	3	3	3	3	3	3	4	4	3	3	4	3	4	3	3	3	3	3	3	4
n_{19}	4	3	3	3	3	3	3	3	4	3	3	3	3	3	3	3	3	3	4	4	3	3	4	3	4	3	3	3	3	3	3
n_{20}	3	4	3	3	3	3	3	3	3	4	3	3	3	3	3	3	3	3	3	4	4	3	3	4	3	4	3	3	3	3	3
n_{21}	3	3	4	3	3	3	3	3	3	3	4	3	3	3	3	3	3	3	3	3	4	4	3	3	4	3	4	3	3	3	3
n_{22}	3	3	3	4	3	3	3	3	3	3	3	4	3	3	3	3	3	3	3	3	3	4	4	3	3	4	3	4	3	3	3
n_{23}	3	3	3	3	4	3	3	3	3	3	3	3	4	3	3	3	3	3	3	3	3	3	4	4	3	3	4	3	4	3	3
n_{24}	3	3	3	3	3	4	3	3	3	3	3	3	3	4	3	3	3	3	3	3	3	3	3	4	4	3	3	4	3	4	3
n_{25}	3	3	3	3	3	3	4	3	3	3	3	3	3	3	4	3	3	3	3	3	3	3	3	3	4	4	3	3	4	3	4
n_{26}	4	3	3	3	3	3	3	4	3	3	3	3	3	3	3	4	3	3	3	3	3	3	3	3	3	4	4	3	3	4	3
n_{27}	3	4	3	3	3	3	3	3	4	3	3	3	3	3	3	3	4	3	3	3	3	3	3	3	3	3	4	4	3	3	4
n_{28}	4	3	4	3	3	3	3	3	3	4	3	3	3	3	3	3	3	4	3	3	3	3	3	3	3	3	3	4	4	3	3
n_{29}	3	4	3	4	3	3	3	3	3	3	4	3	3	3	3	3	3	3	4	3	3	3	3	3	3	3	3	3	4	4	3
n_{30}	3	3	4	3	4	3	3	3	3	3	3	4	3	3	3	3	3	3	3	4	3	3	3	3	3	3	3	3	3	4	4
n_{31}	4	3	3	4	3	4	3	3	3	3	3	3	4	3	3	3	3	3	3	3	4	3	3	3	3	3	3	3	3	3	4

g={4,4,4,4,4,4,4,4,4,4,4,4,4,4,4,4,4,4,4,4,4,4,4,4,4,4,4,4,4,4,4}

$\mathbf{h_{i=g+l_i}}$

Where

i={1,2,3,4,5,6,7,8,9,10,11,12,13,14,15,16,17,18,19,20,21,22,23,24,25,26,27,28,29,30,31}

Table 6: The fourth element is with the incidence matrix

h_1	0	0	4	4	0	4	0	4	4	4	4	4	4	0	4	4	4	4	4	4	4	0	4	4	4	4	4	4	4	4	4
h_2	4	0	0	4	4	0	4	0	4	4	4	4	4	4	0	4	4	4	4	4	4	4	0	4	4	4	4	4	4	4	4
h_3	4	4	0	0	4	4	0	4	0	4	4	4	4	4	4	0	4	4	4	4	4	4	4	0	4	4	4	4	4	4	4
h_4	4	4	4	0	0	4	4	0	4	0	4	4	4	4	4	4	0	4	4	4	4	4	4	4	0	4	4	4	4	4	4
h_5	4	4	4	4	0	0	4	4	0	4	0	4	4	4	4	4	4	0	4	4	4	4	4	4	4	0	4	4	4	4	4
h_6	4	4	4	4	4	0	0	4	4	0	4	0	4	4	4	4	4	4	0	4	4	4	4	4	4	4	0	4	4	4	4
h_7	4	4	4	4	4	4	0	0	4	4	0	4	0	4	4	4	4	4	4	0	4	4	4	4	4	4	4	0	4	4	4
h_8	4	4	4	4	4	4	4	0	0	4	4	0	4	0	4	4	4	4	4	4	0	4	4	4	4	4	4	4	0	4	4
h_9	4	4	4	4	4	4	4	4	0	0	4	4	0	4	0	4	4	4	4	4	4	0	4	4	4	4	4	4	4	0	4
h_{10}	4	4	4	4	4	4	4	4	4	0	0	4	4	0	4	0	4	4	4	4	4	4	0	4	4	4	4	4	4	4	0
h_{11}	0	4	4	4	4	4	4	4	4	4	0	0	4	4	0	4	0	4	4	4	4	4	4	0	4	4	4	4	4	4	4
h_{12}	4	0	4	4	4	4	4	4	4	4	4	0	0	4	4	0	4	0	4	4	4	4	4	4	0	4	4	4	4	4	4
h_{13}	4	4	0	4	4	4	4	4	4	4	4	4	0	0	4	4	0	4	0	4	4	4	4	4	4	0	4	4	4	4	4
h_{14}	4	4	4	0	4	4	4	4	4	4	4	4	4	0	0	4	4	0	4	0	4	4	4	4	4	4	0	4	4	4	4
h_{15}	4	4	4	4	0	4	4	4	4	4	4	4	4	4	0	0	4	4	0	4	0	4	4	4	4	4	4	0	4	4	4
h_{16}	4	4	4	4	4	0	4	4	4	4	4	4	4	4	4	0	0	4	4	0	4	0	4	4	4	4	4	4	0	4	4
h_{17}	4	4	4	4	4	4	0	4	4	4	4	4	4	4	4	4	0	0	4	4	0	4	0	4	4	4	4	4	4	0	4
h_{18}	4	4	4	4	4	4	4	0	4	4	4	4	4	4	4	4	4	0	0	4	4	0	4	0	4	4	4	4	4	4	0
h_{19}	0	4	4	4	4	4	4	4	0	4	4	4	4	4	4	4	4	4	0	0	4	4	0	4	0	4	4	4	4	4	4
h_{20}	4	0	4	4	4	4	4	4	4	0	4	4	4	4	4	4	4	4	4	0	0	4	4	0	4	0	4	4	4	4	4
h_{21}	4	4	0	4	4	4	4	4	4	4	0	4	4	4	4	4	4	4	4	4	0	0	4	4	0	4	0	4	4	4	4
h_{22}	4	4	4	0	4	4	4	4	4	4	4	0	4	4	4	4	4	4	4	4	4	0	0	4	4	0	4	0	4	4	4
h_{23}	4	4	4	4	0	4	4	4	4	4	4	4	0	4	4	4	4	4	4	4	4	4	0	0	4	4	0	4	0	4	4
h_{24}	4	4	4	4	4	0	4	4	4	4	4	4	0	4	4	4	4	4	4	4	4	4	4	0	0	4	4	0	4	0	4
h_{25}	4	4	4	4	4	4	0	4	4	4	4	4	4	0	4	4	4	4	4	4	4	4	4	4	0	0	4	4	0	4	0
h_{26}	0	4	4	4	4	4	4	0	4	4	4	4	4	4	0	4	4	4	4	4	4	4	4	4	0	0	4	4	0	4	4
h_{27}	4	0	4	4	4	4	4	4	0	4	4	4	4	4	4	0	4	4	4	4	4	4	4	4	4	0	0	4	4	0	4
h_{28}	0	4	0	4	4	4	4	4	4	0	4	4	4	4	4	4	0	4	4	4	4	4	4	4	4	4	0	0	4	4	4
h_{29}	4	0	4	0	4	4	4	4	4	4	0	4	4	4	4	4	4	4	0	4	4	4	4	4	4	4	4	0	0	4	4
h_{30}	4	4	0	4	0	4	4	4	4	4	4	0	4	4	4	4	4	4	4	0	4	4	4	4	4	4	4	4	0	0	4
h_{31}	0	4	4	0	4	0	4	4	4	4	4	4	0	4	4	4	4	4	4	4	0	4	4	4	4	4	4	4	4	4	0

Notes:

1- $e = \frac{d-1}{2} = \frac{6-1}{2} = 2$, d=6

2- $M = z^k = z^{31-3}$, k= n-r ,r=3

3- $n = \frac{z^m-1}{z-1} = \frac{5^3-1}{5-1}$,m> 2

4- $n = \frac{z^r-1}{z-1}$,$k = \frac{q^r-1}{q-1}$ -r, r=3

4. Results:

By these results **Table 6**, a comparison was made between 31 lines. We notice that the minimum distance is 6, and this value appeared by comparing u with m, z with l, w with v, f with n, and g with h. This means that only these elements can be relied upon in testing the optimality of the code. It must be noted that the largest distance value is 31. This means that the distance value is limited to the range of 6 and 31, d=31 is the highest value.

Table 6: Results

$d(z, l_i) = 6$	$d(g, m_i) = 31$
$d(u, l_i) = 25$	$d(z, v_i) = 31$
$d(w, l_i) = 31$	$d(u, v_i) = 31$
$d(f, l_i) = 31$	$d(w, v_i) = 6$
$d(g, l_i) = 31$	$d(f, v_i) = 25$
$d(l_i, l_i) = 10$ $i \neq j$	$d(g, v_i) = 31$
$d(z, u) = 31$	$d(w, h_i) = 31$
$d(z, w) = 31$	$d(h_i, l_i) = 31$
$d(z, g) = 31$	$d(m_i, h_i) = 31$
$d(u, w) = 31$	$d(v_i, v_i) = 10$ $i \neq j$
$d(u, f) = 31$	$d(z, n_i) = 31$
$d(u, g) = 31$	$d(u, n_i) = 31$
$d(w, f) = 31$	$d(w, n_i) = 31$
$d(w, g) = 31$	$d(z, l_i) = 6$
$d(f, g) = 31$	$d(f, n_i) = 6$
$d(u, m_i) = 6$	$d(g, n_i) = 25$
$d(z, m_i) = 31$	$d(n_i, n_j) = 10$ $i \neq j$
$d(l_i, m_i) = 31$	$d(v_i, m_i) = 31$
$d(m_i, m_i) = 10$ $i \neq j$	$d(n_i, m_i) = 31$
$d(z, h_i) = 25$	$d(n_i, l_i) = 31$
$d(u, h_i) = 31$	$d(v_i, h_i) = 31$
$d(w, m_i) = 25$	$d(n_i, h_i) = 31$
$d(f, m_i) = 31$	$d(h_i, h_j) = 10$ $i \neq j$
$d(v_i, l_i) = 31$	$d(v_i, n_i) = 31$
$d(f, h_i) = 31$	$d(g, h_i) = 6$

This value is considered large compared to 6. Therefore, when finding the distance between any two lines, it is preferable to write the elements that make the distance value large in a dedicated table, which we call neglected values or values. That is unnecessary when applying the theorem that depends on the minimum distance.

5. Conclusions:

In the conclusions in **Table 7**, we can notice the difference in the distance values, as the large difference between the field in space and the plane was shown, meaning that the smallest difference is 4 between the fields 3,5,2.

Table 7: The Conclusions

z=5	If we substitute the values of n = 31 ,d= 6 ,e =2 ,in inequality of theorem 1,we get M =5^{28}. Hence C is a(31 ,5^{28},6)-code $5^{28}\{\binom{31}{0}+\binom{31}{1}+\binom{31}{2}\}$ $= 5^{28}(1+31(4)+7440)$ $= 5^{28}(7565) < z^n$, n = 31 c is not perfect	
z=3	If we substitute the values of n = 31 ,d= 4 ,e =1 ,in inequality of theorem 1,we get M =3^{10}. Hence C is a(13 ,3^{10},4)-code $3^{10}\{\binom{13}{0}+\binom{13}{1}(3-1)\}$ $= 3^{10}(1+26)$ $= 3^{10}$ c is perfect	
Field	Least distance	The different between plane and space
3	4	9
5	6	25
2	3	4

6. References

[1] Al-Zangana EB, Shehab EA. Certain Types of Linear Codes over the Finite Field of Order Twenty-Five. Iraqi Journal of Science. 2021 Nov 30:4019-31. https://doi.org/10.24996/ijs.2021.62.11.22.

[2] Abdullah HH, Yahya NY. New Applications of Coding Theory in The Projective Space of Order Three. Zanco Journal of Pure and Applied Sciences. 2022 Dec 22;34(s6):119-24. https://doi.org/10.31972/ticma2022.

[3] Hirschfield JWP. Projective Geometries over finite fields. Oxford Claren-don Press, New York,Oxford University Press,1979.

[4] Khalaf AM, Yahya NY. New examples in coding theory for construction optimal linear codes related with weight distribution. InAIP Conference Proceedings 2023 Sep 13 (Vol. 2845, No. 1). AIP Publishing. https://doi.org/10.1063/5.0170590 .

[5] Hirschfeld JW. Projective geometries over finite fields. Oxford University Press; 1998 Jan 8..

[6] Younis AA, Yahya NY. The construction (k+ 1; n)-arcs and (k+ 2; n)-arcs from incomplete (k; n)-arc in PG (3, q). Palestine Journal of Mathematics. 2023 Jan 2;12.

[7] Radhi JS, Al-Zangana EB. Complete (k, r)-Caps From Orbits In PG (3, 11). Iraqi Journal of Science. 2023 Jan 30:347-53. https://doi.org/10.24996/ijs.2023.64.1.32 .

[8] Khalaf HM, Yahya NY. A Geometric Construction of (Ƙ, r)-cap in PG (3, q) for q prime, 2≤ q≤ 997. InJournal of Physics: Conference Series 2022 Aug 1 (Vol. 2322, No. 1, p. 012043). IOP Publishing..

[9] Al-Seraji NA. The Geometry of the Plan of Order Seventeen and Its Application to Error-correcting Codes (Doctoral dissertation, University of Sussex).

[10] AL-Seraji NA, AL-Humaidi RI. Some application of coding theory in the projective plane of order three. Iraqi Journal of Science. 2018 Oct 31:1947-51. https://doi.org/:10.24996/ijs.2018.59.4A.18.

[11] AL-Seraji NA, Ajaj HL. Some Applications of Coding Theory in the Projective Plane of Order Four. Al-Mustansiriyah Journal of Science. 2019 Aug 15;30(1):152-7.

[12] AL-Mukhtar A.SH. Complete Arcs and Surfaces in three-Dimensional Projective Space over Galois Field,PHD.Thesis University of Technology,Iraq,2008.

[13] Hill R. A first course in coding theory. Oxford University Press; 1986.

[14] Al-Zangana EB. The geometry of the plane of order nineteen and its application to error-correcting codes (Doctoral dissertation, University of Sussex).

[15] Al-Seraji NA. Generalized of Optimal Codes. Al-Mustansiriyah Journal of Science. 2013;24(6):101-8.

[16] Al-seraji N. On Almost Maximum Distance Separable Codes. Iraqi Journal of Science. 2013;54(3):638-41.